International Committee for Future Accelerators

Sponsored by the Particles and Fields Commission of IUPAP

Beam Dynamics Newsletter

No. 53

Issue Editors
S. Ivanov, Yu. Shatunov

Editor in Chief:
W. Chou

December 2010

Contents

1 Foreword

1.1 From the Chair

Weiren Chou, Fermilab
Mail to: chou@fnal.gov

What kind of role do accelerators play in the advancement of physics and other sciences? The answer to this question is of critical importance to the accelerator community – especially if we want to attract top-notch scientists and talented young students to work in this field. In no. 50 of this newsletter, we published an article by H. Frederick Dylla, Executive Director and CEO of the American Institute of Physics, entitled "*Big Tools for Science*," in which he pointed out that "*These tools of science (i.e. accelerators), which have existed for almost a century, have had considerable impact on both science and the economy in ways that many outside of the physics community are unaware.*"

In this issue, we publish a letter from Alex Chao (a senior scientist at SLAC) and an article co-authored by him and Enzo Haussecker (a student from UC San Diego) in Sec. 2. The title is "*Influence of Accelerator Science on Physics Research*." They carried out an extensive survey of a large body of literature from Nobel Prize winners, 331 documents all told, and gave a convincing quantitative analysis of such an influence. From 1939 (when Ernest Lawrence received a Nobel Prize for his invention of the cyclotron) to 2009, nearly 30% of the Nobel Prizes in Physics had a direct contribution from accelerators. On the average, accelerator science contributed to a Nobel Prize in Physics every 3 years. These surprising results are impressive and eye-opening. They will have a long lasting positive effect on our community and may also influence government funding agencies when they become aware of these facts.

The Fifth International Accelerator School for Linear Colliders was held from 25 October to 5 November 2010 at Villars-sur-Ollon, Switzerland. Barry Barish, Director of the ILC GDE, wrote an article on the school in Section 3.1. The school web address is http://www.linearcollider.org/school/2010/.

The editors of this issue are Drs. Sergey Ivanov (IHEP, Russia) and Yuri Shatunov (BINP, Russia), both panel members. They took on the editing job at short notice as the original editor of this issue was unavailable. Sergey and Yuri did a great job and collected 20 articles in the theme section "*Accelerator Activities in Russia*." Russia has a remarkable history of important inventions and innovations in the accelerator field: RFQ, electron cooling, H^- injection, Siberian snakes, $\gamma\gamma$ collider – to name but a few. These theme articles give a comprehensive review of a variety of accelerator projects and current activities in that country.

In this issue there is the abstract of a recent doctoral thesis (Simon Mathieu White from Univ. of Paris-Sud and CERN), two ICFA workshop reports (HB2010 and Ecloud2010) and a workshop announcement (DIPAC2011). I thank Sergey and Yuri for editing and producing a valuable newsletter for our accelerator community.

.

1.2 From the Editors

Sergey Ivanov, IHEP, Protvino. 142281, Russia
Mail to: Sergey.Ivanov@ihep.ru

Yuri Shatunov, BINP, Novosibirsk, 630090, Russia
Mail to: Yu.M.Shatunov@ inp.nsk.ru

Theme section of this issue, which was compiled under a tight time schedule, is *Accelerator Activities in Russia*. This topic is disclosed in form of a representative selection of reports presented during the recent 22nd Russian Particle Accelerator Conference. The entire scope of those presentations is available via the JACOW web site at www.jacow.org/r10/.

The editors thank the JACOW collaboration for permission of advanced paper publishing of the selected papers from the conference proceedings electronic volume.

2 Letters to the Editors

2.1 A Letter to the Editors

Alexander Chao
SLAC National Accelerator Laboratory, Menlo Park, California, USA
Mail to: achao@slac.stanford.edu

Enzo Haussecker and I just submitted a report "*Influence of Accelerator Science on Physics Research*" (see Sec 2.2) for your consideration to be included in the ICFA Beam Dynamics Newsletter. That report has an intended technical nature and was written as a technical report. After completing the study, however, I have a few comments to add, not as part of the report, but as my personal comments. I am sending them to see if they might also be included in the Newsletter.

1. To me, this report underscores a general lack of recognition of the contributions by accelerator science to the advancement of physics and other sciences. Indeed, the first initiation of this study has been based on the observation that accelerator science has sometimes been considered a supporting science and not quite worthy of its own standing, in spite of the wealth of facts speaking to the contrary. Surprisingly, some of the people who hold that view are accelerator scientists.
2. This study is also triggered by a more recent observation at the start of the operation of the LCLS project. LCLS is an accelerator project based on a profound physics invention of the free electron laser, together with two decades accumulation of prior accelerator innovations that made the operation of this difficult accelerator technology possible. Once completed, it is turned over to the users, who now have acquired a tool whose power exceeds anything in existence by many orders of magnitude. Using this powerful tool, beautiful results were obtained. It would be ironical and incorrect if the accelerator community is not

recognized accordingly as such, as is already apparently occurring when journals such as Nature and Science are readily publishing new results obtained using the LCLS while a submission of the first lasing of the LCLS was rejected. I have to admit that this has been another observation that was with me when I initiated this study.

3. I have one comment on the Bernoulli plot shown in our report. In this plot, one observes a gap around 1970-1975, and another gap around 1995-2004. It is my belief that, to some degree beyond statistics, the first gap reflects a slowing down of nuclear physics, while the second gap reflects a slowing down of high energy physics. Following this second gap, I am expecting that there will be another surge of prizes in the next two decades, and the theme will be photon sciences. Accelerators will again play a pivotal role in that development. Let us hope that accelerator scientists will have an even and fair opportunity to share some of the glory and the recognition when the time arrives. After all, the lack of recognition for accelerator physics will hinder the recruitment of talented physicists into the field, and will impact its future advancement and contribution to science.

I have been fortunate to have Enzo Hasussecker, my summer student of 2010, as my able co-investigator, and I would like to thank him for joining this study.

2.2 Influence of Accelerator Science on Physics Research

Enzo Haussecker and Alexander Chao[a]
SLAC National Accelerator Laboratory, Menlo Park, California, USA
Mail to: enzo@slac.stanford.edu and achao@slac.stanford.edu

Abstract:

We evaluate accelerator science in the context of its contributions to the physics community. We address the problem of quantifying these contributions and present a scheme for a numerical evaluation of them. We show by using a statistical sample of important developments in modern physics that accelerator science has influenced 28% of post-1938 physicists and also 28% of post-1938 physics research. We also examine how the influence of accelerator science has evolved over time, and show that on average it has contributed to a physics Nobel Prize-winning research every 2.9 years.

2.2.1 **Introduction**

Few would dispute that since the invention of the cyclotron accelerator science has surged in its contributions to research in physics. The extent of these contributions, however, is less well known. A degree of uncertainty exists mainly because until now no one has attempted to evaluate them quantitatively. There are a number of challenges in doing so. One must answer such questions as: How do we establish the existence of an accelerator-science contribution? How do we generate numerical data to provide a reliable measurement of them? By analyzing a well-established index of researches in physics, with well-defined parameters for establishing the existence of accelerator-science contributions, we can take a significant step in answering these questions, minimize uncertainties, and provide a useful and reliable indicator for determining the

extent to which accelerator science has influenced physicists and physics. We devise and analyze such an index below.

2.2.2 **Methodology**

We use an index comprised of all Nobel Prize-winning research in physics from 1939 to 2009. Although this sample is somewhat arbitrary, we have chosen it for three reasons: first, the index begins with the Nobel Prize awarded for the invention of the first modern accelerator, the cyclotron; second, Nobel prize-winning physicists have contributed unequivocally to some of the most significant developments in modern physics; and third, Nobel Prize-winning research is "well defined" in the sense that for every Nobel Prize awarded a press release was issued that clearly cites the key justification for the award. This has allowed us to develop a systematic process for collecting Nobel Prize-winning documents for our analysis; we have assembled a total of 331 such documents upon which we have based our analysis.

2.2.3 **Influence of Accelerator Science on Physicists**

2.2.3.1 ***Defining Accelerator Science Contributions***

We begin our analysis by determining the number of Nobel Prize-winning physicists between 1939 and 2009 who were influenced by accelerator science in performing their Nobel Prize-winning research. To determine this number, we must define a criterion for establishing the existence of an accelerator-science contribution on their research.

Criterion 1:

> *There exists an accelerator-science contribution to a Nobel Prize-winning research in physics if and only if there exists a document, authored or coauthored by a Nobel Prize-winner in physics, that explicitly cites the use of accelerator physics or accelerator instrumentation that was developed after 1928[b] as having contributed directly to his or her research.*

By applying Criterion 1 to the 331 Nobel Prize-winning documents we collected, we obtained the names of all of the Nobel Prize-winning physicists between 1939 and 2009 who were influenced by accelerator science. Several are obvious, namely, accelerator physicists such as Ernest O. Lawrence, who received the Nobel Prize for Physics in 1939 "for the invention and development of the cyclotron and for results obtained with it"; John D. Cockcroft and Ernest T.S. Walton, who shared the Nobel Prize for Physics in 1951 "for their pioneer work on the transmutation of atomic nuclei by artificially accelerated atomic particles"; and Simon van der Meer, who shared the Nobel Prize for Physics in 1984 for developing the method of stochastic cooling for storage of antiprotons, "which led to the discovery of the field particles *W* and *Z*."

Other obvious Nobel Prize-winning physicists who were influenced by accelerator science were nuclear and high-energy experimentalists such as Emilio G. Segrè and Owen Chamberlain, who shared the Nobel Prize for Physics in 1959 "for their discovery of the antiproton" using the Bevatron at the Lawrence Berkeley Laboratory; Robert Hofstadter, who shared the Nobel Prize for Physics in 1961 "for his pioneering studies of electron scattering in atomic nuclei and for his thereby achieved discoveries concerning the structure of the nucleons" using the Stanford Linear Accelerator; Burton

Richter and Samuel C.C. Ting, who shared the Nobel Prize for Physics in 1976 "for their pioneering work in the discovery of a heavy elementary particle of a new kind," the J/Ψ particle, using the SPEAR (Stanford Positron-Electron Accelerating Ring) collider and the Brookhaven Alternating Gradient Synchrotron, respectively; Carlo Rubbia, who shared the Nobel Prize for Physics in 1984 for his "decisive contributions … to the discovery of the field particles *W* and *Z*" using the Super Proton Synchrotron at CERN; Jerome I. Friedman, Henry W. Kendall, and Richard E. Taylor, who shared the Nobel Prize for Physics in 1990 "for their pioneering investigations concerning deep inelastic scattering of electrons on protons and bound neutrons" using the Stanford Linear Accelerator; and Martin L. Perl, who shared the Nobel Prize for Physics in 1995 "for the discovery the tau lepton" using the SPEAR collider.

We give the results of our study in Appendix I. Note that the list of names extends well beyond the above accelerator, nuclear, and high-energy physicists. For example, consider the following two case studies in the application of Criterion 1 that reflect the influence of accelerator science on research that superficially appears to be unrelated to it.

2.2.3.2 *Case Studies in the Application of Criterion 1*

Wolfgang Paul, an atomic physicist, was awarded one-quarter of the Nobel Prize for Physics in 1989 "for the development of the ion trap technique." He states in his Nobel Lecture that, "The idea of building traps grew out of molecular beam physics, mass spectrometry and particle accelerator physics…" [1]. He goes on to explain how, "If one extends the rules of two-dimensional focusing to three dimensions, one possesses all ingredients for particle traps," and that "the particle dynamics in such focusing devices is very closely related to that of accelerators…." Paul's Nobel Lecture thus satisfies Criterion 1, so we add his name to the list of Nobel Prize-winning physicists who were influenced by accelerator science.

The astrophysicist William A. Fowler shared the Nobel Prize for Physics in 1983 "for his theoretical and experimental studies of the nuclear reactions of importance in the formation of the chemical elements in the universe." Several of his theoretical studies were based on accelerator experiments, including an important one carried out by Harry D. Holmgren and Richard L. Johnston at the Naval Research Laboratory [2], on which Fowler collaborated and used to support his hypothesis on stellar-fusion processes [3]. Holmgren and Johnston used a Van de Graaff accelerator to produce 2-MeV (million-electron-volt) singly-ionized alpha particles to study the proton-proton reaction chains $He^3(\alpha,\gamma)Li^7$ and $He^3(\alpha,\gamma)Be^7$. Fowler noted in his analysis that, "The large cross-section found for the $He^3(\alpha,\gamma)Be^7$ capture process means that this process will complete successfully with $He^3(He^3,2p)He^4$" [4], and that "it is the completion of the *pp*-chain through $He^3(He^3,2p)He^4$ which is of key importance in the conversion of hydrogen into helium in the theory of stellar nucleogenesis. Only in this way can a star consisting originally of pure hydrogen produce helium through thermonuclear reactions and thus, bring about the first step in nucleogenesis in stars" [5]. Fowler's paper in which he analyzes Holmgren and Johnston's experiment thus satisfies Criterion 1, so we add his name to the list of Nobel Prize-winning physicists who were influenced by accelerator science.

2.2.3.3 *More on Cases Studies and Methodology*

We also note that there are important cases for which there are no statements that satisfy Criterion 1. For example, Gerardus 't Hooft shared the Nobel Prize for Physics in 1999 "for elucidating the quantum structure of electroweak interactions in physics." We collected two Prize-winning documents for our analysis: his 1972 paper on the regularization and renormalization of gauge fields [6], and his Nobel Lecture [7], in which he claims that "experiments at the Large Electron Positron Collider (LEP) at CERN … have provided us with impressive precision measurements that not only gave a beautiful confirmation of the Standard Model, but also allowed us to extrapolate to higher energies…." This claim, however, is not sufficient to satisfy Criterion 1, because it implies nothing about his confirmation of the Standard Model and, more importantly, the formulation of his theories concerning electroweak interactions. This is confirmed by his 1972 paper, in which he cites only theoretical work, such as that of C.N. Yang and Robert L. Mills, as having influenced his own. Thus, 't Hooft was not directly influenced by accelerator science, and we do not add his name to the list of Nobel Prize-winning physicists who were influenced by accelerator science.

Other cases allow us to underscore our distinction between direct and indirect influence of accelerator science on the work of Nobel Prize-winning physicists. We add to our list only the names of those whose work was directly influenced by accelerator science. Consider, for example, the case of Maria Goeppert Mayer and J. Hans D. Jensen, who shared half of the Nobel Prize for Physics in 1963 "for their discoveries concerning nuclear shell structure." The corresponding press release alluded to Goeppert Mayer's discovery of high magic numbers (at which protons and neutrons form particularly stable nuclei) and stressed that there was strong experimental support for them [8]; in particular, the neutron beams produced by the University of Chicago cyclotron were used to measure the nuclear binding energies of krypton and xenon. Goeppert Mayer analyzed them in her paper, in which she noted that: "If 50 or 82 neutrons form a closed shell, and the 51^{st} and 83^{rd} neutrons have less than average binding energy, one would expect especially low binding energies for the last neutron in Kr^{87} and Xe^{137}, which have 51 and 83 neutrons, respectively, and the smallest charge compatible with a stable nucleus with 50 or 82 neutrons, respectively. It so happens that the only two delayed neutron emitters identified are these two nuclei" [9]. Goeppert Mayer's discovery therefore was directly influenced by accelerator science, and her paper on the existence of high magic numbers satisfies Criterion 1. We therefore add her name to the list of Nobel Prize-winning physicists who were influenced by accelerator science.

One might expect that Jensen's research also was influenced by accelerator science, but this was not the case. His key contribution was his paper on the explanation of high magic numbers [10], in which he explained that a nucleon has different energies when its spin is parallel or antiparallel to its orbital angular momentum. Jensen's research clearly was influenced by Goeppert Mayer's discovery, but that means it was influenced only indirectly by accelerator science. Jensen's research therefore does not satisfy Criterion 1, and we do not add his name to the list of Nobel Prize-winning physicists who were influenced by accelerator science.

2.2.3.4 *Numerical Results*

In proceeding as above in applying Criterion 1 to all of the 141 Nobel Prize winners for Physics in the 71 years between 1939 and 2009, we find that the researches of 39 of them were influenced by accelerator science. Since our sampling methodology has virtually ruled out the possibility that we did not collect a document satisfying Criterion 1 that was authored or co-authored by one of the other 102 Nobel Prize winners, we are inclined to believe that the ratio of 39 to 141 or 28% is an accurate indicator of the proportion of post-1938 physicists who were influenced by accelerator science.

2.2.4 **Influence of Accelerator Science on Physics Research**

2.2.4.1 *Defining the Independence of Researches*

A separate but related problem is to determine the proportion of research in physics that was influenced by accelerator science. This is a separate problem, because it involves a modification of our previous determination, but a related one, because this modification will allow us to restate our earlier findings within the context of research in physics, which provides us with yet another indicator for measuring the influence of accelerator science on them.

We begin by drawing on Criterion 1 to determine all of the works influenced by accelerator science, but this time we do not count the physicists who participated in these researches, but the number of researches themselves, to determine how many were influenced by accelerator science; we then divide this number by the total number of Nobel Prize-winning researches in physics that were awarded in the 71 years between 1939 and 2009. To count these researches, however, we require an appropriate criterion to define their scope to prevent the possibility of counting those that overlap twice.

Criterion 2:

> *The scope of a Nobel Prize-winning research in physics is defined by its motivation as determined by the Nobel Foundation; two researches are independent if and only if they have separate motivations.*

By applying Criterion 2 to each year in which a Nobel Prize for Physics was awarded, we obtain the number of independent Nobel Prize-winning researches for that year. For example, Martin L. Perl was cited as having won the Nobel Prize for Physics in 1995 "for the discovery of the tau lepton," and Frederick Reines was cited as having won the Nobel Prize for Physics that same year "for the detection of the neutrino." Thus, there were two independent Nobel Prize-winning researches in 1995.

2.2.4.2 *Numerical Results*

By applying Criterion 2 in this way to all of the Nobel Prizes for Physics, we find that there were 85 independent Nobel Prize-winning researches that were awarded in the 71 years between 1939 and 2009. When we further apply Criterion 1 to these 85 independent researches, we find that 24 of them were influenced by accelerator science. We therefore believe that the ratio of 24 to 85 or 28% is an accurate indicator of the proportion of post-1938 researches in physics that have been influenced by accelerator science.

2.2.5 Influence of Accelerator Science over Time

2.2.5.1 *A Bernoulli Counting Process*

To examine the influence of accelerator science over time, we considered the years in which a Nobel Prize for Physics was awarded to a research that was influenced by accelerator science as successes in a Bernoulli counting process. The probability of a success in any one year then equals the number of years in which a Nobel Prize for Physics was awarded to a research that was influenced by accelerator science, which we have determined by Criterion 1 to be 23, divided by the total number of years investigated, 67. In this case, we investigated only the last 67 years (1943 to 2009), because of the discontinuity owing to World War II. Thus, for the sequence of Bernoulli random variables X_{1943}, X_{1944}, … X_{2009}, the Pr[X_i] = 23/67.

2.2.5.2 *Numerical Results*

The number of trials needed to get one success is a random variable, T, having a geometric distribution with parameter p = Pr[X_i] = 23/67. T can be interpreted as the average time in years between the awarding of two Nobel Prizes for Physics that were influenced by accelerator science. We calculated the expectation of T to be E[T] = 1/p = 2.9 years. Thus, on average accelerator science contributed to a Nobel Prize-winning research in physics every 2.9 years.

2.2.5.1 *Plotting the Data*

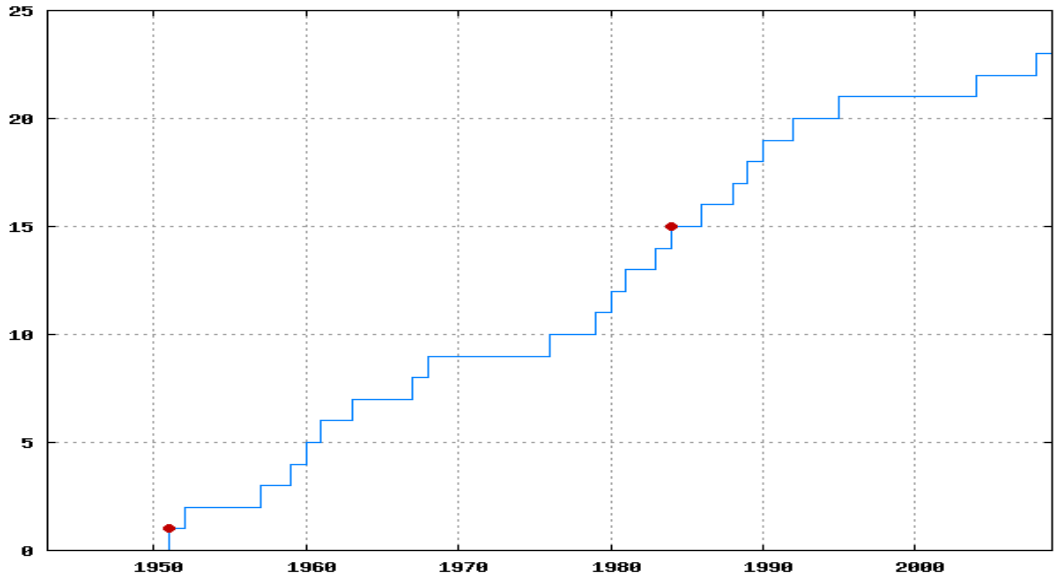

Figure 1: A plot of the Bernoulli count data.

In Figure 1 we see that the Bernoulli-counting process yields a step function that goes up by one unit for each year in which a Nobel Prize for Physics was influenced by accelerator science. The long horizontal lines, for example from 1968 to 1976 and from 1995 to 2004, represent the years in which accelerator science made no contribution to Nobel Prize-winning research; these intervals might be interpreted as a slowing down in recognizing nuclear and high-energy physicists, respectively. The dots indicate the

years in which an accelerator physicist was awarded a Nobel Prize for Phyiscs. (Lawrence is not included because he won the Nobel Prize prior to 1943.)

2.2.6 **Accelerators as an Independent Research Discipline**

The percentages of physicists who and researches that were influenced by accelerator science are sufficiently high to support the view that accelerator science is an important contributor to developments in modern physics. This raises the question as to whether there are more accelerator physicists during the past 71 years who were worthy of high recognition in addition to Lawrence, Cockcroft, Walton, and van der Meer, who together constitute only 2.8% of the 141 Nobel Prize winners in physics between 1939 and 2009. This question is beyond the scope of our present study, but we note that there were many important contributions to accelerator science after World War I, as listed in Appendix II [11], many of which supported research in fields other than physics. Perhaps, therefore, it is time to forgo the view that accelerator science is mainly or exclusively a supporting engineering science, as has been argued by some in the accelerator and the high-energy physics communities. Perhaps it is time to treat and accept accelerator science as an independent research field, deserving of distinction in its own right.

2.2.7 **Conclusion**

Our analysis indicates that accelerator science has played an integral role in influencing 28% of physicists working between 1939 and 2009 by either inspiring or facilitating their research. We also determined that 28% of the research in physics between 1939 and 2009 has been influenced by accelerator science and that on average accelerator science contributed to a Nobel Prize for Physics every 2.9 years. This indicates to us that accelerator science should be regarded as an independent discipline worthy of distinction in its own right.

2.2.8 **Appendix I**

Table 1: A list of physics Nobel Prize-winners who were influenced by accelerator science.

Year	Name	Accelerator-Science Contribution to Nobel Prize-Winning Research
1939	Ernest O. Lawrence	Lawrence invented the cyclotron at the University of Californian at Berkeley in 1929 [12].
1951	John D. Cockcroft and Ernest T.S. Walton	Cockcroft and Walton invented their eponymous linear positive-ion accelerator at the Cavendish Laboratory in Cambridge, England, in 1932 [13].
1952	Felix Bloch	Bloch used a cyclotron at the Crocker Radiation Laboratory at the University of California at Berkeley in his discovery of the magnetic moment of the neutron in 1940 [14].
1957	Tsung-Dao Lee and Chen Ning Yang	Lee and Yang analyzed data on K mesons (θ and τ) from Bevatron experiments at the Lawrence Radiation Laboratory in 1955 [15], which supported their idea in 1956 that parity is not

		conserved in weak interactions [16].
1959	Emilio G. Segrè and Owen Chamberlain	Segrè and Chamberlain discovered the antiproton in 1955 using the Bevatron at the Lawrence Radiation Laboratory [17].
1960	Donald A. Glaser	Glaser tested his first experimental six-inch bubble chamber in 1955 with high-energy protons produced by the Brookhaven Cosmotron [18].
1961	Robert Hofstadter	Hofstadter carried out electron-scattering experiments on carbon-12 and oxygen-16 in 1959 using the SLAC linac and thereby made discoveries on the structure of nucleons [19].
1963	Maria Goeppert Mayer	Goeppert Mayer analyzed experiments using neutron beams produced by the University of Chicago cyclotron in 1947 to measure the nuclear binding energies of krypton and xenon [20], which led to her discoveries on high magic numbers in 1948 [21].
1967	Hans A. Bethe	Bethe analyzed nuclear reactions involving accelerated protons and other nuclei whereby he discovered in 1939 how energy is produced in stars [22].
1968	Luis W. Alvarez	Alvarez discovered a large number of resonance states using his fifteen-inch hydrogen bubble chamber and high-energy proton beams from the Bevatron at the Lawrence Radiation Laboratory [23].
1976	Burton Richter and Samuel C.C. Ting	Richter discovered the J/Ψ particle in 1974 using the SPEAR collider at Stanford [24], and Ting discovered the J/Ψ particle independently in 1974 using the Brookhaven Alternating Gradient Synchrotron [25].
1979	Sheldon L. Glashow, Abdus Salam, and Steven Weinberg	Glashow, Salam, and Weinberg cited experiments on the bombardment of nuclei with neutrinos at CERN in 1973 [26] as confirmation of their prediction of weak neutral currents [27].
1980	James W. Cronin and Val L. Fitch	Cronin and Fitch concluded in 1964 that CP (charge-parity) symmetry is violated in the decay of neutral K mesons based upon their experiments using the Brookhaven Alternating Gradient Synchrotron [28].
1981	Kai M. Siegbahn	Siegbahn invented a weak-focusing principle for betatrons in 1944 with which he made significant improvements in high-resolution electron spectroscopy [29].
1983	William A. Fowler	Fowler collaborated on and analyzed accelerator-based experiments in 1958 [30], which he used to support his hypothesis on stellar-fusion processes in 1957 [31].

1984	Carlo Rubbia and Simon van der Meer	Rubbia led a team of physicists who observed the intermediate vector bosons W and Z in 1983 using CERN's proton-antiproton collider [32], and van der Meer developed much of the instrumentation needed for these experiments [33].
1986	Ernst Ruska	Ruska built the first electron microscope in 1933 based upon a magnetic optical system that provided large magnification [34].
1988	Leon M. Lederman, Melvin Schwartz, and Jack Steinberger	Lederman, Schwartz, and Steinberger discovered the muon neutrino in 1962 using Brookhaven's Alternating Gradient Synchrotron [35].
1989	Wolfgang Paul	Paul's idea in the early 1950s of building ion traps grew out of accelerator physics [36].
1990	Jerome I. Friedman, Henry W. Kendall, and Richard E. Taylor	Friedman, Kendall, and Taylor's experiments in 1974 on deep inelastic scattering of electrons on protons and bound neutrons used the SLAC linac [37].
1992	Georges Charpak	Charpak's development of multiwire proportional chambers in 1970 were made possible by accelerator-based testing at CERN [38].
1995	Martin L. Perl	Perl discovered the tau lepton in 1975 using Stanford's SPEAR collider [39].
2004	David J. Gross, Frank Wilczek, and H. David Politzer	Gross, Wilczek, and Politzer discovered asymptotic freedom in the theory of strong interactions in 1973 based upon results from the SLAC linac on electron-proton scattering [40].
2008	Makoto Kobayashi and Toshihide Maskawa	Kobayashi and Maskawa's theory of quark mixing in 1973 was confirmed by results from the KEKB accelerator at KEK (High Energy Accelerator Research Organization) in Tsukuba, Ibaraki Prefecture, Japan, and the PEP II (Positron Electron Project II) at SLAC [41], which showed that quark mixing in the six-quark model is the dominant source of broken symmetry [42].

2.2.9 **Appendix II**

Table 2: A list of a list of important developments in accelerator science.

Year	*Important Development in Accelerator Science*
1918	Ernest Rutherford discovers artificial nuclear disintegration by bombarding nitrogen nuclei with RaC ($_{83}Bi^{214}$) alpha particles.
1924	Gustav Ising develops the concept of a linear particle accelerator, and four years later Rolf Wideröe builds the world's first linac in an eighty-eight-centimeter glass tube in Aachen, Germany.
1929	Robert J. Van de Graaff invents his eponymous generator at Princeton University. In 1959 he also constructs the first tandem accelerator at Chalk River, Canada.

1929	Ernest O. Lawrence invents the cyclotron at the University of California at Berkeley. In 1930 his student M. Stanley Livingston builds a four-inch-diameter cyclotron.
1932	John D. Cockcroft and Ernest T.S. Walton invent their eponymous electrostatic accelerator at the Cavendish Laboratory in Cambridge, England, and use it to produce the first man-made nuclear reaction.
1937	The brothers Russell and Sigurd Varian invent the klystron, a high-frequency amplifier for generating microwaves, and William Hansen is instrumental in its development at Stanford University. In 1935 Oskar Heil and Agnesa Arsenjewa-Heil at the Cavendish Laboratory, but while on a trip to Italy, had proposed a similar device.
1940	Donald W. Kerst constructs the first betatron at the University of Illinois, an electron accelerator that Joseph Slepian and others had proposed in the 1920s.
1943	Marcus (Mark) Oliphant develops the concept for a new type of accelerator, which Edwin McMillan later named the synchrotron.
1944	Vladimir Veksler at the Lebedev Physical Institute in Moscow, and later Edwin McMillan at the University of California at Berkeley independently discover the principle of phase stability, a cornerstone of modern accelerators, which is first demonstrated on a modified cyclotron at Berkeley in 1946.
1946	Frank Goward constructs the first electron synchrotron in Woolwich, England, which is followed by one built at the General Electric Research Laboratory in Schenectady, New York, where synchrotron radiation is first observed, thus opening up a new era of accelerator-based light sources.
1946	William Walkinshaw and his team in Malvern, England, build the first electron linac powered by a magnetron. William Hansen and his team at Stanford University independently build a similar electron linac a few months later.
1947	Luis Alvarez builds the first drift-tube linac for accelerating protons at the University of California at Berkeley.
1952	Ernest Courant, M. Stanley Livingston, and Hartland Snyder at Brookhaven National Laboratory discover the principle of strong focusing, which Nicholas Christofilos in Athens, Greece, had conceived independently in 1949 and had patented but did not publish. Strong focusing and phase stability form the foundation of all modern high-energy accelerators.
1956	The first Fixed-Field Alternating-Gradient accelerator is commissioned at the Midwestern Universities Research Association, based upon a concept that Tihiro Ohkawa, Andrei Kolomensky, and Keith Symon invented independently. In 1938 Llewellyn Thomas had conceived an earlier variation of it.
1959	The first two proton synchrotrons using strong focusing – the Proton Synchrotron at CERN and the Alternating Gradient Synchrotron at Brookhaven – are built. An electron synchrotron using strong focusing had been built at Cornell University in 1954.
1961	AdA (*Anello di Accumulazione*), the first electron-positron collider, is built at Frascati, Italy [43]. It is followed by two electron-electron colliders, the Princeton-Stanford double-ring collider in the United States and the VEP-1 double-ring collider at Novosibirsk, Russia.
1964	Astron, the first induction linac that Nicholas Christofilos had proposed for

	nuclear fusion, is built at a branch of the Lawrence Radiation Laboratory, later renamed the Lawrence Livermore National Laboratory.
1966	Gersh Budker invents electron-beam cooling at the Institute for Nuclear Physics in Akademgorodok, Russia.
1968	Simon van der Meer invents stochastic cooling for cooling antiproton beams. The proton-antiproton collisions studied at CERN lead to the discovery of the *W* and *Z* bosons in 1983.
1969	Vladimir Teplyakov and Ilya Kapchinskii invent the radio-frequency quadrupole linac at the Institute for Theoretical and Experimental Physics in Moscow.
1971	Intersecting Storage Rings, the first large proton-proton collider, begins operation at CERN.
1971	John M.J. Madey invents and builds the first free-electron laser at Stanford University.
1983	The Tevatron, the first large accelerator using superconducting magnet technology, is commissioned at Fermilab.
1989	The Stanford Linear Collider, first proposed by Burton Richter, is built at SLAC. Maury Tigner had developed the linear-collider concept in 1965.
1993	Construction of the Superconducting Super Collider, a would-be largest accelerator in the world, begins in 1989. The project is cancelled by the U.S. Congress in 1993 [44].
1994	The Continuous Electron Beam Accelerator Facility, the first large accelerator using superconducting radio-frequency technology, is built at the facility now called the Thomas Jefferson National Accelerator Facility.
2005	FLASH (**F**ree-Electron **LAS**er in **H**amburg), the first Vacuum Ultraviolet and soft X-ray free-electron laser-user facility, is built at DESY (Deutsches Elektronen-Synchrotron) in Hamburg, Germany.
2008	The Large Hadron Collider with a twenty-seven-kilometer circumference begins operation at CERN.

2.2.10 **Acknowledgment**

We thank Roger H. Stuewer for his thoughtful and careful editorial work on our paper.

2.2.11 **Notes**

a. Enzo F. Haussecker is an Applied Mathematics Major at the University of California, San Diego and Adjunct Researcher at the SLAC National Accelerator Laboratory; Alexander W. Chao is Professor of Physics at the SLAC National Accelerator Laboratory.
b. We have defined accelerator instrumentation as being developed after 1928 to omit cathode-ray tubes from our analysis, and to begin with the invention of the Van de Graaff accelerator in 1929.

2.2.12 **References**

1. Wolfgang Paul, “Electromagnetic Traps for Charged and Neutral Particles” [Nobel

Lecture, December 8, 1989], in Gösta Ekspong, ed., *Nobel Lectures Including Presentation Speeches and Laureates' Biographies. Physics 1981-1990* (Singapore, New Jersey, London, Hong Kong: World Scientific, 1993), pp. 601-622, on p. 602.
2. H. D. Holmgren and R. L. Johnston, "$He^3(\alpha,\gamma)Li^7$ and $He^3(\alpha,\gamma)Be^7$ Reactions," *Physical Review* **113** (1958), 1556-1559.
3. E. Margaret Burbidge, G.R. Burbidge, William A. Fowler, and F. Hoyle, "Synthesis of the Elements in Stars," *Reviews of Modern Physics* **29** (1957), 547-650.
4. William A. Fowler, "Completion of the Proton-Proton Reaction Chain and the Possibility of Energetic Neutrino Emission by Hot Stars," *The Astrophysical Journal* **127** (1958), 551-556, on 551.
5. *Ibid.*, p. 552.
6. G. 't Hooft and M. Veltman, "Regularization and Renormalization of Gauge Fields," *Nuclear Physics B* **44** (1972), 189-213.
7. Gerardus 't Hooft, "A Confrontation with Infinity" [Nobel Lecture, December 8, 1999], in Gösta Ekspong, ed., *Nobel Lectures Including Presentation Speeches and Laureates' Biographies. Physics 1981-1990* (New Jersey, London, Singapore, Hong Kong: World Scientific, 2002), pp. 359-370, on pp. 366-367.
8. Arthur H. Snell, J.S. Levinger, E.P. Meiners, M.B. Sampson, and R.G. Wilkinson, "Studies of the Delayed Neutrons. II. Chemical Isolation of the 56-Second and the 23-Second Activities," *Phys. Rev.* **72** (1947), 545-549.
9. Maria G. Mayer, "On Closed Shells in Nuclei," *Phys. Rev.* **74** (1948). 235-239, on 238.
10. Otto Haxel, J. Hans D. Jensen and Hans E. Suess, "On the 'Magic Numbers' in Nuclear Structure," *Phys. Rev.* **75** (1949). 1766.
11. Alexander W. Chao and Weiron Chou, "A Brief History of Particle Accelerators" [poster], in Alexander W. Chao and Weiron Chou, ed., *Reviews of Accelerator Science and Technology* (Singapore and Hackensack, N.J.: World Scientific, 2008).
12. E.O. Lawrence and M.S. Livingston, ""The Production of High Speed Light Ions Without the Use of High Voltages," *Phys. Rev.* **40** (1932), 19-35; reprinted in M. Stanley Livingston, ed., *The Development of High-Energy Accelerators* (New York: Dover, 1966), pp. 118-134.
13. J.D. Cockcroft and E.T.S. Walton, "Experiments with High Velocity Positive Ions. I. Further Developments in the Method of Obtaining High Velocity Positive Ions," *Proceedings of the Royal Society of London* [A] **136** (1932), 619-630; reprinted in Livingston, *Development* (ref. 12), pp. 11-23.
14. Luis W. Alvarez and F. Bloch, "A Quantitative Determination of the Neutron Moment in Absolute Nuclear Magnetons," *Phys. Rev.* **57** (1940), 111-122.
15. G. Harris, J. Orear, and S. Taylor, "Lifetimes of the τ^+ and K_L^+-Mesons," *Phys. Rev.* **100** (1955), 932.
16. T.D. Lee and C.N. Yang, "Question of Parity Conservation in Weak Interactions," *Phys. Rev.* **104** (1956), 254-258.
17. Owen Chamberlin, Emilio Segrè, Clyde Wiegand, and Thomas Ypsilantis, "Observation of Antiprotons," *Phys. Rev.* **100** (1955), 947-950.
18. Donald A. Glaser and David C. Rahm, "Characteristics of Bubble Chambers," *Phys. Rev.* **97** (1955), 474-479.
19. Hans F. Ehrenberg, Robert Hofstadter, Ulrich Meyer-Berkhout, D.G. Ravenhall, and Stanley E. Sobottka, "High-Energy Electron Scattering and the Charge Distribution of Carbon-12 and Oxygen-16," *Phys. Rev.* **113** (1959), 666-674.
20. Snell, *et. al.*, "Studies of the Delayed Neutrons" (ref. 8).
21. Mayer, "On Closed Shells in Nuclei" (ref. 9).
22. H.A. Bethe, "Energy Production in Stars," *Phys. Rev.* **55** (1939), 103.
23. Margaret Alston, Luis W. Alvarez, Philippe Eberhard, Myron L. Good, William

Graziano, Harold K. Ticho, and Stanley G. Wojcicki, "Resonance in the Λπ System," *Physical Review Letters* **5** (1960), 520-524; *idem*, "Errata," *ibid.* **7** (1961), 472.

24. J.-E. Augustin, *et al.*, "Discovery of a Narrow Resonance in e^+e^- Annihilation," *Phys. Rev. Lett.* **33** (1974), 1406-1408; reprinted in Bogdan Maglich, ed., *Adventures in Experimental Physics* "Discovery of Massive Neutral Vector Mesons," *Adventures in Experimental Physics*. Vol. 5 (Princeton: World Science Education, 1976), pp. 141-142, and in Robert N. Cahn and Gerson Goldhaber, *The Experimental Foundations of Particle Physics* (Cambridge, New York, New Rochelle, Melbourne, Sydney: Cambridge University Press, 1989), pp. 281-283.
25. J.J. Aubert, *et al.*, "Experimental Observation of a Heavy Particle *J*," *Phys. Rev. Lett.* **33** (1974), 1404-1406; reprinted in Maglich, *Adventures in Experimental Physics* (ref. 24). pp. 128-131, and in Cahn and Goldhaber, *Experimental Foundations of Particle Physics* (ref. 24), pp. 279-281.
26. F.J. Hasert *et al*., "Search for Elastic Muon-Neutrino Electron Scattering," *Physics Letters B* **46 (**1973), 121-124.
27. Sheldon Lee Glashow, "Toward a Unified Theory – Threads in a Tapestry" [Nobel Lecture, December 8, 1979], in Stig Lundqvist, ed., *Nobel Lectures Including Presentation Speeches and Laureates' Biographies. Physics 1971-1980* (Singapore, New Jersey, London, Hong Kong: World Scientific, 1992), pp. 494-504; Abdus Salam, "Gauge Unification of Fundamental Forces" [Nobel Lecture, December 8, 1979], in *ibid.*, pp. 513-538; Steven Weinberg, "Conceptual Foundations of the Unified Theory of Weak and Electromagnetic Interactions," [Nobel Lecture, December 8, 1979], in *ibid.*, pp. 543-559.
28. J.H. Christenson, J.W. Cronin, V.L. Fitch and R. Turlay, "Evidence for the 2π Decay of the K_2^0 Meson," *Phys. Rev. Lett.* **13** (1964), 138-140.
29. Kai Siegahn, "Electron Spectroscopy for Atoms, Molecules and Condensed Matter" [Nobel Lecture, December 8, 1981], in Gösta Ekspong, ed., *Nobel Lectures Including Presentation Speeches and Laureates' Biographies. Physics 1981-1990* (Singapore, New Jersey, London, Hong Kong: World Scientific, 1993), pp. 63-92.
30. Holmgren and Johnston, "$He^3(\alpha,\gamma)Li^7$ and $He^3(\alpha,\gamma)Be^7$ Reactions" (ref. 2); Fowler, "Completion of the Proton-Proton Reaction Chain" (ref. 4).
31. Burbidge, Burbidge, Fowler, Hoyle, "Synthesis of the Elements in Stars" (ref. 3).
32. Carlo Rubbia, "Experimental Observation of the Intermediate Vector Bosons W^+, W^- and Z^0" [Nobel Lecture, December 8, 1984], in Ekspong, *Nobel Lectures. Physics 1981-1990* (ref. 29), pp. 240-287.
33. Simon van der Meer, "Stochastic Cooling and the Accumulation of Antiprotons" [Nobel Lecture, December 8, 1984], in *ibid.*, pp. 291-308.
34. Ernst Ruska, "The Development of the Electron Microscope and of Electron Microscopy" [Nobel Lecture, December 8, 1986], in *ibid.*, pp. 355-380.
35. G. Danby, J-M. Gaillard, K. Goulianos, L.M. Lederman, N. Mistry, M. Schwartz, and J. Steinberger, "Observation of High-Energy Neutrino Reactions and the Existence of Two Kinds of Neutrinos," *Phys. Rev. Lett.* **9** (1962), 36-44.
36. Paul, "Electromagnetic Traps" (ref. 1).
37. J.S. Poucher *et al*., "High-Energy Single-Arm Inelastic *e-p* and *e-d* Scattering at 6 and 10°," *Phys. Rev. Lett.* **32** (1974), 118-121.
38. G. Charpak, D. Rahm and H. Steiner, "Some Developments in the Operation of Multiwire Proportional Chambers," *Nuclear Instruments and Methods* **80** (1970), 13-34.
39. M.L. Perl, *et al.*, "Evidence for Anomalous Lepton Production in e^+-e^- Annihilation," *Phys. Rev. Lett.* **35** (1975), 1489-1492.
40. David J. Gross and Frank Wilczek, "Ultraviolet Behavior of Non-Abelian Gauge Theories," *Phys. Rev. Lett.* **30** (1973), 1343-1346; H. David Politzer, "Reliable Perturbative Results for Strong Interactions," *ibid.*, 1346-1349.

41. Makoto Kobayashi and Toshihide Maskawa, "CP-Violation in the Renormalizable Theory of Weak Interaction," *Progress of Theoretical Physics* **49**, No. 2 (February 1973), 652-657.
42. Makoto Kobayashi, "CP Violation and Flavor Mixing" [Nobel Lecture, December 8, 2008], in Karl Grandin, ed., *Les Prix Nobel. The Nobel Prizes 2008* (Stockholm: Nobel Foundation, 2009), pp. 68-84; website <http://nobelprize.org/nobel_prizes/physics/laureates/2008/kobayashi-lecture.html>.
43. Carlo Bernardini, "AdA: The First Electron-Positron Collider," *Physics in Perspective* **6** (2004), 156-183.
44. Michael Riordan, "The Demise of the Superconducting Super Collider," *Phys. in Perspec.* **2** (2000), 411-425.

3 International Linear Collider (ILC)

3.1 Linear Collider Accelerator School

Barry Barish, ILC GDE
Mail to: barish@ligo.caltech.edu

Following the very intense joint ILC/CLIC workshop (IWLC10) in Geneva last month, I went around Lake Geneva to Villars-sur-Ollon. Our fifth Linear Collider Accelerator School, and the first one sponsored jointly by ILC and CLIC, was held there from 25 October to 5 November 2010. This was a beautiful and comfortable setting for the school, conducive to academic teaching, situated in the mountains and fostering social interactions. In my opinion, one of the most important outcomes of the ILC Global Design Effort is the role we play in the training of future generations of accelerator scientists. The lecturers at the school are leaders of the field, the topics covered are both academically interesting and involve today's forefront research issues, the organization by Alex Chao and Weiren Chou is superb, and the combination of all these aspects has made this a very special yearly event.

Figure 1: 2010 Linear Collider Accelerator School group photo.

The Village of Villars is a couple hours away from Geneva and is very beautiful. It overlooks the Rhône Valley, has views of Mont Blanc from parts of the village, as well as the local ski area. It may sound hard to give six hours of lectures in one day, followed by conducting an interactive homework session with the students in the evening, but in fact it was fun, and I found it a very stimulating environment for students and teachers alike. Admission to the school is extremely competitive, resulting in a highly qualified and motivated student body that comes from all over the world.

Hermann Schmickler, Local Committee Chair

Rolf Heuer, CERN Director General, presenting one of the student awards to Xinlu Xu of Tsinghua Univ., Beijing, China

CERN was the host for this year's school and provided generous support. Hermann Schmickler of CERN served as chair of the local committee and very capably took care of the local arrangements. Rolf Heuer, the CERN Director General, has been a lecturer at several previous schools. He came this year for the final day and presented the student awards.

The school format consisted of two three-hour lectures each day, one in the morning and one in the afternoon, followed by a homework problem session, where the lecturers were available for questions.

This is our fifth school, and while the first schools were dedicated to the ILC, we have now expanded the scope to include both CLIC and the muon collider. After a set of introductory lectures, the school broke into two tracks:

1. Accelerator physics for sources, damping rings, linacs and beam delivery system
2. Superconducting and warm RF technology, LLRF and high power RF

Some students have come to the school twice to cover both tracks. The courses are very rigorous and an examination on the materials is given at the end of the school. The students with the best scores are given a prize.

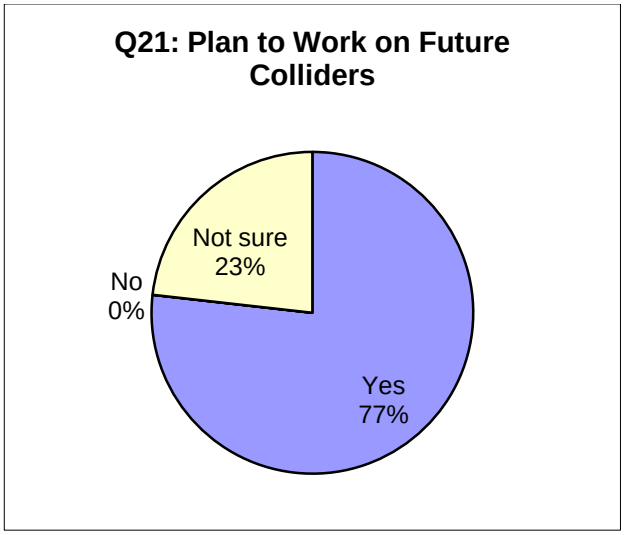

Figure 2: A majority of the students plan to work on future colliders

Few universities include accelerator physics in their academic curriculums for a PhD, so the profession is made up to a large extent of researchers who have migrated into accelerator science from particle physics or some other discipline. Accelerator schools play a very important role in providing the academic training for the field, while accelerator laboratories also provide these students with mentoring to supplement that education. The Linear Collider Accelerator School provides academic training by using current state-of-the-art problems in the field. I find that the students are particularly stimulated by learning from leading accelerator scientists on topics of current interest. I am very proud of our school and am happy I was once again able to participate.

4 Theme Section: Accelerator Activities in Russia

This theme section constitutes a representative selection of reports presented to the recent 22nd Russian Particle Accelerator Conference.

4.1 Overview of RuPAC2010

Nikolay Tyurin and Sergey Ivanov, IHEP, Protvino, Russia
Mail to: tyurin@ihep.ru and sergey.ivanov@ihep.ru

Igor Meshkov, JINR, Dubna, Russia
Mail to: meshkov@jinr.ru

The 22nd Russian Particle Accelerator Conference (RuPAC-2010) was held in Protvino, Moscow region, September 27 – October 1, 2010. It was hosted by the Institute for High Energy Physics (IHEP) and organized jointly by IHEP, Scientific Council for Accelerators of the Russian Academy of Sciences, Joint Institute for Nuclear Research (JINR), and Budker Institute of Nuclear Physics (BINP), Siberian Branch (SB) of the Russian Academy of Sciences. The Conference was supported in

part by the State Corporation for Atomic Energy ROSATOM. Nikolay Tyurin is the Chair of the Organizing Committee, Sergey Ivanov and Igor Meshkov are Co-Chairs.

The first Conference of the series was held in 1968 and was chaired by Prof. Alexander L. Minz, "the father" of powerful radio-electronics in the USSR. Since that time, the Conference became a biennial convention of experts in accelerators and related topics attracting participants from both, the USSR and other countries all over the world.

The venues of the Conference were changed from time to time and the Conference moved from Moscow to Dubna (JINR), then to Protvino (IHEP), Obninsk (Leypunsky IPPE), Novosibirsk (Budker INP), Zvenigorod, vicinity of Moscow (Lebedev PI RAN and Alikhanov ITEP) and now — back to Protvino. Even during the economically hard time of the 1990th, the Conference performance and periodicity was maintained by IHEP that required significant efforts of the organizers.

Until 2004, it had the name of All-Russian (All-Union earlier on) Conference on Particle Accelerators. Quite recently, its name was changed to Russian Particle Accelerators Conference (RuPAC). During all the times RuPAC remains a traditional meeting of accelerator physicists and engineers not only from Russia, but also from the FSU republics, and from foreign laboratories, many of which having active collaborations with the Russian accelerator institutes.

Traditionally, the goal of the event, presented here, is to facilitate information exchange and discussion of various aspects of accelerator science and technologies, beam physics, new accelerator development, upgrade of the existing facilities, and use of accelerators for basic and applied research. The scientific program included the topics to follow:

1. Circular Colliders
2. Linear Colliders, Lepton Accelerators and New Acceleration Techniques
3. Hadron Accelerators
4. Synchrotron Light Sources and FELs
5. Cooler Storage Rings
6. Particle Dynamics in Accelerators and Storage Rings, Cooling Methods, New Methods of Acceleration
7. Accelerator Technologies
8. Applications of Accelerators
9. Radiation Problems in Accelerators
10. Instrumentation, Controls, Feedback, and Operational Aspects

During the RuPAC-2010, the Accelerator Conference Prizes for young physicists and engineers for the best reports presented at the Conference have been nominated for the second time, since the previous RuPAC-2008.

The First Prize was attributed to Dmitry Shwartz (BINP, Novosibirsk) who presented the report "Present Status of VEPP–2000".

Two Second Prizes went to Mariya Gusarova (NRNU MEPhI, Moscow) for her report "MultP-M Code Expansions" and to Andrey Kobets (JINR, Dubna) for his report "Advance in the LEPTA Project".

The Prizes were awarded by the Selection Committee chaired be Vasily Parkhomchuk, Corresponding Member of the Russian Academy of Sciences. All the three reports mentioned above are included into the selection to follow.

The Conference Proceedings are published only electronically. Processing of the electronic files of the contributions prior to, during and short after the Conference was fulfi1led by the RuPAC editing team headed by Maxim Kuzin (BINP) and comprising persons experienced in preparation of the Proceedings of several other Conferences (RuPAC, EPAC, and others), which are members of the Joint Accelerator Conferences Website (JACOW) collaboration. The final version was published at the JACOW website in the early days of November 2010.

The success of the RuPAC-2010 can be attributed to the cooperative efforts of the Program and Organizing Committees, the 1ocal staff of the host institution – IHEP-Protvino, and, of course, a11 of the participants.

4.2 Present Status of VEPP-2000

Dmitry Shwartz, Dmitry Berkaev, Alexander Kirpotin, Ivan Koop,
Alexander Lysenko, Igor Nesterenko, Evgeny Perevedentsev, Yury Rogovsky,
Alexander Romanov, Petr Shatunov, Yuri Shatunov, Alexander Skrinsky,
Ilya Zemlyansky
BINP SB RAS, 630090 Novosibirsk, Russia
Mail to: dshwartz@inp.nsk.su

Abstract:

VEPP-2000 electron-positron collider has been completed in the Budker INP in 2007. First beam was captured in a special lattice with switched off final focus solenoids. This regime is used for all machine subsystems test and calibration as well as vacuum chamber treatment by synchrotron radiation with electron beam current up to 150 mA. Another special low-beta lattice with solenoids switched on partially was used for the first test of the round beam option at the energy of 508 MeV. Studies of the beam-beam interaction were done in “weak-strong” and “strong-strong” regimes. Measurements of the beam sizes in both cases have indicated beam behavior similar to expectations for the round colliding beams. Also the first collider energy calibration at the phi-meson resonance was performed with SND detector. Since the end of 2009 VEPP-2000 started first experimental work with both particle detectors SND and CMD-3 at the energies of 500-950 MeV range with the lattice mode close to project. The precise energy calibration via resonant depolarization method is in progress.

4.2.1 Introduction

At BINP for more than quarter of century the electron-positron collider VEPP-2M has been operated in the energy range of 0.4 ÷ 1.4 GeV. For a long time its results were the main source of information about hadrons production in this energy range. On the other hand, a whole number of events collected by different experimental groups in the energy span above VEPP-2M (up to 2 GeV) does not exceed 10 % of the data accumulated by VEPP-2M. These motivations caused a decision to create instead of VEPP-2M collider a new machine with higher luminosity (up to 10^{32} $cm^{-2}s^{-1}$) and the beam energy up to 2×1 GeV.

To achieve the final goals (luminosity and energy), the Round Beam Concept was applied in design of the machine optics [1]. The main feature of this concept is rotational symmetry of the kick from the round opposite beam. Together with the x – z

symmetry of the betatron transfer matrix between the collisions, it results in particle's angular momentum conservation ($M = xz' - zx' = const$). As a consequence, it yields an enhancement of dynamical stability, even with nonlinear effects from the beam-beam force taken into account.

Computer simulations of the beam-beam interaction in “weak-strong” and “strong-strong” situations confirmed these expectations [2, 3].

4.2.2 **Collider Overview**

The accelerator complex consists of VEPP-2000 collider itself and injection system including 900 MeV booster of electrons and positrons BEP and injection channels also designed for energy of 900 MeV.

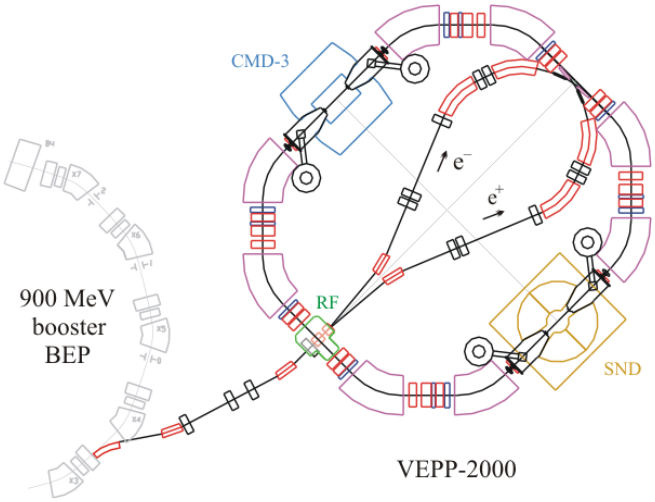

Figure 1: VEPP-2000 layout.

Magnetic structure of VEPP-2000 [4] has the 2-fold symmetry. It includes two (3 m long) experimental straight sections, two straights (2.5 m) for beams injection and RF cavity and 4 short technical straights with 4 triplets of quadrupole magnets. Each triplet together with two 2.4 T bending magnets forms an 90° achromat.

The RBC at VEPP-2000 was implemented by placing into Interaction Regions two pairs of superconducting solenoids symmetrically with respect to collision points.

Table 1: VEPP-2000 Main Parameters (at E = 1 GeV).

Parameter	*Unit*	Value
Circumference, Π	m	24.39 m
Betatron functions at IP, $\beta^*_{x,z}$	cm	10 cm
Betatron tunes, $\nu_{x,z}$		4.1, 2.1
Beam emittance, $\varepsilon_{x,z}$	mm·mrad	1.4×10^{-7} m rad
Momentum compaction, α		0.036
Synchrotron tune, ν_s		0.0035
Energy spread, $\sigma_{\Delta E/E}$		6.4×10^{-4}
RF frequency	MHz	172 MHz
RF harmonic number, q		14
RF voltage	kV	100 kV
Number of particles per bunch, N		10^{11}
Beam-beam parameters, $\xi_{x,z}$		0.075
Luminosity, L	$cm^{-2}s^{-1}$	10^{32} $cm^{-2}s^{-1}$

The strong solenoid focusing provides equal beta-functions of the horizontal and vertical betatron oscillations. There are two combinations of solenoid polarities (+ + – –) and (+ + + +), that rotate the betatron oscillation plane by ±90 degrees and give alternating horizontal orientation of the normal betatron modes. It results in equal tunes and equal radiation emittances of the betatron oscillations. But the simplest case (+ – + –) with an additional small decompensation of solenoid fields also gives round colliding beams and satisfies the RBC requirements.

4.2.2.1 *Superconducting Solenoids*

Each solenoid is designed in two sections: main 13 T solenoid 50 cm in length, and 10 cm anti-solenoid (8 T). In part, the main solenoid consists of two identical units each of these has an inner coil wound with Nb_3Sn wire and an outer coil wound with NbTi wire. To feed the solenoid, we use separate power supplies for the outer and inner coils and for the anti-solenoid. All coils are embedded in the iron yoke located in a common LHe cryostat. During first run 2007/2008 the LHe consumption appeared to be surprisingly high. After the modernization of all solenoids in 2008 consumption decreased from 6 to 4 l/h. The investigations for further consumption decrease are in progress.

4.2.3 **Lattice Options**

Several lattice schemes are available at VEPP-2000 all of them being useful for operation.

4.2.3.1 *Switched off Solenoids*

At the first stage the optics of VEPP-2000 was simplified to the conventional option without solenoids. This “soft” optics (ν_x = 2.4; ν_z = 1.4) is quite different from the

round beam lattice (see Fig. 2, 4). But a part of the lattice near injection is preserved similar to the project one to produce proper betatron phase advance between injection and kicker. Optics without solenoids is available only at energy range below 600 MeV due to gradient limitation in weak F-lenses situated in IR.

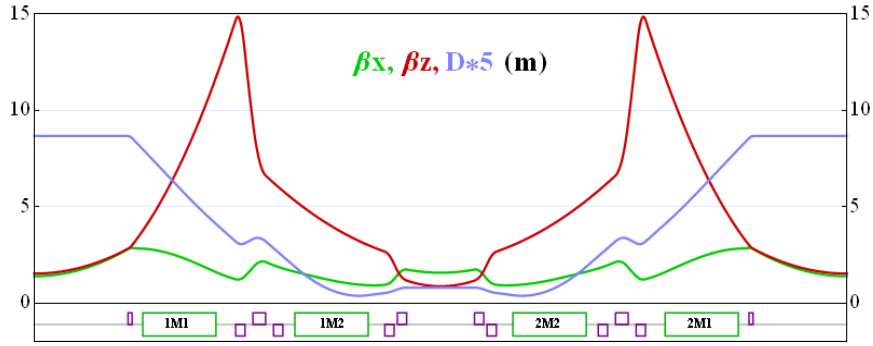

Figure 2: Half period lattice functions. "Soft" optics.

"Soft" lattice was used for the first beam capture, beam transfer efficiency tuning, calibration of the beam diagnostic system, etc. The procedure of vacuum chamber treatment by the synchrotron radiation was also done in this optics scheme, with electron beam in both directions, with several RF-buckets being populated. Beam current, while few days training, raised up to 150 mA and the beam lifetime achieved 1000 sec. At that condition, the lifetime of low beam current (about 1mA) exceeds 10 hours.

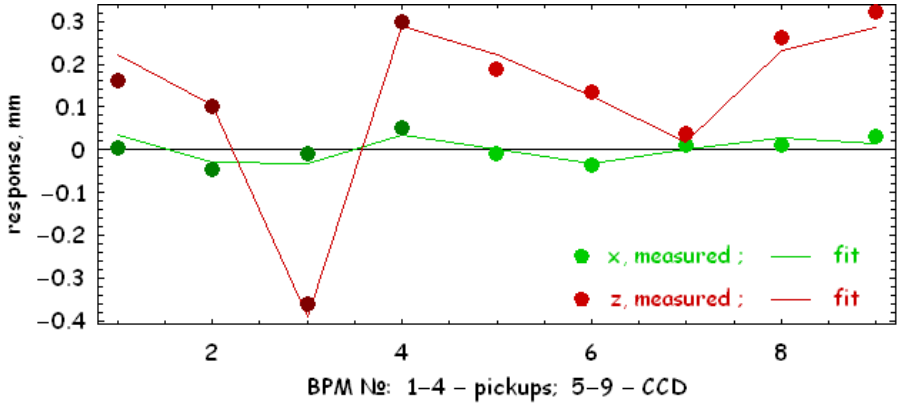

Figure 3: An example of fitted CO response exited by solenoid's coil field.

To start the round beam operation, first of all, we had to align the cooled solenoids. It was done in the same "weak focusing" regime by the CO deviation measurements as a response to the solenoids coils excitation (see Fig. 3). Each section of all 4 solenoids has been tested with magnetic field level up to 4 T. So, coordinates of each i-th solenoid section center (xi, zi, x'i, z'i) have been obtained from the Orbit Response Matrix analysis, and necessary mechanical adjustments of the solenoids have been done.

4.2.3.2 *Short Solenoids*

Round beams optics introduces solenoid focusing, but at low energy of two main solenoid's units it is possible to use only one, closest to IP. It requires 10 T field at 500 MeV and allow to produce β-function at IP as small as $\beta^* = 4.5\ cm$. This optics in

the simplest round beam regime (+ – + –) was used for the first round colliding beam tests in 2008. The colliding beam sizes measurements vs. beam current in "strong-weak" and "strong-strong" cases showed the behavior close to simulations results [5]. The space charge parameter defined by expression

$$\xi = \frac{N r_e \beta^*}{4\pi\gamma\sigma_0^2} \tag{1}$$

achieved the value of ~0.1 and the corresponding maximum peak luminosity expressed as

$$L = \frac{f_0 N^2}{4\pi\sigma^2} \tag{2}$$

or

$$L = \frac{4\pi\gamma^2 f_0}{r_e}\frac{\varepsilon}{\beta^*}\xi^2 \tag{3}$$

was equal to $L = 1\times10^{31}\ cm^{-2}s^{-1}$. In the end of 2008/2009 run VEPP-2000 worked in this optics with collecting the data SND detector that allowed to make first absolute energy calibration at the φ-meson resonance.

4.2.3.3 *Full Solenoids*

Operation at higher energy requires the full solenoid use. Lattice functions for this option are presented at Fig. 4. This optics corresponds to almost twice larger $\beta^* = 8.5\ cm$, while the beam emittance is almost the same. That means that for the same beam currents the luminosity (2, 3) should be near twice lower.

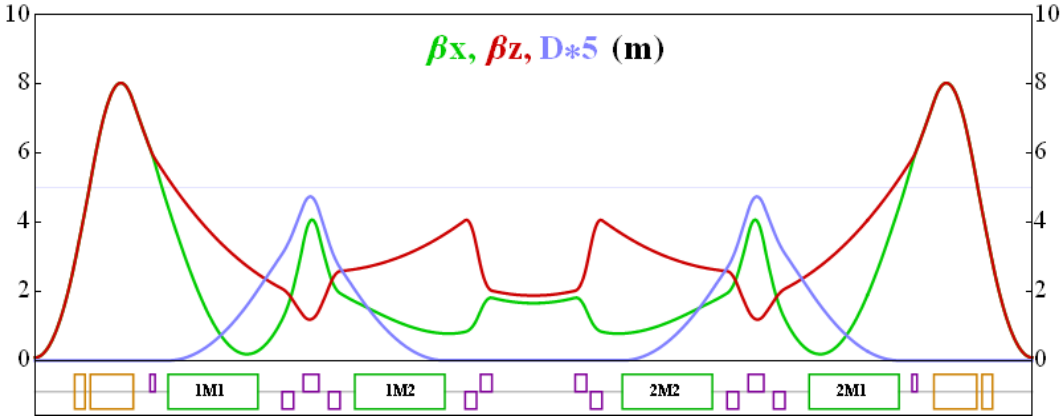

Figure 4: Half period lattice functions. Regular optics with full solenoids.

In the beginning of 2009/2010 run CMD-3 detector became ready for operation. After its installation together with VEPP-2000 final focus solenoids into the IR of the ring, to compensate longitudinal field of the detector ($B = 1\ T$, $L = 1\ m$) anti-solenoids' coils were switched on.

Up to now round beams at VEPP-2000 were always carried out in simple mode where solenoids in each IR have opposite polarity (+ – + –). This corresponds to usual betatron modes, horizontal and vertical elsewhere except IR, where they are rotated on the large angle (roughly π/4). Equal beam emittances required for RBC are produced by finite betatron coupling and betatron tunes being at the coupling resonance $\nu_x - \nu_z = 2$.

We plan to try another optic schemes (+ + – –) and (+ + + +) during the next experimental run 2010/2011, but expect difficulties with smaller dynamic aperture.

4.2.4 **Response Matrix Techniques**

The ORM analysis is widely applied at VEPP-2000 complex. It was used in “soft” optics for rough alignment of cooled solenoids. The precision of coils' position and tilt restored from measured CO response at BPMs does not exceed 0.1 mm and 1 mrad correspondingly. More precise experiments of solenoid position determination with respect to CO was done in regular “round beam” optics also with use of ORM measurements [7].

Another ORM routine application is the measurement and correction of CO distortions at BEP and VEPP-2000 rings. Varying the gradient strength of each quadrupole one can get the CO distortion value there by comparison of measured CO response to model one. This technique is the only one for BEP, where the number of BPMs is poor, but it is also necessary for VEPP-2000 since 16 CCD cameras registering beam synchrotron radiation have high precision of 1 μm but haven't absolute calibration.

The use of SVD technique for ORM inversion also allows us to minimize steering coils currents for given CO. This is important for dynamic aperture optimization since many dipole correctors being embedded in quadrupole lenses have strong nonlinear field components.

Finally, the analysis of orbit responses to dipole correctors variation became a routine but powerful instrument for lattice correction at VEPP-2000 [6, 7]. In Fig. 5 the lattice functions for low-beta optics are presented before lattice correction and after 4-th iteration of the procedure.

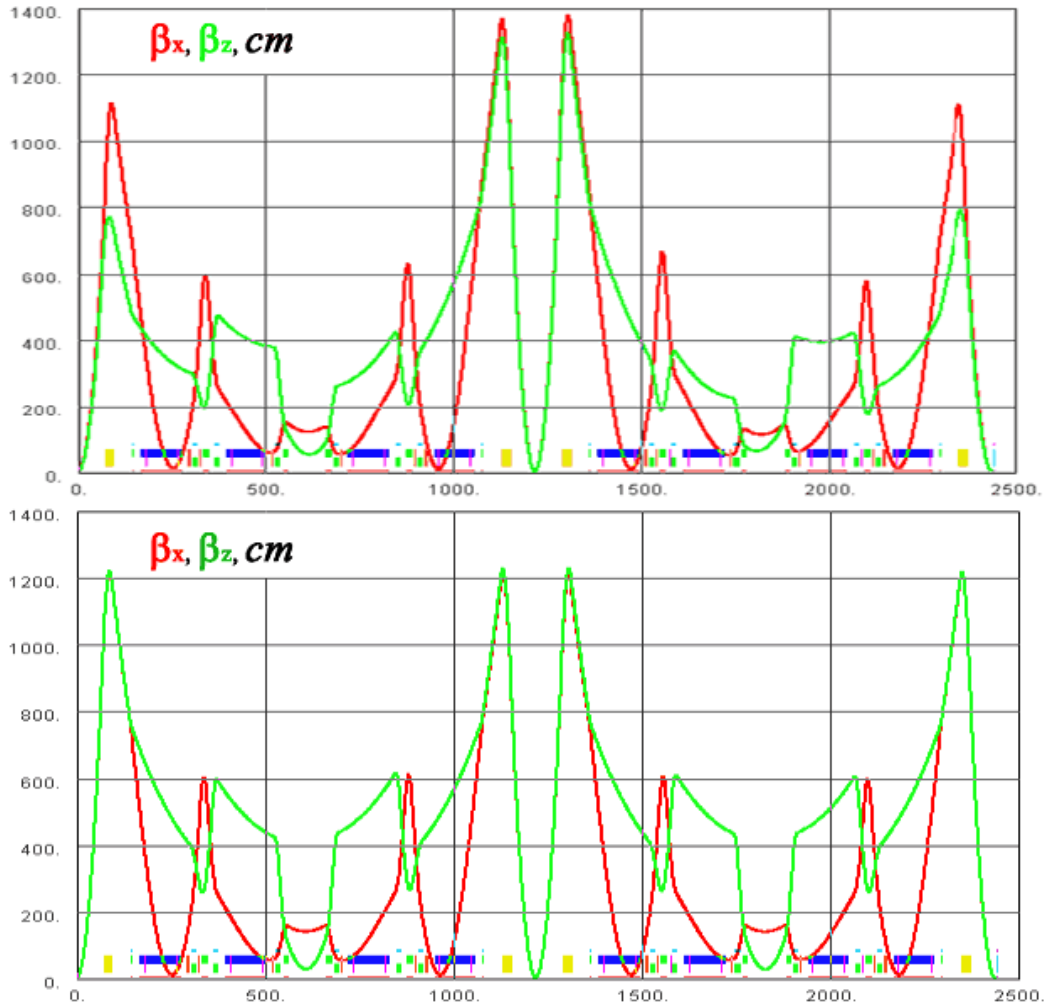

Figure 5: Lattice functions restored from ORM analysis before and after lattice correction.

4.2.5 **Luminosity Integral**

In 2009/2010 first experimental run with both detectors SND and CMD-3 was carried out. Rude energy scan was done from 500 MeV to 950 MeV. The total luminosity integral collected by both detectors amounts to $\int L \sim 10$ pb-1. In Fig. 6 one can see the luminosity integral collected by SND at each point of energy scan. The integral collected by CMD-3 is ~1.6 times smaller.

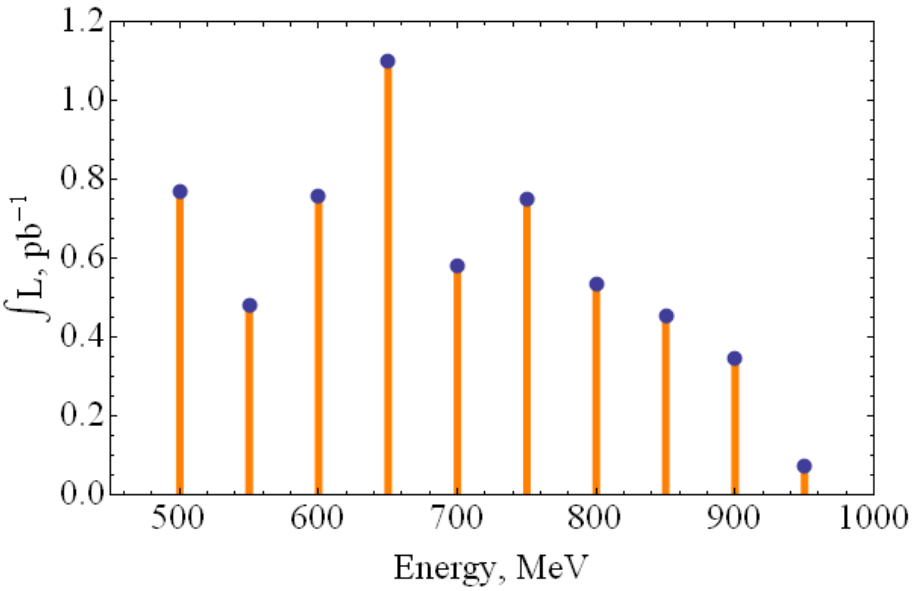

Figure 6: Integrated luminosity collected by SND.

Although the peak luminosity with given beam-beam parameter (3) should grow rapidly with energy ($L \propto \varepsilon\gamma 2$), at present several restrictions exists which do not allow us to provide maximum beam currents at high energy. First one is the insufficient positrons production by the old injection system (part of VEPP-2M complex). It would be fixed after the start up of new VEPP-5 injection complex at BINP. Another problem is low maximum energy of booster BEP and injection channels (900 MeV). In fact the energy ramping in VEPP-2000 was introduced for operation over 800 MeV due to head-tail instabilities in BEP at the higher energies. Firstly ramping inevitably causes large dead time. Moreover, even with enough positrons production the beam currents couldn't be on the beam-beam limit after ramping due to strong energy dependence of space charge parameter (1). In the case of ramping the luminosity dependence L(E) is defined by (2) but with fixed beam current N and thus degrade with energy. Due to mentioned restrictions together with β* change the luminosity value decreased during 2009/2010 run from 1×10^{31} $cm^{-2}s^{-1}$ at 500 MeV to 1.5×10^{30} $cm^{-2}s^{-1}$ at 950 MeV. The project luminosity would be achieved only after BEP upgrade up to 1 GeV. The designing of upgrade is already in progress.

4.2.6 **Energy Calibration**

The requirement on the beam energy measurement precision is $\Delta E/E \leq 10^{-4}$. All VEPP-2000 bending dipoles are equipped with 2 NMR probes each. Probes themselves have high accuracy and show good stability of magnetic field ($\sim10^{-5}$). At the same time they are situated in the dipole gap, but outside of the vacuum volume i.e. rather far from the CO. Rude calibration of the NMR probes was done through the maps of magnetic field obtained from the magnetic measurements. For higher accuracy we use two methods.

4.2.6.1 *Phi-meson*

The φ-meson mass is known with high precision $M\varphi = 1019.455 \pm 0.020$ MeV (PDG). So, the first absolute VEPP-2000 energy calibration was done at the φ-meson resonance with SND detector. It showed an error of previous calibration as large as 3.5 MeV (see Fig.7).

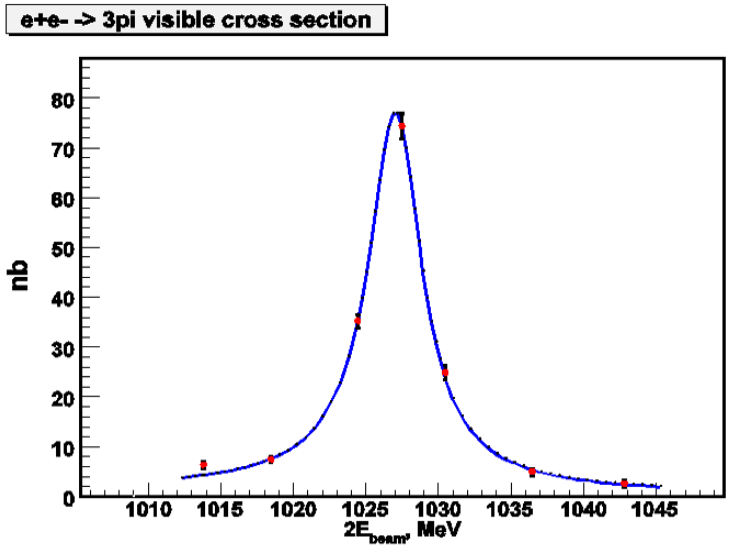

Figure 7: φ-meson resonance before energy calibration (SND data).

4.2.6.2 *Resonant Depolarization*

For more precise energy measurement in addition available at other energy values the method of resonance depolarization is assumed. At the end of 2009/2010 run two weeks were spent for polarization experiments at VEPP-2000. Two counters were installed into one of the technical straights to detect scattered particles. Counters are positioned in horizontal plane one from inner side and another from outer side at some distance from CO. At high energies the main contribution to counting rate is done by Intra Beam Scattering. By comparison of beam lifetime for the case of one bunch and two bunches with the same total beam current it was shown that IBS gives more than 80% of counting rate at 800 MeV. Moreover, to select precisely only good Touschek events only coincident data from two counters was taken. Since the Touschek effect depends on beam polarization the jump in the counting rate should happen during the polarization destruction. The special RF depolarizator was installed into center of injection straight.

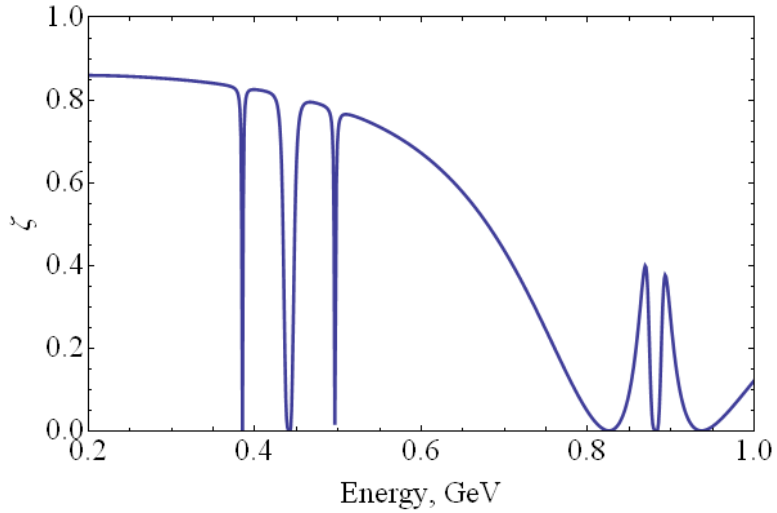

Figure 8: Calculated polarization degree vs. beam energy. Solenoids polarity scheme for low energy experiments.

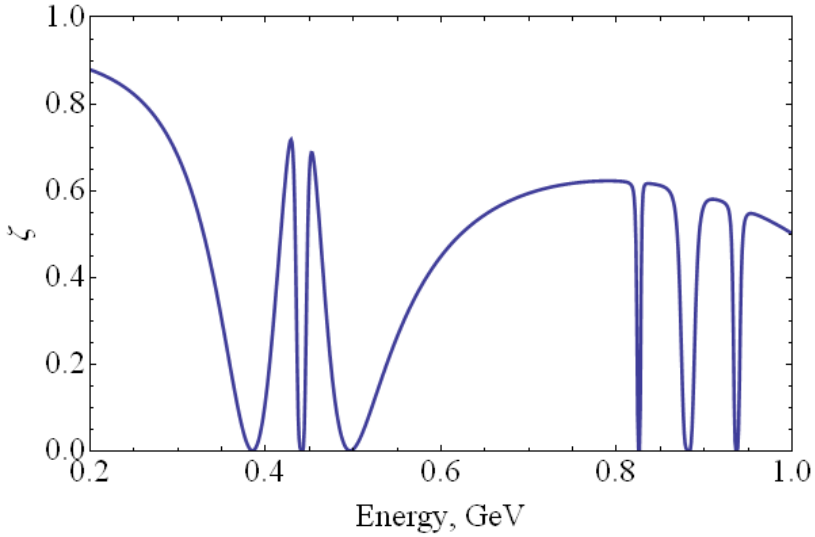

Figure 9: The case of solenoids polarity scheme for high energy polarization experiments.

According to theoretical calculations [8] the jump in Touschek scattering rate depends on the beam emittances ratio being suppressed for the round beam case comparatively to the flat one. So, experiments were held with flat beam: opposite solenoids polarity in each IR; betatron tunes away from coupling resonance; betatron coupling suppressed with skew quadrupole correctors family. To avoid problems with beam parameters drift due to ion cloud focusing the positron beam was chosen for experiments. Radiative polarization time at experiment energy of 750 MeV amounts to ~ 45 minutes according to calculations.

Simulations made with ASPIRRIN code [9] show the great difference for solenoids polarity schemes. In Fig. 8 the beam polarization degree is shown for the (+ – + –) scheme. This scheme includes 2-nd harmonic of longitudinal field that provide strong integer spin resonance at 880 MeV that destroy the polarization at this energy. Thus, such a polarity is suitable for beam polarization only at low energy. Narrow resonance at 440 MeV with two betatron satellites appears in case of solenoids detuning

($\Delta B_s/B \sim 10^{-3}$ at Fig. 8, 9) that is inevitable for real operation. Another scheme (+ – – +) generates the first longitudinal field harmonic, and provide ~60% polarization at 700-800 MeV energy span (see Fig. 9). This scheme was used in attempts of energy calibration at 750 MeV.

Experimental results were dramatically obtained only last night before the complex shut down in the end of July 2010. The first results for the counting rate jump are shown in Fig.10. One can see three scans with the 2.5 ÷ 3 % jump in counting rate. The energy obtained is 750.67 ± 0.03 MeV.

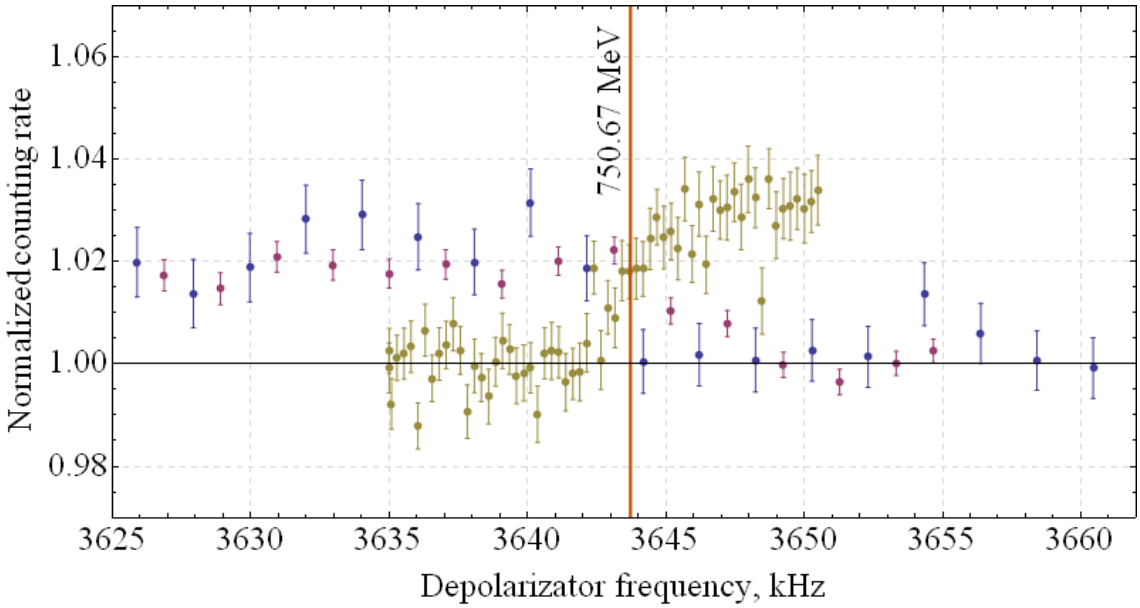

Figure 10: The jump in counting rate.

We plan to continue polarization activity at the beginning of the next run.

4.2.7 **Conclusion**

VEPP-2000 started up the data taking. First energy scan was done. All subsystems were tested at the energies up to 950 MeV. Different optics regimes were tried: technical solenoids-free option; regular round beam optics with $\beta^* = 8.5$ cm and CMD field switched on; low beta optics with higher luminosity; flat beam lattice for resonance depolarization method implementation.

The experimental results of the beam-beam study in the round beams mode have confirmed our expectations for the beam size behaviour in the "weak-strong" and "strong-strong" situations. In the "weak-strong" case the space charge parameter achieved the value of $\xi = 0.1$. The peak luminosity $L = 1\times10^{31}\ cm^{-2}s^{-1}$ has been achieved at energy of 500 *MeV* with beam currents $I^+ \times I^- = 40 \times 40\ mA^2$. To reach the target luminosity (1×10^{32}) at high energy (1 GeV) more positrons are required and booster BEP upgrade is need.

Energy calibration is in progress. NMR probes system was calibrated at the φ-meson resonance. First results of energy measurements via resonance depolarization method were obtained.

4.2.8 References

1. V.V.Danilov et al., in Proc of the EPAC 1996, Sitges, vol. 2, p.1149.
2. Yu.M.Shatunov at. al., in Proc. of the EPAC 2000, Vienna, p.439.
3. A.A.Valishev et al., in Proc. of the PAC 2003, Oregon, p.3398.
4. P.Yu.Shatunov et. al., in Proc. of the EPAC 2006, Edinburg, p. 628.
5. D.E.Berkaev, et. al., in Proc. of the EPAC 2008, Genoa, p. 956.
6. A.L.Romanov, et. al., in Proc. of the RuPAC 2008, Zvenigorod, p. 64.
7. A.L.Romanov, et. al., in Proc. of the IPAC 2010, Kyoto, p. 4542.
8. V.M.Strakhovenko, e-Print: arXiv:0912.5429 [physics.acc-ph], 2009.
9. E.A.Perevedentsev, et al., AIP Conf. Proc. vol. 675, p.761, 2003.

4.3 Project of the Nuclotron-based Ion Collider fAcility (NICA) at JINR

O. S. Kozlov for the NICA Team
JINR, Dubna, Russia
Mail to: okozlov@jinr.ru

4.3.1 Introduction

The Nuclotron-based Ion Collider fAcility (NICA) is the new accelerator complex being constructed at JINR aimed to provide collider experiments with heavy ions up to uranium at the center of mass energy from 4 to 11 GeV/amu. It includes 6 MeV/amu heavy ion linac, 600 MeV/amu booster, upgraded Super Conducting (SC) synchrotron Nuclotron and collider consisting of two SC rings, which provide average luminosity of the level of $10^{27}cm^{-2}s^{-1}$.

The goal of the NICA project is construction at JINR of the new accelerator facility that consists of (see Figure 1):

- cryogenic heavy ion source of Electron String type (ESIS);
- source of polarized protons and deuterons;
- the existing linac LU-20;
- a new heavy ion linear accelerator (HILAc) [1];
- a new SC Booster-synchrotron (that will be placed inside the decommissioned Synchrophasotron yoke);
- the existing proton and heavy ion synchrotron Nuclotron (located in the basement of the Synchrophasatron building) [2];
- two new SC storage rings of the collider;
- a new system of beam transfer channels.

The facility will have to provide ion-ion (1-4.5 GeV/amu of the ion kinetic energy), ion-proton collisions and polarized proton-proton (5-12.6 GeV) and deuteron-deuteron (2-5.8 GeV/amu) beams collisions.

As a result of the project realization, the potential of the Nuclotron accelerator complex will be sufficiently increased in all the fields of its current physics program. The fixed target experiments with slow extracted Nuclotron beams are presumed the experiments with internal target as well. The Booster will be equipped with a slow

extraction system to perform radio-biological and applied researches using heavy ion beams.

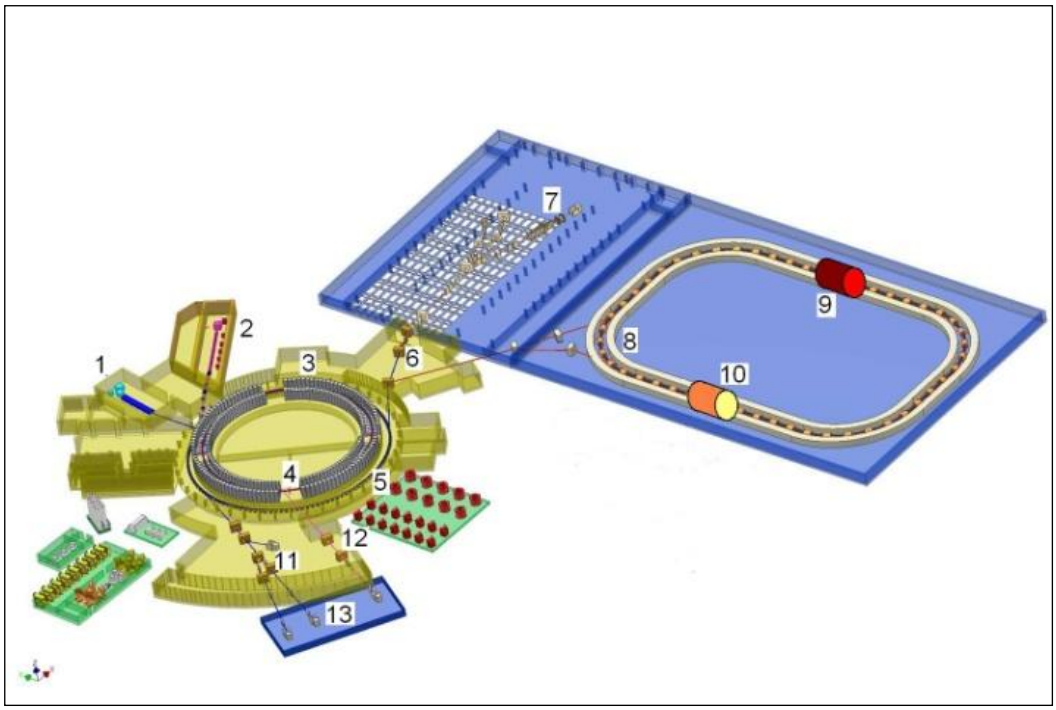

Figure 1: Scheme of NICA facility: 1 – light and polarized ion sources and "old" Alvarez-type linac; 2 – ESIS source and new RFQ linac; 3 – Synchrophasotron yoke; 4 – Booster; 5 – Nuclotron; 6 – beam transfer line; 7 – Nuclotron beam lines and fixed target experiments; 8 – Collider; 9 – MPD; 10 – SPD; 11, 12 – transfer lines; 13 – new research.

The collider will have two interaction points. The Multi Purpose Detector (MPD), aimed for experimental study of hot and dense strongly interacting QCD matter and search for possible manifestation of signs of the mixed phase and critical endpoint in heavy ion collisions, is located in one of them. The second one is used for the Spin Physics Detector (SPD).

Main goal of the NICA facility construction is to provide collider experiment with heavy ions like Au, Pb or U at luminosity above 1×10^{27} $cm^{-2}s^{-1}$ at the energy of 3.5 GeV/amu. It was decided to choose the Gold nuclei $_{197}Au^{79+}$ as the reference particles for the heavy ion collider mode. In the collisions of polarized beams the luminosity above 1×10^{31} $cm^{-2}s^{-1}$ is planned to be achieved in the total energy range.

The essential features of the project permitting to minimize its cost, the construction period and to realize a wide experimental program are the following:

- Collider facility does allow independent carrying out the fixed target experiments;
- The facility can be used for collider experiments with light and middle weight ions including polarized deuterons;
- The required modifications of the Nuclotron ring including development of the ion sources are realizing within the project of the Nuclotron upgrade, which will be completed in 2010 [3];

- Choice of the optimal Booster design based on a few possible versions made before;
- Application of recent world data obtained at BNL, CERN and GSI for achievement of a high collider luminosity;
- Wide co-operation with JINR Member State institutions and active participation of Russian institutions;
- Application of relevant experience available at JINR in superconducting magnets design and fabrication (the magnet cryostat systems of the collider rings and Booster can be made by the institute workshops).

4.3.2 **NICA Operation**

Collider will be operated at a fixed energy without acceleration of an injected beam. Correspondingly the maximum energy of the experiment is determined by the Nuclotron magnetic rigidity that is equal to about 45 Tm at the field value of about 2 T. The collider rings will be placed one above the other one and elements of SC magnetic system are being design as a "twin bore" magnets. For luminosity preservation in the heavy ion collision mode an electron and stochastic cooling systems are planned to be used. To cover the total ion energy range the electron energy of the electron cooling system has to be varied from 0.5 to 2.4 MeV. For optimum operation of the stochastic cooling system the collider optic structure is designed to permit variation of the ring critical energy [4].

To achieve the maximum design energy the Nuclotron has to accelerate fully stripped ions. To provide the ion stripping at high efficiency the ions have to be accelerated to the energy of a few hundreds of MeV/amu. For this goal is used a new synchrotron ring – the Booster. To obtain maximum ion number after single turn injection the Booster has to have a circumference as long as possible. It is realized at the Booster location inside the Synchrophasotron yoke. The yoke will provide also a necessary radiation shielding of the Booster ring .

The heavy ion beam accumulation in the collider rings will be realized with application of RF barrier bucket technique. Intensity of the injected portion influences on the stacking process duration only and could be arbitrary in principle. The required beam emittance is formed during the stacking by the cooling application. The maximum bunch number in the collision mode is limited by requirement to avoid parasitic collisions in the interaction region. The collider will be equipped with Barrier Bucket RF system and two sinusoidal RF systems – one of them is operated at the harmonics number coinciding with the bunch number at the collisions (it is used for the bunching of the stacked beam), another one is operated at significantly larger harmonics number that is necessary to keep a short bunch length at reasonable RF voltage value.

The suggested Project allows one to collide mass asymmetric beams including proton-ion (pA) collisions. Alongside of proper physics meaning, it is quite important as a reference point for comparison with heavy ion data. The experiment will be performed at the same MPD detector therefore the luminosity significantly larger than 10^{27} $cm^{-2}s^{-1}$ is not necessary. This level is achievable quite easily because of large proton number in the beam comparing with heavy ions.

In this mode the collider injection chain has to be switched fast (during a time of a few seconds) from acceleration of heavy ions to acceleration of protons. Two

acceleration and stacking chains of heavy ions and protons (or light polarized ions) are proposed:

ESIS → HILAc → Booster → Nuclotron → Collider
Duoplasmatron (polarized ions source) →LU-20 → Nuclotron → Collider

For the proton acceleration the Booster is not necessary. The proton beam generated by duoplasmatron source is accelerated by LU-20 up to energy of 20 MeV. Single-turn injection allows Nuclotron to have more than 10^{11} protons. After adiabatic bunching they are accelerated at the 5-th harmonic of the revolution frequency to the experimental energy and transferred, bunch by bunch, to the collider ring. If necessary the accelerated proton beam can be rebunched in the Nuclotron after the acceleration to form a single bunch of larger intensity.

Another mode of the facility operation will be proton-proton and deuteron-deuteron polarized colliding beams in the energy range 5-12.6 GeV for protons and 2-5.8 GeV/amu for deuterons. The luminosity above 1×10^{31} $cm^{-2}s^{-1}$ is required over the total energy range.

For the spin physics program the Booster is not used because it has only 4 superperiods instead of 8 in the Nuclotron. The polarized particles are accelerated with LU-20, single-turn injected into the Nuclotron where accelerated up to the experiment energy.

In the Nuclotron ring the deuteron depolarization resonances are absent in the total achievable energy range. The possibility of acceleration and extraction of polarized deuterons in the Nuclotron has been demonstrated a few years ago. The measurements of polarization degree performed by three independent groups on internal and extracted beams in November 2003 gave the value of 65% agreed with the expected value.

For acceleration of the polarized proton beam, the Nuclotron has to be equipped with insertion devices for the spin tune control to cross the depolarization resonances without loose of the polarization degree. Preliminary design of such devices was prepared and the Nuclotron straight section length is sufficiently long to place them.

Presently the maximum achieved intensity of polarized beam in the Nuclotron is about 2×10^{8} particles per cycle. The main direction of work aimed at increase of the intensity is connected with the design and construction of a new high current polarized ion source with charge-exchanged plasma ionizer (IPSN) based on the equipment of CIPIOS polarized proton and deuteron source transferred to Dubna from Bloomington (Indiana University, USA). The work is carried out in collaboration with INR (Troitsk). Some parts of suitable equipment for the new source were presented by DAPHNIA (Saclay). The IPSN will provide the output beam current up to 10 mA of $\uparrow p$ and $\uparrow d^{+}$ ions. $\uparrow d^{+}$ ion polarization of 90% of the nominal vector mode +/-1 and tensor mode +1,-2 is expected. That will result in increase of the accelerated polarized beam intensity at the Nuclotron up to above 10^{10} particle/cycle.

The collider operational cycle assumes feeding the collider with ions during a few minutes after that the collision experiment will be provided during a few hours at almost constant luminosity without additional injections. At this time the Booster and Nuclotron will be used for independent experimental programs. The Nuclotron with LU-20 as injector will provide light ion beams for internal target experiments and its slow extraction system will be used for fixed target experiments and test of the MPD elements. The Booster will be used as a heavy ion synchrotron. Its designed magnetic

rigidity of 25 Tm allows providing the wide range of radio-biological and applied experiments as well as cancer therapy researches with carbon and heavy ions.

4.3.3 **Plans for Realization**

The Nuclotron upgrade program considered as a first stage of the NICA project [4] is in the final stage now. Main goal of the program is to prepare the synchrotron for operation as a part of the NICA collider injection chain. To the moment the upgrade of the Nuclotron vacuum system is completed, deep reconstruction of the liquid helium factory was provided during 2008-2009, modernization of the magnetic system power supply and energy evacuation system will be completed this year. As a result of the works at the Nuclotron run in March 2010 the ions Xe^{42+} were successfully accelerated up to energy of about 1.5 GeV/amu, and the magnetic system was operated at the dipole magnetic field of about 1.8 T (the designed value is 2 T). Development of the new heavy ion source and the polarized ion source is the part of the Nuclotron upgrade as well.

In parallel with the accelerator modernization, the technical design of the collider injection chain elements (HILAc, Booster, LU-20 upgrade program) was prepared.

One of the most important problems determining the facility construction period is the possibility of the collider location close to the Nuclotron with minimum civil constructions. The collider ring circumference has to be about 550 m. However, it is not possible to locate such a ring in the existing experimental building. The project of the new location of the collider (see Figure 1) is under development by State Specialized Design Institution (Moscow) and we expect it the completion at the end of 2010. As a result the price and the required reconstruction period will be determined.

The structural dipole and quadrupole magnets for the collider, as well as for the Booster, will be based on the design developed during the Nuclotron construction. The Nuclotron superconducting magnets are based on a cold-iron window frame type yoke and low inductance winding made of a hollow composite superconductor. The magnetic field distribution is formed by the iron yoke. The Nuclotron magnet fabrication has brought a great experience to the Institute staff in the field of SC magnet design and manufacturing. Such type of magnets one plans to use for construction of SIS-100 synchrotron of the FAIR project. The collider dipole magnet will be about 2 m long, the distance between apertures is about 30 cm. Construction of the magnet model based on the preliminary design has been started in 2010.

To construct the Booster and collider rings we need to fabricate more than two hundreds of the dipole magnets and lenses during short period of time. The working area for the magnet fabrication and test benches required for the magnet commissioning are under preparation now.

A few elements of the facility (such as electron and stochastic cooling) require R&D works and long term of the construction (HILAc).

Taking into account all these problems, the beginning of the facility element commissioning in 2015 looks realistic at the moment. In the optimistic expectations, the experiments with circulating beam in the collider rings can be started at the end of 2015. At the first stage of the collider operation the heavy ion collisions will be realized and the design luminosity level can be achieved to 2017. After upgrade of the ring optics near the collision point the heavy ion–proton collisions will be performed. Collisions of light polarized ions are scheduled for the third stage of the collider operation.

4.3.4 References

1. A.O. Sidorin et al., “Injector Complex of the NICA Facility”, RuPAC2010 Proceedings, TUPSA015.
2. A.O. Sidorin et al., “Design of the Nuclotron Booster in the NICA Project”, RuPAC2010 Proceedings, TUPSA014.
3. A.O. Sidorin et al., “Status of the Nuclotron”, RuPAC2010 Proceedings, WECHA01.
4. S.A. Kostromin et al., “Optics Design for the NICA Collider”, RuPAC2010 Proceedings, TUCHB03.

4.4 Optics Design for Heavy Ion Collider with Changeable Energy Range 1÷5 GeV/u

S.Kostromin[1], A. Bolshakov[4], O.Kozlov[1], V.Lebedev[3], V.Mikhailov[1], I.Meshkov[1], S.Nagaitsev[3], Yu.Senichev[2], A.Sidorin[1], P.Zenkevich[4]
[1]JINR, [2]Forschungszentrum Juelich, [3]FNAL, [4]ITEP
Mail to: kostromin@jinr.ru

Abstract:

The Nuclotron-based Ion Collider fAcility (NICA) [1] is a new accelerator complex being constructed at JINR. It is designed for collider experiments with ions and protons and has to provide ion-ion (Au79+) and ion-proton collisions in the energy range 1÷4.5 GeV/u and collisions of polarized proton-proton and deuteron-deuteron beams.

Collider conceptions with constant γ_t and with possibility of its variation are considered. The ring has the racetrack shape with two arcs and two long straight sections. Its circumference is about 450 m. The straight sections are optimized to have β^*~35 cm in two IPs and a possibility of final betatron tune adjustment.

4.4.1 Introduction

NICA collider lattice development has a number of challenges which must be overcome in the design process. The requirements set by physics goals are: changeable energy of the Au-ions collision in the range 1÷4.5 GeV/u, operation with different ion mass (Au79+, deuterons and protons), the peak luminosity up to $5 \cdot 10^{27}$ $cm^{-2}s^{-1}$ at 4.5 GeV/u, and, additionally, the collider rings must fit into existing JINR infrastructure.

The ring lattice is based on super-ferric magnets with 2 T bending field. The technology of fabrication of such magnets operating at 4.5 K with hollow composite NbTi cable is well established in JINR.

The main luminosity limitation is set by the direct space charge tune shift. In this case the luminosity is proportional to the beam emittance and, consequently, to the collider acceptance. Thus, good optics for NICA implies that in addition to the standard requirement of small beta-function in IP, β^*, there is a requirement of maximizing the machine acceptance.

4.4.2 **Intra-Beam Scattering Study**

The intra-beam scattering (IBS) is one of the main factors which have to be taken into account in a collider ring design. For operation below transition IBS is significantly reduced if the local beam temperatures averaged over the ring are equal. In this case the emittance growth rate due to IBS is equal to zero for a perfectly smooth lattice. Beta-function and dispersion variations destroy this thermal equilibrium resulting in an emittance growth in all three planes: larger variations excite faster emittance growth.

First, the IBS rates were computed for the ideal rings (without straight sections) constructed from ODFDO - and FODO -cells [2]. For the same number of particles the beam emittances were adjusted to have the same growth rates for all planes (thermal equilibrium) and to have the same vertical space charge tune shift (bunch density). Due to "smother" optics the IBS heating rate, τ_{IBS}^{-1}, for the ring based on the triplet cells is ~5 times smaller than for the singlet cells ring with the same phase advance per cell. Therefore the ODFDO-cell ring was chosen as a reference for the collider optics.

A transition from the ideal ring to the collider optics with low-β straight sections increases β-function and dispersion variations and yields an increase of IBS rates. Finally, the collider ring lattice based on FODO-cells has only ~1.5 times larger rates: the growth time of ~890 s versus ~1350 s for the luminosity of $6 \cdot 10^{27}$ $cm^{-2}s^{-1}$.

Table 1: Main parameters of the collider rings optics.

Beam species and energy	***Au^{79+}, 4.5 GeV/n***
Ring circumference	454 m
Gamma-transition, γ_{tr}	6.22
Betatron tunes	9.46 / 9.46
Particles per bunch (of 20 bunches)	$5.3 \cdot 10^9$
Acceptance	40 π mm mrad
Longitudinal acceptance, Δp/p	+/- 0.0125
RMS emittance, $\varepsilon_x/\varepsilon_y$	1.1/0.6 π mm mrad
Beta function at IP, β^*	35 cm
Rms bunch length	60 cm
IBS growth time	1350 s
Luminosity (for Au^{79+} 4.5 GeV/n)	$6 \cdot 10^{27}$ cm^{-2} s^{-1}

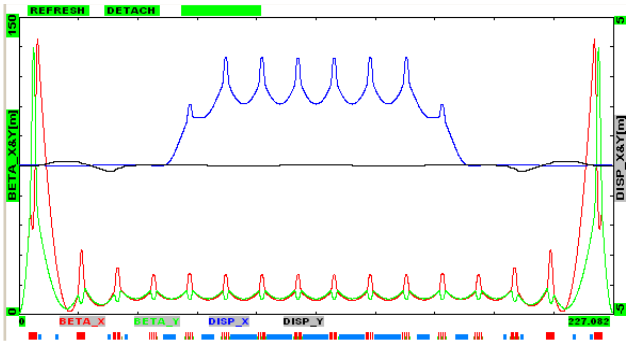

Figure 1: β-function & dispersions for half of the ring.

4.4.3 Collider Ring Optics Structure

Two main options of the NICA optics were considered.

4.4.3.1 *Triplet based Racetrack with γ_t=6.22*

This option was considered in Ref. [3] (see Fig.1). The objectives for the optics design are: (1) small β*, (2) an operation near thermal equilibrium where IBS rates can be minimized, (3) large transverse and momentum acceptances, (4) small circumference, (5) optimal location of collider tune and (6) two IPs. That determined the following design choices: (1) mirror symmetric racetrack with IP in each straight section, (2) triplet focusing through the entire machine (including IPs), (3) phase advance of 90° per cell, (4) dispersion zeroing in the straight sections by a half-dipole without changing phase advance per cell, and (5) vertical beam separation at IPs with two-step vertical elevation for zeroing the vertical dispersion in IPs. The ring parameters are listed in Table 1.

Important to note, that a relative smoothness of the optics resulted in a 3.5 times difference between the heating of all degrees of freedom and the temperature exchange time between different planes (τexchange≈380 s).

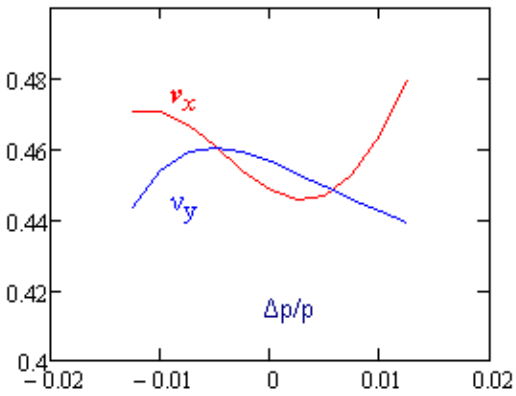

Figure 2: Tune dependence on the momentum offset.

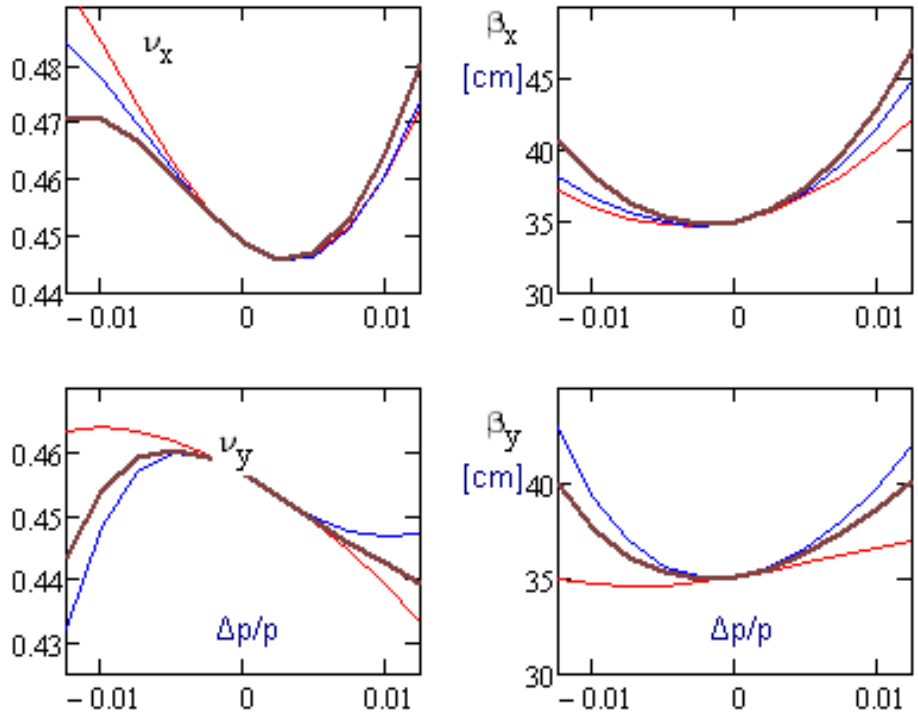

Figure 3: Dependence of the tune and β^* on $\Delta p/p$ with different sextupoles strength.

A chromaticity correction includes four families of sextupoles (two focusing and two defocusing ones). It allows one to correct both the tune chromaticity and the beta-function chromaticity excited by IP quadrupoles. Sextupoles of each family are located with 180° betatron phase advances for their nonlinearity compensation. The dependence of the collider tune on $\Delta p/p$ is shown in Fig. 2. It is very nonlinear due to large β^* which excites large tune and β-function chromaticity. The natural chromaticity of the ring are: ξ_x=-27.1, ξ_y=-23.2 ($\Delta\xi_{x,y} \approx 17$ from two IPs). Corrected chromaticities are: ξ_x =1.54, ξ_y =1.50. The sextupole strength is ~0.35 kG/cm^2. A non-linear dependence of tunes and β-functions on $\Delta p/p$ and the optics smoothness requirement do not allow the perfect chromaticity correction. However sextupole settings making reasonably good compensation were found (see Fig. 3). That allowed us to avoid adding octupoles. Note also that the nonlinearity of tunes is actually profitable. It allows us to have large tune chromaticity required for transverse instabilities suppression with moderate tune variation across the momentum aperture.

The stochastic cooling system is assumed to be used in the collider. The slip-factor was chosen for optimal cooling at 4.5 GeV/u. The cooling time is ~200 s which is significantly smaller than the IBS heating time. The slip factor is increasing fast with beam energy decrease. For fixed momentum spread and bunch length it would result in an unacceptably high RF voltage. However, the beam thermal equilibrium yields a momentum spread decrease with energy decrease as the beam emittance is determined by the ring acceptance and stays constant. That results in that the maximum RF voltage of 0.9 MV is achieved at 2.5 GeV/u. This is only 2 times larger than at 4.5 GeV/u – the energy where optics was optimized.

4.4.3.2 *FODO Cell based Racetrack with Changeable γ_t*

To meet the NICA requirements of operation with Au-ions in range 1÷4.5 GeV/u and with proton 6÷13 GeV lattice with changeable transition energy is considered. Such lattice has to be capable to operate with the minimum IBS heating for Au-ions, to provide increased transition energy for operation with protons [4] and ensure slippage factor in a range 0.01÷0.05 for acceptable RF-voltage and efficient stochastic cooling.

Table 2: Main Parameters of optics with changeable γ_t

Energy of the experiment	Ion-ion and ion-proton collisions			Polarized protons 5÷12 GeV
	1.5 GeV/u	3.5 GeV/u	4.5 GeV/u	
Ring circumference, m	534.2			
Transition energy, γ_{tr}	3.2	5.8	7.6	68
Phase advance per cell, °	30	60	90	varied
Slippage factor, $\eta\omega$	0.051	0.015	0.013	0.004
Betatron tune Q_x/Q_y	8.44/ 7.44	10.44/ 10.44	12.44/ 12.44	12.44/ 12.44
Number of bunches, n_{bunch}	26			
Total chromaticity of the ring (before correction), ξ_x/ξ_y	-28.8/ -27.5	-29.6/ -32.4	-38.3/ -36.6	-37.2/ -33.5
Ring acceptance, π·mm·mrad	200/300	200/200	40/40	40/70
Ring long. acceptance, Δp/p	±0.005			±0.005
Maximum acceptable RMS emittance, $\varepsilon_x/\varepsilon_y$ π·mm·mrad	1.1/0.5	1.1/0.6	1.2/0.6	1.1/0.6
RMS momentum spread	0.6·10-3	1.3·10-3	1.7·10-3	1.2·10-3
Particle per bunch corresponding to tune shift (ΔQ +ξ) = 0.05	0.4·109	2.5·109	4.9·109	2.5·1011
β*, cm	35			35
Bunch length, cm	60	60	60	60
IBS growth time, s	110	600	710	8700
Maximum achievable luminosity, cm^{-2} s^{-1}	$1.8\cdot10^{25}$	$2.0\cdot10^{27}$	$4.2\cdot10^{27}$	$4.2\cdot10^{31}$

The ring optics (Table 2) is optimized for operation with Au79+ ions at the energy of 4.5 GeV/u. Increasing of γ_t was carried out by adjusting gradients in structural lenses [4]. Decrease of γ_t was fulfilled by decrease of the phase advance in each FODO-cell in the arcs. Optics structure of the ring for different regimes of operation is presented in Fig. 4.

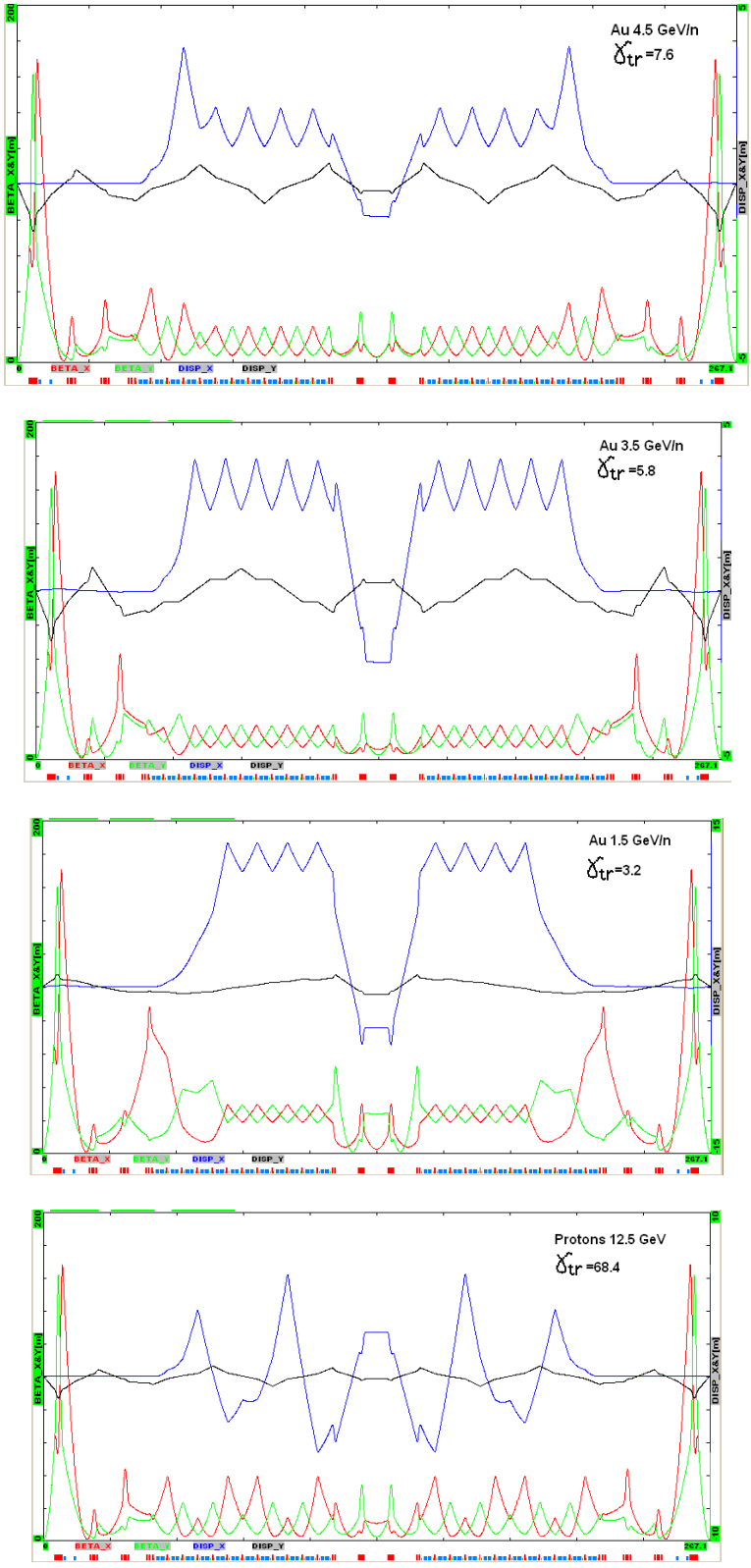

Figure 4: β-functions & dispersions for half of the ring.

The horizontal dispersion suppression was provided by adjusting of focusing gradients in cells near the entrance to the straight section. Such a choice allows tuning of the suppressor at different lattice options when phase advance per cell is changed.

In the proton mode the number of cells in one superperiod N_{cell} and the number of superperiods Sarc per arc are dictated by the required betatron phase advance in the horizontal plane. Horizontal betatron phase advance in the arc ν_{arc} is close to the number of superperiods S_{arc} as possible keeping them both being integers. This means that the phase advance in one superperiod should be $2\pi\nu_{arc}/S_{arc}$, and the phase advance of radial oscillations between the cells located in different superperiods and separated by $S_{arc}/2$ superperiods is $\pi+2\pi n$. It corresponds to the condition of first-order compensation for the nonlinear effects of sextupoles in the arcs. Considering all implications arc consist from 12 FODO cells. They are grouped into 4 superperiods by gradient modulation in the case of proton mode and remain a regular periodic structure (no modulation) for Au-ions (see fig.4). A transition from one option to another is done by gradient change in two focusing quadrupole families in the arcs and then by optics match to the straight sections.

The horizontal dispersion suppression was provided by adjusting of focusing gradients in cells near the entrance to the straight section. Such a choice allows tuning of the suppressor at different lattice options when phase advance per cell is changed. In the proton mode the dispersion in the straight sections is suppressed due to the 2π integer betatron phase advance in the arc.

Straight sections were designed to provide $\beta^*\sim35$ cm, to bring minimum chromaticity into the ring, to ensure total ring tune adjustment, and to have space for non-structural equipment positioning.

Nevertheless due to two IP the NICA has sufficiently high normalized chromaticity value $\xi_{x,y}/\nu_{x,y}\sim3.5$, and use of quite strong sextupole magnets for chromaticity correction sharply restricts the dynamic aperture (see Table 2). The ring tunes have non-linear dependence on $\Delta p/p$ especially for Au 1.5 GeV/u and Protons options. Thus, may be, adding of the octupoles is needed. However in the region of momentum acceptance $\Delta p/p$ ±0.005 the tunes have acceptable values to avoid crossing of dangerous resonances (especially half-integer).

4.4.4 **References**

1. G. Trubnikov et al., “Project of the Nuclotron-based Ion Collider fAcility (NICA) at JINR, Proceedings of RuPAC 2008, Zvenigorod, Russia/
2. S. Nagaitsev, “Intrabeam scattering formulas for fast numerical evaluations”, Physical Review Special Topics – Accelerators and Beams, 8, 064403, (2005) and V. Lebedev, OptiM - Computer code for linear and non-linear optics calculations, 2009.
3. V. Lebedev, “NICA: Conceptual proposal for collider”, MAC2010, January, 2010.
4. Yu. Senichev and A. Chechenin, Theory of “Resonant” Lattices for Synchrotrons with Negative Momentum Compaction Factor, Journal of Experimental and Theoretical Physics, December 2007, vol. 105, No. 5, pp. 1127–1137.

4.5 Accelerator Complex U70 of IHEP: Present Status and Recent Upgrades

S. Ivanov, on behalf of the U70 Light-Ion Task Team[#]
Institute for High Energy Physics (IHEP), Protvino, 142281, Russia
Mail to: Sergey.Ivanov@ihep.ru

[#] Team members: Yu. Fedotov, A. Minchenko, A. Afonin, E. Ludmirsky O. Lebedev, D. Demihovskiy, A. Ermolaev, Yu. Milichenko, I. Tsygankov, I. Sulygin, N. Ignashin, S. Sytov, O. Belyaev, V. Zenin, S. Pilipenko, Yu. Antipov, D. Khmaruk, V. Dan'shin and G. Kuznetsov.

Abstract:

The report overviews status of the U70, accelerator complex of IHEP-Protvino comprising four machines (2 linear accelerators and 2 synchrotrons). Particular emphasis is put on the recent upgrades implemented since the previous conference RuPAC-2008.

4.5.1 Generalities

Layout and technical specification of the entire Accelerator complex U70 of IHEP-Protvino was specified in the previous status report [1] whose general part remains up-to-date.

On December 30, 2009, the Russian Federal Government issued an executive order enrolling the complex into the national List-Register of Unique Nuclear-Physics Facilities. It constitutes a prerequisite for an awaited revision of a funding scheme to maintain special and general-purpose engineering infrastructure of the IHEP facilities.

Efforts were continued to attain the following goals:

1. to ensure stable operation and high beam availability during the regular machine runs,
2. to improve proton beam quality,
3. to implement a program to accelerate light ions with a charge-to-mass ratio q/A = 0.4–0.5, and
4. to put forward a sound long-range option to diversify and develop accelerator and experimental facilities on the IHEP grounds, with a bias towards fixed-target research beyond elementary particle physics.

4.5.2 Routine Operation

Since RuPAC-2008, the U70 complex worked for four runs in total. Table 1 lists their calendar data (end of the text). The first run of a year is shorter and solves, mainly, developmental and methodological tasks.

Dedicated machine development (MD) activity is split into two sessions per a run. One takes about a week prior to delivering beam to experimental facilities. Another (2-day long) occurs amidst the fixed-target physics program, under conditions of a smooth sustained operation of the machines thus facilitating R&D on beam physics.

Table 1: Four runs of the U70 in between RuPAC-2008 and -2010

Run	2008-2	2009-1	2009-2	2010-1
Launching linac URAL30, booster U1.5 and U70 sequentially	October, 10	March, 10	October, 12	March, 15
Proton beam in the U70 ring since	November, 3	April, 1	November, 5	April, 7
Fixed-target physics program with extracted beams	November, 19 – December, 10, 28 days	April 6–21, 14½ days	November, 12 – December, 9, 25 days	April, 12–22, 10 days
No. of multiple beam users (of which the 1st priority ones)	11 (8)	8 (5)	10 (6)	9 (6)
MD sessions and R&D on beam and accelerator physics, days	9	6 ½	11	7
Light-ion acceleration MD program	December, 10–12, 2 ½ days	April, 21–25, 3 ½ days	December, 11–15, 3 ½ days	April , 24–27, 3 ½ days

Fig. 1 shows beam availability data during MDs and a fixed-target experimental physics program (XPh) with averages over 2002–10. Run 2009-2 has set a record with experimental facilities acquiring the extracted beam with its availability exceeding 90%.

During the runs, all the beam extraction systems available in the U70 were engaged — fast single-turn, slow 3rd-order resonant, internal targets, and deflectors made of bent silicon crystals. Fig. 2 demonstrates a period of smooth operation of the U70. Fig. 3 presents operation of slow extraction system.

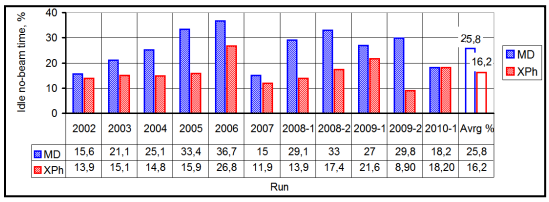

Figure 1: Beam availability statistics.

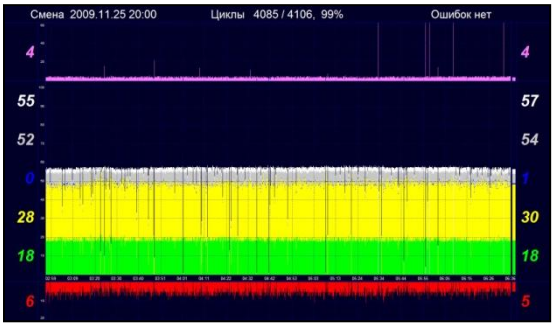

Figure 2: Screenshot of the on-line monitoring over the U70 operation. Time interval (abscissa) extends over 3 hr, or 1000 cycles of acceleration. Yellow trace slows intensity of stochastic extraction, green trace — operation of internal targets. Red (inverted) trace indicates spent beam remains damped onto internal absorber.

4.5.3 **Machine Development**

This Section reports on recent updates in equipment.

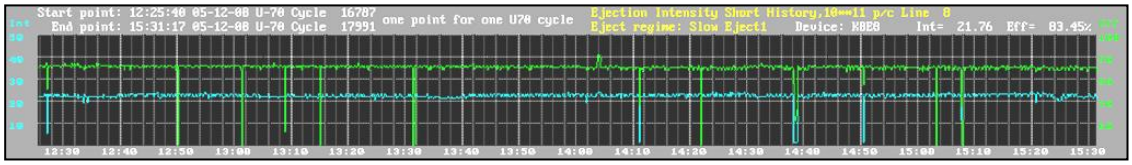

Figure 3: Efficiency factor of slow extraction (90–95%), upper trace. Slowly extracted beam current, lower trace.

4.5.3.1 ***New Septum Magnet SM26***

In 2008, a new septum magnet SM26, manufactured at IHEP workshops, was installed in 4.9 m long straight section SS#26 of the U70 lattice, see Fig. 4. It was a step in upgrade of the slow extraction system aimed at enlarging vertical gap for extracted beam from 25 to 35 mm.

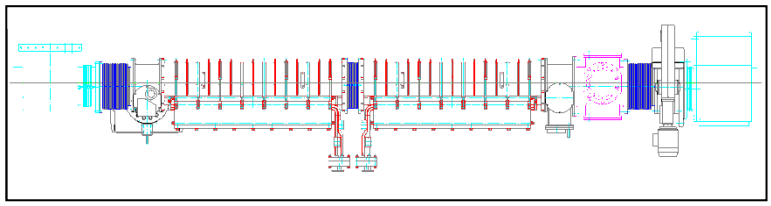

Figure 4: Layout of equipment in SS26 of the U70.

SM26 is sectioned into 2 identical units. Other auxiliary equipment housed in SS#26 (beam diagnostics, vacuum pumps and valves, bellows) was rearranged to a new configuration which also accommodated an universal 3-port docking box (right block in Fig. 4) suitable for inserting diagnostics devices or, say, bent-silicon-crystal deflectors.

4.5.3.2 ***Wide-Band Transverse Feedback***

It is a fast bunch-by-bunch 1-turn delay feedback employing variable delay line ($\Delta\tau/\tau$ is about –10%) and the "virtual pickup" concept, see Fig. 5. In 2008, the former analogue delay was traded for an up-to-date digital delay clocked at the 16th harmonic of radiofrequency.

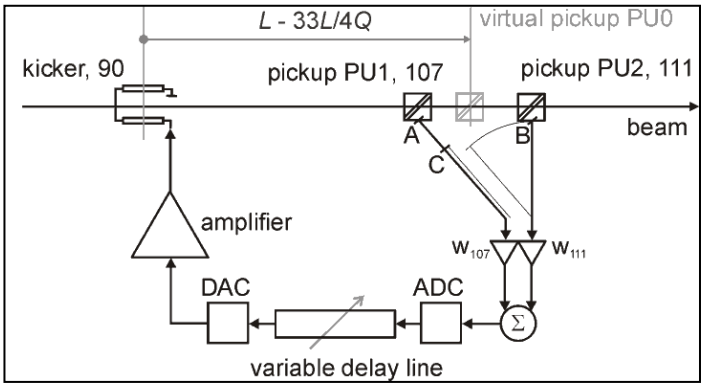

Figure 5: Layout of the wide-band feedback.

A natural byproduct of going to DSP is flexibility in implementation of various feedback algorithms, from linear proportional to nonlinear "bang-bang", sensitive to sign of the beam offset. In practice, an intermediates regime constituting a combination of the two was found most effective with its factor of 50 in shortening decay time of coherent transverse oscillations. Details of the technical solutions adopted by now are reported in [2].

Our intent is to continue efforts in this direction and test a promising one-pickup 3-turn digital delay feedback solution that behaves as a 3-tap periodical notch FIR filter and imposes a purely imaginary coherent tune shift [3].

4.5.3.3 *Intensity of Proton Beam*

For the first time in many years, we have run the U70 complex with a high intensity and 29 bunches injected. Here is a summary of beam parameters in the run 2009-1.

Proton synchrotron U70 has achieved operating intensity of $0.7–1.1\cdot10^{13}$ protons per pulse. Beam top energy is 50 GeV (kinetic). Beam losses over cycle are 2–3%. Bunch length through a cycle is 96 ns (injection) – 17 ns (transition) – 20 ns (extraction). Horizontal beam size is 9–11 mm at 50 GeV. Slow stochastic extraction to beam-line #21 to the OKA experimental facility (study of rare kaon decays) yielded $6–9.5\cdot10^{12}$ protons per a low-ripple 1.4–1.85 s long spill. Booster synchrotron U1.5 has attained top intensity of $5.3\cdot10^{11}$ protons per a (single) bunch under a very reliable operation (relative idle time 6%). Fig. 6 illustrates operation of the U70.

On going to higher beam intensities, mainly, due to uniform orbit filling patterns involved, we have encountered problems with transition crossing. They were tentatively evaded by switching back the 200 MHz spill cavity that dilutes longitudinal phase volume (notice a kink in the peak-current trace of Fig. 6). Still, efforts were and are being spent to better understand transition crossing with compact bunches (high local density) and work out appropriate working point, betatron resonance- and chromaticity-correction scenarios close to γ_t.

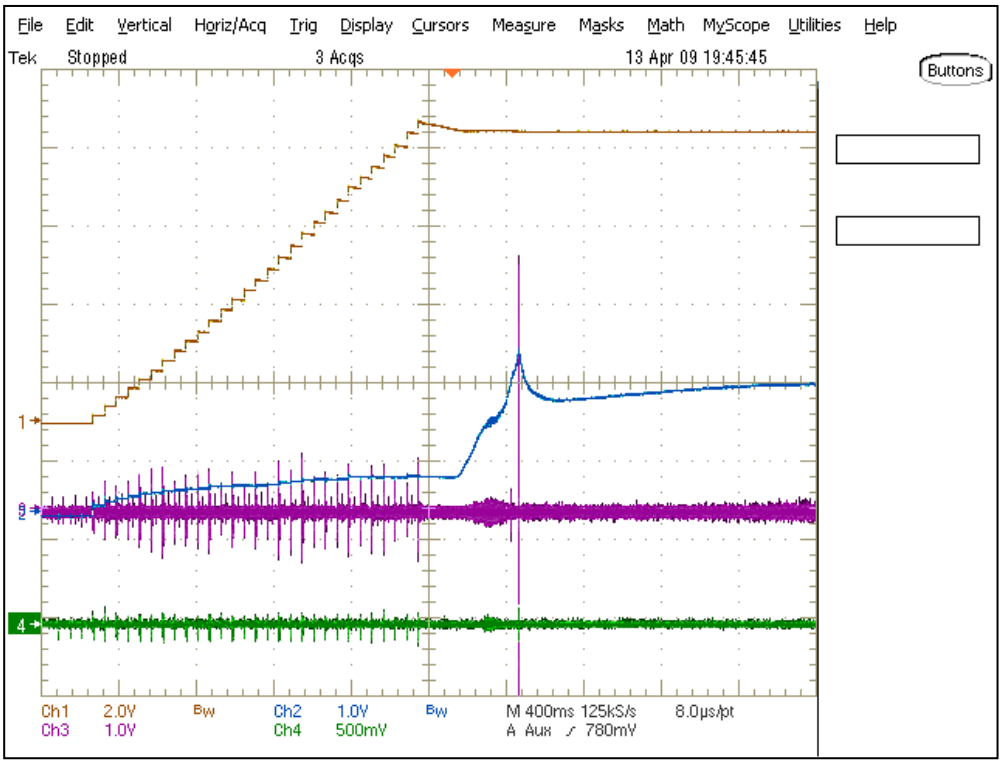

Figure 6: Accumulated beam intensity (upper trace, DCCT monitor, 29 bunches) and peak current of beam (second trace). Lower traces show transverse beam offset signals (H/V injection errors).

4.5.3.4 *Slow Stochastic Extraction*

Fig. 7 illustrates operation of slow extraction system delivering beam to the OKA experimental facility. It shows both, technological signals acquired in the U70 ring and readouts of front-end counters in the OKA setup proper (courtesy of the OKA team). Distance between these two data acquisition points is around 1 km.

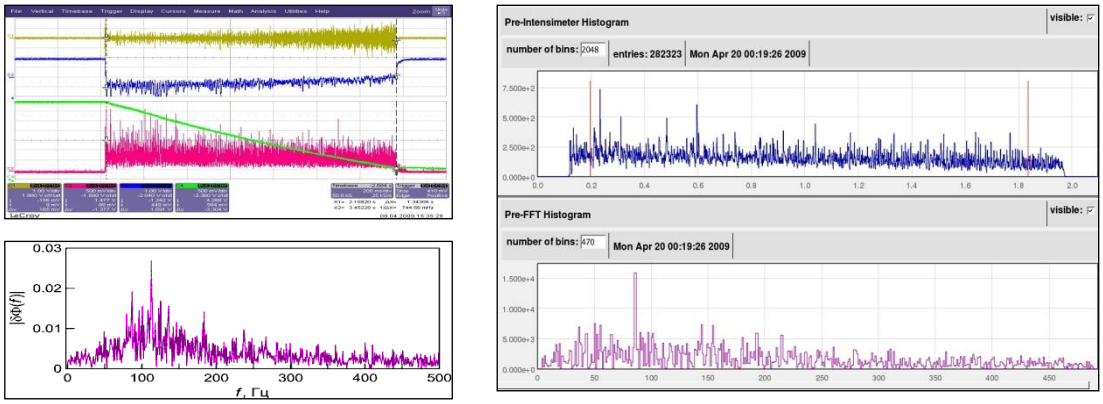

Figure 7: Left, signals from the U70. (1, brown) AM-modulated extraction noise. (2, blue) Feedback signal to modulate noise amplitude. (3, green) Population of waiting beam stack monitored with a DCCT. (4, red) Spill current measured with a BLM in SS#106. (5, purple) Amplitude Fourier spectrum of spill. Right, slowly extracted beam seen at the OKA facility. (1, blue) Spill current. (2, purple) Amplitude Fourier spectrum of spill.

Left-side spill trace (4) in Fig. 7 originates from the beam loss monitor in the ring hall that sees secondary particles emerging due to interception of extracted beam halo by a wire septum of electro-static deflector ESD106. Right-side signal shows intensity of the slowly extracted beam core delivered to the terminal beam consumer.

The data confirms that the U70 now possesses a high-intensity low-ripple long-spill slow extraction system.

4.5.3.5 *Fast Extraction below Flattop*

To meet the demand of beam users, we have successfully tested a fast 1-turn extraction of bunches at 50 GeV (B-field 0.8590 T) during a ramp with dB/dt ≠ 0 and flattop 1.0331 T corresponding to beam energy 60 GeV.

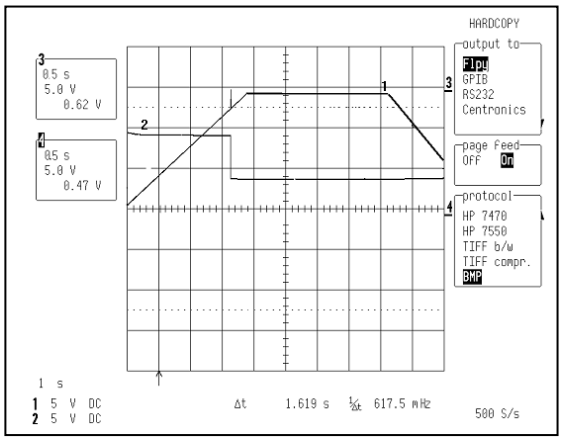

Figure 8: Fast extraction from the U70 during B-field ramp (trace 1). Intensity of circulating bean is shown by trace 2

To this end, new cable traces in the ring hall of the U70 were laid that allowed reshaping horizontal closed-orbit bump near deflecting magnets DM62, 64 from a half-

to a full-wavelength (cancellation of electromotive force due to dB/dt ≠ 0 at bump-coil power supply outlets). Beam trace angle at entry to transfer line has required adjusting with a dipole corrector DCH66 (switched polarity).

Fig. 8 shows experimental data. Stability of operation of fast-extraction synchronization (especially, in its updated configuration) and reproducibility of the extracted beam energy was confirmed in runs 2009-1 and 2009-2.

The similar goal — to diversify extracted beams available in a given magnetic cycle of the U70 — was pursued during tests of acceleration with an intermediate plateau of the B-field. The first plateau (flat bottom) at .0.03537 T corresponds to injection energy 1.32 GeV. The second (new) plateau at 0.8590 T accepts 50 GeV beam, while the third plateau (flattop) is at 1.0330 T and 60 GeV.

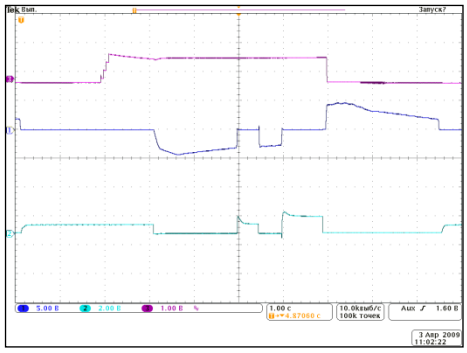

Figure 9: Here and on the right, traces are listed from top to bottom. (1) Beam current (DCCT). (2) Derivative *dB*/*dt*, inverted. (3) Feedback signal to stabilize level of plateau.

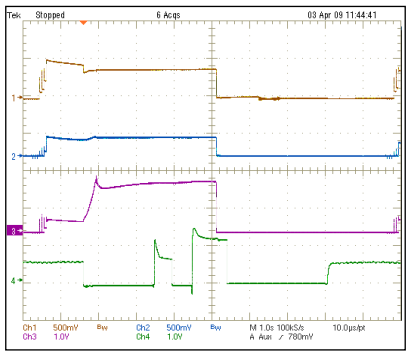

Figure 10: (1) Beam intensity (pickup). (2) Beam current (DCCT). (3) Peak current of bunches. (4) Feedback signal to stabilize level of plateau.

On the one hand, this task constitutes a backup alternative to the on-the-fly fast extraction mentioned above. On the other hand, it set a sound work-pad to Department of Power Engineering Facilities of the U70 to develop and test a new set of tools to control, synchronize and stabilize magnetic cycle, with both 3 and 2 (routine) plateaus.

This regime was safely implemented in the run 2009-1. There were no beam loss observed in course of (a well adiabatic) traversal of the intermediate plateau. Experimental signals acquired from ring magnet supplies and beam monitors are shown in Fig. 9 and 10.

Both the tasks in question related to fast extraction below flattop put forward new options for a more flexible operation of the U70 in the future.

4.5.3.6 *Proton Linear Accelerator URAL30*

This machine stands in the start position in the Accelerator complex U70. Its stable operation is crucial to maintain high overall beam availability.

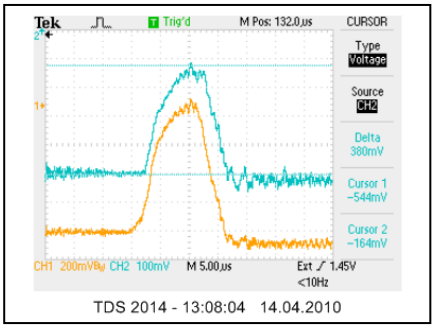

Figure 11: Beam pulse in the URAL30. Pulse current is 25–40 mA.

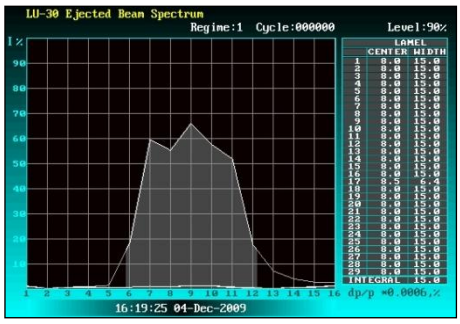

Figure 12: Bunch distribution over momentum at exit from the URAL30.

To maintain stable operation of the proton ion source (duoplasmatron), its vacuum pumping system was renovated. To this end, a pair of new high-tech turbo molecular pumps SHIMADZU 3203LM (speed 3200 l/s (in N2), 2400 l/s (in H2)) was mounted. Since then, no failures of ion source due to vacuum conditions were observed. Reproducibility of bunches has improved, which can be noticed, say, as a linear slope of the upper, beam accumulation trace in Fig. 6. Fig. 11, 12 shows other beam data.

The upgrade plans foresee renewal of pulsed power supplies in the ion gun, of RF powering scheme of the first two sections, and installing a commercially available subsystem to stabilize temperature of cooling water.

4.5.3.7 *Digital Master Oscillator*

A new DDS master oscillator for the U70 proton synchrotron was developed and tested in the run 2010-1. This activity pursues many goals. These are (in priority order):

1. To attain more flexibility in generating “B-field–radiofrequency” law allowing acceleration of protons and light ions with charge-to-mass ratio about ½.
2. To provide a tool for coordinated variation through cycle of gains in radial and phase-frequency feedback loops around the maser oscillator.
3. To introduce, as a routine, bunch-rotation RF gymnastics prior to de-bunching at flattop for prompt control over momentum spread in circulating beam.
4. To introduce a straightforward procedure of bunch smoothing and lengthening with an off-line digitally synthesized and uploaded phase noise samples of accelerating voltage.

All items of this list were beam-tested successfully. The capabilities of the DDS master oscillator are very promising, though an in-depth study of the newly opened options is yet to be completed. Figs. 13–15 present a few experimental results on the items in question.

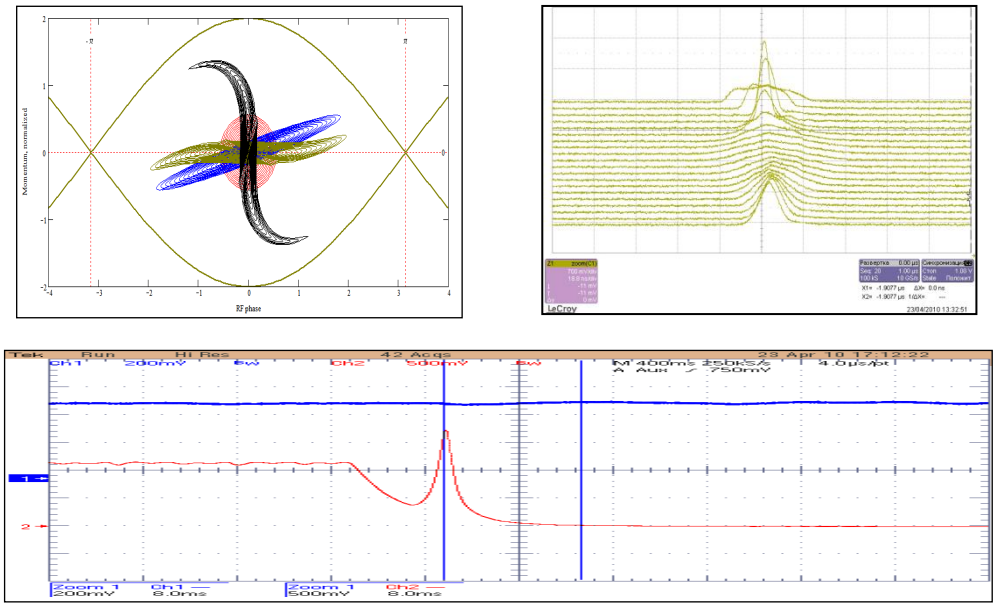

Figure 13: Bunch rotation in the longitudinal phase-plane. Top left – calculation, right– observed "mountain range" display, bottom – peak current of beam. Notice a fast 1.5 ms de-bunching with no symptoms of a spurious re-bunching due to a widened ±Δp/p0.

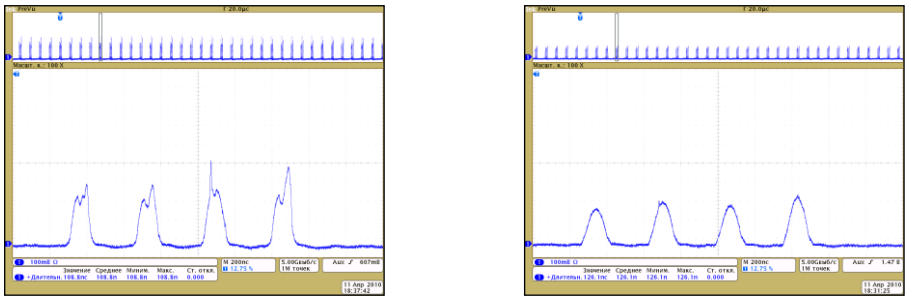

Figure 14: Bunch smoothing and lengthening with external phase noise.

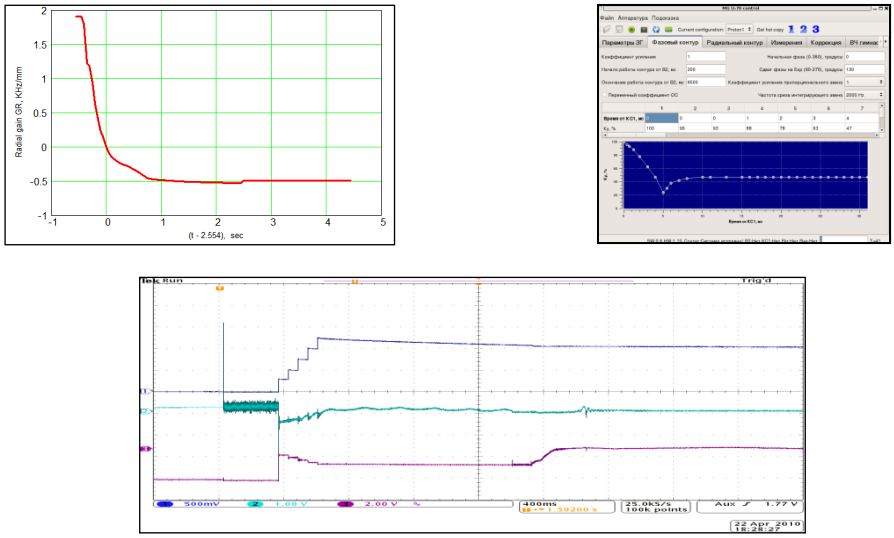

Figure 15: Variable gains in feedback loops. Top left – calculated optimal gain in radial loop for a fixed gain 0.15 kHz/deg in phase-frequency loop, right– its view in a control screen of the DDS MO, sign reversal at transition is implied. Bottom – traces of beam intensity, radial position, and beam phase about RF voltage.

4.5.3.8 *Light-Ion Program*

This program proceeds at a steady pace. By the last run 2010-1, deuterons were accelerated to 23.6 GeV per nucleon (kinetic) through a chain of the I`100, U1.5, and U70 proper. Chronology of the progress is reported in [4].

4.5.3.9 *Crystal Deflectors*

These types of beam transverse deflectors are extensively employed for routine technological purposes and in a dedicated R&D program accomplished with beams of the U70. Ref. [5] reports on details of this activity.

4.5.4 **AC-IHB**

4.5.4.1 *Generalities*

This acronym stands for Accelerator Complex of Intense Hadron Beams. It is a multi-purpose mega-project discussed at IHEP now [6]; refer to Fig. 16. The proposal offers a long-range plan to develop accelerator and experimental facilities on the IHEP grounds for fixed-target research, within and beyond elementary particle physics.

The base-line design foresees construction of a pulsed facility having more than 1 MW of proton beam average power, a pulse rate of 25 Hz, pulse width ≤ 1.5 μs, clear staging, site-specific integration and upgrade plans, and a reduced technical risk (use of proven technologies).

The facility comprises a non-SC 400 MeV linear accelerator LU400 followed by a 3.5 GeV rapid cycled proton synchrotron (RC PS) U3.5.

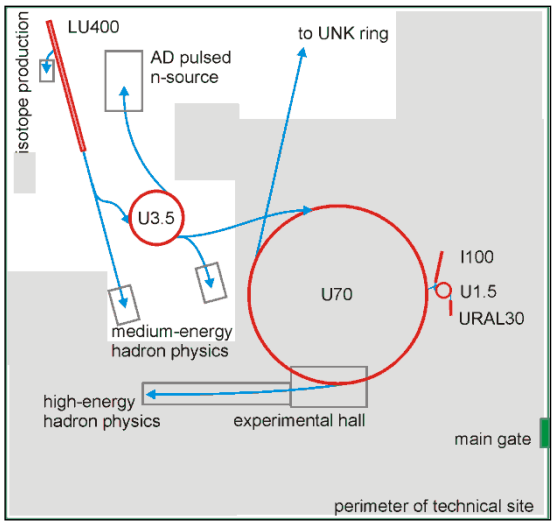

Area of a dense civil engineering and utility infrastructure existing is shadowed. Blue arrows show directions of beam transfer.

Figure 16: Layout of the AC-IHB facility.

4.5.4.2 *Staging*

A particular stage of the project addresses either applied or fundamental science (see Fig. 16).

Stage-1 assumes construction of a short-pulse accelerator-driven 1 MW neutron source for applied research (material and life sciences).

Goal of the next stage-2 is to develop the second direction of fast extraction from the U3.5 to feed a new experimental zone dedicated to intense-beam medium-energy hadron physics.

At a later stage, the U3.5 is engaged as a new injector to the existing U70 PS, or its updated successor. To this end, orbit length and RF harmonic number of the U3.5 amount to 3/10 of those in the U70. It facilitates, at most, a 3-train bunch-to-bucket transfer from U3.5 to the U70 ring thus yielding a beam pattern 3 × (9 filled + 1 empty) bunches there. Apart from the lower-energy mode of a 3.5 GeV proton beam stretcher delivering slow spills, the U70 will accelerate intense beam to higher energies.

This staging does not intervene drastically into the present operation of the URAL30(I100)/U1.5/U70 chain. Even more, at stage-0, the existing machines will be beam test benches and pilot consumers of the key project-related technologies (like source of H–, ions, RFQ linac, stripping-foil insertion, ferrite-loaded RF cavities, etc).

4.5.4.3 *RC PS U3.5*

Core of the AC-IHB project constitutes a new 3.5 GeV rapid cycled proton synchrotron U3.5 ramped at 25 Hz (sinusoidal) and yielding $7.5 \cdot 10^{13}$ ppp. Other specifications of the machine are listed in Table 2.

A multi-turn (145 turns around) charge-exchange injection into the RC PS U3.5 is performed at 400 MeV from a new linear accelerator LU400 (H–, 40 mA).

Lattice of the U3.5 is based on a synthesis of a plain FODO stricture, “missing dipole” and “quadruple-bent achromat” (QBA) concepts with 6 dispersion-free straights half-the-ring long totally, Fig. 17.

Table 2: Specifications of U3.5 (project)

Energy (kinetic), E	0.4–3.5	GeV
Orbit length, L	445.11	m
Curvature radius, ρ	15.28	m
Magnetic rigidity, $B\rho$	3.18–14.47	T·m
Compaction factor, α	0.0173	
Transition gamma, γ_t	7.60	
Intensity, N	$7.5 \cdot 10^{13}$	ppp
Ramping time, t_R	0.020	s
Cycle period, T	0.040	s
Average beam current	300	μA
Beam power, P	>1	MW
RF harmonic, h	9	
Radio frequency, f_{RF}	4.322–5.925	MHz
Net RF voltage, V_{RF}	720	kV/turn
Lattice period	FODO(90°)	
No. of periods	36	
No. of super periods	6	
Betatron tune (H/V)	9.15/7.20	

The lattice has 24 dipole magnets (length 4 m, field 0.95 T, and gap 150 mm). There are 72 identical quadrupole lenses (length 0.6 m, gradient < 5.6 T/m, and bore radius 102.8 mm). The quads are arranged into three families (36 QF, 30 QD, and 6 QD1 at arc mid-points).

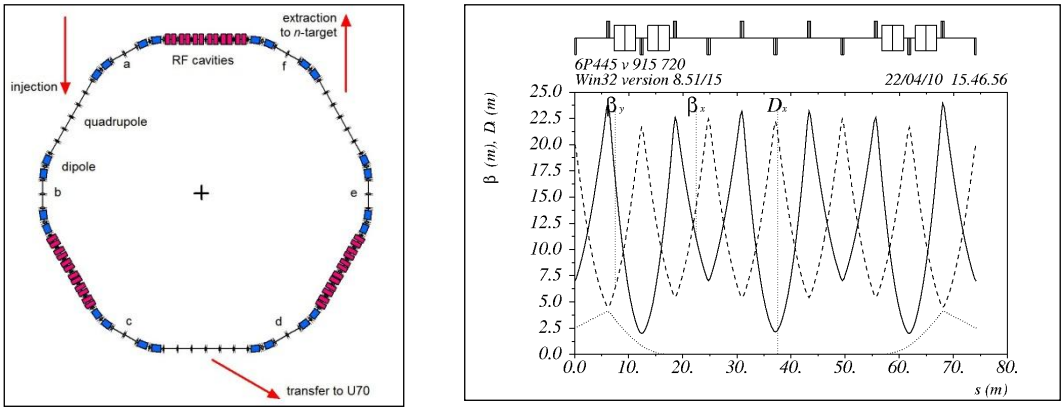

Figure 17: Backbone equipment and optical functions of the U3.5 RC PS ring.

Aperture margin is set at a conservative ±4σ level. The betatron acceptance is about 660/160 π·mm·mrad (horizontal/vertical). Momentum acceptance is ±3.1% (pencil beam), or ±1.6% (full beam).

Coulomb tune shift at injection is –0.08/–0.15 (horizontal/vertical).

Protons are accelerated by 36 two-gap ferrite-loaded cavities yielding 20 kV peak voltage each. An RF station occupies < 2.5 m of a dispersion-free straight flange-to-flange. Stable phase angle is ≥ 55–56° (cosine convention). Estimated power consumption is around 130 kW per a cavity. Beam loading factor (ratio of beam fundamental RF harmonic to peak current through shunting resistance) is 3.8 ca, which is manageable.

Outline for other subsystems is being elaborated, [6].

4.5.5 Conclusion

Accelerator complex U70 of IHEP-Protvino is the sole national proton facility running for the fixed-target research in high-energy physics. It is a subject of an ongoing upgrade program affecting the key technological systems and promising still better beam quality. To maintain and develop expertise available at IHEP in hadron beam accelerators and experimental physics, a new AC-IHB project is put forward and is under development.

4.5.6 References

1. S. Ivanov and the U70 staff, Proc. of RUPAC-2008, Zvenigorod, 2008, p. 130–133.
2. O. Lebedev et al, these Proceedings.
3. S. Ivanov, Preprint IHEP 97–64, Protvino, 1997.
4. S. Ivanov et al, these Proceedings.
5. A. Afonin et al, these Proceedings.
6. Accelerator Complex of Intense Hadron Beams, IHEP Internal Rep., September 2010.

4.6 Maintenance of ITEP-TWAC Facility Operation and Machine Capabilities Development

N.N.Alexeev, P.N.Alekseev,V.A.Andreev, A.N.Balabaev, V.I.Nikolaev,
A.S.Rjabtsev, Yu.A.Satov, V.S.Stolbunov, V.A.Schegolev, B.Yu.Sharkov,
A.V.Shumshurov, V.P. Zavodov
ITEP, Moscow, Russia
Mail to: nalex@itep.ru

4.6.1 Introduction

The ITEP-TWAC Facility consisting of main synchrotron-accumulator U-10 with 25 MeV proton injector I-2 and linked to U-10 ring booster synchrotron UK with 4 MV ion injector I-3 runs now in several operation modes accelerating protons in the energy range of 0.1-9.3 GeV, accelerating ions in the energy range of 0.1-4 GeV/u and accumulating nuclei at the energy of 200-300 MeV/u. Accelerated beams are used in several modes: secondary beams generated in internal targets of U-10 ring are transferred for experiments to Big experimental hall (BEH); beams extracted from U-10 ring in one turn are transferred to Target hall (TH); and proton beam bunch extracted from U-10 ring is transferred to Biological research hall (BRH). Some of secondary beam transfer lines are used now for transferring of slow extracted beams from U-10 ring.

4.6.2 Machine Operation

Next year will be 50-th anniversary of ITEP Ring Accelerator was started for operation that continues up today in parallels with machine modernization. Statistic of

ITEP-TWAC operation time is shown on Fig.1. The total machine run time of near 4000 hours per year is divided between three operation modes: acceleration of protons (~50%), acceleration of ions to relativistic energy (~10%) and nuclei stacking (~40%). Statistic of beam using for different research fields shows the tendancy of machine operation time increase for applications as proton and ion beams using in biology, medicine and radiation treatment of electronics for cosmic apparatus. The required beam time for users exceeds the possible one by factor of two. This discrepancy has to be cardinally reduced in a result of machine infrastructure development and extension of its experimental area.

New modes of Fe-nuclei acceleration up to the energy of 3.6 GeV/u and of Ag^{19+}-ions acceleration up to the energy of 100 MeV/u realized in 2008-2009 are illustrated by oscillograms in Fig.2 and Fig.3. In the mode of Ag^{19+}-ions acceleration from very low level of injection energy as 0.7 MeV/u at vacuum in the beampipe as $1x10^{-9}$ Torr, particle losses at acceleration exceeds 90%.

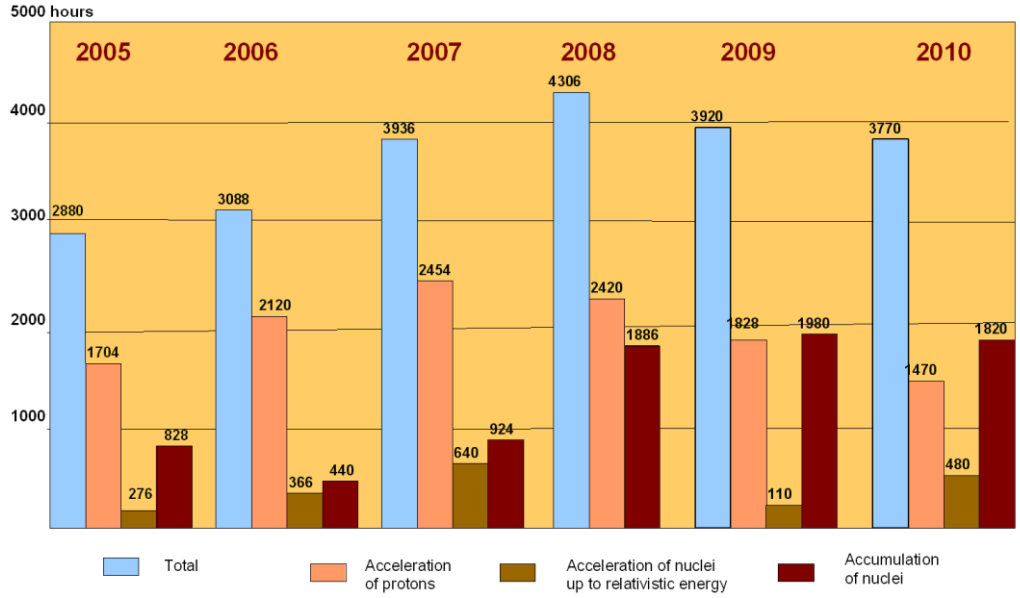

Figure 1: Statistic of ITEP-TWAC operation time.

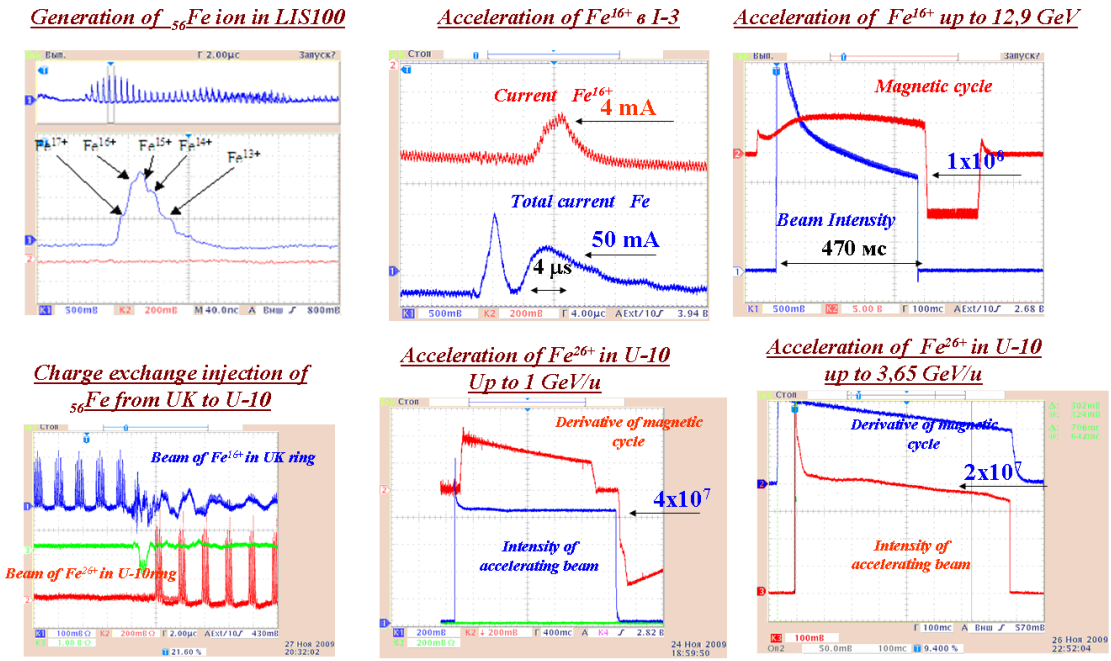

Figure 2: Acceleration of Fe-nuclei up to relativistic energy.

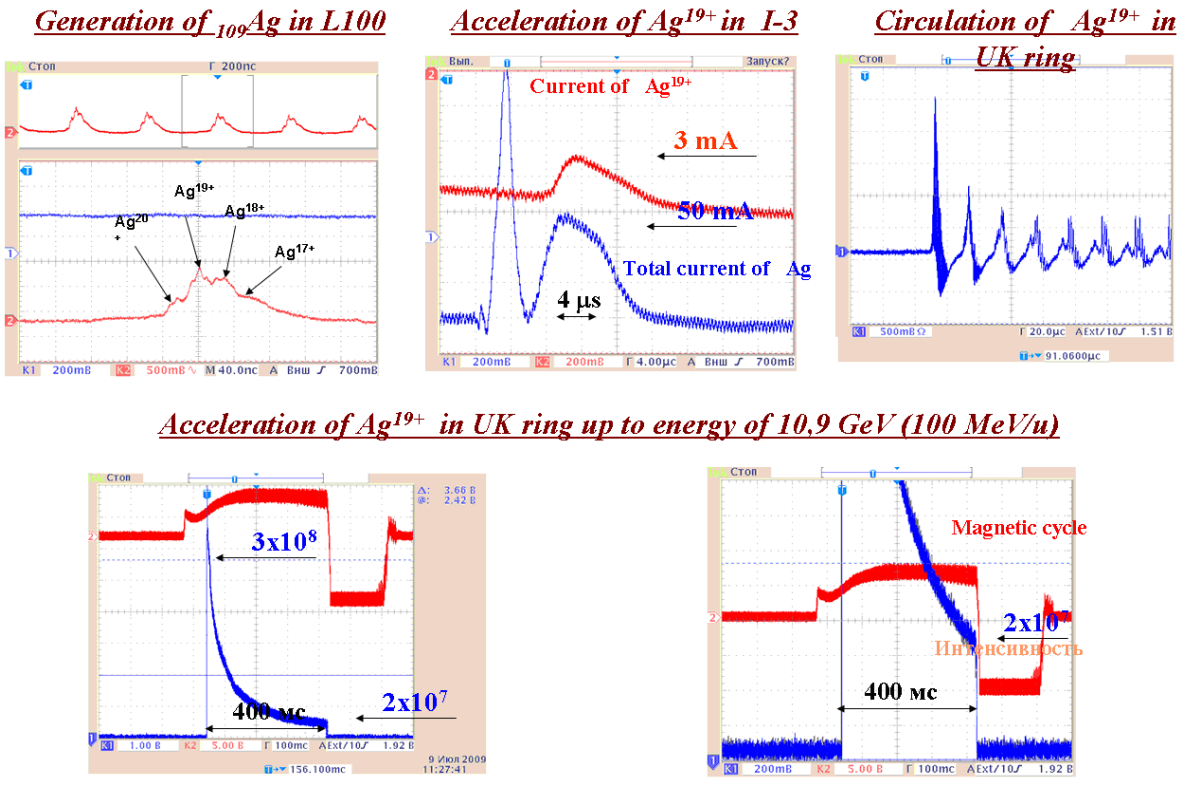

Figure 3: Acceleration of Ag19+ ions in UK Ring.

4.6.3 **Experience with LIS Operation**

First compact configuration of LIS with 5J CO_2 laser L5 [1] has been in operation at injector I-3 until 2006 when it was reconstructed under using in the frame of a new universal optical scheme the 100J CO_2 laser L100 which was assembled and prepared for operation [2]. Old LIS was used for generation of C-ions only (Fig.4) and maximal charge state specie C^{5+} had been observed in this beam which shows that ionization potential (IP) in the laser plasma exceeds 374 V.

The new LIS with laser L100 is in operation from 2008 and it's used with target materials of Al, Fe and Ag. Generation of Fe-ions (Fig.5) shows maximal charge state specie Fe^{16+} with IP= 506 V. The higher level of charge state specie Fe^{17+} with IP=1168 V has been also observed in some measurements but in very few quantity. Generation of Ag-ions (Fig.6) shows maximal charge state specie Ag^{20+} with IP= 816 V and very few specie Ag^{21+} with IP= 960 V has been also observed in some measurements. Summarizing results of ion generation in old and new configurations of LIS at injector I-3 is shown on Fig.7 with another data obtained from different publications. [3-6]

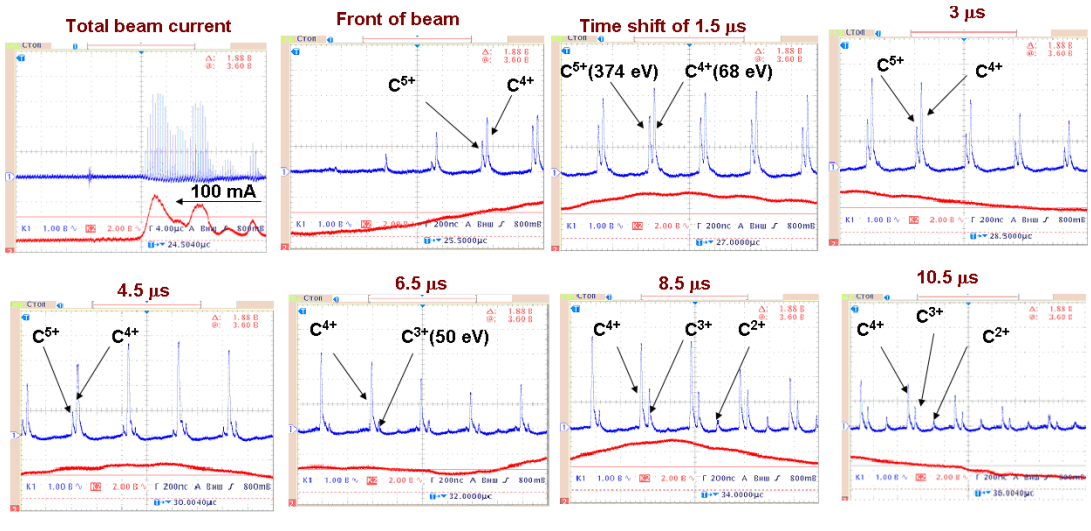

Beam parameters

	C^{5+}	C^{4+}
Pulse width, μs	3.5	10
Number of particles	$3x10^{10}$	$5x10^{11}$

Figure 4: C-ions generation in old LIS with L5 (2006).

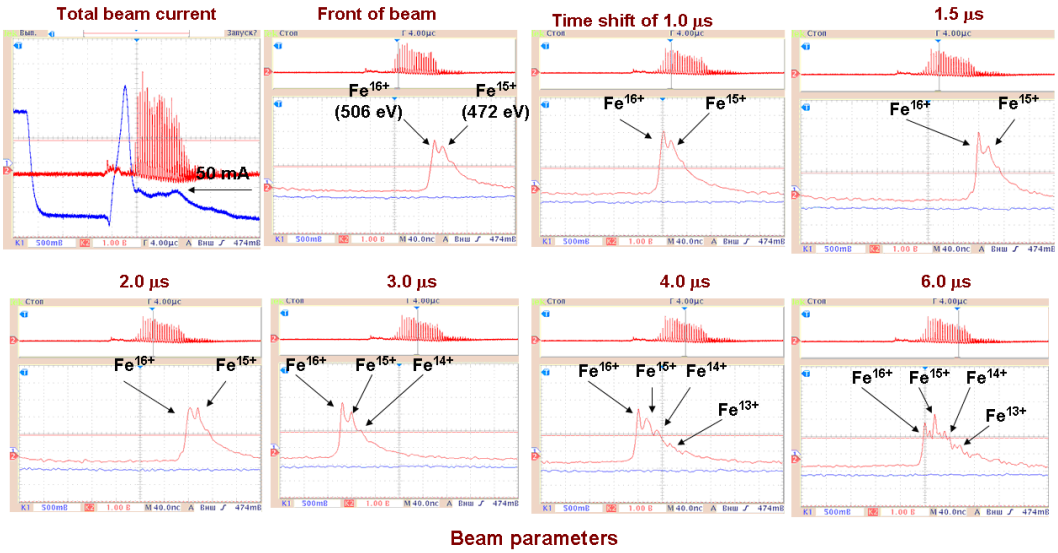

Beam parameters

	Fe^{16+}	Fe^{15+}
Pulse width, μs	4.5	5
Number of particles	$1x10^{10}$	$8x10^{9}$

Figure 5: Fe-ions generation in new LIS with laser L100.

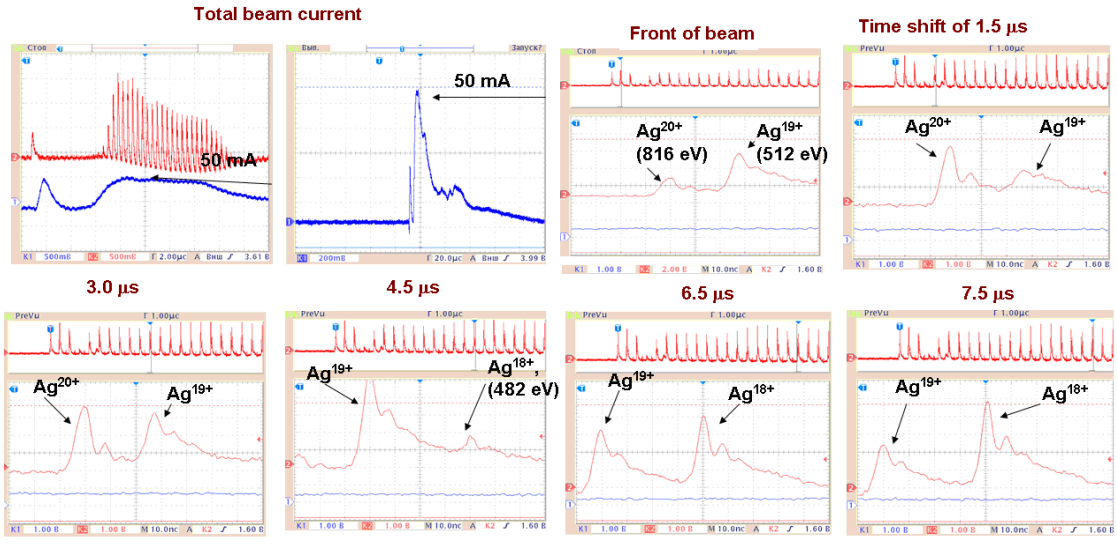

Ag beam parameters

	Ag^{20+}	Ag^{19+}
Pulse width, ms	2.5	6
Number of particles	$2x10^{9}$	$1x10^{10}$

Figure 6: Ag-ions generation in new LIS with laser L100.

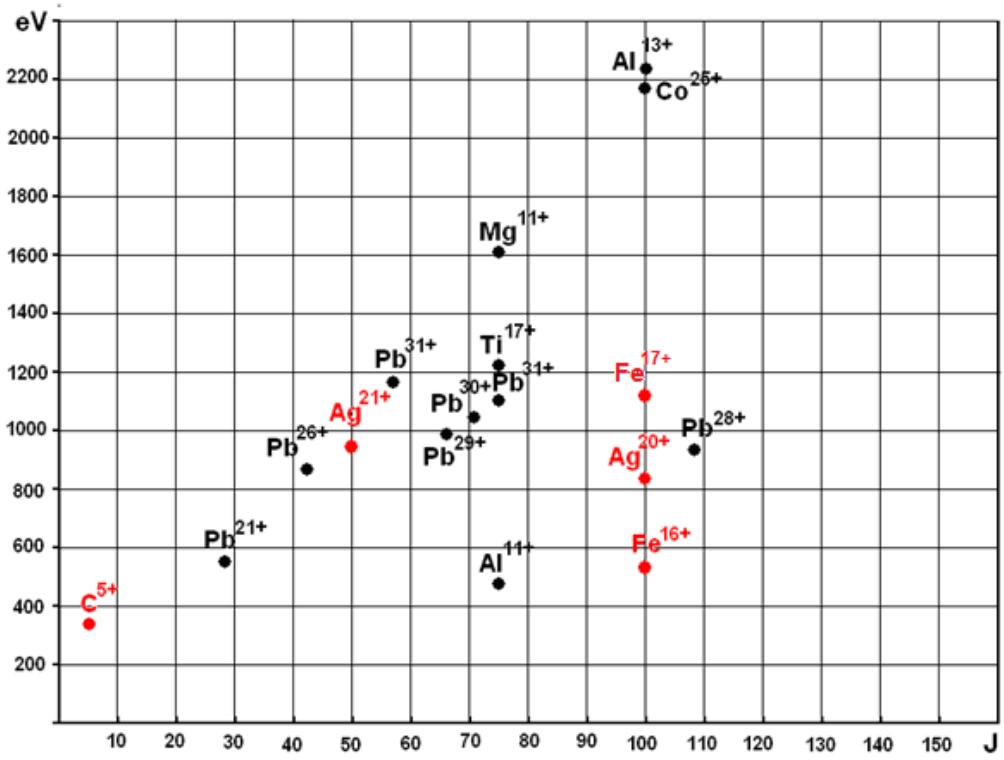

Figure 7: Ionization potentials reached in LIS stand tests from different publications (black points) and in LIS at injector I-3 (red points) from laser used radiation energy.

4.6.4 **Development of Heavy Nuclei Stacking Technique**

The charge exchange injection technique is used now with stacking factor of 70 for C-nuclei stacking at the beam energy of 300 MeV/u [7]. The efficiency of Fe-nuclei stacking at the energy of 230 MeV/u is limited on the level of stacking factor 10 due to disturbing effects of beam interaction with stripping foil. Efficiency of beam stacking for nuclei of mass number A~60 will be increased many times with increasing of injected beam energy up to 600-700 MeV/u. For nuclei with A < 30, disturbing effects of beam interaction with stripping foil are small enough and efficiency of beam stacking is a function of injection scheme parameters and of storage ring dynamic aperture. We are planning to start experiments on the beam stacking process optimization at the end of this year with stacking of $Si12^{+}$=>Si^{14+} ions at the energy of > 500 MeV/u. Expected results of stacking process improvement are shown on Fig.8/

Parameters of beam stacking with laser L5 (L100 for Si) and 4MV injector I-3

Parameters	Reached for C^{4+}=>C^{6+}	Expected for C^{4+} =>C^{6+}	Expected for Si^{12+} =>Si^{14+}
Energy	300 MeV/u	400 MeV/u	650 MeV/u
Injected beam intensity	$6x10^8$	~$5x10^9$	~$5x10^9$
Cycle time , s	3	2	2
Acceptance, A_{x}, π mm mrad	10	30-50	30-50
Vacuum, Torr	~$1x10^8$	~$1x10^9$	~$1x10^9$
Stacking factor	~70	~200	~200
Stacked beam intensity	$4x10^{10}$	~10^{12}	~10^{12}

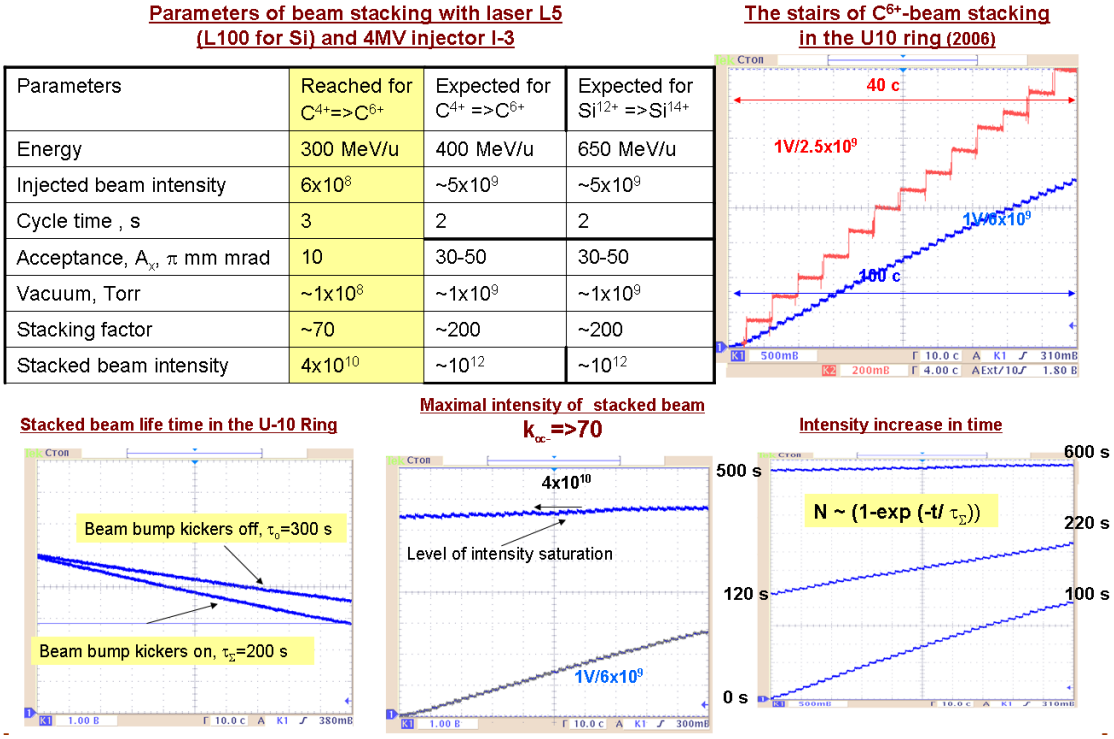

Figure 8: Optimization of beam stacking at A<30.

4.6.5 **Development of ITEP-TWAC Infrastructure**

Elaborated strategy of ITEP-TWAC infrastructure development is aimed to redouble beam time for physical experiments and applications extending of functionality of UK synchrotron for protons acceleration too and for generation of slow extracted beams to the area of beam using for applications. Layout of expanded Injection Complex with additional beam lines from injectors both I-2 and I-4 to UK Ring is shown on Fig. 9.

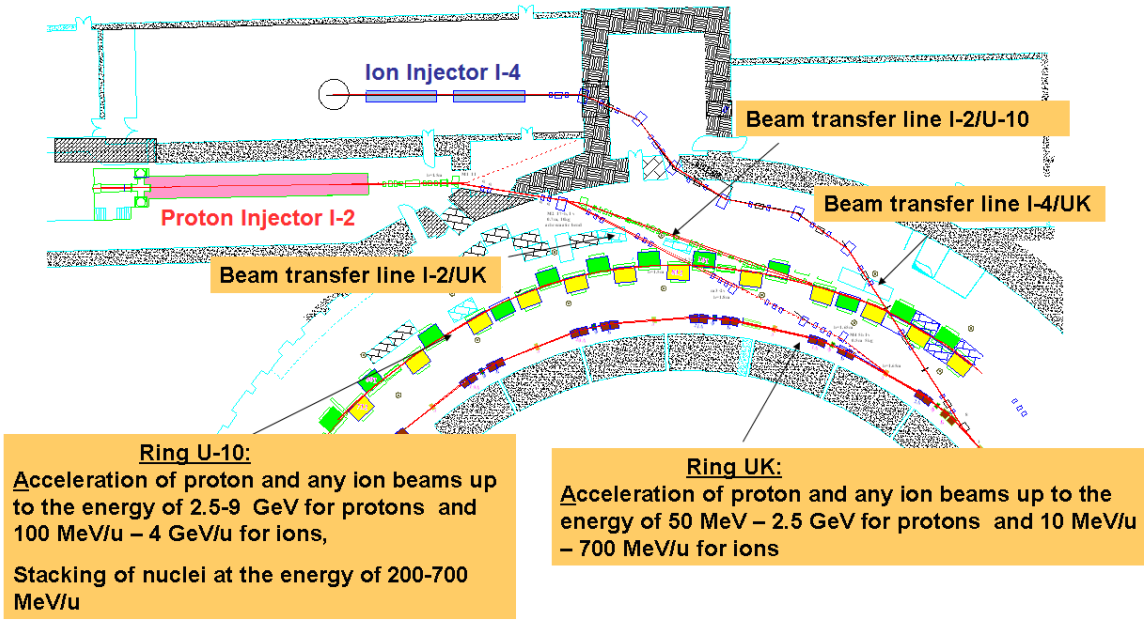

Figure 9: Expanding of ITEP-TWAC Injection Complex.

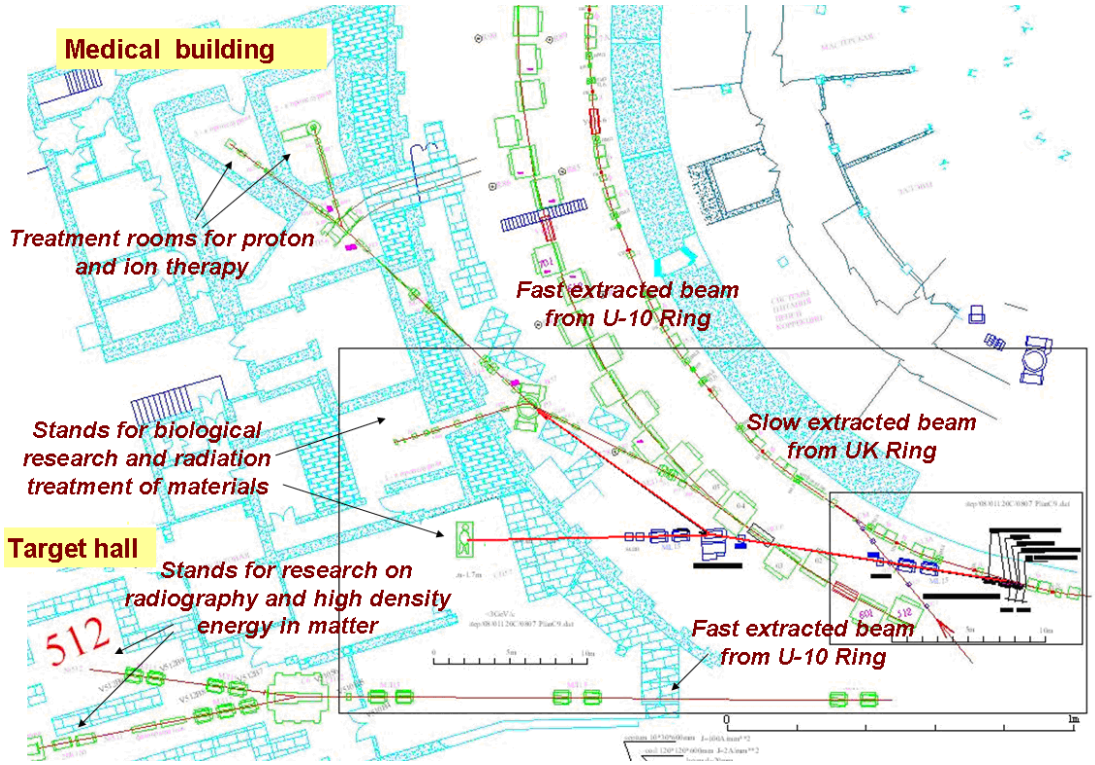

Figure 10: Expanding of beam area for applications.

Layout of beam using area for applications is shown on Fig.10. New projected beam line for slow extracted beam from UK Ring is directed to free space of Target hall (where stand will be installed for biological research) and linked with beam line from U10 Ring used now for proton therapy.

We consider also possibility of construction the second slow extraction system for U-10 Ring to BEH [8] for the beam of maximal beam momentum of 10Z GeV/c. Area of this beam using in the corner of BEH has to be rounded by radiation shielding.

4.6.6 **Conclusion**

The ITEP Accelerator Facility is in operation by ~4000 hours yearly accelerating proton and ion beams and stacking nuclei for physics experiments, methodical research and radiation technologies.

The progress has been achieved in acceleration of heavy ion: specie of Ag^{19+} have been generated in LIS and accelerated in synchrotron UK up to the energy 100 MeV/u with intensity of 2×10^7; nuclei of Fe^{26+} have been accelerated using three stage scheme I-3/UK/U-10 up to record energy of 3.6 GeV/u or 200 GeV per particle with intensity of 5×10^7.

Experiments on the ion beam generation in LIS with 100J CO_2 laser L100 give evidence of optic used imperfection reducing the laser radiation power density on the target surface by factor of more than ten. New focusing scheme for target station is elaborated on a base of parabolic short focusing mirror to increase the power density by factor of three. Next factor of power density increase will be achieved replacing windows by them of better quality.

Construction of the new heavy ion injector I-4 is in progress: the RFQ section for the energy of 1.5 MeV/u of Z/A=0.3 ions is constructed and successfully tested for resonator parameters measuring and RF power loading [9]. Preparations of RFQ section for the beam test is now started to be carried out in the first quarter of next year.

The progress in intensity of heavy ion beam stacked in U-10 Ring using multiple charge exchange injection technique is expected in the experiments planned for the end of this year with ions Si^{12+}=> Si^{14+} stacking at the energy of 500 MeV/u.

Development of ITEP-TWAC facility Infrastructure is aimed to redouble beam time for physical experiments and applications making operation of both U-10 and UK synchrotrons in parallels.

4.6.7 **References**

1. N.N. Alexeev, S.L. Bereznitsky, V.I.Nikolaev.,"Bean dynamics in matching channel of ITEP-TWAC heavy ion injector I-3", proceedings of the 2000 European Particle Accelerator Conference, Austria, Vein, (2000), 1283-1285.
3. B.Ju.Sharkov, N.N.Alexeev, P.N.Alekseev, A.N.Balabaev,. V.I.Nikolaev, V.A.Schegolev, A.V.Shumshurov, V.P. Zavodov, Yu.A.Satov, " Experiments with Fe-ion beam generation acceleration and accumulation in ITEP-TWAC facility ", proceedings of the 2008 European Particle Accelerator Conference, Genoa, Italy, (2008) 352-354.
4. S. Kondrashev, A. Balabaev, K. Konukov, B.Y. Sharkov, A. Shumshurov, " New Developments of a Laser Ion Source for Ion Synchrotrons" proceedings of the 2004 European Particle Accelerator Conference, Lucerne, Switzerland, (2004) 1402-1404.
5. S.Kondrashev, N.Mescheryakov, B.Sharkov, A.V.Shumshurov, S.V.Homenko, K.N.Makarov, Yu.A.Satov, Yu.B. Smakovskii "Production of He-like light and medium mass ions in laser ion source", Rev.Sci. Ins., 71, 3, 1409–1412, (2000)
6. V.V.Appolonov, Ju.A.Byckovsky, N.N.Degtjarenko, V.F.Elesin, Ju.P.Kozyrev, S.M.Sil'nov, "Multi charge state ions generation at power laser radiation pulse

interaction with solid.". Pisma JETF, v.11 (1970), p.377
7. N.N.Alexeev, D.G.Koshkarev, B.Ju.Sharkov,"ITEP-TWAC Status Report" proceedings of the 2006 European Particle Accelerator Conference, Edinburg, UK, (2004), 243-245.
8. N.N.Alexeev, P.N.Alekseev, A.N.Balabaev,. V.I.Nikolaev, V.A.Schegolev, B.Ju.Sharkov, A.V.Shumshurov, V.P. Zavodov, Yu.A.Satov, "ITEP-TWAC Status Report" proceedings of the 2008 Rusia Particle Accelerator Conference -2008, Zvenigorod, Russia, (2008), 134-136
9. V. Andreev, N.N. Alexeev, A.Kolomiets, V. Koshelev, V. Kuzmichev, S. Minaev, B.Sharkov, " Progress Work on High-current Heavy Ion Linac for ITEP TWAC Facility " proceedings of the 2010 International Particle Accelerator Conference, Japan, (2010) 801-803

4.7 Status of the Nuclotron

A. Sidorin, N. Agapov, V. Alexandrov, O. Brovko, V.Batin, A. Butenko,
E.D. Donets, A. Eliseev, A.Govorov, V. Karpinsky, V. Kekelidze,
H. Khodzhibagiyan, A.Kirichenko, A. Kovalenko, O. Kozlov, I. Meshkov,
V. Mikhaylov, V. Monchinsky, S.Romanov, V. Shevtsov, V. Slepnev, I. Slepnev,
A. Sissakian, G. Trubnikov, B.Vasilishin, V. Volkov
JINR, Dubna, Moscow Region, Russia
Mail to: sidorin@jinr.ru

4.7.1 **Introduction**

The project “Nuclotron-M” is considered as a key part of the first stage of the JINR general project NICA/MPD (**N**uclotron-based **I**on **C**ollider f**A**cility and **M**ulty **P**urpose **D**etector) [1]. The extension of JINR basic facility capabilities for generation of intense heavy ion and high intensity light polarized nuclear beams, including design and construction of heavy ion collider aimed at reaching the collision energy of $\sqrt{s_{NN}}$ = 4÷11 GeV and averaged luminosity of $1 \cdot 10^{27}$ $cm^{-2}s^{-1}$ is necessary for realization of the NICA/MPD.

The first stage of the NICA/MPD realization includes the following tasks:

- Upgrade the Nuclotron facility (the “Nuclotron-M” project);
- Elaboration of the NICA technical design report;
- Development of the laboratory infrastructure aimed for long term stable operation of the accelerator complex and preparation for construction of the NICA elements;
- R&D works for MPD elements.

The “Nuclotron-M” program includes all necessary works on the development of the existing Nuclotron accelerator complex [2] to the facility for generation of relativistic ion beams over atomic mass range from protons to gold and uranium ions at the energies corresponding to the maximum design magnetic field (2 T) in the lattice dipole magnets. Realization of the project will make it possible to reach new level of the beam parameters and to improve substantially reliability and efficiency of the accelerator operation, renovate or replace some part of the equipment that have been under operation since 1992-93 as well.

As an element of the NICA collider injection chain the Nuclotron has to accelerate single bunch of fully stripped heavy ions (U^{92+}, Pb^{82+} or Au^{79+}) from 0.6 to about 4.5 GeV/u. The required bunch intensity is about $1 \div 1.5 \cdot 10^9$ ions. The particle losses during acceleration have to be minimized and do not exceed 10%. The magnetic field ramp has to be ≥ 1 T/s. To demonstrate the ability of the Nuclotron complex to satisfy these requirements, the general milestones of the project are specified as an acceleration of heavy ions (at atomic number larger than 100) and stable and safety operation at 2 T of the dipole magnet field. The project has been started in 2007. During the project realization almost all the Nuclotron systems were modernized and 5 runs of the Nuclotron operation were carried out. During the last run performed from 25 of February to 25 of March 2010 the Xe ions were accelerated and the magnetic system was operated at 1.8 T. Completion of the project is scheduled for the fall of 2010.

4.7.2 **Status and Main Parameters of the Nuclotron**

The first run at the Nuclotron (the superconducting synchrotron intended to accelerate nuclei and multi charged heavy ions) was performed in March 1993. Presently the Nuclotron delivers ion beams for experiments on internal targets and for fixed target experiments using slow extraction system. Achieved energy of protons is 5.7 GeV, deuterons – 3.8 GeV/u and nucleons - 2.2 GeV/u. The maximum achieved energy is limited by the system of the energy evacuation of the Nuclotron SC magnets and power supply of the lattice magnets.

Main elements and systems of the Nuclotron facility (Fig. 1) are the following:

1. Superconducting synchrotron Nuclotron, which magnetic-cryostat system of the circumference of 251,5 m is located in the tunnel surrounding the Synchrophasotron basement;
2. Cryogenic supply system consisting of two helium refrigerators KGU-1600/4.5 with required infrastructure for storage and circulation of the gaseous helium, liquid helium transfer lines, tanks for the liquid nitrogen storage and nitrogen tranfer lines for thermal screens of the Nuclotron lattice magnets;
3. The injection complex consisting of HV fore-injector and Alvarez-type linac LU-20. The fore-injector voltage up to 700 kV is produced by pulsed transformer. The LU-20 accelerates the protons up to the energy of 20 MeV and ions at Z/A ≥ 0.33 up to the energy of 5 MeV/u. The wide range of the ion species is provided by the heavy ion source “KRION-2”, duoplasmatron ion source, polarized deuteron source POLARIS and laser ion source.
4. Beam transport line from LU-20 to the Nuclotron ring including equipment for the beam injection onto the orbit;
5. System of the resonant slow extraction of the accelerated beam in the direction to main experimental hall (bld. 205);
6. Transport lines for the extracted beam;
7. Power supply units for the Nuclotron lattice magnets and the transport lines to the experimental facilities located in the separated building 1A (it does not shown in the Fig. 1);
8. Control system, diagnostics of the beam and the accelerator complex parameters;

9. RF system for the beam acceleration in the Nuclotron;
10. Radiation shielding and automatic system for the radiation measurements.

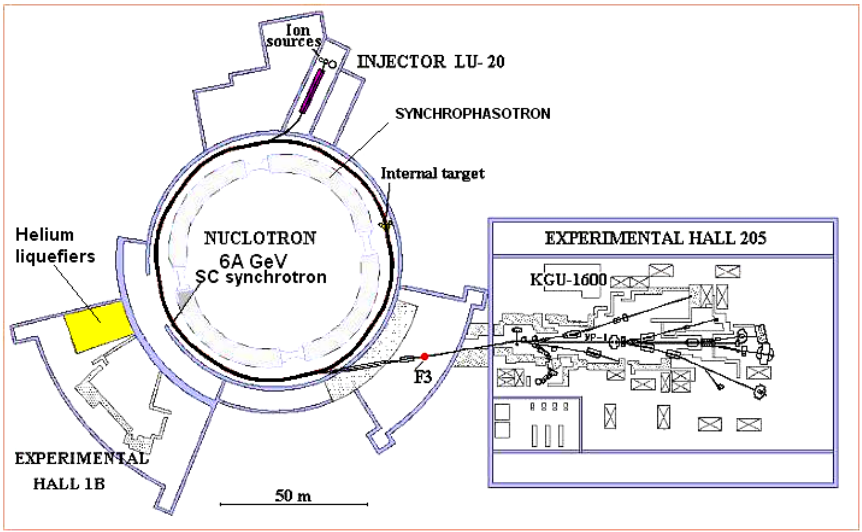

Figure 1. Schematics of the Nuclotron facility.

4.7.3 **Nuclotron-M Project**

General goal of the project is to prepare all the existing systems of the Nuclotron for its long and reliable operation as a part of the NICA facility. Additionally the project realization will increase the Nuclotron ability for realization of its current experimental program. The project working program includes the next main tasks:

1. Development of the heavy ion source.
2. Development of the polarized deuteron source.
3. Sufficient improvement of the vacuum conditions in the Nuclotron beam pipe and linear accelerator-injector.
4. Development of the power supply system and energy evacuation system in order to reach magnetic field in dipole magnets of 1.8 - 2 T.
5. Upgrade of the Nuclotron RF system, realization of the adiabatic trapping into acceleration.
6. Development of the slow extraction system.
7. Development of the beam transfer lines and radiation shielding.
8. Beam dynamics investigations, minimizations of the particle loss at all stages of the acceleration.
9. Preparation of the KRION-2 ion source for generation of the ion beam at A > 100 and q/A > 0.33.
10. Design of new heavy ion linear injector.

Sufficient part of the first run performed after beginning of the project - #37 (November of 2007) - was devoted to the test of the status of the Nuclotron systems and machine development experiments. During this run experimental estimate of average vacuum in the Nuclotron was made based on the studies of $^{2}H^{+}$ and deuteron beam circulation at the injection energy (5 MeV/u). It was shown, the beam pipe pressure

scaled to equivalent concentration of N_2 molecules at T = 300 K is measured to about p $\approx 2 \cdot 10^{-8}$ Torr, that is not sufficient for heavy ion acceleration. To start modernization of the system for orbit position measurements and the orbit correction the existing PU stations and correctors were tested and calibrated. Preliminary test of new scheme of the structural magnet supply based on the consequent magnet connection was performed. It was demonstrated that the large inductivity sufficiently suppresses the magnetic field ripple. It leads to stable acceleration process and improve the quality of slow extracted beam.

4.7.4 **Results of Last Runs**

During the "Nuclotron-M" project realization four runs of the Nuclotron operation were carried out - #38 (June of 2008), #39 (June of 2009), #40 (November 2009) and #41 (March 2010). Sufficient part of them was devoted to the test of new equipment installed at the Nuclotron accelerator complex. Within this period two stages of the ring vacuum system upgrade were completed. Deep reconstruction of the cryogenic system was performed. New supply system for electrostatic septum of the slow extraction system was constructed and tested at a test bench and at the ring. New power supplies for the closed orbit corrector magnets were designed and first 4 units were tested at the ring. Partial upgrade of the ring RF system aiming to increase RF voltage and realize the adiabatic trapping into acceleration was performed. A set of works at LU-20 accelerator was performed to improve the vacuum conditions and to increase the acceleration efficiency.

In parallel with the Nuclotron modernization a good progress was achieved in design and construction of the new heavy ion and polarized light ion sources.

4.7.4.1 ***Upgrade of the Nuclotron Ring Vacuum System***

The Nuclotron vacuum system consists of two sub-systems: insulation vacuum system of the cryostat and high vacuum system for the beam pipe. Insulation vacuum system satisfied to all the requirements of the accelerator operation and its serious upgrade is not necessary. Before beginning of the "Nuclotron-M" project the Nuclotron beam pipe had no effective pumping of gaseous hydrogen and helium, while gaseous helium can to penetrate into the pipe due to diffusion from insulation vacuum volume of the cryostat through non welded connection between beam extraction channel and circulating beam chamber.

Upgrade of the vacuum system was performed in two stages:

- Reconstruction of a few sections of the ring and installation of new vacuum pumps and diagnostic equipment;
- Creation of automatic control system for the vacuum equipment.

The first stage was realized in a general between the runs #37 and #38. Installed vacuum equipment was tested and put into operation during the run #38 and its application was resulted in improvement of the vacuum conditions by about one order of magnitude.

The automatic control system was put into operation during the runs #40 and #41 that permitted to provide experimental study of evolution of the residual gas pressure and composition during long period of the ring operation. At the moment the vacuum

conditions in the beam pipe satisfies to requirements of the NICA project that was additionnaly demonstrated during the #41 run in acceleration of Xe ions.

4.7.4.2 *Upgrade of the Cryogenic System*

Starting from August of 2008 the Nuclotron cryogenic system was deeply reconstructed. Almost all the equipment was dismounted, transferred to specialized factories, repaired and transferred back into JINR. From the February of 2009 the equipment was tested and step by step put into operation.

4.7.4.3 *Heavy Ion Acceleration*

During the run #41 the ions of 124Xe42+ were accelerated up to about 1.5 GeV/u. At 1 GeV/u the slow extraction of the accelerated beam was used for a few methodical and physics experiments. To reach this goal the following works were performed during 2009 and first month of 2010:

- Four stand runs (five weeks each) at multi charged heavy ion source Krion-2 have been done in order to optimize operational parameters;
- Modernization of power supply system of the beam transfer line from LU-20 to the Nuclotron;
- Readjustment of the LU-20 accelerating-focusing system in order to improve the acceleration efficiency;
- Three runs at LU-20 dedicated to test all the systems at acceleration of deuteron, C^{+4} and heavy ion beams.

During LU-20 run performed in January – February of 2010 the following ions were obtained with Krion-2 source in the pulse of 6.7 μs of duration:

- a) 84Kr28+ $3.5 \cdot 10^7$ ions per pulse,
- b) 84Kr29+ $3.2 \cdot 10^7$ ions per pulse,
- c) 84Kr30+ $3.0 \cdot 10^7$ ions per pulse,
- d) 124Xe41+ $3.0 \cdot 10^7$ ions per pulse,
- e) 124Xe42+ $3.0 \cdot 10^7$ ions per pulse,
- f) 124Xe43+ $2.7 \cdot 10^7$ ions per pulse,
- g) 124Xe44+ $1.5 \cdot 10^7$ ions per pulse.
-

The beams of $_{84}Kr^{29+}$ and $_{124}Xe^{42+}$ ions were accelerated with LU-20 up to 5 MeV/u.

The Nuclotron run #41 was started with laser ion source. All the ring systems were tested and tuned with deuteron beam initially. Thereafter initial part of the beam acceleration was optimized for acceleration of ions at charge to mass ration closed to 1/3 with C^{+4} beam. The C^{+4} beam life-time due to stripping on residual gas is not long enough to accelerate them to energy of the range of 1 GeV/u. The slow extraction system was tuned with Xe ions after change of the ion source. The Xe beam intensity during the acceleration was measured with the ionization monitor and even relative change of the intensity is complicated to estimate due to variation of the ionization cross-section. Intensity of the accelerated beam was at the sensitivity threshold therefore accurate tuning of the slow extraction was not provided. Even at these conditions the beam intensity at the exit of the ring was about a few thousands ions per pulse. Most

likely the source of the ion loss during the acceleration was interaction with the residual gas. As a part of the NICA injection chain the Nuclotron will be operated for acceleration of fully striped gold ions from 600 MeV/u up to 4.5 GeV/u. During Xe ion acceleration it was demonstrated that the vacuum conditions in the Nuclotron beam pipe is sufficient for this goal.

4.7.5 **Further Development**

During # 41 run the magnetic system was operated at 1.8 T of the dipole magnetic field for a few hundred of cycles. It was demonstrated that after more than 15 years of the operation a degradation of the magnet properties is practically absent. The long and safe operation of the accelerator magnetic system at maximum design level of the magnetic field (2 T) is related to the following modifications of the power supply system:

- Manufacturing, assembling and put into operation seven units of the new switches for energy damp from the magnets in a case of quench for both the dipoles and the quadrupoles power supply circuits;
- Upgrade of the quench detection system;
- Development of scheme of the Nuclotron magnet power supply.

The works are in the final stage, and beginning of the commissioning of the new power supply and quench protection systems is scheduled for the Autumn Nuclotron run in 2010. After that the Nuclotron upgrade project will be completed. The next stage of the development is connected with construction of the NICA facility elements.

4.7.6 **References**

1. NICA Conceptual Design Report, JINR, January 2008. http://www.jinr.ru/
2. A.A.Smirnov, A.D.Kovalenko, “Nuclotron-superconducting accelerator of nuclei at LHE JINR (Creation, Operation, Development)” Particles and Nuclei, Letters, 2004, v.1, № 6 (123), p.11-40

4.8 Acceleration of Deuterons up to 23.6 GeV per Nucleon through I100, U1.5, and U70 of IHEP

S. Ivanov, on behalf of the U70 Light-Ion Task Team[#]
Institute for High Energy Physics (IHEP), Protvino, 142281, Russia
Mail to: Sergey.Ivanov@ihep.ru

[#] Team members: O. Lebedev, A. Ermolaev, G. Hitev, V. Lapygin, Yu. Milichenko, V. Bezkrovnyy, V. Stolpovsky, I. Sulygin, E. Nelipovich, A. Bulychev, Yu. Antipov, S. Pilipenko, N. Anferov, D. Khmaruk, S. Semin, V. Dan’shin, N. Ignashin, S. Sytov, and G. Kuznetsov.

Abstract:

The paper reports on the recent progress en route of implementing the program of accelerating light ions in the Accelerator Complex U70 of IHEP-Protvino. The crucial milestone of guiding the deuteron beam through entire cascade of three accelerators available to a specific kinetic energy of 23.6 GeV per nucleon was accomplished in April 2010, which confirms feasibility of the project goal to diversify our main proton machine U70 to a light-ion synchrotron as well.

4.8.1 **Introduction**

The program to accelerate light ions with a charge-to-mass ratio q/A = 0.4–0.5 in the Accelerator complex U70 of IHEP-Protvino aims at diversification and development of our accelerator facilities. The ion mode of operation involves a sequence of Alvarez DTL I100, rapid cycled synchrotron U1.5, and the main synchrotron U70 proper.

Refs. [1, 2] reported on the first attempts of operation with a deuteron beam of a yet truncated cascade comprising I100 and U1.5. Since then, consisted efforts were continued to adapt and upgrade technological systems of the proton machines to better accommodate the ion beam. This report chronologically overviews the progress achieved since the previous conference RuPAC-2008.

4.8.2 **Run 2008-2**

During this run, in the period of 10–12.12.08, acceleration of deuterons from 16.7 to 455 MeV per nucleon was accomplished for the second time in the U1.5 record of service (Fig. 1). Achieving this goal was hampered by improper vector adding at beam of RF voltages from 8 accelerating ferrite-loaded cavities whose start frequency is lowered from 0.747 (design value) to 0.563 MHz.

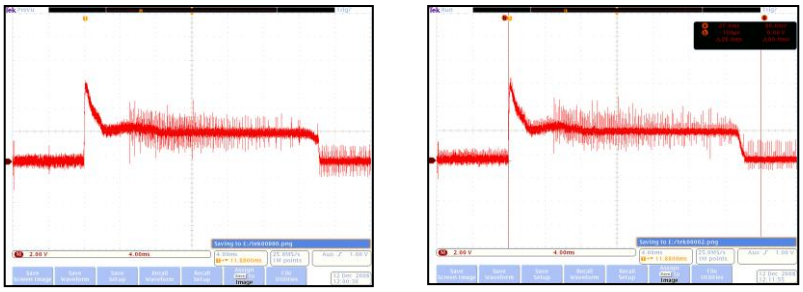

Figure 1: Deuteron beam in the U1.5 seen by a DCCT.

A bit earlier, while being in a proton mode, the U70 was trained to accept the ions. To this end, 1.32 GeV proton beam accumulation and circulation on flat-bottom was studied. The lattice magnets were powered a stand-alone DC power supply (131.1 A, 354 G). Coasting beam circulation (with RF off) and injection of bunches populated by as small as $3 \cdot 10^{10}$ ppb (imitation of a low-intensity deuteron bunch) were tried.

Attempts to transfer a full deuteron beam to the U70 ring and get a circulation there were not successful. Still, first deuterons in the U70 were observed with scintillating screen in straight section #10 indicating beam traversal through at least 4 of 120 combined-function magnets.

4.8.3 **Run 2009-1**

In the closing days of this run (on April 25, 2010), the first ever stable circulation of a light-ion beam (ions of deuterium) at flat-bottom values of magnetic guide field of the main synchrotron U70 was obtained.

To start with, the Alvarez DTL I100 safely accelerated deuterons to 16.7 MeV per nucleon at the 4π-mode. The gas ion source yielded 16–17 mA of pulsed current at 40 μs pulse width with chopper off, and 15 mA; 5 μs with chopper on.

Specific kinetic energy was then ramped in the U1.5 ring from 16.7 to 448.6 MeV per nucleon. Overall in-out transfer efficiency through the machine amounted to 50%. The output intensity of $4.5 \cdot 10^{10}$ dpb complies with design expectations. Beam observation over the regime is shown in Fig. 2.

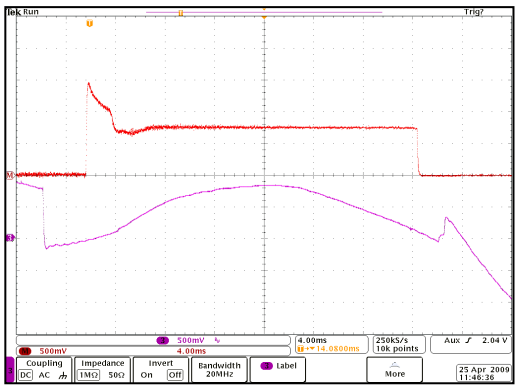

Figure 2: Ramping rate of the U1.5 guide field (lower trace) and deuteron beam intensity monitored with a DCCT (upper trace). Acceleration is accomplished in 26 ms. Compare with Fig. 1 to notice much improved performance of beam diagnostics made free of EM interferences.

Finally, the deuterons at 448.6 MeV per nucleon were transferred onto the waiting flat-bottom of the U70 ring (field 350.9 G, DC PSU current 128.4 A).

As a result, the U70 got a stable circulation of a coasting deuteron beam for about 7.5 s. This limit was imposed by an operational constraint in the existing timing system rather than by any physical reason. Momentum spread of the bunch injected is equal to $\pm 3.6 \cdot 10^{-3}$, bunch full length at base is about 100 ns, intensity is $4.5 \cdot 10_{10}$ dpb.

Estimated decay time of de-bunched beam (RF field off) is about 30–40 s.

Beam signals observed are shown in Figs. 3, 4.

4.8.4 **Run 2009-2**

In course of maintenance activity for this run, 8 (of 40 available) ferrite-loaded RF cavities in the U70 ring were accommodated to an extended band of radiofrequency 2.6–6.1 MHz (essentially, reset to the factory default). These and only these cavities were fit to operate with the light-ion beam. To this end, they were driven to the top gap voltages feasible to compensate for a deficit in an overall number of cavities adapted.

This group of cavities had lower frequency sufficient to capture light-ion beam longitudinally at the flat-bottom guide field of the U70.

A new digital (DDS) RF master oscillator was put into service and coded to start from a lower RF of 4.46 MHz.

On taking full advantage of these hardware updates, we have continued with light-ion acceleration program during closing days of the run (December 11–15, 2010).

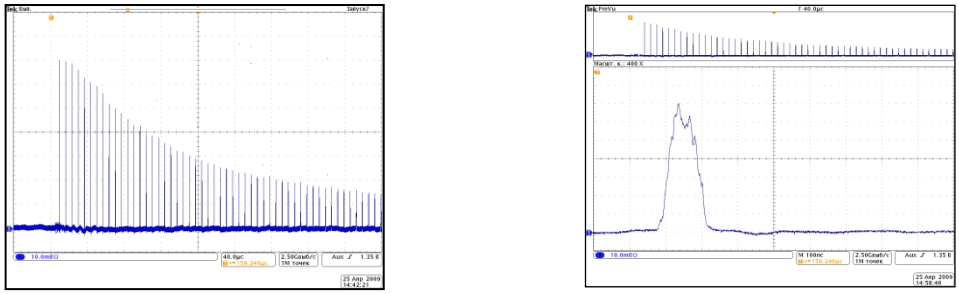

Figure 3: Circulation of a deuteron beam in the U70. (Left) AC beam current acquired by a pickup electrode. Rotation period is 6.72 μs. The same guide field would have forced lighter and faster protons rotate with 5.44 μs recurrence. The signal decays due to de-bunching given RF accelerating field switched off. Envelope of this signal bears data about beam momentum spread. (Right) First-turn shape of a deuteron bunch injected.

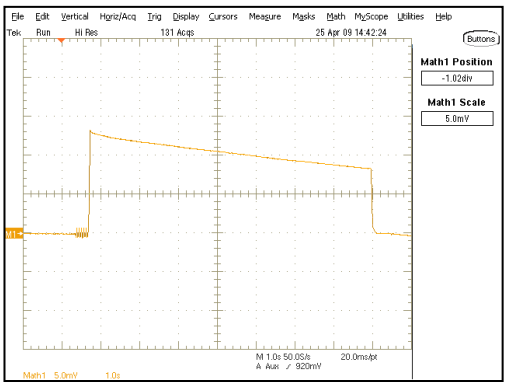

Figure 4: Deuteron beam intensity monitored with a DCCT. It dyes out much slower than beam peak current shown in Fig. 3. Scan tome base is 10 s.

The injector cascade comprising ion source, Alvarez DTL I100 and transfer line to the booster ring U1.5 operated reliably, as is shown in Figs. 5, 6.

Troubles with vector summing of RF voltages in accelerating system of the U1.5 persisted. They were even aggravated by a certain misbalance of performances of a renovated Automated Frequency Control (in 8 cavities of 8), well adapted for light-ion program, and an out-dated wide-band intermediate amplifiers (in 7 of 8) that stayed yet beyond the upgrade activity by the run in question.

In spite of the obstacles encountered, we have managed to get circulation of both, an azimuthally uniform beam (like in run 2009-1) and capture deuterons into RF buckets to get circulation of deuteron bunches in the U70.

Then, after a smooth ramp of RF by +10 kHz in 3 s we have safely tried the fixed-field mode of acceleration of a deuteron bunch (the so called phasotron regime). This

way, kinetic energy was ramped by +3.8 MeV per nucleon unless deuterons had been lost at the outer wall of the vacuum chamber (Fig. 7).

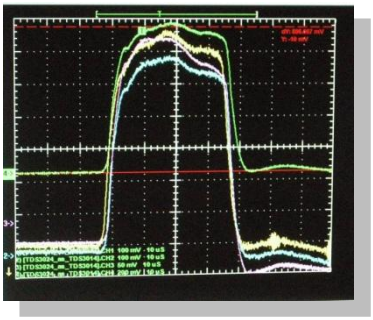

Figure 5: Deuterons in the DTL I100. Pulsed current 19 mA, pulse width 40 μs. Beam chopper is off.

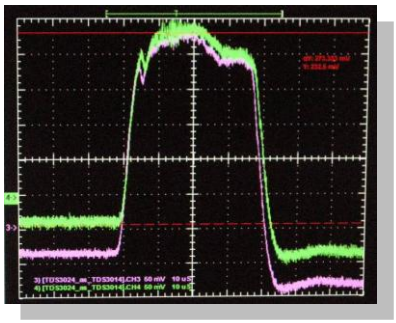

Figure 6: Beam current at entry to and exit from beam transfer line from I100 to U1.5. In-out transfer efficiency is 90% ca.

Formally, this exercise might be recorded as the first ever attempt of acceleration of light ions in the U70.

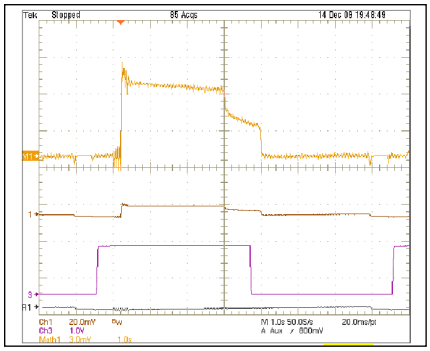

Figure 7: Acceleration of deuterons in the U70, fixed-field regime. Upper trace is beam intensity. First step down occurs when the captured beam fraction goes to outer radii and impacts horizontal aperture limitation. The surviving residual is azimuthally continuous fraction that is intercepted later on by internal beam dump target. Meander shows RF voltage amplitude program.

4.8.5 **Run 2010-1**

This run succeeded on April 27, 2010 in the first acceleration to specific kinetic energy 23.6 GeV per nucleon of a light-ion beam (deuterons) in the main ring U70.

Booster U1.5 ramped the beam energy, as usual, from 16.7 to 448.6 MeV per nucleon. Top intensity observed amounted to 2·1011 and $1.2 \cdot 10^{11}$ dpb at start and end of a cycle, respectively. In-out transfer efficiency improved to 60% thus exceeding that of the previous runs.

Lattice magnets of the U70 were powered via the conventional scheme, by rotor machine generators (guide field 351–8441 G, cycle period (shortened) 7.5 s). Ultimately, the transition energy (at 8.0 GeV per nucleon) was safely crossed, and U70

accelerated deuterons to 23.6 GeV per nucleon. Maximum beam intensity observed was $7 \cdot 10^{10}$ and $5 \cdot 10^{10}$ dpb at start and end of a cycle, respectively.

The top energy of 23.6 GeV per nucleon was imposed by the particular magnet cycle inherited from a preceding regular 50 GeV proton mode of the U70. Going to the top magnetic field of 12 kG would have resulted in a deuteron beam having 34.1 GeV per nucleon which energy now seems surely attainable from the technical viewpoint.

Figs. 8, 9 and 10 present beam observations along the cascade of machines engaged.

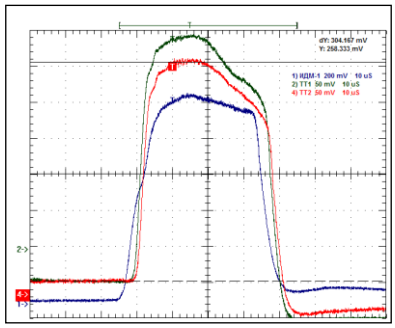

Figure 8: Acceleration of deuterons in the Alvarez DTL I100. Lower trace — beam pulse at exit from the fore injector. First and second traces from top — beam current at entry to and exit from beam transfer line I100/U1.5, respectively. In-out transfer factor is 91%. Top-pulsed current at exit from I100 amounted to 21 mA. All the pulses are 40 μs wide.

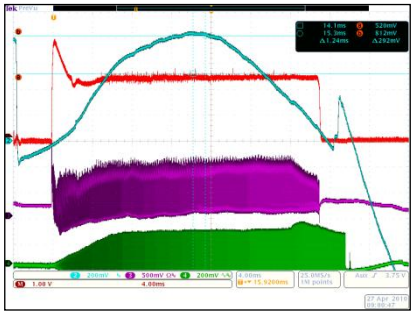

Figure 9: Acceleration of deuterons in the booster U1.5. Traces are listed from top to bottom. First (blue) signal is ramp rate of guide field. Second (red) signal is beam intensity monitored with a DCCT. It stands for $1.4 \cdot 10^{11}$dpb at start and $8.6 \cdot 10^{10}$ dpb at end of acceleration. Third (purple) ray is a signal from pickup electrode that sees combination of longitudinal and transverse beam motions. Fourth (green) trace is envelope of the net accelerating field. Ramping time is 26 ms, cycle period is 60 ms long.

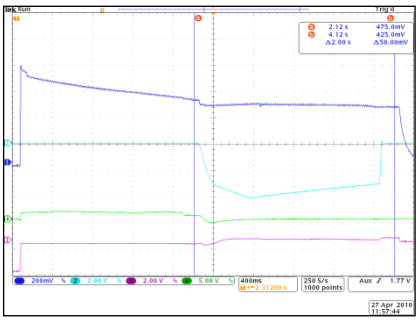

Figure 10: Acceleration of a deuteron bunch in the main ring U70. Traces are listed from top to bottom. First (blue) signal is acquired from an electrostatic pickup. It stands for $4 \cdot 10^{10}$ dpb at start and $2.5 \cdot 10^{10}$ dpb at end of acceleration. Second (cyan) trace shows ramping rate of magnetic field. Third (green) ray is a technological signal from beam radial position detector. Fourth (purple) ray is a technological signal from beam phase detector. Phase jump occurs at transition crossing (at 8 GeV per nucleon).

4.8.6 **Conclusion**

The important milestone of the program to accelerate beams of light ions in the Accelerator complex U70 of IHEP-Protvino was achieved in April of 2010 by accelerating deuterons to 23.6 GeV per nucleon in the U70 ring.

The main accelerator faculty of IHEP— its proton synchrotron U70 can now be substantially referred to as an ion (to be more precise, a light-ion) synchrotron as well.

Next step planned for the end of 2010, or beginning of 2011, is to accumulate and accelerate carbon ions and to put on trial a new slow extraction system delivering spills at the flat-bottom energies of the U70.

4.8.7 **References**

1. S. Ivanov and the U70 staff, Proc. of RUPAC-2008, Zvenigorod, 2008, p. 130–133.
2. Yu. Antipov et al, ibid, p. 104–106.

4.9 Status and Prospects of the Novosibirsk FEL Facility

N.A. Vinokurov, E.N. Dementyev, B.A. Dovzhenko, A.A. Galt, Ya.V. Getmanov, B.A. Knyazev, E.I. Kolobanov, V.V. Kubarev, G.N. Kulipanov, L.E. Medvedev, S.V. Miginsky, L.A. Mironenko, V.K. Ovchar, B.Z. Persov, V.M. Popik, T.V. Salikova, M.A. Scheglov, S.S. Serednyakov, O.A. Shevchenko, A.N. Skrinsky, V.G. Tcheskidov, M.G. Vlasenko, P.D. Vobly, N.S. Zaigraeva
Budker INP, Novosibirsk, Russia
Mail to: vinokurov@inp.nsk.su

Abstract:

Multiturn energy recovery linacs (ERL) looks very promising for making ERLs less expensive and more flexible, but have serious intrinsic problems. At this time only one multiturn ERL exists. This Novosibirsk ERL operates with two orbits and two free electron lasers now. The Novosibirsk terahertz radiation user facility provides 0.5 kW

average power at 50 - 240 micron wavelength range. Different users work at six stations. Two another orbits and third free electron laser are under construction. The operation experience revealed specific problems of ERLs (especially, of multiturn ones). Some solutions were proposed recently.

4.9.1 The First Orbit FEL

A source of terahertz radiation was commissioned in Novosibirsk in 2003 [1]. It is CW FEL based on an accelerator–recuperator, or an energy recovery linac (ERL). It differs from other ERL-based FELs [2, 3] in the low frequency non-superconducting RF cavities and longer wavelength operation range. The one-turn ERL (which is the first stage of the full-scale four-turn ERL) parameters are listed in Table 1, and its scheme is shown in Fig. 1.

Table 1: Parameters of the first stage of Novosibirsk ERL.

Parameter	*Unit*	Value
Beam energy	MeV	11
Maximum average electron current	mA	30
RF frequency	MHz	180.4
Maximum bunch repetition rate	MHz	22.5
Bunch length	ps	100
Normalized emittance	mm·mrad	30
Charge per bunch	nC	1.5
RF cavities Q factor		$4 \cdot 10^4$

This first stage of the Novosibirsk free electron laser generates coherent radiation tunable in the range 120-240 micron as a continuous train of 40-100 ps pulses at the repetition rate of 2.8 - 22.5 MHz. Maximum average output power is 500 W, the peak power is more than 1 MW [4,5]. The minimum measured linewidth is 0.3%, which is close to the Fourier-transform limit. The third harmonics lasing was obtained recently.

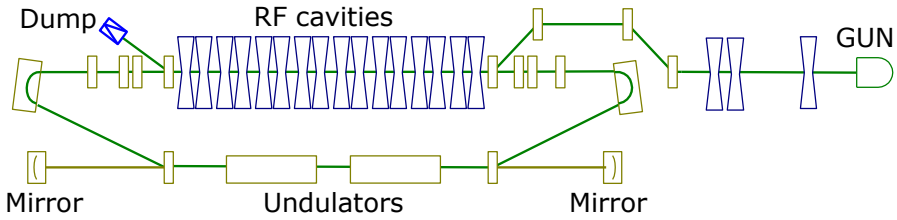

Figure 1: Scheme of the Novosibirsk terahertz free electron laser.

It was achieved by suppression of the first harmonics lasing using aperture-decreasing scrapers.

Five user stations are in operation now. Two other are in progress.

4.9.2 **The Second Stage of ERL and FEL**

Full-scale Novosibirsk free electron laser facility is to be based on the four-orbit 40 MeV electron accelerator-recuperator (see Fig. 2). It is to generate radiation in the range from 5 micrometer to 0.24 mm [6, 7].

Manufacturing, assembly, and commissioning of the full-scale four-turn ERL are underway. The orbit of the first stage with the terahertz FEL lies in the vertical plane. The new four turns are in the horizontal one. One FEL will be installed at the fourth orbit (40 MeV energy), and the second one is already installed and works at the bypass of the second orbit (20 MeV energy).

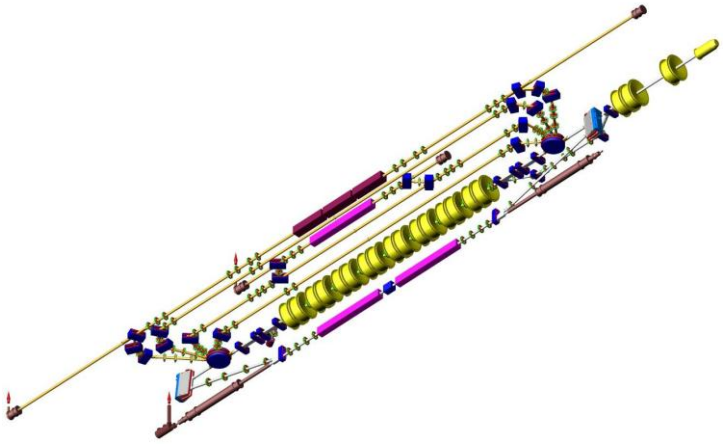

Figure 2: The full-scale Novosibirsk ERL with 3 FELs (bottom view).

The bypass provides about 0.7 m lengthening of the second orbit. Therefore, when the bypass magnets are switched on, the deceleration of beam take place at the third passing through the accelerating system, and after that electrons come to the first orbit and, after the second deceleration, to the beam dump.

All 180-degree bends are achromatic. To reduce sensitivity to the power supply ripples, all magnets are connected in series. To simplify the mechanical design, all non-round (small) magnets are similar and parallel-edge. Water-cooled vacuum chambers are made from aluminum.

The bypass magnetic system contains four bending magnets, quadrupoles, and undulator. The second orbit undulator is very similar to the old undulators of the first-orbit FEL, but its gap is lower. It is fixed-gap electromagnetic undulator. The main parameters of the undulator are listed in Table 2.

Table 2: Parameters of the second orbit undulator.

Parameter	***Unit***	**Value**
Period	mm	120
Gap	mm	70
Maximum field amplitude	T	0.12
Total length	m	3.9
Maximum bus current	kA	2.2
Maximum power consumption	kW	30

The undulator poles have the concave shape to equalize focusing in both transverse coordinates. It is necessary, as at 20 MeV this focusing is strong (matched beta function at the 0.12 T field amplitude is 1.1 m only).

The optical resonator length is 20 m (12 RF wavelengths). Therefore the bunch repetition rate for initial operation is 7.5 MHz (24^{th} subharmonics of the RF frequency). Mirrors are made of copper, water-cooled, and covered by gold. Outcoupling holes (3 and 4 mm diameter) serve also for alignment by visible reference laser.

The location of two FELs in accelerator hall is shown in Fig.3. The first lasing of the FEL at bypass was achieved in 2009. The radiation wavelength range is 40 - 80 micron. The maximum gain was about 40%. The significant (percents) increase of beam losses took place during lasing. Therefore sextupole corrections were installed to some of quadrupoles to make the 180-degree bends second-order achromatic. It increased the energy acceptance for used electron beam.

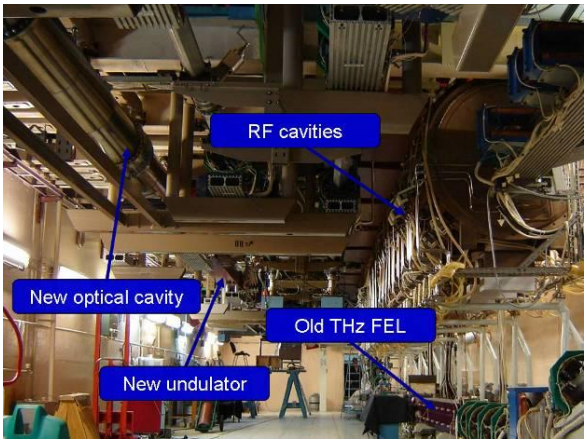

Figure 3: The location of two FELs in accelerator hall.

The beamline (Fig. 4), which delivered radiation from new FEL to existing user stations, is assembled and commissioned. The output power is about 0.5 kW at the 9 mA ERL average current. Thus, the first in the world multiturn ERL operates for the far infrared FEL.

Figure 4: The optical beamline, which transports the radiation of the second FEL to the user stations.

4.9.3 **The Prospects**

The assembly of third and fourth orbits is in progress. The four-orbit ERL commissioning will start the next year.

4.9.4 **References**

1. E. A. Antokhin et al. NIM A528 (2004) p.15.
2. G.R. Neil et al. Phys. Rev. Lett. 84 (2000), p. 662.
3. E.J. Minehara. NIM A483 (2002) p. 8.
4. V.P. Bolotin et al. NIM A 557 (2006) p.23.
5. E.A.Antokhin et al., Problems of Atomic Science and Technology, p.3, №1, 2004.
6. N.G. Gavrilov et al. IEEE J. Quantum Electron. QE-27, p. 2626, 1991.
7. V.P.Bolotin et al. Proc. of FEL-2000, Durham, USA, p. II-37 (2000).

4.10 Kurchatov Synchrotron Radiation Source Facilities Modernization

M.Blokhov, V.Leonov, E.Fomin, G.Kovachev, V.Korchuganov, M.Kovalchuk, Yu.Krylov, V.Kvardakov, V.Moryakov, D.Odintsov, N. Smoliakov, S.Tomin, Yu.Tarasov, V.Ushkov, A.Valentinov, A.Vernov,Yu.Yupinov and A.Zabelin
RRC Kurchatov Institute, Moscow 123182, Russia
Mail to: vnkorchuganov@mail.ru

Abstract:

Kurchatov Synchrotron Radiation Source (KSRS) operates in the range of SR from VUV up to hard X-ray. Technical modernization of KSRS systems is under way. It includes a replacement of the power supplies and the nano- and micro-second generators by the new ones, the installation of the new third RF accelerator cavity on 2.5 GeV storage ring SIBERIA-2. The projects of the feedback system for the longitudinal coherent multi-bunch instabilities dumping and of the new sensitive electronics for pick-up stations on Siberia-2 storage ring start in 2010. Three 7.5 T wiggler beam lines were mounted and tested with SR beam in December 2009. The 7.5 T (19+2) poles SC wiggler and new 3 RF cavities are doing the KSRS spectrum harder and intensive. The program tools for KSRS operation are introduced in accelerator control system with a new electronics. The new scheme of top-up energy injection placed outside of Siberia-2 storage ring tunnel is carried out. The report describes a statistics works and plans on KSRS facilities.

4.10.1 **Introduction**

The accelerator complex of KSRS consists of the linear accelerator and two storage rings [1]. Main parameters of the KSRS accelerator facilities are shown in Table 1.

Table 1: Parameters of KSRS facilities

Linac	*SIBERIA-1*	*SIBERIA-2*
E = 80 MeV	E = 80÷450 MeV	E = 0.45÷2.5 GeV
I = 0.2 A	I = 0.2÷0.3 A (singlebunch)	I = 0.1÷0.3 A (multibunch)
L = 6 m	C = 8.68 m	C = 124.13 m
DE/E = 0.005	B = 1.5 T	B = 1.7 T
ε0=300 nm·rad	εx0=800 nm·rad	εx0=78÷100 nm·rad
T = 18 ns	T0 = 29 ns	T0 = 414 ns
frep = 1 Hz	Trep = 25 s	τ =10÷25 hrs
	λc=61 Å , BMs	λc=1.75 Å, BMs λc=0.40 Å, SCW
Forinjector	Booster, VUV and soft X-ray source	Dedicated SR source 0.1-2000Å [1]

Possible number of photon beam lines from BMs equals to 24, SR sources like SC wigglers and warm wigglers (undulators) are planned to offer 6-8 SR beam lines from IR to hard X-ray radiation.

4.10.2 KSRS Facilities Work

The work of SIBERIA-2 on experiments is carried out with use of SR from bending magnets in energy range of photons 4-40 keV and spectral flux (1013-1011) ph/s/mrad/0.1%BW during week runs in a round-the-clock mode. Within one week 9 working 12-hour shifts are presented.

Table 2: SR Experimental time in 2005-2009 years

	2005	2006	2007	2008	2009
Siberia-1: experiment, hrs	238	236	205	471	634
Integral, A-hrs	16.1	21.1	13.4	41.7	67.4
Siberia-2: experiment, hrs	1292	2035	1629	1437	1527
Integral, A-hrs	94.9	165.5	126.2	56.3	77.5

Table 2 shows the integral time devoted for SR experimental work in 2005 - 2009 years. Fig.1 contains some statistics of the time which was spent on experiment, injection and tuning of SR source.

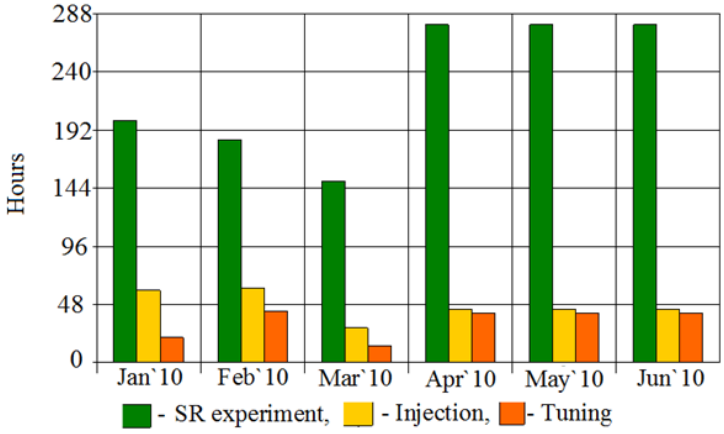

Figure 1: The Siberia-2 work in 2010.

4.10.3 **Modernization of 2008-2010**

4.10.3.1 ***New Septum Magnet of Siberia-1(KCSR-INP)***

The new pulse septum-magnet was installed with aim to increase the effectiveness of electron beam ejection from Siberia -1 into the electron transport line - ETL-2. The new septum-magnet is the modified version of the old one that worked during previous 8 years. It has more homogeneous magnetic field distribution. The results are obtained: stable control of the pulse generator of the septum-magnet, an increase in the coefficient of the release of electron beam from the Siberia-1 storage ring into the ETL-2 up to 70%.

4.10.3.2 ***New SR Beamline at Siberia-1 (KCSR – NIIOFI)***

SR from 3d BM of Siberia-1 was conducted in VUV experimental hall after the completion of mechanical and vacuum works on the new beamline D3.2. First metrology experiments were made by NIIOFI and KCSR staff.

4.10.3.3 ***RF System of Siberia-2 Upgrade***

The RF system upgrade was target to increased reliability of the machine operation and to adapt Siberia-2 storage ring to operate with new high magnetic field sc wigglers. Now RF system of Siberia-2 has two channels. Each channel includes 200 kW RF generator (with two GU-101A tetrodes), a waveguide and one or two 181 MHz cavity with own feeders. Three bi-metal cavities (7 mm of stainless steel and 8 mm of copper joint together by diffusion bonding) were installed in the storage ring upon completion of the upgrade. Initially, on December 2007 one old cavity has been replaced by a section of two new cavities. Second old cavity was replaced by a single new bi-metal cavity on October 2009.

So total accelerating voltage is increased up to 1.5 (1.8 MV max). New set of parameters of the storage ring and its RF system is listed in Table 3.

Table 3. Parameters of Siberia-2 and its RF system [9].

Parameters of the Siberia-2 storage ring		Energy of electrons	EMAX	GeV	2.5
	SR losses with BMs and wigglers		ΔEBMs ΔEBM+WIG	keV/ turn	681 1021
	Beam current		I B MAX	A	0.29
	Total accelerating voltage		2U1+U2	kV	1500
First RF channel : 200 kW generator, two cavities (№1, №3)		Accelerating voltage	2U1	kV	820
	Shunt impedance		2ZT2	MOhm	8.6
	Power dissipated in the cavities		2P1	kW	39
	Power transferred to the beam		2P1b	kW	157
Second RF channel: 200 kW generator, one cavity (№2)		Accelerating voltage	U1	kV	680
	Shunt impedance		ZT2	MOhm	4.3
	Power dissipated in the cavity		P2	kW	54
	Power transferred to the beam		P2b	kW	139

A new 2 feeders connected with the waveguide of RF generator № 1 deliver RF power to the lateral cavities (№ 1 and № 3). The middle cavity (№ 2) is fed by the RF generator № 2, see Fig.2.

At the moment we observe the mutual influence of two RF generator control systems through the electron beam which leads to unstable operation of the RF generators.

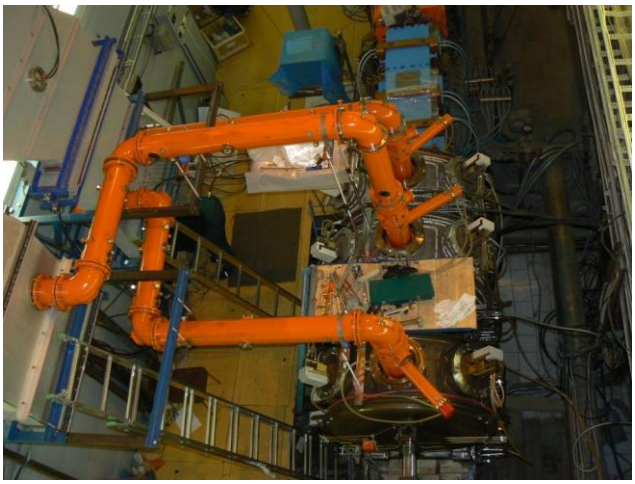

Figure 2: New cavities and feeders at SIBERIA-2 ring.

According to a simulation, the stability will grow with tuning the RF feeders and the waveguides at a wavelength of (n+1/8) l. We plane to do it to the end of 2010.

The synchrotron oscillations collective modes appear after injection of first four or five bunches. The energy ramping of the electrons with current in many bunches exceeding 150 mA is characterized by synchrotron motion in coherent modes and possible losses of the beam part. The losses depend on the number of bunches and modulate the particles numbers in bunches correspondingly with the synchrotron mode number, see Fig.3.

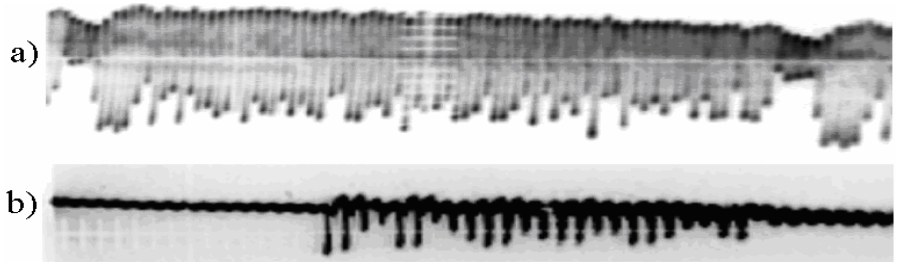

Figure 3: The modulation of bunches with different filling due to collective mode instability losses.

The decision was made to carry out “Bunch-to-bunch longitudinal feedback” to dump the coherent synchrotron oscillation. It will include a wide-band cavity as a kicker, a wide-band pick-up electrode, a phase detector, a modulator, RF control electronics, a wide-band power amplifier.

4.10.3.4 *New Nanosecond Generator (KCSR)*

The prototype of new low voltage sin-like pulse nanosecond generator with 100-200 ns semi-period was created at a base of the pseudo-spark thyratron “ТПИ1-10К/50”with the cold cathode. Maximum anode amplitude is of 25-30 kV. It was successfully tested with the electron beam. The short-circuited plates of the Siberia-2 inflector were switched on as parallel electrical loads of the new ns generator (<1.5kA, 14 kV). In result, the high temporary stability of capture of electrons was reached in the regime of injection in Siberia-2 with high efficiency (up to 70- 75%). The features of new device are low voltage, absence of spark discharge and a work only with magnetic field between the kiker plates. It will be a real alternative to high voltage existing inflector and preinflector nanosecond generators of Siberia-2, which work on the electric spark dischargers.

4.10.3.5 *New SR Beam Lines from BMs of Siberia-2*

Currently under construction are 3 experimental stations and 3 SR beamlines from the 1.7.T bending magnets of Siberia-2: “PES” - Photoelectron Spectroscopy (PES, ARPES, NEXAFS) - K6.5, “PHASE”- X-Ray precision optic-2 - K2.3, "NANOFAB-2” – micro- and nano-electro-mechanical systems researches (MEMS and NEMS)- K2.6. These SR beamlines and experimental stations are producing with a firm “NT-MDT”, Zelenograd.

4.10.3.6 *New SC Wiggler Beam Lines*

We note the production and the consequent mounting of wiggler`s beam lines elements were effectuated according to KCSR`s drawings with the help of a firm «Megaterm», Briansk.

In the first half-year 2009 the installation of three SC wiggler`s beam lines elements was first executed inside the tunnel of Siberia-2, then they were conducted through the shielding wall and installed in the experimental hall. A specially designed 100 kW SR absorber–distributor was mounted near the ring of Siberia-2. Inside its vacuum volume it contains one stationary and three movable absorbers for each of three separate SR beam lines. Before 100 kW absorber the DU250 shatter was posed for the separation of the vacuum systems of the X-ray beam lines and Siberia-2. These works were alternated with the work on SR experiments.

In September - October 2009, the work was carried out with the opening of the vacuum chamber of Siberia-2. A new camera with three SR absorbers to limit sc wiggler`s SR divergence was installed in the triplet following 7.5T wiggler. A refinement was also made of the existing pumping unit and diagnosis (PDU), located after the first bending magnet (following the triplet). It was introduced in PDU volume two immobile and single movable absorbers to protect the DU250 shatter against SR, coming from the bending magnet. In addition, engineering equipment, visualization elements of SR and TV monitor were mounted on the beam lines.

4.10.4 **Insertion Devices**

4.10.4.1 *Work with 7.5Tt SC Wiggler*

Project SC wiggler parameters are presented in Table 4.

Table 4: Project SC wiggler parameters at 2.5 GeV

Max. field, T	3-7.5
Period, mm	164
Npoles	19+2
Elliptic liner, Cu. V*H, mm	13*120
Eph crit, keV	31.2
Flux, ph/s/0.1%BW	10^{14}-10^{12}
Working spectrum, keV	5-200
Θx max, mrad	± 23.5
Energy loss/turn, keV	365
Ptot (100 mA), kW	36.5
Coils	NbTi

First run of SC wiggler was carried out on 2008, June, 7 with the 3 T magnetic field [2].

In November 2009, after the mounting of 3 wiggler beam lines was completed the vacuum conditions in Siberia-2 for the work with the electron beam were restored. The control code was debugged for new bipolar power units of wiggler and the ramping of magnetic field up to 7.5T was accomplished in the automatic regime. The measured shifts of betatron tunes have coincided with theoretical ones with good accuracy, Fig.4.

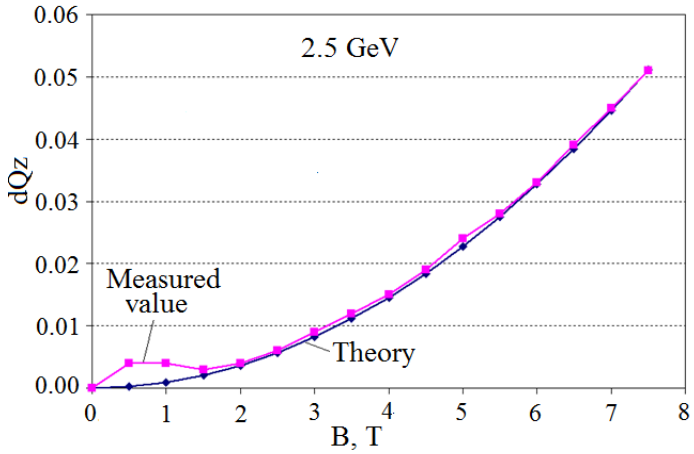

Figure 4: Measured and theoretical vertical betatron shift vs SCW magnetic field amplitude.

Hard component of SR was observed in an experimental hall with a TV camera at luminescent screens fixed on flanges, closing the ends of each of 3 tubes, Fig.5.

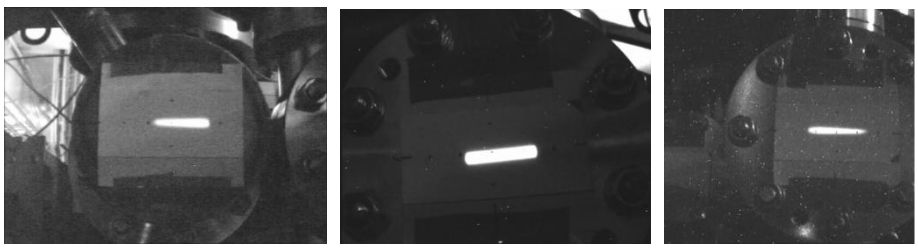

Figure 5: X-Ray beam from 7.5T SCW at output of three beam lines in the experimental hall of Siberia-2.

Measurements of position of x-ray beams relative to axes of channels and its operative adjustment have been simultaneously implemented. Besides, the card of

radiation fields has been measured in an experimental hall with the deduced X-ray beams.

Unfortunately, in December 2009 the breakdown of superconductivity has occurred in the coils of the wiggler magnets at 7.5T. Under the action of resulting ponderomotive forces, the liner of wiggler - intra-vacuum thin-walled copper tube of almost elliptical cross section - collapsed, completely blocking the aperture. Therefore, the wiggler was evacuated from the ring of Siberia-2 and replaced by a spacer. In June 2010 new modified more durable liner was manufactured (BINP, Novosibirsk) and wiggler was again put on the storage ring in early July 2010.

In July-September, the vacuum chamber was degassing by means of SR. Last decade of September, after collecting the integral 2.1 A-hrs of electron current, Siberia-2 works at 2.5 GeV with 40-50 mA electron current and a lifetime of 2-4 hours. We plan to continue the work with the wiggler in October 2010.

4.10.4.2 *New IDs Planned at Siberia-2*

The planned scheme of the insertion devices location on the Siberia - 2 storage ring is shown in Fig.6. Eight IDs are to be installed, among them 4 superconducting, 3 normal conducting wigglers and one mini-undulator. Besides that one photon line of infra-red (IR) edge radiation (ER) will be taken out [3,4]. IDs approached parameters are given in the Table 5.

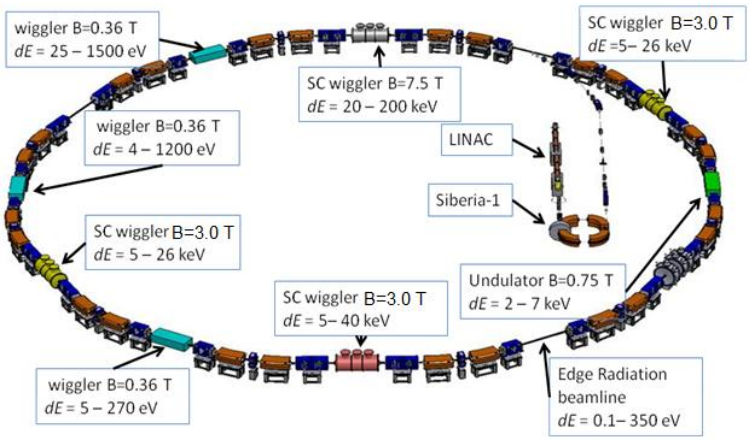

Figure 6: Plan of IDs location at Siberia-2

Table 5. Main parameters of planed insertion devices

IDs	Bmax T	λu, mm	N per	Eph	SR station, planed
1 SCW	7.5	164	10	4-200 keV	RSA, RS-MCD, Hard X-Ray
3 SCW	3.0	44	35	5-40 keV	Belok-1, Belok-2, Lengmuir-2, Standing X-Ray
3 NCW	0.36	80	51	5.5-270eV	PES microscop, PES-SH Resol., Spectro-Lumi, VUV, MR
Mini-U	0.75	7	300	2-7 keV	1.3 GeV: X-Ray holography
IR ER	-	-	-	0.1-350eV	IR, VUV, Soft-X-Ray

4.10.4.3 *New Experimental Stations on 7.5T SCW*

Now there is a progress in the creation of next 3 new experimental station based on SR from 7.5 T SC wiggler:

1. EXAFS/XANES and X-ray Magnetic Circular Dichroism (XMCD): q= (13.3 ± 1) mrad, λc = 0.5 Å, P = 760 W/mrad – beam line K1.4.2;
2. Hard X-ray: λc=0.4Å, P=940 W/mrad, q= (0 ± 1) mrad – beam line K1.4.3;
3. X-ray structure analysis-RSA: q=(-17 ± 1) mrad, λc=0.58 Å, P = 650 W/mrad – beam line K1.4.4.

Here the SR power data correspond to 100 mA current and 2.5 GeV energy of the electron.

4.10.5 **Improvement of Beam Parameters**

Ultimate goal of improvements of parameters of electron and photon beams is the increase of brightness, spatial and time stability of SR source.

4.10.5.1 *Diagnostics and Control System*

A new electronics and computer control codes were run at Siberia - 1 and Siberia – 2 for betatron tunes measurement. The betatron spectra are measured and demonstrated on operator monitor with high precision. [5]

A new NMR probe with auxiliary electronics and control code was installed in the calibration bending magnet of Siberia-2. New electronics serve as a part of feedback system of electron energy stabilization scheme.

A new electronic devices (crate controllers K167), computer control codes (miniMODUL167 processor and ARTX-166 real time OS) and operator interface were elaborated and run. On the base of CC K167 and managing server of class Pentium IV several application were improved: the measuring of an electron current value in Siberia-1 and a transverse beam position in the electron transport line ETL-2 became rather simple and reliable; the modernization of synchronization system and control system of the pulse power supplies of accelerator complex were realized; new control system of Siberia–2 RF generators is developed and successfully introduced; management of power supplies of the quads and steering magnets of Siberia – 2; new operational control software and the experimental data archives in on-line mode are started in routine work.

4.10.5.2 *An Increasing of Electron Life Time at Siberia-2*

The lifetime at injection energy of 450 MeV is much less - not more than 30 min in single-bunch mode with a typical current in one bunch 3 - 4 mA. It is mainly determined by Touschek effect in the presence of limiting the horizontal aperture. According life time studies we have found that the most accessible method to increase the lifetime was the control of betatron oscillations coupling at low energy.

The betatron coupling was adjusted by two families of skew-quadrupole. As a result, at the injection energy an increase of lifetime was reached from 30% to 40% depending on the number of particles in one bunch. As a consequence the storage rate

of electrons was increased also. Besides that, the lifetime was increased in process of the energy ramping, thus reducing the loss of current during the ramping process from 5 - 6% to 1.5 - 2%.

The lifetime of the electron beam at 2.5 GeV in Siberia-2 storage ring is determined by the vacuum conditions and is now more than 15 hrs at a current of 100 mA.

Beam lifetime τ(t) at 2.5 GeV depends on time t as follows: $\tau(t)^{-1} = \tau_0^{-1} + C \cdot I(t)$, where I(t) - electron current, τ_0 - lifetime when the current approaches to zero, C - constant, τ0 is determined by the level of vacuum in absence of the beam. The second term can be determined by the effect of Touschek or by a gas desorption stimulated by SR from the walls of the vacuum chamber. In our case, the second mechanism is running, since the values τ_0 and C depend on the collected current integral at 2.5 GeV (see Fig.7).

Let's note, that after closing the vacuum chamber, for the achievement of life time of 12 hours at the 100 mA electron current it was required to collect an integrated doze of 16 A*hrs, that is 10 times less, than it was required at the very beginning of SIBERIA-2 work with electron beam.

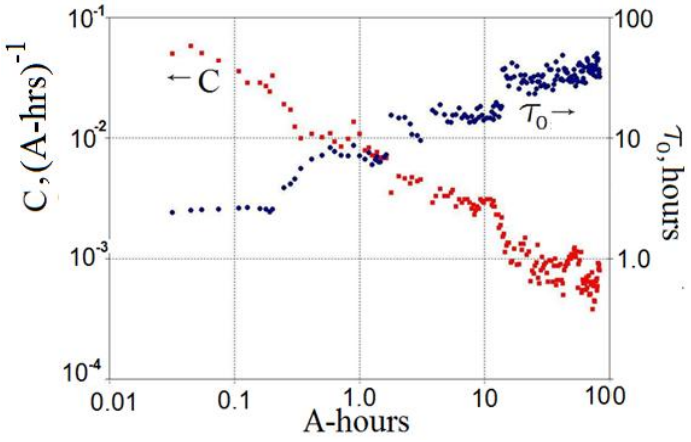

Figure 7: Parameters of τ0(in blue) and C(in red) vs collected integral of electron current at 2.5 GeV.

4.10.6 **Modernization of SR Source**

4.10.6.1 ***Top-up Energy Injection with Synchrotron***

In KCSR the Project of technical upgrade of accelerator complex as SR source was developed [6]. The purpose of the Project is to create SR source of 2.5÷3 generations on the base of existing accelerator complex. This will increase the spectral brightness more than in 30÷100 times in comparison with the realized project. To reach this aim means to develop the new optical structures for SIBERIA-2 with small natural horizontal emittance 6÷18 nm-rad at the electron energy 1.3 GeV and 2.5 GeV accordingly.

An achievement of the purposes means a radical improvement of an injection part of a SR complex. According to the Project, injection in Siberia - 2 will be made from a booster synchrotron (BS) with rather small natural emittance. The parameters of BS-1 and BS-2 are given in the Table 6.

Table 6: Calculated parameters of Booster Synchrotrons

Parameter	***BS-1***	***BS-2***
Injection energy, MeV	80-160	80-160
Extraction energy, GeV	2.5	2.5
Circumference, m	110.9	56.27
Cycling frequency, Hz	1	1
Emittance nm·rad	52.6	90.1
Momentum compaction	0.0107	0.032
Betatron tunes: Qx/Qy	6.83 / 4.57	5.186/2.352
Chromaticity: ξx/ξy	–14.12/–8.89	-8.85/-4.45
R.m.s. energy spread	9×10-4	1.95x10-3
Energy loss per turn, keV	622	622
Damping times: τx, τy, τs , ms	3.08, 2.97, 1.46	0.59/1.52/3.49
Beam current, mA	10	10
RF frequency, MHz	181.13	181.13
Harmonic number	67	34

BS will ramp the energy from 0.08 (0.16) GeV till 2.5 GeV with repetition rate of 1 Hz. BS will support the constant level of electron current in SIBERIA-2 and SR for the users (an “infinite beam life time”). Now there are two schemes (BS-1 and BS-2) of the BS location relative to Siberia-2 storage ring. [7]

In Fig.8 the modernized complex is shown. Left: an external ring - Siberia-2, an internal ring - BS-1 is in the same tunnel, the linac with a projected magnetic mirror, the small ring - a SR source Siberia -1. Right: BS-2 is outside of tunnel of Siberia-2, Siberia-1 is dismounted.

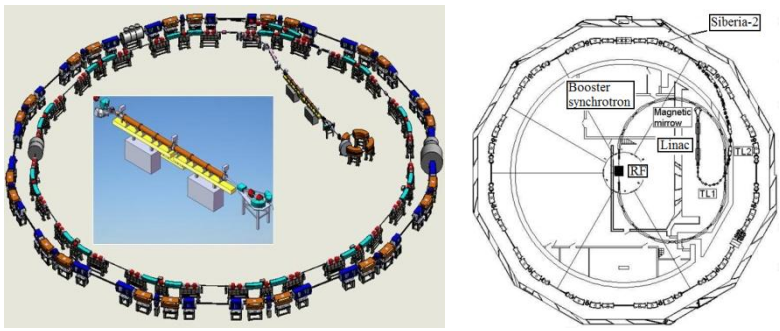

Figure 8: Two schemes of top-up energy injection.

Existing linear accelerator [8] will continue to work as injector for SIBERIA-1 with electron energy 80 MeV. Besides, linac with a magnetic mirror will work as injector for BS-1 or BS-2 with doubled up to 160 MeV electron energy.

4.10.7 **Conclusion**

We hope that the scientific and technical decisions offered in the current modernization process will provide for a scientific attractiveness and competitiveness of SR source in Russian Research Center “Kurchatov Institute”.

4.10.8 References

1. V. Anashin et al., Nucl. Instr. Meth., A282 (1989), p. 369-374.
2. V.Korchuganov,…,N.Mezentsev at al., ”First Results of Siberia-2 storage ring operation with 7.5 T superconducting wiggler”, RUPAC2008.
3. A. Anoshin, E.Fomin, V.Korchuganov, S.Tomin, ”Possibility to reach the diffraction limited X- ray source in Kurchatov Center of SR”, RUPAC2008.
4. V.Korchuganov, N.Smolyakov, N.Svechnikov, S.Tomin, “Radiation sources at Siberia-2 storage ring”, RUPAC2010.
5. E.Kaportsev at al., , “The expanded program tools for KSRS operation with archivation of data”, RUPAC2010.
6. V. Korchuganov at al., Nucl. Instr. Meth., A543 (2005), p.14 -18.
7. A.Anoshin, E. Fomin, V. Korchuganov at al., ”A new injection system for KSSR”, RUPAC2008.
8. A.Anoshin, E.Fomin, V.Korchuganov, S.Tomin, “Electron beam dynamics in the linac of Kurchatov source of SR with energy doubling”, RUPAC2008.
9. Proc. of the 8th EPAC, 3-7 June, 2002, Paris, p.2169-2171.
10. V.Korchuganov, Yu.Krylov, A.Valentinov, Yu.Yupinov, “An increasing of electron beam lifetime at injection energy in SIBERIA-2 storage ring by regulating betatron coupling”, RUPAC2010.

4.11 Radiation Sources at Siberia-2 Storage Ring

V.N. Korchuganov, N.V. Smolyakov, N.Yu. Svechnikov and S.I. Tomin
RRC Kurchatov Institute, Moscow 123182, Russia
Mail to: tominsi@mail.ru

Abstract:

In this report, two projects of radiation sources at Siberia-2 storage ring are considered. The first one is in-vacuum short period mini-undulator, which is intended for generation of bright X-ray beams. It is shown the feasibility of diffraction-limited in vertical direction X-ray source, which is to say that vertical emittance of the electron beam is equal to diffraction emittance of generated by undulator 2 KeV photon beam.

The second source will utilize edge radiation, which is generated in the fringe fields of the bending magnets. Numerical simulations show that the edge radiation is more intensive in infrared – ultraviolet spectral range as compared with standard synchrotron radiation (SR) from regular part of the same bending magnet.

4.11.1 Introduction

The magnetic system of Siberia-2 storage ring (electron beam energy of 2.5 GeV) consists of six mirror-symmetrical cells, each containing an achromatic bend and a gap with a zero dispersion function, see Fig.1 [1, 2]. The distance between the down- and upstream edges of the bending magnets is 5340 mm. The portion of straight section, suitable for insertion device loading, is about 3 m in length. The Siberia-2 lattice is so designed that the different requirements for wigglers and undulators are satisfied. So, the straight sections with small values of betatron functions, where electron beam has minimum sizes, provide optimum performance for wigglers, while the straight sections

with large betatron functions, where the electron beam has small angular divergences, are optimum for undulators.

Now at Siberia-2 storage ring SR is mainly in use. Its flux is of the order of 10^{11}-10^{13} phot/s/mrad/(BW=0.1%) in 4 – 40 KeV spectral range. One superconducting wiggler with 7.5 T magnetic field amplitude is also installed. At the same time nearly all straight sections are planed to complete with different insertion devices in the nearest future, see Fig.1 and Table 1.

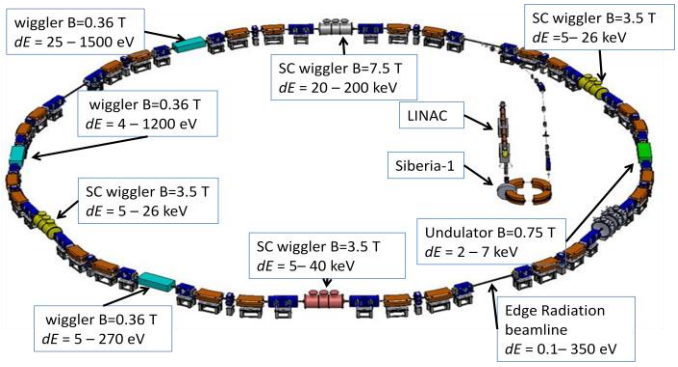

Figure 1: Siberia-2 layout with projected insertion devices.

Table 1. Main parameters of insertion devices

	Bmax T	***λu, mm***	***Number of periods***	***Spectral range KeV***
s/c wiggler	7.5	164	10	20-200
s/c wiggler	3	44	35	5-40
wiggler	0.36	80	51	5.5-270 eV
undulator	0.75	7	300	2-7
edge radiation	-	-	-	0.1-350 eV

4.11.2 **UNDUlator Radiation**

The most important feature of undulator radiation beam is its brilliance, which is mainly determined by the electron beam emittances and radiation diffraction phase volume, which is equal to $\lambda/4\pi$, where λ is radiation wavelength. A light source is called diffraction - limited if the electron beam emittance is smaller than that of the photon beam.

Nowadays a natural horizontal emittance of electron beam in Siberia-2 at 2.5 GeV is equal to 98 nm·rad [1]. Operating parameters of storage ring are listed in the Table 2. In addition to existing optical lattice new more brilliant lattice with horizontal emittance 18 nm·rad (at 2.5 GeV energy) has been developed (Table 2), The new lattice allows to obtain the horizontal emittance of 4.9 nm·rad at 1.3 GeV. Vertical emittance of electron beam is 49 pm·rad with a coupling factor of betatron oscillation $k \approx 0.01$ for Siberia-2. Thus, vertical emittance is equal to emittance of 2 keV photons. It is important to note that the new brilliant lattice can be obtained by changing of currents in lattice magnetic elements only.

Table 2: Siberia-2 Storage Ring Parameters

Lattice	***"standard"***	***"brilliance"***
Energy	2.5 GeV	1.3 GeV
Emittance	98 nm·rad	4.9 nm·rad
Beam size: σx/ σy	1500/78	363/17
Circumference	124.128 m	
Coupling	0.01	
Momentum compaction	0.0103	4.2×10-3
Betatron tunes: Qx/Qy	7.775/6.695	9.707/5.622
R.m.s. energy spread	9.5×10-4	5×10-4
Damping times: τx, τy, τs	3.2; 3;1.5 ms	22;22;11 ms
Beam current	100-300 mA	

For generation of 2 KeV photons by 1.3 GeV electron beam, undulator should match rigid requirements, see Table 3. Undulator has very short 7 mm period and high peak field 0.75 T. In the last years technology for undulators was greatly advanced [3, 4, 5]. It gives us a hope that production of the undulator with such record parameters will be possible.

Table 3: Main parameters of the undulator.

Gap	2.2 mm
Permanent magnet material	NdFeB
Residual field, μ0Hc	1.2 T
Undulator period, λu	7 mm
Poles width, w	50 mm
Field amplitude, B0	0.75 T
Undulator parameter, K	0.492
Number of periods	300
Undulator length, LID	2.1 m
Wavelength of fundamental, λ1	6.06 Å
Photon energy of fundamental, ε1	2.045 KeV

A set of computer codes SMELRAD [6] has been used for undulator radiation simulation. Flux density distributions of fundamental harmonic in horizontal and vertical directions are shown in Fig. 2. Three cases were considered: 1) electron beam with zero horizontal and vertical emittances: $\varepsilon_x=\varepsilon_z= 0$; 2) $\varepsilon_x=4.9$ nm·rad, $\varepsilon_z=49$ pm·rad; 2) $\varepsilon_x=4.9$ nm·rad, $\varepsilon_z=4.9$ pm·rad. One can see that electron beam emittance essentially influence on radiation angular distribution. At the same time a tenfold decrease of electron beam emittance in vertical direction from $\varepsilon_z=49$ pm·rad to $\varepsilon_z=4.9$ pm·rad does not change notably the radiation distributions. Thus we can conclude that in vertical plane the diffraction limit is achieved.

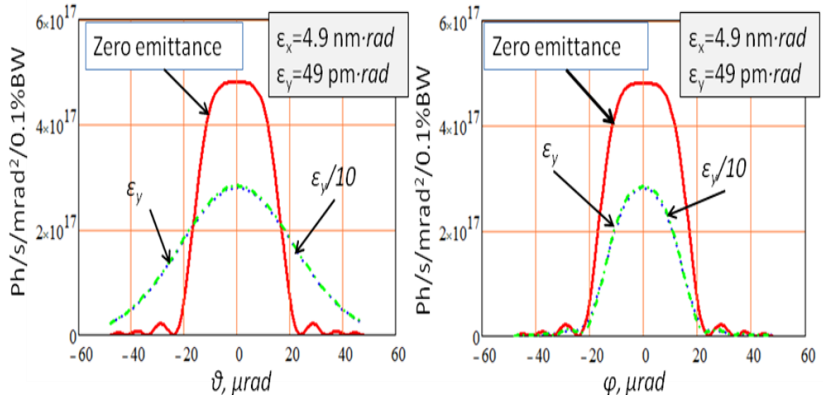

Figure .2: Horizontal (left) and vertical (right) angular distribution of fundamental harmonic.

4.11.3 **Edge Radiation**

The pole of each bending magnet is divided into two parts: the long one with the main field $B = 1.7$ T (bending radii of 490.54 cm) and a shorter one with a quarter field B/4=0.425 T. The shorter part of the magnetic pole with quarter field adjoins to the long straight section. The measured field of the bending magnets is shown in Fig. 3.

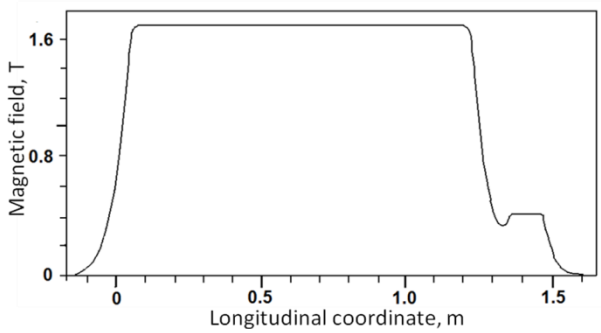

Figure 3: Magnetic field of Siberia-2 bending

Electromagnetic edge radiation (ER) is produced by a relativistic charged particle in its passage through the fringe fields at the bending magnet edges. In long-wavelength spectral range (at radiation wavelengths much longer than synchrotron radiation critical wavelength) its intensity is much higher than corresponding intensity of synchrotron radiation from uniform magnetic field of the same bending magnet [7, 8, 9]. Measurements of long-wave ER [10, 11] strengthened the belief that electron beam ER can be used as a bright source of electromagnetic radiation in the infrared - vacuum ultraviolet spectral range. Several infrared beam lines utilizing ER are now in operation [12, 13, 14].

The photons emitted at two adjacent bending magnets bounding a straight section, appear in the same narrow cone and are subsequently synchronized by the electron itself. This leads to the interference of ER. The interference manifests itself as additional oscillations in the radiation intensity distribution [15, 16, 17].

The distance between the down- and upstream edges of the bending magnets is 5340 mm. Synchrotron radiation with 7.2 keV critical energy from the homogeneous 1.7 T field is extracted by 10x10 mrad2 beam lines. The radiation distributions were

calculated at the following beam parameters [1]: 100 mA beam current, $\sigma_x = 0.72$ mm, $\sigma_{x'} = 0.11$ mrad, $\sigma_z = 0.014$ mm, $\sigma_{z'} = 0.056$ mrad. Since 0° port has a mask with entrance aperture 44 mm hor. × 16 mm vert. which is installed at 1580 mm downstream from the straight section, ER distributions were calculated in the plane of this mask. The numerical evaluations are carried out with the package of computer codes SMELRAD (SiMulation of ELectromagnetic RADiation) [6]. Simulations include so-called "velocity term" and near-field effects. The program computes step by step the electron's trajectory in the given magnetic field, which should be prescribed in the input file with the magnetic field data. It makes possible to use experimentally measured data. Electron beam emittance effects are calculated via numerical convolution.

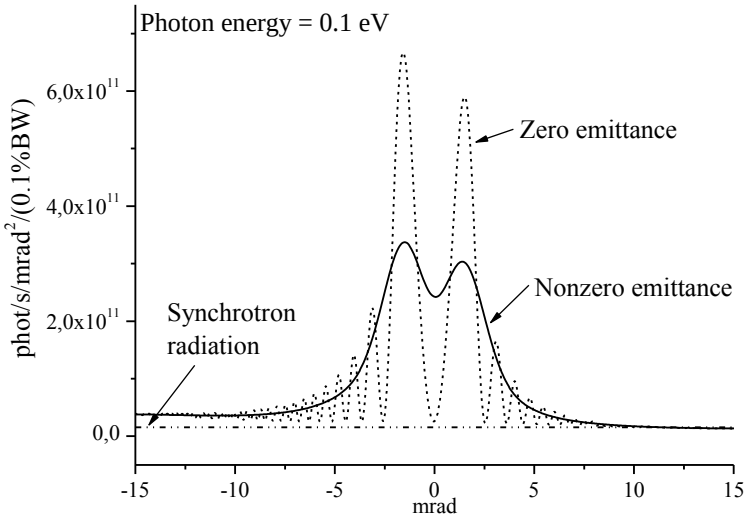

Figure 4: Horizontal distributions of ER in the median plane.

Figure 4 displays the computed flux density in the Siberia-2 electron orbit plane 1580 mm downstream of a straight section. The flux density with 0.1 eV photon energy is plotted versus horizontal angle. The calculations were carried out for the electron beam with zero and nonzero electron beam emittance. One can readily see that the nonzero emittance effects smooth out the fine interference oscillations. The distributions are substantially asymmetric about the straight section axis because of the relatively short distance from the screen to the straight section. The radiation distribution tends to the correspondent SR intensity as the distance from the straight section axis in the median plane increases.

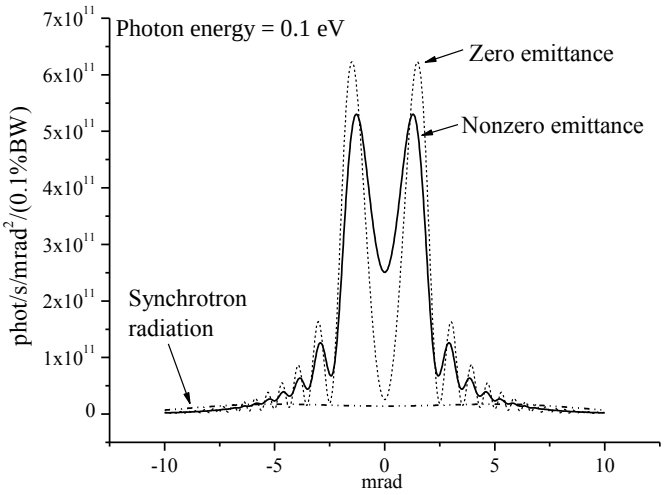

Figure 5: Vertical distributions of edge radiation.

The vertical cross sections of 0.1 eV ER distributions along straight section axis (with zero horizontal angle) is shown in Fig. 5. For comparison the correspondent distribution of synchrotron radiation from 1.7 T bending field is also plotted in the same figure. It is easy to see from Figs. 4 and 5 that ER is much brighter than synchrotron radiation in long wavelength spectral range.

In Fig. 6, the ER and synchrotron radiation fluxes into 10x10 mrad2 solid angle centered on the straight section axis are shown. From this figure we notice that for a given aperture the flux of edge radiation far exceeds the synchrotron radiation flux for the photon energies less than 350 eV.

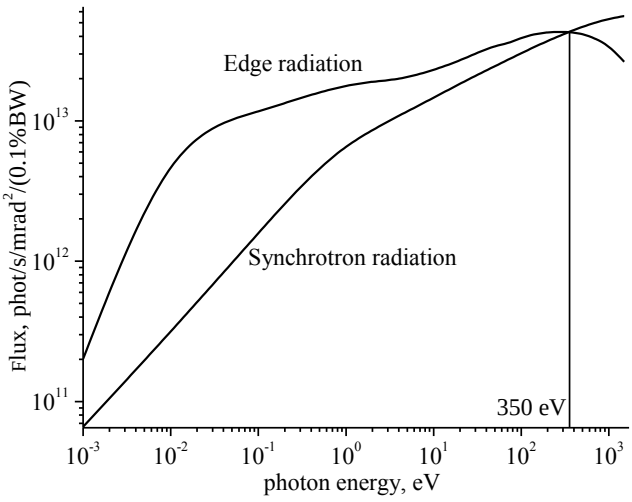

Figure 6: ER and SR fluxes into 10x10 mrad2 solid angle.

It is worthy of note that application of ER considerably reduces thermal and radioactive load on beam line elements. Indeed, the generation of hard X-rays is suppressed along the straight section because the magnetic field is depressed at fringe

regions. The total power generated in 1.7 Tesla bending field by the 100 mA electron beam into 10×10 mrad^2 solid angle is equal to 113 W. At the same time the total power generated by this electron beam along straight section axis into 28×10 mrad^2 (entrance aperture of mask) is equal to 18 W only.

4.11.4 **References**

1. V.V. Anashin, A.G. Valentinov, V.G. Veshcherevich et al., Nucl. Instr. and Meth. A282 (1989) 369.
2. Korchuganov V., Blokhov M., Kovalchuk M. et al., Nucl. Instr. Meth. A543 (2005) 14.
3. Rakowsky G., Aspenleiter J.J., Graves W.S. et al. Proceedings of 1997 Particle Accelerator Conference. 1997. V. 3. P. 3497.
4. Sasaki S. Proceedings of 2005 Particle Accelerator Conference. 2005. P. 982.
5. Kim D.E., Park K.H., Oh J.S. et al. Proceedings of 2007 Asian Particle Accelerator Conference. 2007. P. 190.
6. Smolyakov N.V. Nucl. Instr. and Meth. A467-468 (2001) 210.
7. E.G. Bessonov, Sov. Phys. JETP 53 (1981) 433.
8. O.V. Chubar, N.V. Smolyakov, J. Optics (Paris) 24, No. 3 (1993) 117.
9. O.V. Chubar, N.V. Smolyakov, Proc. of the 1993 IEEE PAC Conf., Washington (1993) 1626.
10. Shirasawa K., Smolyakov N.V., Hiraya A., Muneyoshi T. Nucl. Instr. and Meth. B199 (2003) 526.
11. Smolyakov N.V., Hiraya A. Nucl. Instr. and Meth. A543 (2005) 51.
12. Y.-L. Mathis, P. Roy, B. Tremblay et al., Phys. Rev. Letters 80 (1998) 1220.
13. T.E. May, R.A. Bosch and R.L. Julian, Proc. of the 1999 PAC Conf., New York (1999) 2394.
14. R.A. Bosch, R.L. Julian, R.W.C. Hansen et al., Proc. of the 2003 PAC Conf., Portland (2003) 929.
15. M.M. Nikitin, A.F. Medvedyev, M.B. Moiseev, Sov. Tech. Phys. Lett. 5 (1979) 347.
16. M.M. Nikitin, A.F. Medvedyev, M.B. Moiseev, V.Ya. Epp, Sov. Phys. JETP 52 (1980) 388.
17. M.M. Nikitin, A.F. Medvedyev, M.B. Moiseev, IEEE Trans. Nucl. Sci. NS-28 (1981) 3130.

4.12 Advance in the LEPTA Project

E.Ahmanova , V.Bykovsky, V.Kaplin, V.Karpinsky, A.Kobets,
V.Lokhmatov,V.Malakhov, I.Meshkov, V.Pavlov, A.Rudakov, A.A.Sidorin,
S.Yakovenko
JINR, Russia

M.Eseev, M.V.Lomonosov
Pomor State University, Russia

A.Kobets
Institute of Electrophysics and Radiation Technologies, Ukraine
Mail to: kobets@jinr.ru

4.12.1 **Introduction**

The Low Energy Positron Toroidal Accumulator (LEPTA) at JINR is close to be commissioned with circulating positron beam. The LEPTA facility is a small positron storage ring equipped with the electron cooling system and positron injector. The maximum positron energy is of 10 keV. The main goal of the project is generation of intensive flux of Positronium (Ps) atoms - the bound state of electron and positron, and setting up experiments on Ps in-flight. The report presents an advance in the project: up-grade of LEPTA ring magnetic system, status of the construction of positron transfer channel, and the electron cooling system, first results of low energy positron beam formation with ^{22}Na radioactive positron source of radioactivity of 25 mCi

4.12.2 **Lepta Ring Development**

The Low Energy Particle Toroidal Accumulator (LEPTA) is designed for studies of particle beam dynamics in a storage ring with longitudinal magnetic field focusing (so called "stellatron"), application of circulating electron beam to electron cooling of antiprotons and ions in adjoining storage electron cooling of positrons and positronium in-flight generation.

For the first time a circulating electron beam was obtained in the LEPTA ring in September 2004 [1]. First experience of the LEPTA operation demonstrated main advantage of the focusing system with longitudinal magnetic field: long life-time of the circulating beam of low energy electrons. At average pressure in the ring of 10-8 Torr the life-time of 4 keV electron beam of about 20 ms was achieved that is by 2 orders of magnitude longer than in usual strong focusing system. However, experiments showed a decrease of the beam life-time at increase of electron energy. So, at the beam energy of 10 keV the life time was not longer than 0.1 ms. The possible reasons of this effect are the magnetic inhomogeneity and resonant behaviors of the focusing system.

4.12.2.1 ***Magnetic and Vacuum System Improvements***

During March-May 2009 new measurements of the longitudinal magnetic field at solenoids connections were performed. According to the measurement results water cooled correction coils have been fabricated and mounted. As result, the inhomogeneity has been decreased down to $\Delta B/B \leq 0{,}02$ (Fig.1).

The new water cooled helical quadrupole lens was designed and fabricated that allowed us to improve significantly the vacuum conditions in the straight section.

In old design the distance between kicker plates was off 32 mm that limited the aperture. New kicker design allows us to increase aperture up to 120 mm.

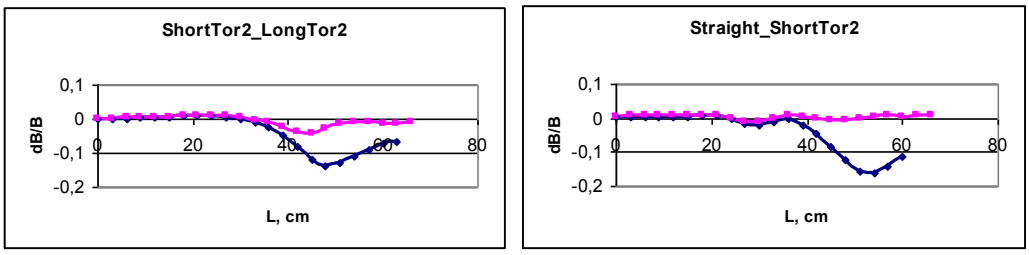

Figure 1: Magnetic field distribution along the toroidal solenoid axis**.**

4.12.2.2 *Testing after Upgrading*

After all the improvements and modifications the ring has been reassembled, the electron beam circulation has been obtained again and its life time has been remeasured. Typical life time dependence on electron energy, τe(Ee), has two slopes (Fig.2). The left one, where τe increases with Ee, is defined by electron scattering on residual gas. The right slope, descending with Ee, relates to violation of electron motion adiabaticity on inhomogeneities of solenoid magnetic field.

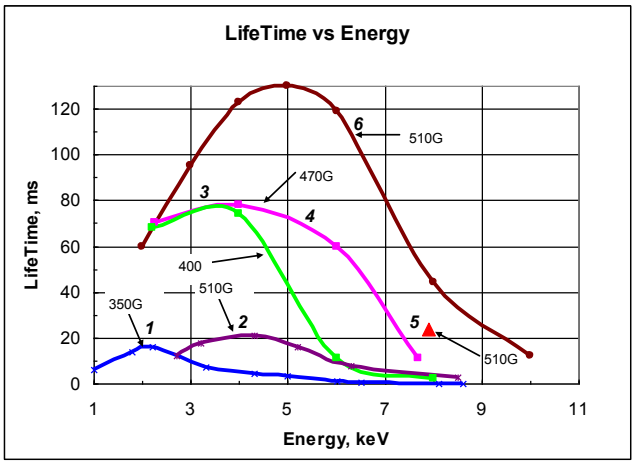

Figure 2: Lifetime vs electron energy**.**

The curves 1 and 2 were obtained in 2005, whereas the curves 3, 4 and the point 5 have been measured in June 2008. The curve 6 was measured in August 2009, after all modifications of the ring described above. One can see significant increase of the electron life time. Of the main importance is the increase of the life time (comparing with the values of the year 2005, 2008) in the energy range above 4 keV by 6÷10 times. It proves the necessity of a further improvement of the solenoid field homogeneity.

An essential influence of magnetic field quality on τe value is demonstrated in Fig. 3: the lifetime of 8 keV electrons increases significantly with correction coil current enhancement.

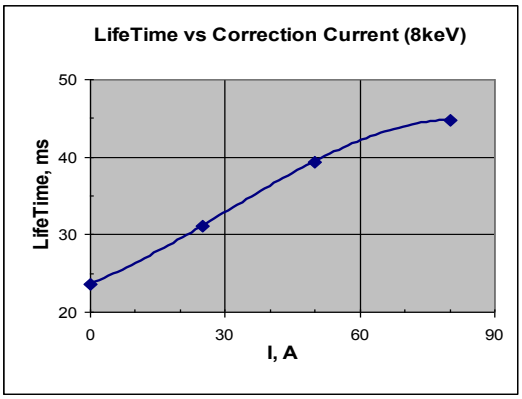

Figure 3: Lifetime vs correction coil current at electron energy of 8 keV.

4.12.2.3 *Electron Cooling System Construction*

The manufacturing of the system for generation, transportation and energy recovering of single pass electron beam has been completed. Test of the electron beam transportation from the gun to the collector begun in pulsed mode and continued in DC mode of the gun operation. Result is in Table 1.

Table 1. Parameters of electron cooling system.

Electron energy	**Current**		
	Ie, mA	**ΔIe, uA**	**ΔIe/Ie**
3	20	230	0,011
5	50	290	0,006
7	64	620	0,01
8,7	105	430	0,004

4.12.2.4 *Positron Transfer Channel*

The channel is aimed to transport positrons extracted from the trap of the injector (see below) and accelerate them up to 10 keV (maximum) in electrostatic field in the gap between the trap and the channel entrance. The designing and manufacturing of the channel elements was completed in 2010. The manufacturing of solenoids of the positron beam transfer channel is in progress presently.

4.12.3 **Test of the New Positron Source**

The slow monochromatic positron flux is formed from broad spectrum of positrons from radioactive isotope 22Na. The positrons with energy up to 0.54 MeV are moderated to the energy of few eV in the solid neon [2]. The neon is frozen on the copper cone surface where capsule with isotope is located (Fig.4).

22Na positron source of activity of 25mCi for LEPTA facility has been donated by iThemba LABS (RSA) and transferred to JINR in February 2008. After completion of the very long procedure of formalities it was mounted in the LEPTA injector and tested.

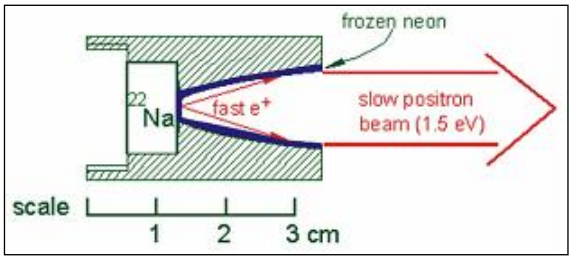

Figure 4: Positron moderation principle.

To detect slow positron flux we used microchannel plate (MCP) detector and scintillater detector both working by coincidence scheme and independently. Integral spectra of slow positrons were measured with MCP and electrostatic analyzer - a short drift tube suspended at variable positive potential. The fitting of the experimental results are presented (Fig. 5).

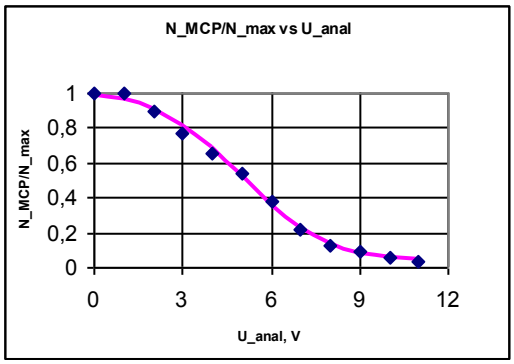

Figure 5: Gaussian fitting of positron energy spectrum curve measured at T = 7,35 K, d = 10 mcm, (dN/dE)max = 5.5 eV, spectrum width σ = 2.3 eV.

Maximum flux of slow positrons determined by standard method for coincidence scheme was equal $N_{max} \approx 1.5 \cdot 10^5$ positrons/ sec**.**

4.12.4 **The Positron Trap**

When slow positron beam is formed, it enters the Penning-Malmberg trap where the positron cloud is accumulated [3]. The trap is a device which uses static electric and magnetic fields to confine charged particles using the principle of buffer gas trapping. The confinement time for particles in the Penning-Malmberg traps can be easily extended into hours allowing for unprecedented measurement accuracy. Such devices have been used to measure the properties of atoms and fundamental particles, to capture antimatter, to ascertain reaction rate constants and in the study of fluid dynamics. The JINR positron trap (Fig. 6) was constructed to store slow positrons and inject positron bunch into the LEPTA ring.

The research of the accumulation process was carried out using electron flux. For this purpose the test electron gun allowing to emit dN/dt = 1*106 electrons per second with energy 50 eV and spectrum width of a few eV was made. These parameters correspond to slow monochromatic positron beam which we expect from a radioactive source at activity of 50 mCi.

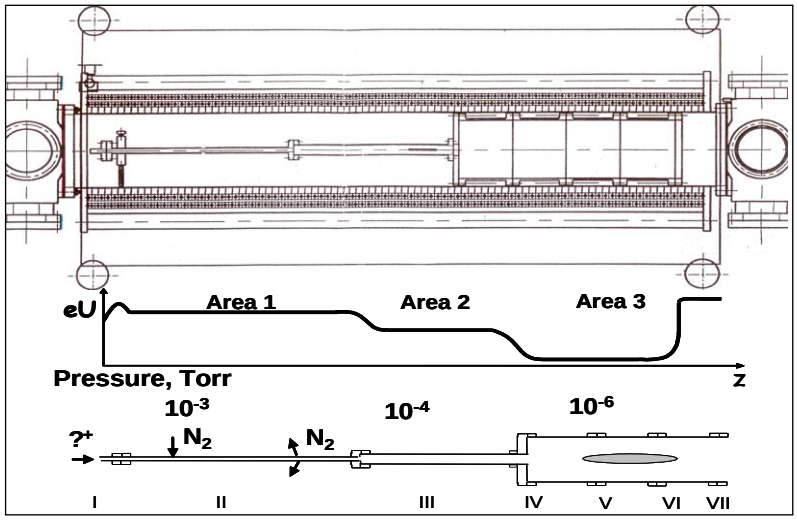

Figure 6: Assembly drawing of the positron trap (upper picture), potential and pressure distributions along the electrode system**.**

Electron accumulation in the trap with application of rotating electrical field so called "rotating wall" (RW) [4], was studied during December 2006 and repeated in July 2009. The test electron beam shrinking was observed when RW parameters were optimized (Fig.7).

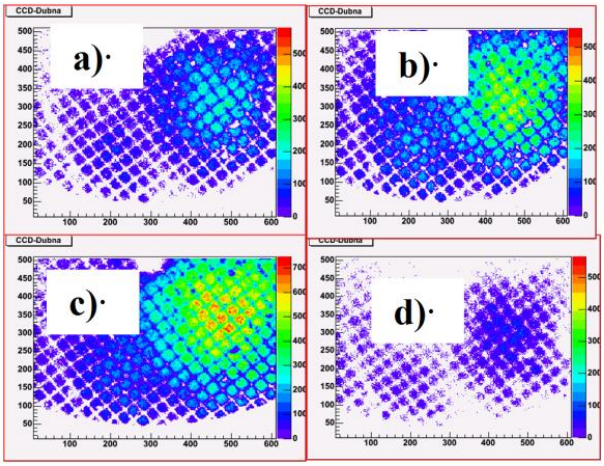

Figure 7: Profiles of the stored test electron beam at different storage time: a) 5s, RF On; b) 20s, RF On; c) 50s, RF On, d) 30s, RF Off**.**

4.12.5 **The Positron Injector**

In summer 2010 the slow positron source and the trap have been assembled. The first attempts of slow positron storage were performed (Fig. 8) and stored positrons were extracted to the collector.

Upt is the amplitude of the signal from the phototube (PT), RW amplitude is equal to 0.5 V.

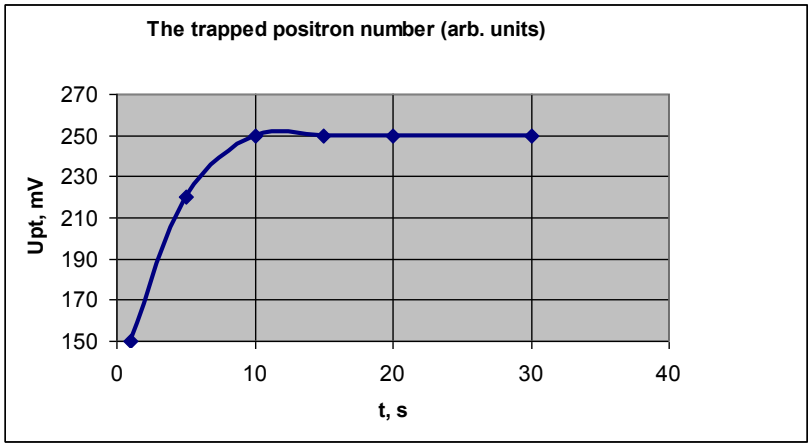

Figure 8: The trapped positron number vs storage time.

4.12.6 **Concluding Remarks**

The development of the LEPTA project is approaching the stage of experiments with circulating positron beam. All main elements of the ring and the injector are ready and have been tested.

All work is supported by RFBR, grant No. 09-02-00084.

4.12.7 **References**

1. A. Kobets, et. al., Status of the LEPTA project, proceeding of Beam Cooling and Related Topics, http://accelconf.web.cern.ch/accelconf/
2. A. P. Mills, Jr. and E. M. Gullikson, "Solid Neon Moderator for Producing Slow Positrons". Appl. Phys. Lett. 49, 1121 (1986)
3. M. Amoretti et al., The ATHENA antihydrogen apparatus, Nucl. Inst.Meth. Phys. Res. A 518 (2004) 679-711
4. C.M. Surko, R.G. Greaves, Radial compression and inward transport of positron plasmas using a rotating electric field, Phisics of plasmas, 8 (2001), 1879-1885.

4.13 Present Status of FLNR (JINR) ECR Ion Sources

S.Bogomolov, A.Efremov, V.Loginov, A.Lebedev, N.Yazvitsky, V.Bekhterev,
Yu.Kostukhov, G.Gulbekian, B.Gikal, V.Drobin and V.Seleznev
JINR, Dubna, Russia
Mail to: bogomol@nrmail.jinr.ru

4.13.1 **Introduction**

Main theme of FLNR JINR is super heavy elements research. From 2000 up to 2010 more than 40 isotopes of elements 112, 113, 114, 115, 116, 117, 118 were synthesized in the laboratory.

At present four isochronous cyclotrons: U-400, U-400M, U-200 and IC-100 are in operation at the JINR FLNR. Three of them are equipped with ECR ion sources. In the DRIBs project for production of accelerated exotic nuclides as ^{6}He, ^{8}He etc. the U-400M is used as radioactive beam generator and U-400 is used as a post-accelerator.

Layout of FLNR accelerators complex is presented at Fig.1 [1]. Red stars indicate the location of the ECR ion sources.

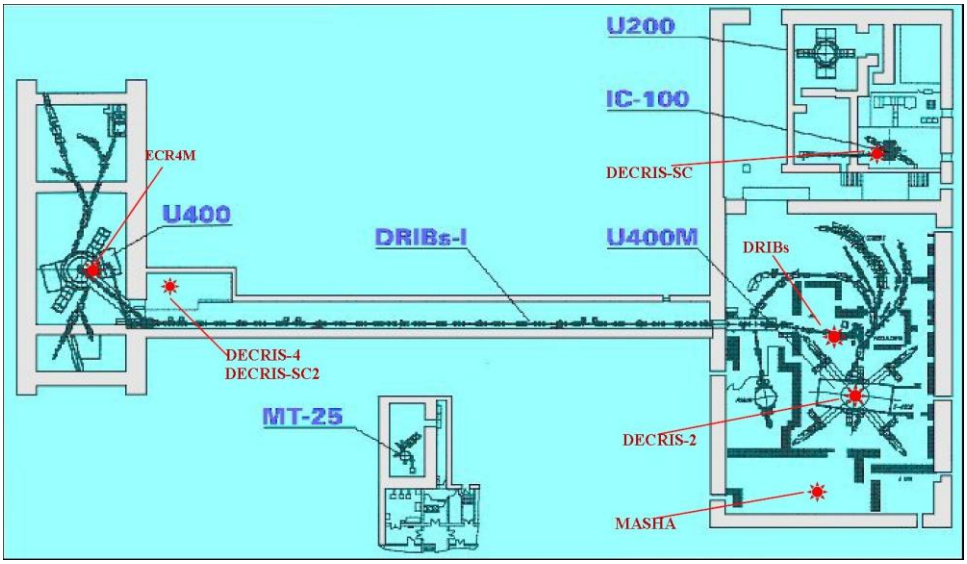

Figure 1: Layout of FLNR JINR accelerator complex. Red stars indicate the location of the ECR ion sources.

4.13.2 **DECRIS-2 Ion Source**

The ion source DECRIS-2 is in regular operation at the U400M cyclotron since 1995 [2]. Nowadays the main physical setups at the cyclotron U400M are the fragment-separators ACCULINNA and COMBAS. Besides, the accelerator is used for the secondary beam production at the DRIBs facility. Intensive beams of ^{7}Li, ^{11}B, ^{13}C, ^{15}N, ^{18}O ions with energies of 35 -55 MeV/nucleon on the U400M cyclotron provide good possibilities for generation secondary beams of ^{6}He, ^{15}B, ^{9}Li, ^{11}Li, ^{12}Be, ^{14}Be, ^{8}He. The intensity of light ion beams such as ^{7}Li or ^{11}B on the targets is $(3\div5)10^{13}$ pps.

Typical intensities of ion beams, produced by DECRIS-2 source, are listed in Table 1.

Table 1: Typical intensities of ion beams (eμA), produced by DECRIS-2 source

Ion	***Li***	***B***	***O***	***Ar***	***Kr***	Xe
2+	300					
3+	70	200				
4+		80				
5+			660			
6+			450			
7+			40			
8+				600		
9+				340	100	
18+						45
20+						40

At recent time the cyclotron ensures two acceleration modes:

- acceleration of high-energy ion beams up to 100 MeV/nucleon;
- acceleration of low-energy ion beams (the mode providing the beam energy of 4.5-9 MeV/nucleon was implemented in 2008). This low energy ion beams (such as ^{48}Ca) will be used for synthesis and study of new elements.

4.13.3 **The ECR4M Ion Source**

The ECR4M source and the axial injection system were assembled and commissioned in 1996. First accelerated Ar beam was produced in November 1996 [3]. The main goal was to provide the intense beam of the ^{48}Ca ion beam for the experiments on synthesis of super heavy elements at a minimal consumption of this enriched and expensive isotope. First experiment on the synthesis of super heavy elements with the beam of ^{48}Ca was performed in November 1997. Since that total operation time of the U400 amounts more than 70000 hours. About 66% of this time was used for acceleration $^{48}Ca^{5+,6+}$ ions for research on synthesis and investigation of properties of new elements. The production of the ^{48}Ca ion beam was performed with the use of micro oven with the maximal temperature of 900 °C and thin cylindrical Ta sheet placed inside the discharge chamber to prevent the condensation of metal at the chamber wall [4]. In a long-term operation an average consumption of calcium is about of 0.4÷0.8 mg/h depending on the required beam intensity.

The modernization of the U400 axial injection, which included sharp shortening of the injection channel horizontal part, was performed. These changes allow us to increase the $^{48}Ca^{18+}$ ion intensity at the U400 output from 0.9 to 1.4 pμA

According to the plans of the reconstruction of the U400 cyclotron (U400R project) the project of the modernization of the ECR4M source was developed. This modernization include the increase of the plasma chamber diameter from 64 to 74 mm; production of the higher magnetic field in the injection region by insertion an iron plug in the injection side; waveguide UHF injection into plasma chamber. The modified magnetic structure of the ECR4M and the axial magnetic field distribution are shown at Figure 2.

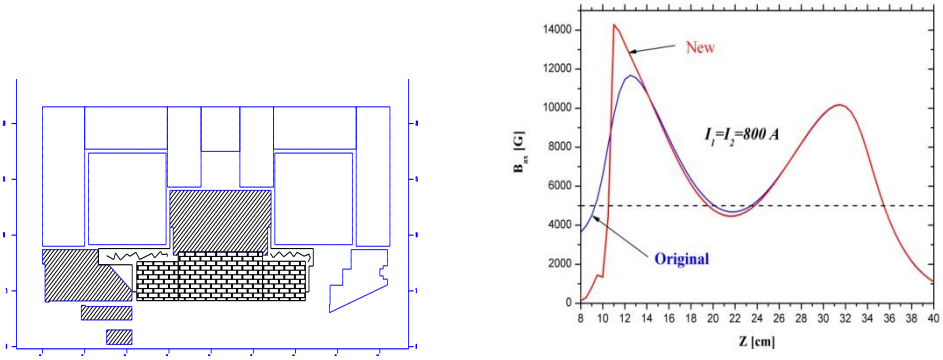

Figure 2: The modified magnetic structure of the ECR4M source (left) and axial magnetic field distribution (right).

4.13.4 **DECRIS-4 Ion Source**

The DECRIS-4 ion source [5] was designed for the use as an injector of heavy multiply charged ions for the U-400 cyclotron as well as a “charge breeder” for the

second phase of the DRIBs project. The design of the magnetic structure of the source was based on the idea of the so-called "magnetic plateau". The axial magnetic field is formed by three independent solenoids enclosed in separated iron yokes. Since 2005 the source is in operation at the test bench and is used for the experiments in the solid state physics and for beam development.

Test experiments on production of Ti ion beam were performed. The best results were obtained using MIVOC method with $(CH_3)_5C_5Ti(CH_3)_3$ compound, first used by Jyvaskyla group [6]. More than 60 μA of $^{48}Ti^{5+}$ were produced in stable mode, but there is a problem in synthesizing such a compound from a small quantity of enriched ^{50}Ti. Also the titanium isopropoxide was tested with MIVOC method, but the results were very pure, not more than 1 μA of $^{48}Ti^{5+}$ were produced.

Also TiF_4 was tested using the micro oven. The compound was loaded into the crucible with thin capillary, and micro oven was moved further from the plasma chamber. About 10÷20 μA of $^{48}Ti^{5+}$ were obtained in stable mode of operation, the further increase of intensity leads to instability of source regime due to overheating of crucible by plasma.

4.13.5 **DECRIS-SC Ion Source**

DECRIS-SC ion source [7] has been designed to be used as an injector for the IC-100 compact cyclotron. DECRIS-SC is a hybrid type electron cyclotron resonance ion source using permanent magnet hexapole, providing the radial magnetic field at the plasma chamber wall of 1.3 T, and a set of four superconducting solenoids to make min-|B| structure suitable for operation up to 28 GHz. The compact refrigerator of Gifford-McMahon type is used to cool the solenoid coils. At present the operating frequency of the source is 18 GHz.

After modernization the cyclotron is able to accelerate such ions as Kr^{15+}, Xe^{22+} up to energies of about 1 MeV/n

Since May 2004 the source is in regular operation at the IC-100 cyclotron for production of polymer membranes and solid state physics. Accelerated beam currents are listed in Table 2.

Table 2: Typical intensities of ion beams (eμA), accelerated at the IC-100 cyclotron

Ion	***A/Z***	Current, μA
$^{22}Ne^{4+}$	5.5	0.7
$^{40}Ar^{7+}$	5.714	2.5
$^{56}Fe^{10+}$	5.6	0.5
$^{86}Kr^{15+}$	5.733	2
$^{127}I^{22+}$	5.773	0.25
$^{132}Xe^{23+}$	5.739	1.2
$^{184}W^{31+}$	5.9355	0.035

4.13.6 **DECRIS-SC2 Ion Source**

Using the experience obtained during construction and operation of the DECRIS-SC source the new source DECRIS-SC2 was developed [8]. The source is planned to be used at the U-400M cyclotron to replace the conventional ECR ion source DECRIS-2. The main goal of the DECRIS-SC2 source is the production of more intense beams of heavy ions in the mass range heavier than Ar. For ECR plasma heating the existing microwave system (14 GHz) will be used.

The design of the superconducting magnet system of the new source differs essentially from the previous source. To decrease the weight and dimensions of the system it was decided to produce the vacuum vessel from chromium plated soft steel, so it will simultaneously serves also as a magnetic yoke. The magnetic field is formed by a set of four coils, magnetic yoke and iron plugs.

The superconducting magnet system passed the full test. The axial magnetic field distribution is shown at Fig. 3, the currents of the coils are shown in the Figure insert. The source is completely assembled and installed at the test bench for beam tests.

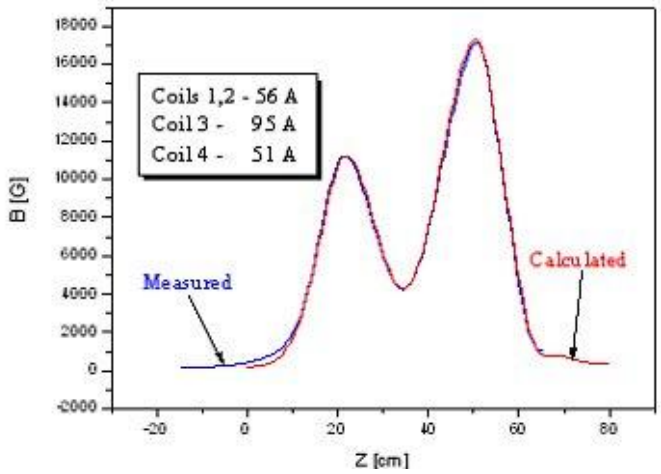

Figure 3: Axial magnetic field distribution of the DECRIS-SC2 ion source

4.13.7 **ECR Ion Sources for Radioactive Ion beams**

The DRIBs (Dubna RIB) project has been running since 2002 [9]. The primary ion beams (^{7}Li or ^{11}B) from U400M used for production nuclides as ^{6}He, ^{8}He at the target (Be or C). The produced radio-nuclides transported from hot catcher by dissision into ECR ion source [10] where are ionized. The 2.45 GHz ion source is dedicated for the production of singly charged radioactive ion beams. The magnetic configuration of the source is made with three radially magnetized permanent magnet rings. That allows to create pseudo-closed resonance surface.

For the primary beam (^{7}Li) intensity of 3 pμA the intensity of accelerated ^{6}He beam reaches of 5 10^{7} pps.

The similar type of the ECR source is used at the MASHA (Mass Analyser of Super Heavy Atoms) setup. The magnetic configuration of this source is made with two permanent magnet rings. The easy axis of the each magnet ring is directed along the axis of the magnetic system.

4.13.8 **DECRIS-5 Ion Source for DC-110 Cyclotron Complex**

The project of the DC-110 [11] cyclotron facility to provide applied research in the nanotechnologies (track pore membranes, surface modification of materials, etc.) has been designed by the Flerov Laboratory of Nuclear Reactions of the Joint Institute for Nuclear Research (Dubna). The facility includes the isochronous cyclotron DC-110 for accelerating the intensive Ar, Kr, Xe ion beams with 2.5 MeV/nucleon fixed energy. The cyclotron has 2m pole diameter, and to provide the energy of 2.5 Mev/nucleon the accelerated ions should have the mass to charge ratio about of A/Z = 6.6, that is $^{40}Ar^{6+}$, $^{86}Kr^{13+}$ and $^{132}Xe^{20+}$. The required intensity of the ion beam produced by the source is determined as about of 150÷300 eμA for $^{132}Xe^{20+}$. Therefore the main parameters of the source were choosed as listed in the Table 3. The magnetic field of the source will be created by the three copper coils and permanent magnet hexapole.

Table 3: Main parameters of the DECRIS-5 ion source

UHF frequency	***18 GHz***
Injection side magnetic field	2.2 T
Extraction side magnetic field	1.35 T
Radial magnetic field	1.3 T
Plasma chamber inner diameter	80 mm
Maximal power consumption	160 kW

4.13.9 **References**

1. G.Gulbekian and CYCLOTRONS Group, “Status of the FLNR JINR Heavy Ion Cyclotrons,” in Proc. Of 14th Int. Conf. on Cyclotrons and Their Applications (Cape Town, South Africa, 1995), pp. 95–98.
2. A.Efremov, V.B.Kutner, A.N.Lebedev, V.N.Loginov, N.Yazvitskiy and H.Zhao. “Dubna electron cyclotron resonance ion source (DECRIS)-14-2: Results of the first operation” Rev. Sci.Instr. 1996, 67(3) p.980 – 982.
3. Yu.Ts.Oganessian et al. “Axial injection system for the U-400 cyclotron with the ECR-4M ion source”. JINR FLNR Scientific Report 1995 – 1996 Heavy Ion Physics. E7-97-206, Dubna 1997, p.270 – 276.
4. V.B.Kutner, S.L.Bogomolov, A.A.Efremov, A.N.Lebedev, V.Ya.Lebedev, V.N.Loginov, A.B.Yakushev, and N. Yu. Yazvitsky, Rev. Sci.Instrum. 71, p.860-862, 2000.
5. M.Leporis, S.Bogomolov, A.Efremov and G.Gulbekian “The new ECR ion source DECRIS-4 (project)” Rev. Sci. Instr. 75 (5), 2004, p. 1492 – 1493
6. H. Koivisto, J. Arje, R. Seppala, M. Nurmia “Production of titanium ion beams in an ECR ion source” NIM B, 187 (2002), p.111-116
7. A.Efremov et al. “Status of the ion source DECRIS-SC” Rev. Sci. Instrum. 77, 03A301, 2006.
8. V.V.Bekhterev et al. “The project of the superconducting ECR ion source DECRIS-SC2” High energy physics and nuclear physics (HEP & NP) A Series Journal of the Chinese Physical Society (C) vol.31, Supp.I, Jul., 2007, p. 23 - 26
9. B. N. Gikal, S. L. Bogomolov, S. N. Dmitriev, et al.,
10. Dubna Cyclotrons - Status and Plans,” in Proc. of Cyclotron04 Int. Conf. (Tokyo, Japan, 2004).
11. A.Efremov, V.Bekhterev, S.Bogomolov et al., “The 2.45 GHz ECR ion source for the first stage of the DRIBs project”, NIM B 204 (2003) p. 368 – 371

12. Gikal B.N. et al. The Project of the DC-110 Heavy Ion Cyclotron for Industrial Application and Applied Research in the Nanotechnology Field. P9-2009-111. Preprint of the Joint Institute for Nuclear Research. Dubna, 2009

4.14 55 MeV Special Purpose Race-Track Microtron Commissioning

A.I.Karev, A.N.Lebedev, V.G.Raevsky
P.N.Lebedev Physical Institute, RAS, 119991 Moscow, Russia

A.N.Ermakov, A.N.Kamanin, V.V.Khankin, N.I.Pahomov, V.I.Shvedunov
SINP MSU, 119992 Moscow, Russia

N.P.Sobenin
MEPhI, Kashirskoe shosse 31, 115409 Moscow, Russia

L.Brothers, L.Wilhide,
Valley Forge Composite Technology Inc. (VFCT)
50 East Rivercenter Blvd., Suite 820, Covington, KY, USA
Mail to: a_ermak1978@mail.ru

Abstract:

Results of Lebedev Physical Institute RAS 55 MeV special-purpose racetrack microtron (RTM) commissioning are presented. RTM is intended for photonuclear detection of hidden explosives based on initiation of photonuclear activation and consequent registration of secondary gamma-rays penetrating possible screening substances.

This work was supported by CRDF Grant #RP0-10732-MO-03 (LLNL)

4.14.1 **Introduction**

The purpose of the work consists in development of an effective photonuclear detector of hidden explosives to be used under stationary conditions and in mobile systems for searches of field mines. The detector consists of a source of high-energy gamma - radiation and counters fixing the secondary radiation from decay of short-living isotopes formed in explosives due to reactions with nitrogen and carbon nuclei [1]. The gamma source is based on a specialized microtron (RTM) for energy of 55 MeV. A RTM photo is presented in Fig. 1, main RTM A RTM photo is presented in Fig. 1, main RTM parameters reached by commissioning are listed in Table 1.

RTM has been built following a classical scheme with two 1 T end magnets and a standing wave linac between them providing 5 MeV energy gain per pass. A 50 keV beam from an electron gun is injected into linac through a 450 magnet and a solenoidal lens. The 5 MeV electron beam after the first acceleration is reflected by the end magnet field back to the linac axis and is accelerated up to 10 MeV - the energy sufficient to bypass the linac at the next turn. The beam is extracted from the last orbit 1with a dipole of 17.50 deflecting angle. More details about the RTM scheme can be found in [2].

Figure 1: RTM photo.

Table 1: RTM parameters

Output energy	55 MeV
Output pulse current	10 mA
Repetition rate	5 – 50 Hz
Number of linac passages	11
Energy gain / turn	5 MeV
Current pulse length	5 μs
Operating frequency	2856 MHz
End magnet field	1.0 T
Maximum RF power	2.5 MW
Orbit circumference increase / turn	1 λ

4.14.2 **RTM Systems**

4.14.2.1 ***RF System***

The RF system is based on a multi-beam klystron KIU-168 [3] with a rare earth permanent magnet focusing system providing 6 MW/6 kW pulsed/average power at 2856 MHz. The klystron is compact, its high voltage pulse amplitude is only 54 kV, so it does not need oil insulation and can be installed under the RTM table. A pumping port, a vacuum window, and a circulator are installed between the linac and the klystron.

The non-vacuum part of the waveguide tract is filled with SF6 at 2 bars. Parameters of the vacuum window and the circulator by commissioning restricted the maximum RF power transported to the linac by 2.5 MW and thus restricted a maximum exit pulsed beam current by 10 mA. The klystron is fed by a “hard” modulator [4] with pulse duration up to 15 μs. To simplify the RF system we use a self-oscillation mode of operation with linac structure included in a feedback loop [5]. Optimal conditions for self-oscillations and for RF power level regulation are controlled with a phase shifter and an attenuator installed in the feedback loop. In Fig. 2 the klystron current, the high voltage and RF field pulses are shown. The 8 μs high voltage pulse duration is set externally. The delay of about 3 μs between the high voltage front and RF pulses is the time required for building-up self-oscillations from the noise. This time can be decreased by adding a low power “igniting” RF signal to the feedback loop.

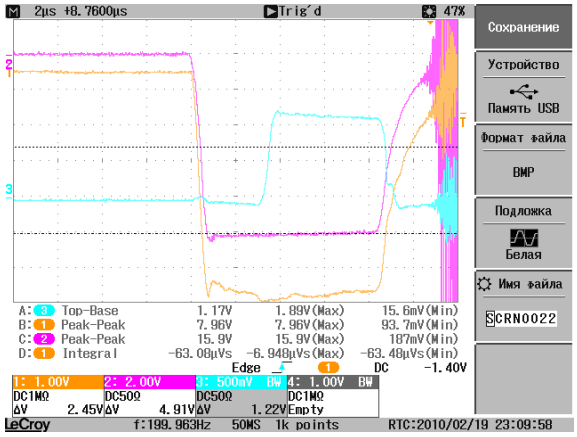

Figure 2: Klystron current (1), high voltage (2), and RF field (3) pulses**.**

4.14.2.2 *Electron Gun*

A three electrodes electron gun with a 8.6 mm diameter tungsten impregnated cathode for nominal current of 400 mA and beam energy of 50 keV is used in RTM (Fig. 3(a)). By varying intermediate anode, voltage the gun current can be controlled within ±100 mA.

(a) (b)

Figure 3: (a) Electron gun, (b) magnets power supply.

The electron gun is fed with the same modulator as the klystron is. A voltage at the intermediate anode regulated in discrete steps is provided from the high voltage divider installed inside the RTM table. The electron gun is pumped with 5 l/s ion pump, vacuum in the gun being better than 10-5 Pa.

4.14.2.3 *Magnets Power Supply System*

To feed the coils of the end magnets current sources Genesys™ type form TDK-LAMBDA [6] are used. Two GEN 12.5-60 current sources feed reverse pole coils while two GEN 60-55 sources are used for the coils of the main poles. The rest magnetic

elements are fed with a multichannel current source of 42 channels designed by Protom company [7]. Magnets power supply system is shown in Fig. 3(b).

4.14.2.4 *Control System and Beam Diagnostics*

RTM control system has been built using standard National Instruments modules for signals control and LabView software [8] for user interface.

Beam diagnostic is provided by beam current monitors (BCM) of 5 mV/mA sensitivity installed at each orbit and at the linac axis, by synchrotron radiation, and by transition radiation. To observe synchrotron radiation from RTM orbits with CCD camera a glass window in the vacuum chamber was installed at the end magnets. Accelerated beam was extracted to atmosphere through 20 μm thick Ti foil. Transition radiation generated by the beam crossing the foil was registered by a CCD camera. Extracted beam absorbed in a Faraday cup provides a beam current signal.

4.14.3 **RTM Tuning**

Before RTM tuning the distance between the edges of the end magnet main poles was set according to calculated value with accuracy ±0.1 mm. The level of the main and reverse field was adjusted to calculated values using a calibrated Hall probe with accuracy 0.1% and 1%, respectively. Care was taken to decrease hysteresis phenomena influence on the field level when switching on/off current sources.

The main factors influencing on the beam propagation in the transverse plane of RTM are end magnets field errors, parasitic and strayed magnetic fields, an inaccuracy in magnets and linac positioning, an inaccuracy in longitudinal beam dynamics tuning. In longitudinal plane, the main factor is uncertainty of the accelerating field level which absolute value cannot be well determined by RF diode calibration or by measuring of linac dissipated RF power via cooling water temperature and flow.

To decouple longitudinal and transverse plane tuning we calibrated the RF diode signal against beam energy using end magnets combined with BCMs placed at 1st and 2d orbits. To accomplish this we calculated electron trajectories in the end magnet for various currents in the coils keeping constant a ratio of the main and reverse fields. Then we found a correspondence between the electron energy and the coils current when the beam passed through the centre of the first and the second orbit tubes.

At the second step, we measured the beam energy spectrum after the first acceleration using 1st orbit BCM for various settings of the accelerating field. After the first acceleration the beam is reflected back to the linac by the end magnet (M1) moving counter clockwise. In order to enter 1st orbit tube at lower magnetic field the beam must move clockwise, so to measure spectrum we reversed the polarity of the M1 coils. In Fig. 4 at the left beam spectra measured after the first acceleration at various field levels are compared with a spectrum found in RTM beam dynamics simulation (black dots). The energy resolution of spectrometer is defined by the inner diameter of the tube and is rather poor. We fixed the RF diode voltage for pink curve as one corresponding to nominal accelerating field.

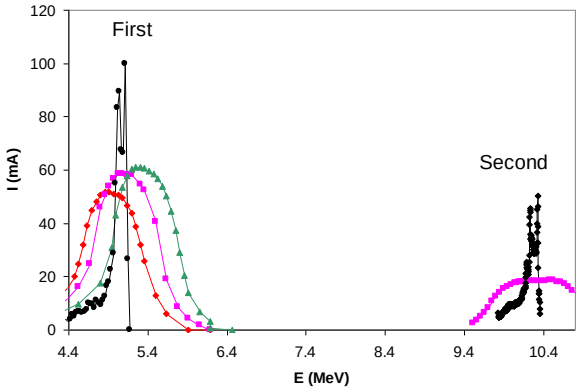

Figure 4: Measured beam spectra after first and second acceleration compared with calculated**.**

At the next step, we set the proper polarity and level of the M1 field, so the beam was reflected back to the linac and accelerated in opposite direction. Than with second magnet (M2) and 2d BCM we controlled beam energy (right pink points curve at Fig. 4). One can see that the measured beam spectrum maximum (~ 10 MeV) well coincides with maximum of spectrum found in beam dynamics simulation (black points). From these results, it follows that the beam enters the linac after reflection by M1 in a proper phase.

Note that after the first acceleration the beam current is about 50-60 mA (this value is defined by the gun current and injection system tuning), while after the second one it falls down to about 16 mA, an essential part of the low energy tail of the beam being stopped by the linac wall. Current losses are somewhat higher than following from calculations – compare amplitudes of calculated spectra (which are in arbitrary units).

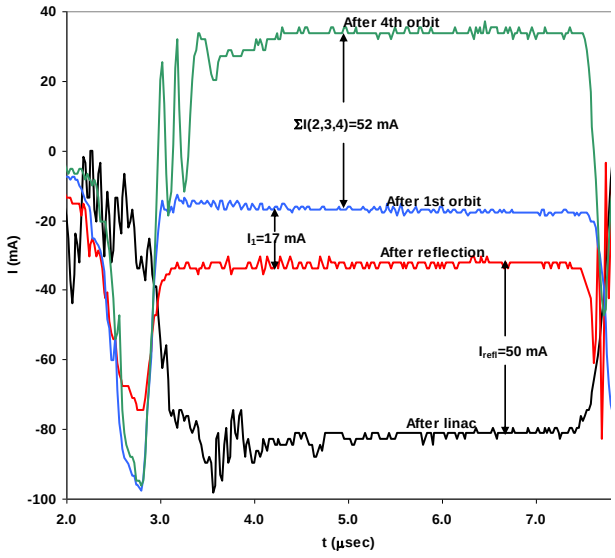

Figure 5: Signals from BCM installed at linac axis.

Additional valuable information about beam reflection by M1 and following acceleration can be obtained from BCM installed at the linac axis between the linac and M1 magnet. In Fig. 5 signals from BCM obtained under different conditions are shown.

Black curve was obtained with M1 magnet off. Beam current coming out of the linac in this case is about 80 mA. After M1 switching on a current registered by BCM decreased for about 50 mA – this was the beam current reflected from M1 and passing BCM in opposite direction. After first orbit the BCM signal dropped to 17 mA and after the forth additionally to 52 mA (meaning a sum of the 2, 3 and 4th orbits current) changing signal polarity. From these data it follows that RTM can be tuned with minimal beam losses after 1st orbit.

In order to get beam transmission shown in Fig. 6 currents of the steering coils installed at the injection path and at RTM orbits were adjusted using information from BCM. We should note that the RF power necessary to accelerate 16 mA beam up to the last orbit exceeds the damage limit of the vacuum window and circulator. So for further RTM tuning the beam current was decreased by decreasing the gun current and by deliberate current losses in the injection path.

In succeeding, RTM tuning by steering coils additional information from CCD camera viewing synchrotron radiation (Fig. 6) and from a Faraday cup was used.

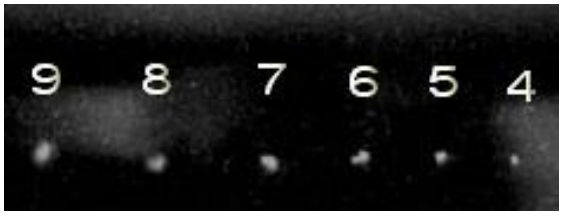

Figure 6: Synchrotron radiation beam image for 4-9 orbits.

4.14.4 **Conclusion**

As a result of RTM tuning the pulsed beam current of 10 mA was obtained at RTM output. This value was limited by parameters of available RF elements. A new 6 MW window and circulator have been purchased. After their installation, a higher beam current is expected.

4.14.5 **References**

1. A.I.Karev, V.G.Raevsky, J.A.Konyaev et al, Patent RF #2226686. Filed Dates: August 14, 2002, RF.
2. A.I. Karev, A.N. Lebedev, V.G. Raevsky et al, RuPAC-2008, p.124
3. I.A. Frejdovich, P.V. Nevsky, V.P. Sakharov et al, Proceedings of IVEC-IVESC 2006, Report N13.5
4. N.V. Matveev and S.F. Kravtsov, in Conference Record of the Twenty-Fifth International Power Modulator Symposium, 2002 and 2002 High-Voltage Workshop, p. 378
5. A.N. Ermakov, D.I. Ermakov, B.S. Ishkhanov et al, Instruments and Experimental Techniques, Vol. 45, No. 4 (2002) 482–489
6. http://www.us.tdk-lambda.com
7. http://www.protom.ru
8. http://www.ni.com

4.15 First Radiocarbon Measurements at BINP AMS

S.A. Rastigeev, A.R. Frolov A.D. Goncharov, V. F. Klyuev, S.G. Konstantinov,
E.S. Konstantinov, L. A. Kutnykova, V. V. Parkhomchuk, M.V. Petrichenkov,
A. V. Petrozhitskii
BINP, Novosibirsk, Russia
Mail to: s.a.rastigeev@inp.nsk.su

Abstract:
Present status of the BINP accelerator mass spectrometry (AMS) facility is described. The results of experiments for beam selection and radiocarbon concentration analysis in trial samples are presented.

4.15.1 **Introduction**

The AMS is mainly dedicated for dating of archaeological, paleontological and geological samples by measurements of the ratio between carbon isotopes.

The BINP AMS facility [1] includes negative ion source, folded type vertical electrostatic tandem accelerator, magnesium vapors stripper [2], the high-energy and low-energy beam lines with analyzers, time-of-flight final detector [3].

The negative ion beam is horizontally extracted from the ion source. Then the beam is vertically injected into the low energy accelerating tube through injection channel with 90° magnet. The negative ions are accelerated to the positively charged high voltage terminal and stripped to charge state 3+ in magnesium vapors stripper. Then they pass through the 180^0 electrostatic bend and then again are accelerated vertically into the high energy accelerating tube to the ground potential. Then ions are horizontally put to the final detector through high-energy channel with 90° magnet.

The most distinguishing feature of our AMS machine is the use of additional electrostatic separator of ion beam, located inside the terminal. Interfering isobaric molecules are destroyed by collisions in the stripper into the terminal and are selected immediately after the stripping process. It is important to decrease the background from molecular fragments before the second stage of acceleration [4], because the energy of fragments is always less than the ion energy (at this moment). The next important distinguishing feature is magnesium vapours stripper instead of the gas stripper. The gas flow into the accelerator tubes leads to big energy spread in the beam thus limiting the sensitivity and accuracy of spectrometer. The molecular destruction and ion recharging by magnesium are localized into the hot tube of the stripper.

4.15.2 **BINP AMS Facility Modifications**

Now the AMS facility created at BINP SB RAS is installed at CCU “Geochronology of the Cenozoic era”. The accelerator is placed into underground room with radiation shielding. The inner size of the room is 6 x 6 x 7.5 meters. The basic parts of electronic devices are located outside of the shielding room and connected with accelerator elements. The local equipment of the water cooling, compressed air and gas transfer system has been installed.

The 500 kV terminal voltage was achieved with 1 atm atmospheric air into pressure tank (without insulating gas). The equipment for gas filling and drying was not used,

but the silica gel was placed directly into the tank. Initially, the terminal voltage was limited by the water vapor condensate on the cool surface of the gas turbine feeding dielectric tube, located along the accelerator column. This tube is used for terminal turbine feeding by compressed air. The electrical conductivity of condensed water distorts the electric fields, which can induce electrical breakdown. For prevention of water condensation, the lower part of the tube (outside of the tank) was heated. Now the electrical breakdowns are occurred only during the first start after tank closing, as we assume, due to the dust accumulation when the tank is open. Recently, 1 MV terminal voltage was achieved by using low cost air-gas mixture. The tank was pumped to the 0.8 atm air pressure, and then the tank pressure was increased to 1.6 atm by four nitrogen gas-cylinder. The 4 kg of SF_6 gas was added (+0.02 atm) to increase the electrical strength of the mixture. The 1 MV has been achieved without breakdowns.

The multi-cathode (for 24 samples) sputter ion source has been recently manufactured and installed. It's needed for synchronous analysis of the samples and for comparison of the tested samples with the reference one. The negative ions are produced by bombarding graphite target with positive cesium ions. The Cs+ ions are produced on a hot tantalum ionizer (1100^0C) by cesium vapor from the oven (180^0C). The cesium ion beam is focused on the carbon sample placed on the cathode, because the working surface of ionizer is a spherical-shape cup. The copper sample holder has the inner diameter of 2 mm. The holder is water cooled to reduce sample heating. The cesium ions leaving the ionizer are accelerated by 7 kV potential. The negative carbon ions are accelerated by the same potential and extracted through the hole 6 mm in diameter in the center of the ionizer. The power consumption of the ion source does not exceed 250 W. The test sample in ion source is selected by sample wheel rotation. The stepping motor with Pi/25600 rad/step resolution is used for sample changing. The process of rotation is controlled by motor driver and checked by optoelectronic sensor system (at every turnover) and by video camera (online).

The new magnesium vapors stripper has been manufactured and installed. All hot parts of striper are located in vacuum. It prevents corrosion of striper surface by the tank gas mixture. The power consumption is about 50 W.

The electronics for time-of-flight detector (ToF) was improved. At present, the ToF channel width is 70ps. Moreover, the moment of time for ion detection can be registered with 16 μs channel width. This data is used for calculation of number of detected ions per unit time, allowing to filter the background ions from electrical breakdowns.

4.15.3 **Experimental Results**

During the experiments, the injection energy of carbon beam was 25 keV. The carbon beam current was about 5 uA. The terminal voltage of tandem accelerator was 1 MV. The 180° electrostatic bend was set to transmit the ions with charge state 3+. The magnesium vapors stripper was heated for obtaining the equilibrium charge state distribution, but not more. The ions transmission of AMS system at this energy is about 10% (includes the stripping yield for 3+ charge state). The ^{14}C ions are counted by ToF detector. The ^{12}C ions are measured in shielded Faraday cups with secondary electron suppression. The current of the mass-12 ions can be measured immediately after the magnet of low energy beam lines (^{12}C- ions) and at the AMS exit ($^{12}C^{3+}$ ions). The vacuum level in the beam line was about 10^{-6} Torr.

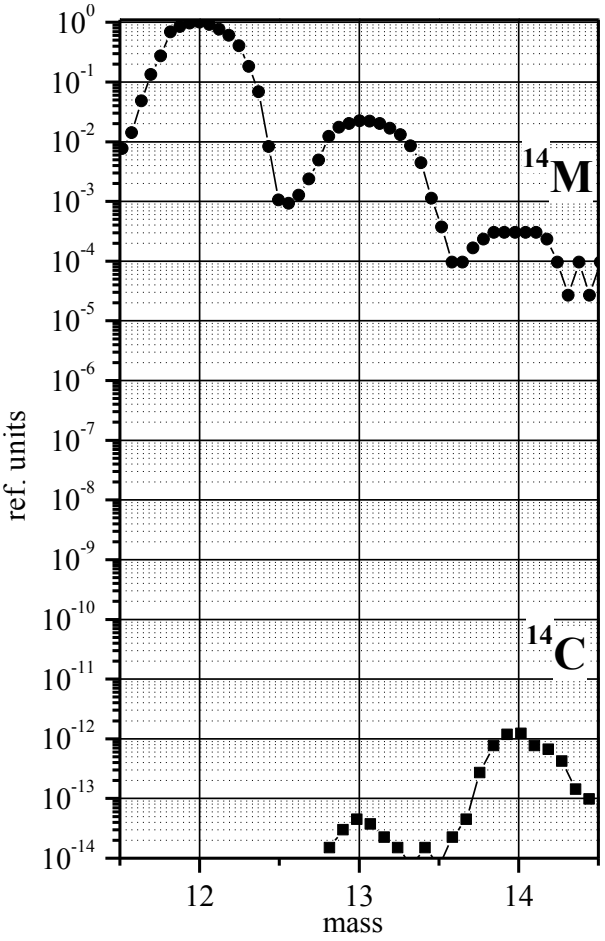

Figure 1: Mass spectrums of the injected (upper curve) and accelerated (lower curve) beams.

The typical mass spectrum of the carbon target before acceleration is shown in Fig. 1 (upper curve). The intensity of the mass-14 peak is more than 10^{-4} per ^{12}C isotope. It is mainly the $^{12}CH_2$ and ^{13}CH molecular currents. The ToF spectrum at the exit of AMS is also shown in Fig. 1 (lower curve). The mass is calculated from ToF channels. The AMS system is tuned for radiocarbon transmission. The molecular background of the mass-14 is suppressed by the destruction process in the magnesium target and then filtered by tandem 180° bend. The small mass-13 peak is also visible in the spectrum, but the mass separation is good enough for radiocarbon measurements.

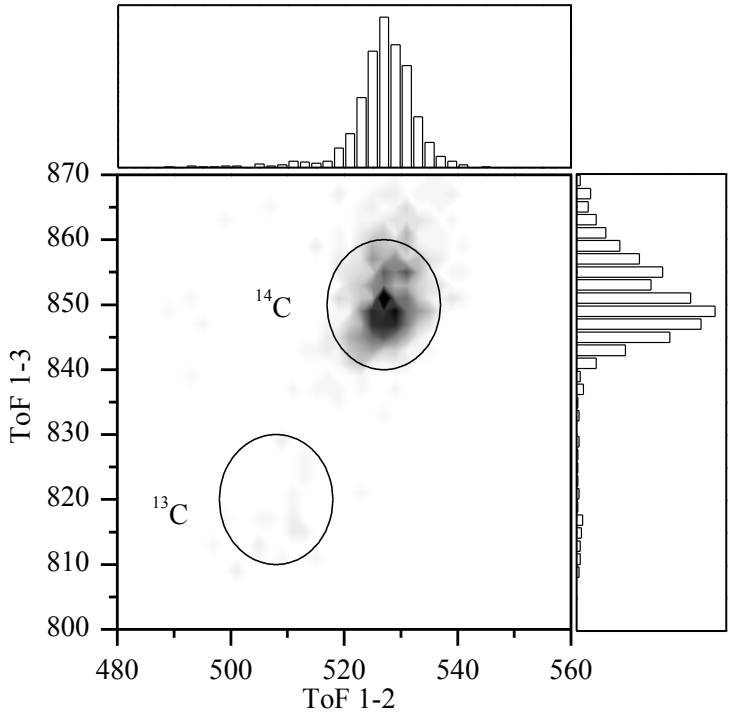

Figure 2: The 2D ToF spectrum at the exit of AMS (70 ps per channel).

The more detailed 2D ToF spectrum with the same AMS tuning is shown in Fig. 2. The solid circles show the locations of the radiocarbon and mass-13 peaks. The particles from mass-14 circle are calculated for radiocarbon concentration determination. The time-of-flight histograms for both ToF distances are also shown in Fig. 2. The peaks separation is bigger about of factor 2 than peak widths (FWHM) for each ToF distance. Such a system of several sequentially positioned detectors on the particles path allows a significantly decrease in the number of random coincidences.

The commercially available carbon fabric is used as test modern sample. The filaments of fabric are pressed into the cathode holder. The carbon fabric is made of organic materials. The radiocarbon isotope ratio of the modern organic matter is about 10^{-12} ($^{14}C/^{12}C$). The graphite MPG is used as test "dead" sample. The radiocarbon concentration in graphite is about 100 times lower than in modern sample.

For radiocarbon concentration analysis, the ^{12}C ions current and ^{14}C ions number are measured for each sample. During the experiments, the $^{12}C^{3+}$ ion current was measured one time of each 400 s interval of radiocarbon counting. During switching between the isotopes, the magnets settings are changed. The $^{12}C^{-}$ ions were measured simultaneously with the ^{14}C counting. The process of isotope measuring and sample changing (wheel rotation) is fully automated.

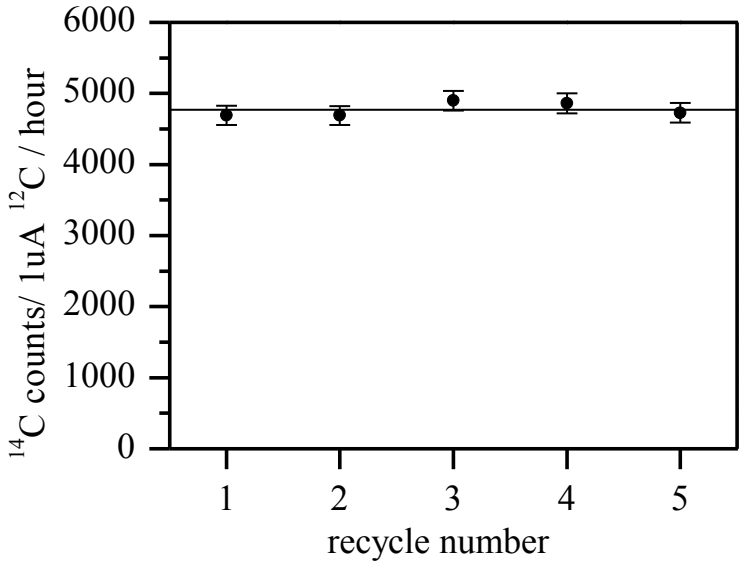

Figure 3: Radiocarbon concentration in modern sample. The sample was measured five times.

For estimation of the reproducibility of measurements, the series of five radiocarbon concentration measurements for one sample is presented at Fig.3. The solid lines show the mean concentration value. The experiment was carried out without rotation of the sample wheel. The ^{14}C counts time is 800 s for each measurement. The statistical uncertainty of radiocarbon registration is about 3% (shown by error bars). It is seen, that the results are in agreement with each other within the error ranges.

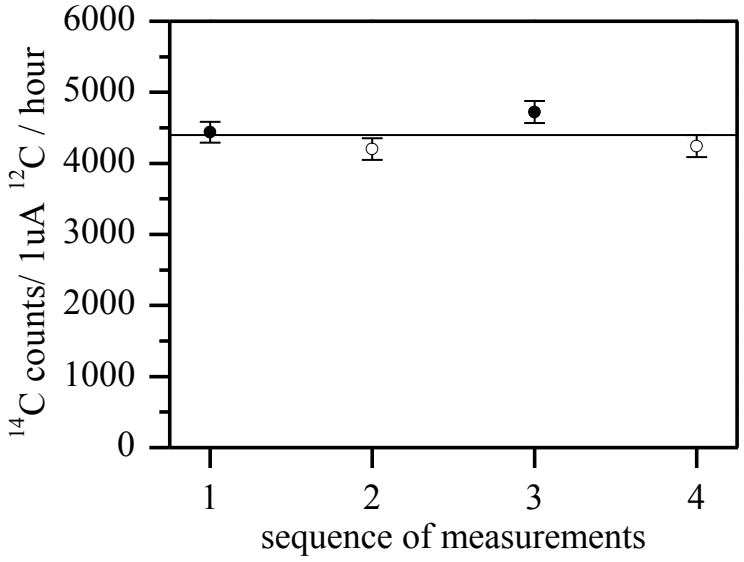

Figure 4: Radiocarbon concentration in two modern samples (measured alternately).

For testing of the reproducibility of measurements after sample wheel turning, another series of measurements is presented in Fig. 4. Here, two modern samples are measured alternately. One can see the results with wheel rotation are similar to ones presented in Fig. 3. The samples were degassed before the measurements by Cs beam. The time of degassing is about 5 min per sample. The effect is visible by vacuum monitoring. The ion source parameters are not stable during the degas process.

For ion background estimation, the modern sample and “dead” sample are measured alternately. The results are shown in Fig. 5. The data are normalized to the radiocarbon concentration in modern sample. As seen the radiocarbon concentration in “dead” sample is about 1% of the modern sample concentration.

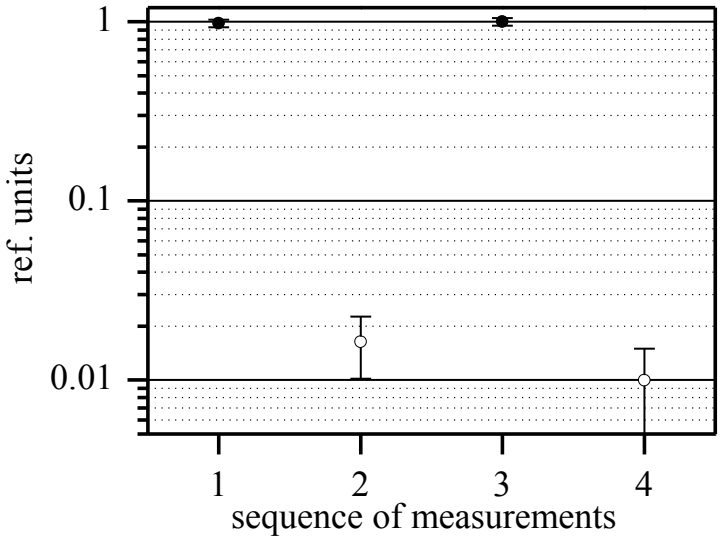

Figure 5: Radiocarbon concentration in the modern and “dead” samples (measured alternately).

For radiocarbon analysis, the samples with large content of carbon /were used. The sample preparation is needed for transformation of natural objects to such samples by combustion and graphitization. We tested more than 100 samples prepared by CCU “Geochronology of the Cenozoic era”. The measured background carbon contamination during sample preparation is about 10%. This work will be continued to the reduction of contamination.

The data presented is the first preliminary estimation of BINP AMS facility for radiocarbon dating. The detailed study of the systematic errors and ion background investigation will be done soon.

4.15.4 **Summary**

The accelerator complex has demonstrated the sustained performance on 1MV running. The reproducibility of first radiocarbon concentration measurements is about 3%. The measured radiocarbon concentration in “dead” sample is about 1% of the modern sample concentration.

4.15.5 **Acknowledgments**

This work is supported by SB RAS Integration Project #14.

4.15.6 **References**

1. N.I. Alinovskii et al, Technical Physics, Accelerator mass spectrometer for the Siberian Branch of the Russian Academy of Sciences, Technical Physics, 2009, Vol. 54, No 9, p 1350.
2. V.F. Klyuev, V. V. Parkhomchuk, S.A. Rastigeev, A magnesium vapor charge-

exchange target for an accelerator mass spectrometer, Instruments and Experimental Techniques, 2009, Vol. 52, No. 2, p. 245.
3. N.I. Alinovskii et al, A time-of-flight detector of low-energy ions for an accelerating mass-spectrometer, Experimental Techniques, 2009, Vol. 52, No. 2, p. 234.
4. V.V. Parkhomchuk and S.A. Rastigeev, Analysis of the ion background in an acceleration mass spectrometer of the Siberian Division of the Russian Academy of Sciences, Technical Physics, 2009, Vol. 54, No. 10, p 1529.

4.16 High Power ELV Accelerators for Industries Application

N.K. Kuksanov, Yu.I. Golubenko, P.I. Nemytov, R.A. Salimov, S.N. Fadeev,
A.V. Lavruhkin, A.I. Korchagin, D.S. Kogut and A.M.Semenov
Budker Institute of Nuclear Physics SB RAS, Novosibirsk, 630090, Russia
Mail to: kuksanov47@mail.ru

Abstract:

Beginning from 1971, the Budker Institute of Nuclear Physics Siberian Branch of Russian Academy of Science (SB RAS) started its activity in the development and manufacturing of electron accelerators of the ELV-type for their use in the industrial and research radiation-technological installations. The ELV-type accelerators were designed with use of the unified systems and units enabling thus to adapt them to the specific requirements of the customer by the main parameters such as the energy range, beam power, length of extraction window, etc. INP proposes a series of electron accelerators of the ELV-type covering the energy range from 0.3 to 2.5 MeV with a beam of accelerated electrons of up to 400 mA and maximum power of up to 400 kW. The design and schematic solutions provide the long term and round-the -clock operation of accelerators under the conditions of industrial production processes. The ELV accelerators are especially popular accelerators not only in Russia, but in China, Korea, and etc. The cross-linking technologies are applied very widely in industries. While the improved maximum operating temperature was one of the initial attractions of cross-linking, there are other important product advantages as a results of cross-linking of the polymers, such as: reduced deformation under load, improved chemical resistance, increased abrasion resistance, improved impact properties, memory characteristics. At present the electron-beam technologies are extensively used in a cable industry for cross-linking of insulation made on the basis of polymer compositions. The use of these technologies enabled to develop the manufacture of a wide range of wires, cables and heat-shrinking goods for different markets (power plant, telecommunications, electronics, oil industry, nuclear power plant, submarine and aircraft, etc). All of them are of high reliability, when being mounted and during operation as under standard and extreme operating conditions.

4.16.1 **Introduction**

The use of electron-beam technologies gave an opportunity to develop the production of wide range of wires, cables, heat-shrinking products (heating cables, power and ship cables, airborne wires and cables, as well as atomic power plant (A-plant) wires). All of them are of improved reliability at assembly and operation as in

regular service and in extreme conditions. The quality of radiation treatment depends on accelerator itself as well as on under-beam equipment. Thus, the accelerators should provide stability of electron beam parameters, such as energy, beam current and width of irradiation area. In order to enhance absorbed dose azimuthal homogeneity they should be provided by 4-side irradiation system.

The main specification of the system of cable transportation through radiation zone is transportation rate of speed, which should be proportional to beam current rate. Proportionality coefficient called “specific rate” depends on the type of irradiated product and accelerator parameters. Taking into account the information mentioned above, there was developed the high-automated systems for electron-beam treatment of cable isolation. Practically, there is no necessity in permanent presence of accelerator control panel operator. Effective visualization of irradiation process (energy, beam current, cable transportation speed) allows the operators of transportation line to control and set the treatment conditions directly at working place close by pay-off and take up machines.

4.16.2 **Accelerators**

The main features of ELV-accelerators are as follows:

1. High power of electron beam in wide energy range, it means high productivity of EB processing;

Figure 1: Accelerator ELV-8.

2. High efficiency of conversation of electricity power to electron beam power. The efficiency is limited by frequency converter and in case of transistors frequency converter efficiency is increased up to 80-92%;
3. Simple procedure of accelerator control by operator due to control system based on computer. It allows operating accelerator in on-line mode.

4. Accelerator control system comprises a set of software and hardware covering all the accelerator units required an operative control and diagnostics.
5. Accelerator itself has simple design and high reliability. If some troubles appear our customers repair accelerator by themselves with our consulting by phone, as a rule.
6. After warranty service. It means we delivery spare parts or parts with limited lifetime or make any accelerator service after warranty period by separate contracts with the low price.
7. A set of additional equipment (such as transportation line, ring or double side irradiation system, 4-side irradiation system) increases the accelerator possibility.
8. ELV accelerators are stable in operation. The energy and beam current instabilities practically do not exceed +/- 2%.

By now, over 120 accelerators had been delivered inside Russia and abroad and the total operation time exceeds 800 accelerator-years**.**

4.16.3 **4-Side Irradiation System**

In due time the laboratory proposed to develop the system of 4-side irradiation, which allowed us to enhance dramatically the quality of cable products treatment. Fig. 2 shows the extraction device with 4-side irradiation system. Together with enhancement of absorbed dose azimuthal homogeneity this method enables to decrease accelerated electrons energy that considerably expands the range of accelerator applications in the area of irradiation of big diameter cables. New system of irradiation exchanged the traditional early applied systems of 2-side irradiation and enhanced the quality of manufactured products and raised labor productivity. The cables are laid out under the beam in such a way that at each turn (lap) the upper and lower surfaces of a cable swap their places. If beam trajectories are crossed 90^0 angularly, than, taking into account the exchange of surfaces, 4-side irradiation is achieved (Fig. 3 and Fig. 4). It is important that the cable passes the irradiation zone few times.

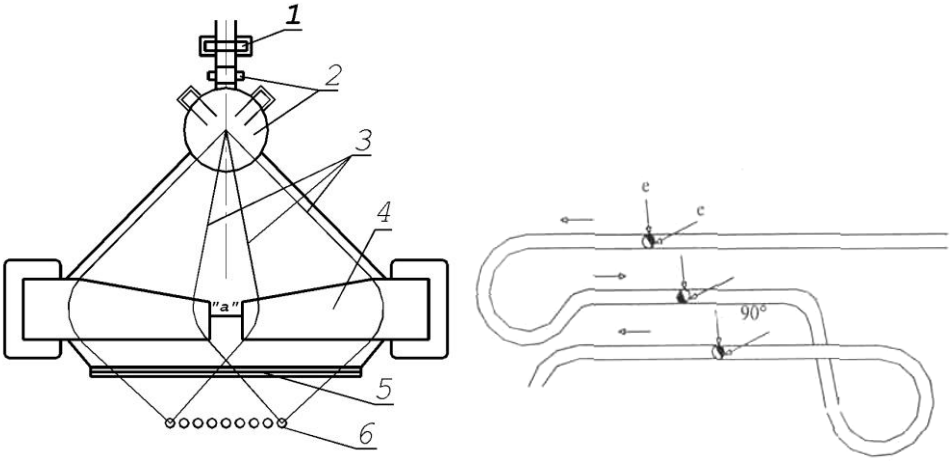

Figure 2-3: 4-side irradiation system.

4.16.4 **Under-Beam Transportation System**

Universal under-beam transportation system (UBTS) was developed in our laboratory. Its design is shown in Fig. 5. UBTS consists of 2 drums, one of which is driving and another one is guided. That reduces the risk of stretching of treated product and prevents the decrease of cable cord diameter.

Figure 4: 4-side irradiation system, continued.

Big diameters of the drums (900 mm) allow treatment of monoconductor cable with 36 mm^2 section (Fig. 5) and exchange tape guide rollers enable to treat multiconductor cables with the diameter up to 42 mm. Minimum pitch diameter of treated wire for this facility is 1 mm, but during the experiment we successfully irradiated cable of 0.12 mm^2 Irradiated chamber with UBTS, extraction device and 4-side irradiation system delivered to “Rosskat Ltd.” is shown in Figure 6. In UBTS we use the asynchronous motor (induction motor) with frequency drive. The rotation frequency is set by accelerator control system. The operation drive has a wide dynamic range, that is proportionality between transportation speed and beam current is saved within wide speed range. That enables to realize a smooth start of the technology and to refuse movable target. Irregularity of absorbed dose at UBTS acceleration from 0 right up to 250 m/min does not exceed 5%.

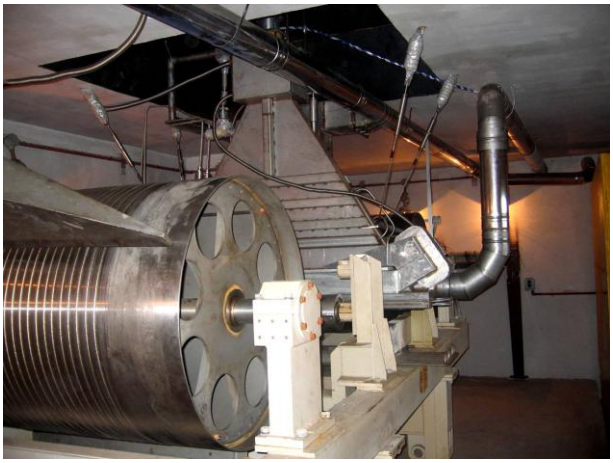

Figure 5: Cable irradiation.

4.16.5 **Data-Computing System**

The information of processing is shown on illuminated indicator board (Figю 6). It's dimensions allow to read information from any point of operation hall. The following parameters are continuously displayed: energy, beam current, speed of line, remainder of cable on bobbin, time to finish of bobbin (Fig. 7). The perfect quality of treatment is proved by reliable operation of cables in extreme conditions of oil industry.

Figure 6: Indicator board.

4.16.6 **Accelerators for Environmental Applications**

ELV-12 accelerator with power 400 kW is used for ecological purpose. The installation for electron-beam waste water treatment was put in operation in Korea.

Simultaneously with manufacturing of high power accelerators we developed movable accelerators. Accelerator together with radiation shielding is arranged inside of trailer. Main purpose of these accelerators is to eliminate small local contamination.

Figure 7: Irradiation hall for wastewater treatment with ELV-12 accelerator.

Figure 8: Movable accelerator.

4.17 The High-Current Deuteron Accelerator for the Neutron Therapy

V. Skorkin, S. Akulinichev and A. Andreev
INR RAS, Moscow, Russia
Mail to: skorkin@inr.ru

Abstract:

Physical project of neutron sources for the neutron therapy and neutron activation analysis is proposed. The neutron sources are based on beam provided by the high-current deuteron accelerator. The fast neutrons with intensity up to $5 \cdot 10^{12}$ $n \cdot s^{-1}$ are produced using T(D,n)4He reaction at the energy of deuteron beam about 430 keV and average current up to 20 mA. Neutron source can be used for the fast neutron and neutron capture therapy. Liquid-crystalline DNA-Gd nano-particles, as a potential biomaterial for the neutron capture therapy were investigated on a thermal neutron beam.

4.17.1 Introduction

Progress in the physics and technology of linear accelerators ion promotes the wider use in various sectors of the linear accelerators of protons and deuterons at low energies. In particular, such accelerators are used for the production of medical radioisotopes, neutron activation analysis, fast neutron therapy and neutron capture therapy of cancer [1]. Creation of fast and thermal neutrons through nuclear reactions (d, n), (p, n) without the use of fissile materials is a safe alternative to nuclear reactors. At low deuteron energy for high intensity neutron fluxes is most preferable DT and DD fusion reactions.

Currently in Russia powerful neutron generators (NG) using DT reaction produces NIIEFA. One of them, NY-12-2, provides a flow of 14 MeV neutrons of about $2 \cdot 10^{12}$ $n \cdot s^{-1}$ at an accelerating voltage of 250 kV and a current of 10 mA of deuterium ions. From foreign producers should be noted the firm "IRELEC" (France), which produces NG with fast neutron flux of about $5 \cdot 10^{12}$ $n \cdot s^{-1}$ at an accelerating voltage of 430 kV and a deuteron current of 20 mA. In the INR, was assembled and tested a NG based on high-current accelerator of deuterons (HCAD). The impact of a 20 mA deuteron beam

accelerated at 430 kV on tritium target produces a neutron flux of $2 \cdot 10^{11}$ $n \cdot s^{-1} \cdot cm^{-2}$ for a neutron output of $5 \cdot 10^{12}$ $n \cdot s^{-1}$.

4.17.2 **Deuteron Accelerator**

The machine consists of: an electrostatic particle accelerator, supplying a 20 mA/430 kV beam of monoatomic deuterium ions, a target assembly, an ISU type high voltage DC power supply, providing the 400 kV acceleration voltage, a control and monitoring system.

The electrostatic particle accelerator consists of a high voltage electrode with the injector and associated power supplies, accelerating tube, quadrupole focalization double, an extension tube, leading to the targets assembly (see Fig. 1). The high voltage (HV) electrode is mechanical assemble designed to house the high voltage components (400 kV) and supported by three insulated legs.

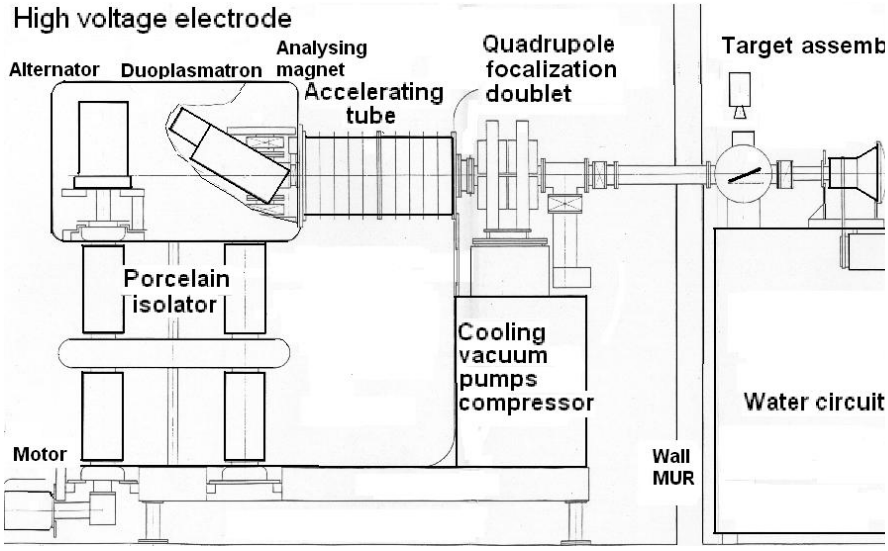

Figure 1: Deuteron accelerator**.**

The HV electrode includes the vacuum chamber of the injector with deflecting magnet and associated power supplies, the magnet enclosure auxiliaries, the ion source equipment, the alternator supplying power to the HV electrode. The injector has the ion source (the duoplasmatron type), beam extraction optics, atomic ion analysing magnet. A low pressure discharge is created between a hot cathode and an anode. The plasma expands through the anode into a expansion cup. Oven-heated oxide cathode has lifetime greater than 300 hours for discharge current of 15 A and discharge voltage of 150 V. The beam extraction optics (the pierce type) has maximum deuterium beam current of 55 mA.

Accelerating tube fixed to the high voltage head and consists of two half-length tubes, each made up of 5 porcelain rings and electrodes bonded together, providing a 12.5 kV/cm outside the accelerating space. A rated voltage, diameter and length of the tube are 400 kV, 0.5 m and 1.03 m respectively. The beam hits the target at a distance of 3.3 m. To compensate for divergence and to adjust the impact dimension, a

quadrupole doublet is located. A throat diameter and a nominal gradient of the doublet are 102 mm and 1.9 T/m respectively.

The target assembly consists of the retractable target designed for beam adjustment, the rotating target containing the tritiated layer, representing the neutron source, a cryopump, the target water cooling system.

The retractable target used to focus the beam by examining the impact dimension on a tantalum network through a window using a video camera. The power of the beam is determined by a calorimetric measurement of the cooling water. Considering the angle of 18° between the target and the horizontal plane, it can receive a maximum power of 8.6 kW for a 20 mm beam diameter.

The rotating target consists of a 345 mm diameter spherical sector, a double rotating seal to ensure an air-tight vacuum, an insulated tube, DC motor rotating the target at 1500 rpm. The axis of rotation is shifted by 30° with respect to the beam axis. The target and the rotating seals are water cooled.

The ISU DC power supply consists of a transformer set enclosed in cylindrical tank. In the ISU 400 kV – 30 mA single – phase configuration, multi-turn induction system is powered directly from a motorized variable auto-transformer connected to mains power. The control and monitoring system includes the Control Bay, centralizing the controls, adjustments for the various beam parameters, operating modes, fault indications and safety; the information transmission system, the power box, centralizing the power components.

Overall dimensions of the deuteron accelerator are 6.8×1.7×3 m. A power consumption is about 60 kW. Dangers related to the use of the accelerator is 400 kV high voltage of the HV electrode, X-rays of secondary electrons at the entrance to the accelerating tube, neutron radiation, radiation from neutron activation, the high radioactivity of the target (1000 curies).

4.17.3 **Neutron Therapy Facility**

The physical project of compact neutron sources for the fast neutron therapy (FNT), the neutron capture therapy (NCT) and the neutron activation analysis (NAA) is proposed. The layout neutron sources based on HCAD for FNT, NCT and NAA is illustrated in Fig. 2. These sources can be used to investigate neutron scattering (NSF).

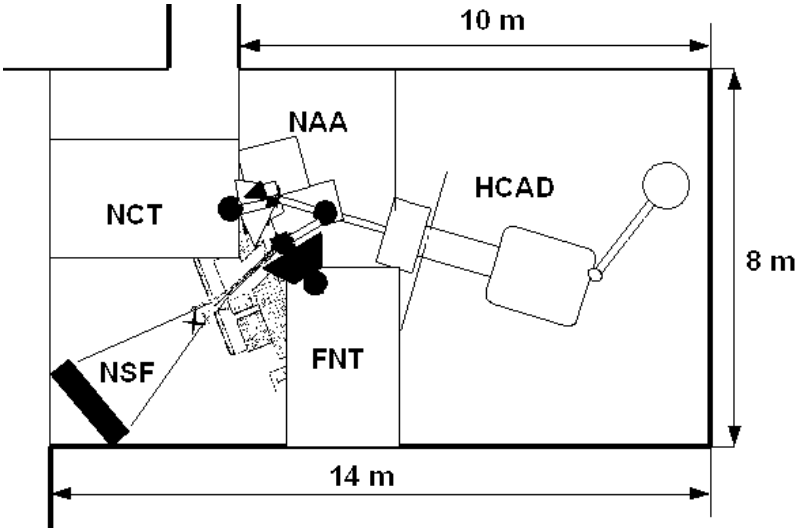

Figure 2: The layout neutron sources and facilities for the FNT, NCT, NAA and NSF.

Thermal neutron flux at moderation DT neutrons is of $1 \cdot 10^{10}$ $n \cdot s^{-1} \cdot cm^{-2}$. This neutron flux can be used for the NAA and will allow several times the sensitivity of NAA in the determination of quantitative properties of the element in the sample (1 ng) [2]. Fast neutron flux is equal to $1 \cdot 10^{8}$ $n \cdot s^{-1} \cdot cm^{-2}$ can be obtained for FNT. The neutron source could be employed for NCT experimental investigations by using an irradiation facility consisted of the tungsten neutron converter, a bismuth reflector, a graphite and polyethylene moderator. The thickness of W converter and Bi reflector is about 10 cm. Thickness of graphite moderator is about 20 cm.

A Monte-Carlo transport program, NCNP4B, was used to calculate the neutron fluxes from such a system. Thermal neutron flux is equal to $1 \cdot 10^{9}$ $n \cdot s^{-1} \cdot cm^{-2}$ can be obtained at the facility for NCT (see Fig.3).

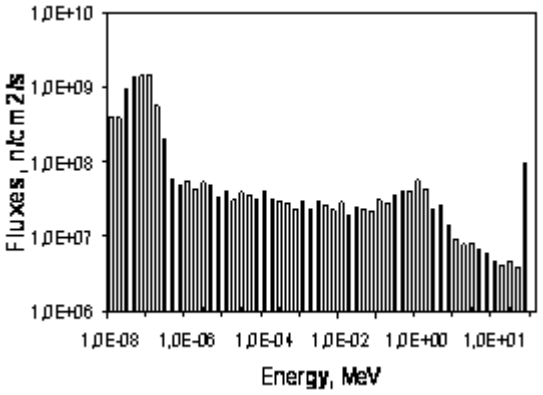

Figure 3: Spectrum of the neutrons from moderator system of the neutron sources for NCT.

4.17.4 **THE DNA-Gd RBE Research**

In [3] have proposed particles of liquid-crystalline dispersions formed by the cholesteric double-stranded DNA and Gd ions as a potential platform for NCT. We have investigated the radiobiological effectiveness (RBE) of the secondary photon and electron radiation, generated after the thermal neutron capture by the DNA-Gd particles. Each particle contains 10^8 gadolinium atoms and the corresponding natural gadolinium concentration in the biomaterial is about 250 mg/g. The conversion electrons, X-rays and gamma rays have a range in tissue about of 50 μm and can induce a tissue dose and DNA double strand breaks in cell nucleus when the DNA-Gd particles located on the surface of cells.

The biological samples containing cell suspension and DNA-Gd particles has been irradiated into the polyethylene phantom by neutrons from generator NG-400. The thermal and fast neutron fluxes for each biological sample were measured by means of the neutron activation analysis. The killing of a major part of tumor cells in biological samples with nano-particles was produced the thermal neutron fluence about 10^{11}cm^{-2} for a nano-particle density of the order of 10^3 particles per cell. In our experiment samples were irradiated inside the polyethylene phantom of the size $20 \times 20 \times 20$ cm^3. We have identically irradiated two sets of samples: one is the cell culture added with the solid particles of (DNA-gadolinium) complex, and another one is the cell culture without these particles. In the latter case, the killing effects can be caused only by fast neutrons. Therefore the difference in the cell killing efficacy for the two sets of samples might be due to the thermal neutron capture by the solid particles only. The irradiation time was about 1 h and the thermal neutron fluence of about $5 \cdot 10^{11}$ n·cm^{-2}. The thermal and fast neutron fluence was measured by means of the activation method. The fast neutron (~ 1 MeV) fluence of about $1 \cdot 10^{11}$ n·cm^{-2}. The absorbed dose of the thermal neutron was ~ 20 Gy. The absorbed dose of the fast neutron was ~ 2 Gy and the effect of these types of radiation was smaller and did not produce the cell killing. The examination of irradiated samples has proved it: the tumor cells in the samples with gadolinium were killed while the cells in control samples survived under the same conditions.

4.17.5 **References**

1. B.F. Bayanov, V.P. Belov, E.D. Bender et al., Nucl. Instr. and Meth. A 413 (1998) 397.
2. C. Zhang, Z.Y. Guo, A. Schempp, et al., Nucl. Instr. and Meth. A 521 (2004) 326.
3. Yu.M. Yevdokimov, V.I. Salyanov, O.V. Kondrashina et al., Int. J. Biol. Macromol. 370 (2005) 165.

4.18 ELLUS-6M Linear Electron Accelerator for Radiotherapy

A.A. Budtov, M.F. Vorogushin, V.A. Shyshov
FSUE "D.V. Efremov Scientific Research Institute of Electrophysical Apparatus",
St. Petersburg, Russia

S.V. Kanaev, N.N. Petrov
Scientific Research Oncology Institute, Pesochny, St. Petersburg, Russia
Mail to: vorogushin@luts.niiefa.spb.su

4.18.1 The Compact Medical Accelerator

"ELLUS-6M", a compact medical accelerator of new generation, has been designed and manufactured for radiotherapy by 6MeV photons in the multi-static and arc modes. The gantry of the accelerator can be rotated through ±1850 and ensures setting accuracies of the irradiator rotation velocity and positioning sufficient for the IMRT mode. The computerized control system is compatible with the treatment planning system and allows upgrading by adding new modules.

To realize the conformal radiotherapy, the following additional medical equipment has been developed: a multi-leaf collimator, a portal vision system for the dose field verification during irradiation and an upgraded treatment table made as a semi-pantograph.

In 2010, it is planned to finish clinical tests of the "ELLUS-6M" accelerator with the additional medical equipment carried out in the N.N. Petrov Scientific Research Oncology Institute, Pesochny, St. Petersburg.

In countries with a highly-developed economics, radiotherapy is used for treatment of more than 70% of oncological patients, and more than 60% of such patients are usually successfully cured of cancer. In Russia, this method is used for treatment of less than 20% of the whole number of oncological patients, which mainly depends on insufficient up-to-date radiotherapeutic equipment available in oncologic institutions in our country Linear accelerators, which can be used for the conventional beam therapy, are about 80 in number, and only 20 machines are used for the conformal treatment. It is insufficient to satisfy the needs for these machines; for comparison, the international standards are 1 machine for 250-300 thousand people.

Nowadays in Russia have appeared all necessary prerequisites to change critically the status of radiotherapy. The Government of the Russian Federation has taken a decision on the financial support of activities aimed at the advancement of oncological treatment of the population and fitting out of oncological clinics with up-to-date equipment.

Development of electrophysical equipment for radiotherapy is one of high-priority lines of activity of FSUE "D.V. Efremov Scientific Research Institute of Electrophysical Apparatus". Several generations of accelerators and cyclotrons for medicine have been developed since the foundation of the Institute [1, 2]. A new generation of linear electron accelerators for radiotherapy has been developed by specialists of the Institute, one of these machines is a 6 MeV "ELLUS-6M" shown in Fig. 1.

Figure 1: The “ELLUS-6M” accelerator under technical tests; dose fields are being measured in a water phantom

The new accelerator is equipped with a computerized control system, demountable multileaf collimator to form bremsstrahlung fields with a high accuracy and a portal image-based verification system. The system for radiotherapy developed on the basis of the “ELLUS-6M” accelerator allows the most advanced technologies of the radiation oncology to be realized.

The main block of the accelerator is an irradiator, which includes systems and units for an electron beam generation and acceleration, its transport and forming in compliance with a particular treatment plan, as well as dose monitoring and verification of treatment prescription.

The beam is generated in a three-electrode electron source and injected into the accelerating structure, which is a chain of coupled cavities. A standing-wave accelerating structure is used in the “ELLUS-6M” accelerator. Simultaneously, the RF energy is supplied to the accelerating structure by a magnetron via the waveguide line.

From the accelerating structure, electrons reach a deflection-focusing system where they are deflected by a magnet to an angle of 130° and focused to a tungsten target. Rectangular radiation fields, which are necessary for radiotherapy, are formed by radiation head collimators.

The irradiator can be rotated through an angle of ±1850; the servo drive of the gantry ensures variation of angular velocity and necessary irradiator positioning accuracy.

Mechanical travels of the gantry, radiation head and treatment table can be controlled both from the manual control console and automatically from the host computer located in the control console room.

The computer control system supports DICOM 3, DICOM RT and HL4 communication protocols with the treatment planning and topometric systems.

The accelerator is also equipped with a multileaf collimator (see Fig. 2, 3), which allows individual radiation fields to be formed (see Fig. 4).

Figure 2: Multileaf collimator mounted on the SL-75-5 accelerator

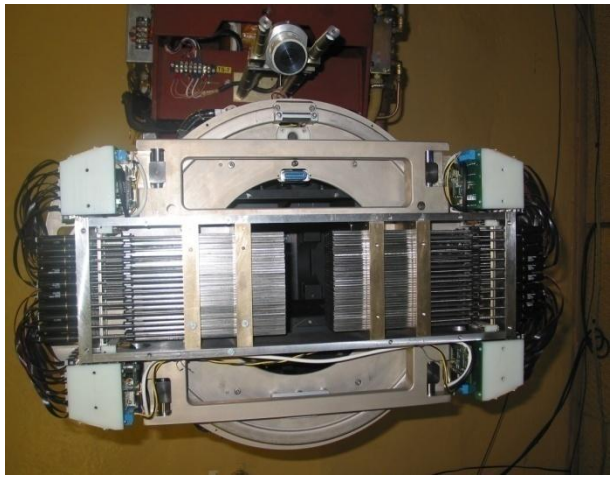

Figure 3: Multileaf collimator without casing

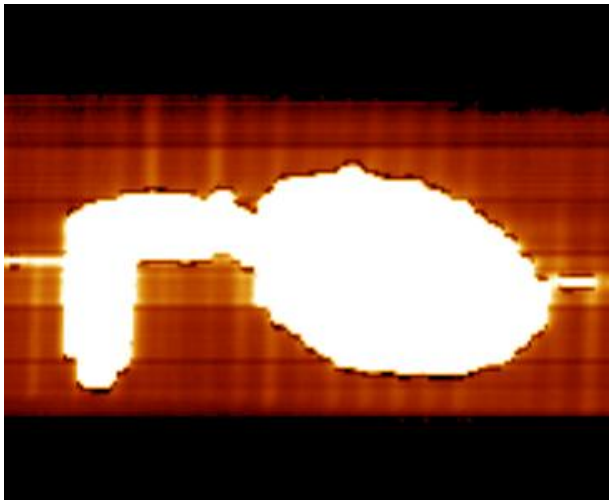

Figure 4: Radiation fields of required configuration formed with the MLC; the field image is obtained by using the portal image-based verification system

Prior to irradiation with an irregular field, an anatomic and topometric preparation is done with an X-ray topometric system TSR-100 [3], which is a component of the radiotherapeutical system developed in NIIEFA.

Fig. 5 shows the preparation of a patient for treatment. On the image of a patient's body a radiologist chooses an area to be treated (on the right of the figure); after that the treatment planning system performs computations of the leaves' position, which most accurately describes a preset contour (on the left of the figure). The data file comprising coordinates of the leaves is transferred to the MLC control system of the accelerator. In the process of patient's set up, the portal image system is used to verify the accuracy of the formed radiation field and the coincidence of the planned treatment area with the actual patient treatment position.

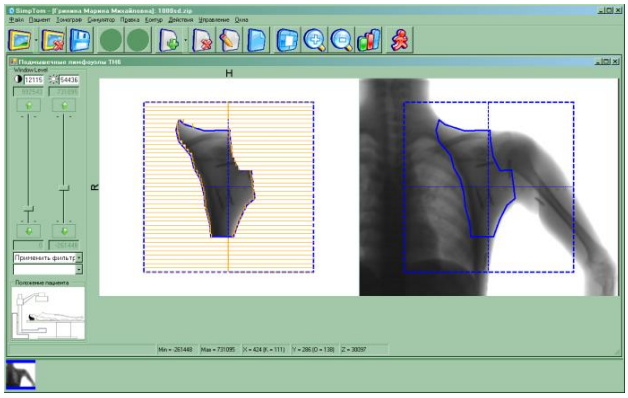

Figure 5: Irregular field chosen for treatment by a radiologist on the basis of a patient body projection image (right) and computations of MLC leaves' coordinates (left)

The collimator is a demountable device; it is so mounted on the accelerator radiation head so that to keep the possibility of the radiation head to rotate around the central axis

of the beam. The collimator drive ensures independent travel of leaves and verification of their position. The width of the area covered with one leaf is 0.5 cm 1m from target. The transmission between the ends of the closely connected leaves is less than 50% and between the neighboring leaves is 5%.

The MLC leaves' positioning system ensures the formation of the field boundary 1 m from target accurate to not worse than ±1mm. Depending on the leaf position, the penumbra width changes less than for 3 mm.

The MLC developed can also be used with SL-75-5 accelerators for conformal and IMRT irradiation techniques. In addition to the MLC, the accelerator is equipped with an independent patient treatment prescription verification system, which allows us to verify the compliance with the treatment prescription of the patient position relative to the beam of the accelerator.

The portal image device is an advanced tool contributing to higher efficiency of radiotherapy due to verification of the most important stages of the treatment process, namely a patient's set up and radiation field formation.

The portal image-based verification system is located directly on the rotating gantry of the accelerator (see Fig. 6). The system visualizes projected images of a patient's treatment position by recording the beam passing through the body of the patient (the portal image device). The dose field verification system developed for the "ELLUS-6M" accelerator can also be used on SL-75-5 accelerators.

As an example, Fig. 7 shows an image of a calf head obtained with the TSR-100 topometric system by using the beam of the SL-75-5 accelerator.

Figure 6: The portal vision system with beam-forming block

The delivery set of the "ELLUS-6M" accelerator includes a treatment table. The table top vertical travel is from 650 up to 1900 mm (above the floor); the table top horizontal longitudinal travel is 800 mm and its transversal travel is ±200 mm. The table can be rotated around the vertical axis passing through the isocenter for ±950.

The treatment table travels are actuated by servo drives with a smoothly regulated velocity. The table travels can be controlled both manually from a local control desk and automatically from the accelerator control system.

The table top is equipped with components to secure fixing accessories. On both sides of the table top, universal rails are made and emergency-off buttons for the whole radiotherapeutic facility and to stop the table traveling are located.

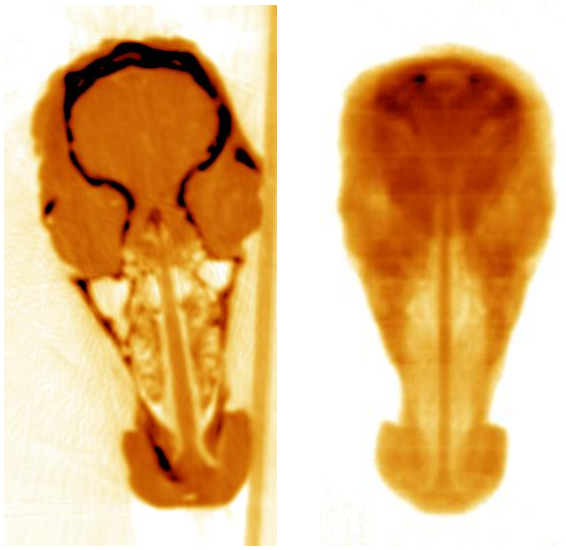

Figure 7: Calf head as a tested object.The image obtained with the therapeutic beam of the SL-75-5 accelerator (left) and a longitudinal tomogram obtained on the TSR-100 topometric system (right)

In addition, the accelerator is equipped with laser isocentor pointers, a TV treatment-room monitoring system and an intercom. The delivery set in addition to the accelerator includes the equipment necessary for maintenance/repair works.

So, the radiotherapeutic system on the basis of the linear electron accelerator "ELLUS-6M" equipped with the multileaf collimator, portal vision system for treatment verification, treatment table and other auxiliary devices allows the main problems of radiotherapy to be successfully solved satisfying the requirements of modern beam therapy techniques.

4.18.2 **References**

1. M.F. Vorogushun, A.S. Tikhomirov, "High-tech medical equipment for radiotherapy", Latest commercial techniques, TSNILOT Minatom RF, Moscow, № 1(312) p. 42 (2003).
2. S.V. Kanaev, M.F. Vorogushun, A.S. Tikhomirov, V.A. Shishov, "Characteristics of the domestic system for radiotherapy of oncological patients", Voprosy Onkologii, V. 49 № 5, p. 668 (2003).
3. S.V. Kanaev, M.F. Vorogushun, A.S. Tikhomirov, V.A. Shishov, "Anatomic and topometric preparation of oncological patients with the TSR-100 topometric system used in radiotherapy", Voprosy Onkologii, V. 49 № 5 p. 676 (2003).

4.19 Multp-M Code Upgrade

N.P. Sobenin, V.I. Kaminskii, S.V. Kutsaev, R.O. Bolgov, I.V. Isaev,
M.A.Gusarova and M.V. Lalayan
NRNU-MEPhI, Moscow, Russia

L.V. Kravchuk, INR, Moscow, Russia
Mail to: gusarovamariya@mail.ru

Abstract:

It is obvious that for all new RF devices all issues potentially influencing on their performance and operation must be considered at design stage. Multipacting discharge is known to be one of such phenomena. This discharge occurs in vacuum areas of RF devices in case resonant conditions for electrons are met and the secondary electron emission is strong enough. The problem of effective design of multipactor-free RF devices can be solved using powerful 3D numeric simulation tool Multp-M developed at MEPhI and INR. [1].

In this paper new features of this code are presented and illustrated by several common tasks solved. Multp-M code was upgraded so it is able to simulate the external magnetic and electric fields influence on discharge behavior and transient mode simulation. Code became more user-friendly thanks to new 3D interface.

4.19.1 **Influence of the External Fields**

There are a lot of ways for multipactor suppression known and used in microwave techniques. Use of external magnetic or electric field is one of the most widely implemented. Besides that a lot of RF devices like electron guns and injectors operate with magnetic field applied for beam focusing. This leads to sufficient change in multipactor properties. In order to simulate these conditions at early design stage Multp-M was expanded with new modules introducing static fields in model.

Algorithms added were tested and proved to yield correct results. As the initial test single electron dynamics was simulated in simple electric and magnetic fields pattern. More comprehensive research were done and their results compared to known data.

New features were used to evaluate external focusing magnetic field in PITZ photoinjector cavity and electric bias applied in “warm” coaxial line area commonly used in high power input couplers [2]. For instance latter having inner conductor radius equals to 14.4 mm and outer of 31 mm is used in Energy Recovery Linac.

Sample results obtained for PITZ photoinjector cavity illustrating Multp-M code simulation and visualization capabilities are presented on Fig.1. For research details refer to [3]. Multipactor trajectories in cell to circular waveguide transition area were found at 27.25 MV/m on-axis field strength.

Multipactor could be a severe problem for coaxial lines operation. Its suppression could be done by applying DC high voltage bias between conductors. As an example the simulated multipactor in coaxial line used in ERL high power input coupler warm part [2] is shown on Fig. 2. Coaxial line model used for simulation has inner conductor radius equal to 14.4 vv and outer one 31 mm. Fig.2 illustrates raise of electrons number vs. transmitted power for different bias applied. RF power on charts is normalized: 1 unit equals to 33 MW.

One could see that applying 3...4 KV DC lead to multipactor suppression for transmitted power up to 250 KW CW. It covers full operating range for this coupler.

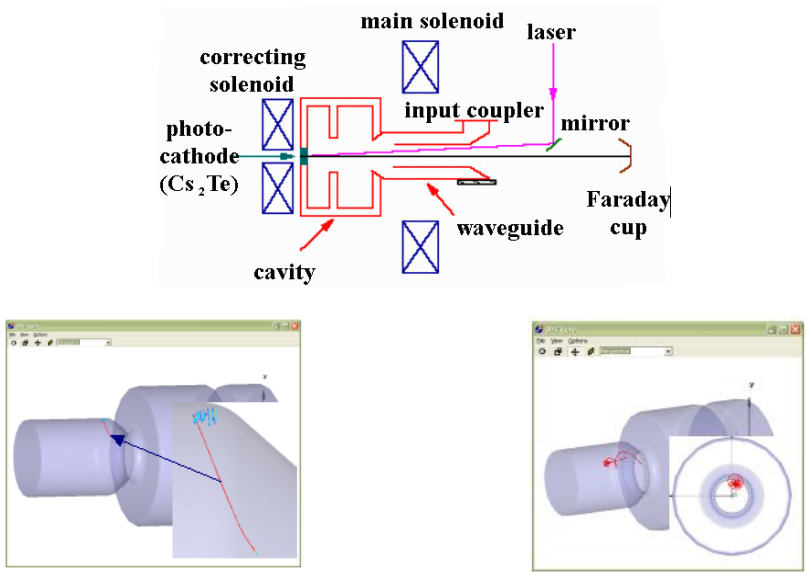

a b

Figure 1: Sample multipactor electron trajectories. a – without external field, b – with focussing magnetic field.

Thus new computation module implemented in Multp-M code allows to make correct simulation for devices with static magnetic or electric fields and to choose of bias parameters.

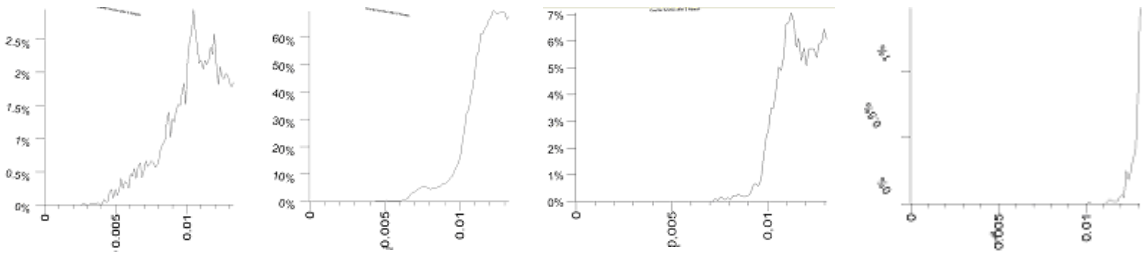

0 V 3 kV 3 kV 4 kV

Figure 2: Multipactor electrons number in coaxial line for different DC bias applied to inner conductor.

4.19.2 **3D Interface**

Initially MultP-M had only 2D visualization mode. Both model and simulation results showed via three planes aligned to coordinate axes (see Fig. 3).

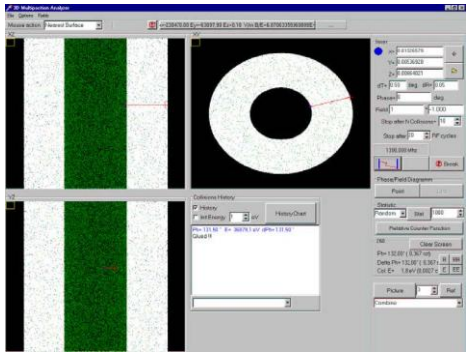

Figure 3: MultP-M: 2D interface.

However, electron trajectories analysis is very important for multipactor study. For complex models multipactor localization and its features is hard to find without true 3D figures and corresponding tools. For this reason, Multp-M code was upgraded with 3D visualization module.

Code itself operates in MS Windows environment, so 3D graphics was made using OpenGL library. Fig. 4 illustrates Multp-M snapshot for disk loaded waveguide model and simulated multipactor electron trajectories.

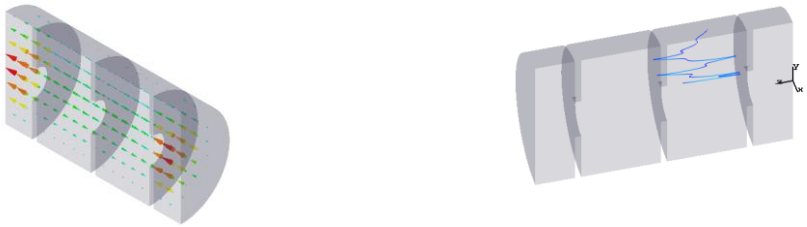

Figure 4: MultP-M: multipactor in DLW simulation results (left - electric field distribution, right – electron trajectory).

New 3D interface allows full visualization of model, electromagnetic field distributions and found electron trajectories. Panning, zoom, rotation, cut-off plane placing, transparency control and other functions are available.

4.19.3 **Transient Mode**

New simulation module for transient case development became an important code upgrade. This feature allows one to study multipactor in RF devices operating not only in steady state but also for different transient conditions occurring for example at power-on. New module for pre-calculated time-dependant fields using general purpose electromagnetic solver import was created. Transient fields distribution is interpolated using set of field matrices at different discrete time steps.

Both single and group multipacting electron trajectories simulation in transient mode made ready for use. Sample model for transient solver demonstration is rectangular waveguide of 20x40 mm cross section operating on 5712 MHz. Input signal waveform used in simulation is shown on Fig. 6. Electromagnetic field distribution along the waveguide for 2 ns after pulse launch is shown on Fig. 6.

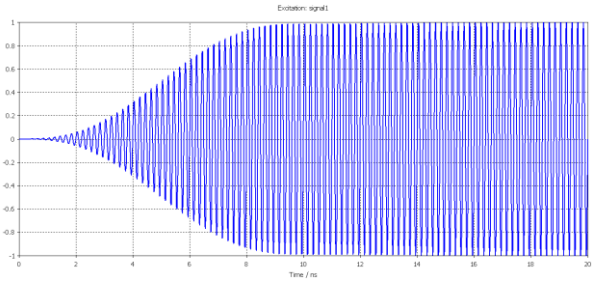

Figure 5: Transient signal waveform

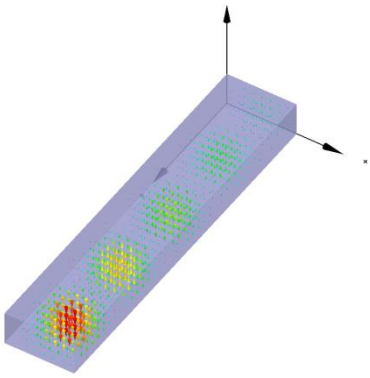

Figure 6: Electric field in waveguide distribution 2 ns after pulse rise (MultP-M).

Fig. 7 presents the rectangular wavegude operating on 5712 MHz example test simulation results. Multipacting electrons trajectories are shown along with overall electron number vs. time.

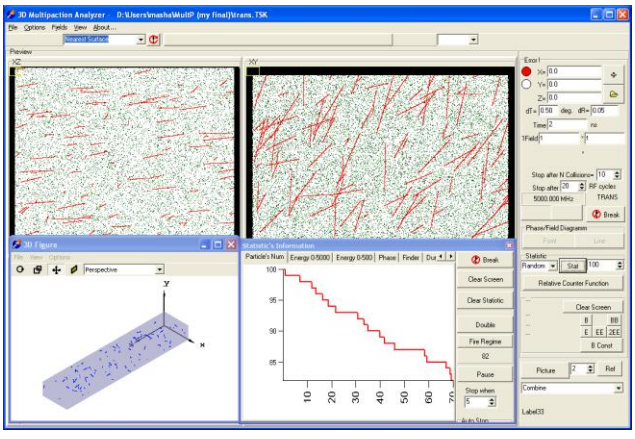

Figure 7: Multipactor electrons trajectories and overall electron number vs. time for transient mode

4.19.4 Conclusions

New modules for multipactor simulation Multp-M code upgrade were developed and tested. Series of examples were presented to show code capabilities for simulation of devices with static fields and in transient conditions. 3D interface developed for this code is also.

4.19.5 References

1. M.A. Gusarova, S.V.Kutsaev, V.I.Kaminsky, M.V.Lalayan, N.P.Sobenin, L.V.Kravchuk, S.G.Tarasov, "Multipacting simulation in accelerator RF structure", Nuclear Instrument and Methods in Physics Research A, 599. P. 100-105, 2009. ISSN 0168-9002.
2. B. Yu. Bogdanovich, M. A. Gusarova, A.A.Zavadtsev, D.A.Zavadtsev, V. I. Kaminskii, A. A. Krasnov, M. V. Lalayan, and N. P. Sobenin "High Average Power Input Couplers for Superconducting Cavities of Charged Particle Accelerators ", Instruments and Experimental Techniques, Vol. 50, No. 1, 2007
3. M.A. Gusarova, M.V.Lalayan, S.V.Kutsaev, I.V.Isaev, R.O.Bolgov, "Multipactor discharge in accelerating cavities with external magnetic field simulation", Proc. of the XXI International Workshop on Charged Particle Accelerators, Ukraine, Alushta, the Crimea, September 6-12, 2009

4.20 Development of Accelerators and Detector Systems for Radiation Medicine in DLNP JINR

E.M. Syresin
Joint Institute for Nuclear Research, Dubna, Moscow reg., 141980, Russia
Mail to: syresin@nusun.jinr.ru

4.20.1 Introduction

The DLNP JINR activity is aimed at developing two directions in radiation medicine: development of accelerator technique for proton and carbon treatment of tumors and new types of detector systems for spectrometric computed tomography (CT) and combined magnetic resonance tomography (MRT)/positron emission tomography (PET).

JINR-IBA realized the development and construction of proton medical cyclotron C235-V3. At present time all basic cyclotron systems were constructed. During 2011 we plan to assemble this cyclotron in JINR and in 2012 perform tests with extracted proton beam.

A superconducting isochronous cyclotron C400 has been designed by IBA-JINR collaboration. This cyclotron will be used for radiotherapy with proton, helium and carbon ions. The $^{12}C^{6+}$and $^{4}He^{2+}$ ions will be accelerated to the energy of 400 MeV/amu, the protons will be extracted at the energy 265 MeV. The C400 construction was started in 2010 in frame work of the Archarde project (France).

Modern CT requires modification to allow determining not only density of a substance from the X-ray absorption coefficient but also its chemical composition (development of spectrometric CT tomographs with colored X-ray imaging). JINR develops the principle new pixel detector systems for the spectrometric CT. A combined MRT/PET is of considerable interest for medicine, but is cannot be made

with the existing PET tomographs based on detectors of compact photomultipliers. Change-over to detectors of micro-pixel avalanche photodiodes (MAPDs) developed in JINR allows making a combined PET/MRT.

4.20.2 **Proton Therapy**

Dubna is one of the leading proton therapy research centers of the in Russia [1]. The modern technique of 3D conformal proton radiotherapy was first effectuated in Russia in this center, and now it is effectively used in regular treatment sessions [1-3]. A special Medico-Technical Complex was created at JINR on the basis of the synchrocyclotron (phasotron) used for proton treatment. About 100 patients undergo a course of fractionated treatment here every year. During last 10 years were treated by proton beams about 660 patients (Table 1). The methodic of 3 D conformal proton radiotherapy was effectuated there, when the irradiated dose distribution coincident with the tumor target shape with an accuracy of 1 mm [2-3].

Table 1: Diseases treated in JINR by the proton medical beams in 1990–2009.

Diseases	***Number of patients***
Meningiomas	112
Chordomas, chordosarkomas	19
Gliomas	33
Acoustic Neurinomas	7
Astrocytomas	24
Paragangliomas	5
Pituitary Adenomas	17
AVMs	60
Brain and other metastasis	53
Other head and neck tumors	134
Melanomas	7
Skin diseases	42
Carcinoma metastasis of the lung	9
Breast cancer	44
Prostate Adenomas	1
Sarcomas	9
Other	19

4.20.3 **Proton Cyclotron C235-V3**

A cyclotron C235–V3, superior in its parameters to the medical proton cyclotron IBA C235 installed in 10 proton treatment centers of the world, has been design and manufactures by JINR-IBA collaboration. This cyclotron design is an essentially modified version of IBA C235 cyclotron [4-5] (Table 2).

The one goal is to modify the sectors spiral angle at R>80 cm for improving of the cyclotron working diagram (Fig.1) and reduction of coherent beam losses at acceleration. The coherent beam displacement z from median plane is defined by vertical betatron tune Q_z: $z \propto Q_z^{-2}$. At $Q_z \approx 0.2$ the coherent beam displacement corresponds to 7 mm and at amplitude of free axial oscillations of 2-3 mm can became to beam losses at reduction of the sector gup in the C235-V3 cyclotron. An increase of vertical betatron tune from $Q_z \approx 0.2$-0.25 to $Q_z \approx 0.4$ in C235-V3 permits to reduce by 3-4 times the coherent losses at proton acceleration (Table 2).

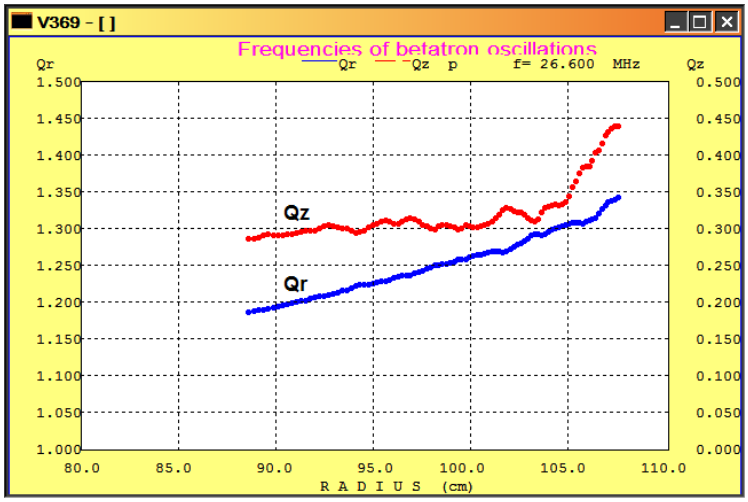

Figure 1: Dependence of betatron tunes on radius in cyclotron C235-V3.

Table 2: JINR-IBA cyclotron C235-V3

Parameter	***C235***	***C235-V3***
Optimization of magnetic field at modification of sector		Modification of sector azimuthal angle at R>80
Vertical betatron frequency at R>80	Qz=0,25	Qz=0,45
Vertical coherent beam displacement related to median plate effects	6-7 mm	1,5-2 mm
Beam losses at proton acceleration	50%	15%
Beam losses at extraction	50%	25%
Reduction of radiation dose of cyclotron elements		by 2-3 times

The modification of extraction system is other aim of new cyclotron C235-V3 [4]. The main peculiarity of the cyclotron extraction system is rather small gap (9 mm) between sectors in this area. The septum surface consists of several parts of circumferences of different radii. The septum thickness is linearly increased from 0.1 mm at entrance to 3 mm at exit. The proton extraction losses essentially depend on septum geometry. In proposed JINR septum geometry when minimum of septum thinness is placed on a distance of 10 cm at entrance the losses were reduced from 25% to 8%. Together with an optimization of deflector entrance and exit positions it leads to increasing of extraction efficiency up 80%. The new extraction system was constructed

and tested on IBA cyclotron C235. The experimentally measured extraction efficiency was improved from 60% for old system to 77% for new one (Fig.2).

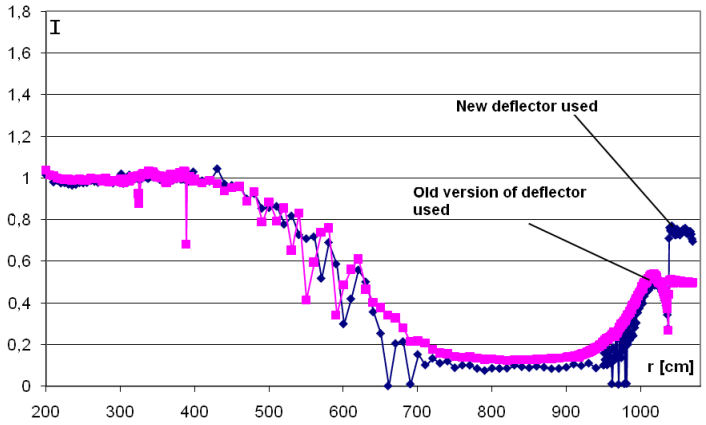

Figure 2: Proton beam extraction in cyclotron C235 with old IBA deflector and new electrostatic deflector developed in JINR.

Advantages of the medical proton cyclotron are simplicity, reliability, small size, and most importantly, the ability to modulate rapidly and accurately the proton beam current (Fig.3). The current modulation of the extracted proton beam at a frequency up to 1 kHz [5] is most advantageous with Pencil Beam Scanning and Intensity Modulated Proton Therapy. The energy of the extracted beam in cyclotron is fixed. However the fast proton energy variation at a rate of 15 MeV/s is easily performed during active cancer treatment by using a wedge degrader. This energy variation rate is few times faster than for typical synchrotron regime.

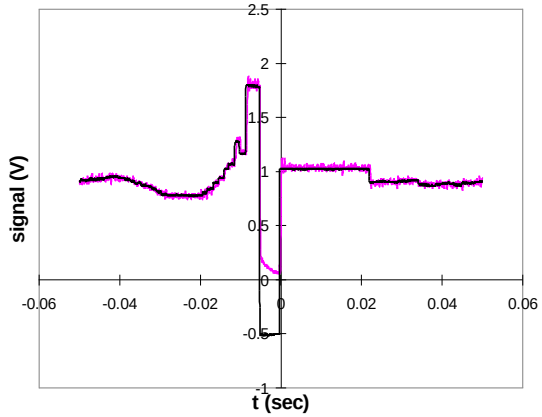

Figure 3: Beam intensity variation at the IBA C235 proton cyclotron.

4.20.4 **Supeconducting Cyclotron C400 Applied for Carbon Therapy**

Carbon therapy is the most effective method to treat the resistant tumors. A compact superconducting isochronous cyclotron C400 (Fig.4) was designed by JINR-IBA collaboration (Table 3) [5-9]. This cyclotron will be used for radiotherapy with protons, helium and carbon ions. The $^{12}C^{6+}$ and $^{4}He^{2+}$ ions will be accelerated to the energy of 400 MeV/amu and H_2^+ ions will be accelerated to the energy 265 MeV/amu and protons will be extracted by stripping.

Three external ion sources will be mounted on the switching magnet on the injection line located below of the cyclotron. The $^{12}C^{6+}$ ions are produced by a high performance ECR at the injection current of 3 μA. The alphas are produced by the other ECR source, while H_2^+ are produced by a multicusp ion source. All species have a Q/M ratio of 1/2.

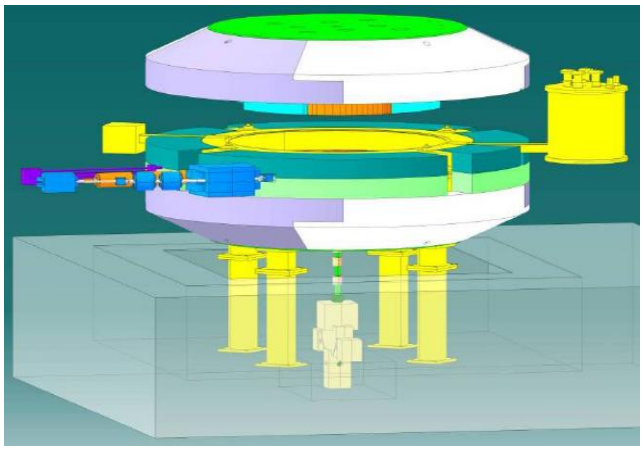

Figure 4: Common view of C400 cyclotron.

Table 3: Main parameters of the C400 cyclotron

General properties	
Accelerated particles	H_2^+, $^4He^{2+}$, $^6Li^{3+}$, $^{10}B^{5+}$, $^{12}C^{6+}$
Injection energy	25 keV/Z
Final energy of ions, Protons	400 MeV/amu 265 MeV
Extraction efficiency	~70 % (by deflector)
Number of turns	~1700
Magnetic system	
Total weight	700 tons
Outer diameter	6.6 m
Height	3.4 m
Pole radius	1.87 m
Valley depth	60 cm
Bending limit	K = 1600
Hill field	4.5 T
Valley field	2.45 T
RF system	
Radial dimension	187 cm
Vertical dimension	116 cm
Frequency	75 MHz
Operation	4 harmonic
Number of dees	2
Dee voltage: center/extraction	80 kV/170 kV

The dee tips have the vertical aperture 1.2 cm in the first turn and 2 cm in the second and further turns. In the first turn the gaps were delimited with pillars reducing the transit time. The azimuth extension between the middles of the accelerating gaps was

chosen to be 45 deg. The electric field in the inflector was chosen to be 20 kV/cm. Thus, the height (electric radius) of the inflector is 2.5 cm. The gap between electrodes was taken to be 6 mm, tilt parameter is equal to k′=0.1. The aspect ratio between the width and the spacing of the electrodes was taken to be 2 to avoid the fringe field effect.

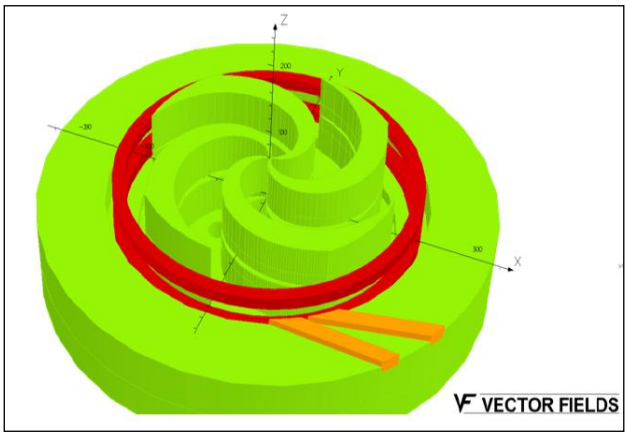

Figure 5: 3D TOSCA simulation of C400 magnetic system.

The 3D TOSCA simulation (Fig.5) and design of the C400 magnetic system was based on its main characteristics: four-fold symmetry and spiral sectors; deep-valley concept with RF cavities placed in the valleys; elliptical pole gap is 120 mm at the center decreasing to 12 mm at extraction; accelerate up to 10 mm from the pole edge to facilitate extraction; pole radius is 187 cm; hill field is 4.5 T, valley field is 2.45 T; magnetic induction inside yoke is less 2-2.2 T; the magnet weight is 700 tons and the magnet yoke diameter is 6.6 m; the main coil current is 1.2 MA.

The sectors are designed by way with flat top surface and without additional grooves, holes etc. The sectors have following parameters: the initial spiral law with parameter Nλ=77 cm with increasing spiral angle to the final radius with parameter Nλ~55 cm; the sectors azimuth width is varying from 25º in the cyclotron center to 45º at the sectors edge; axial profile is the ellipse with 60/1874 mm semi-axis, at the final radii the ellipse axial profile is cut by the planes at the distance z= ± 6 mm. The optimized sector geometry provides vertical focusing Qz~ 0.4 in the extraction region (Fig. 6).

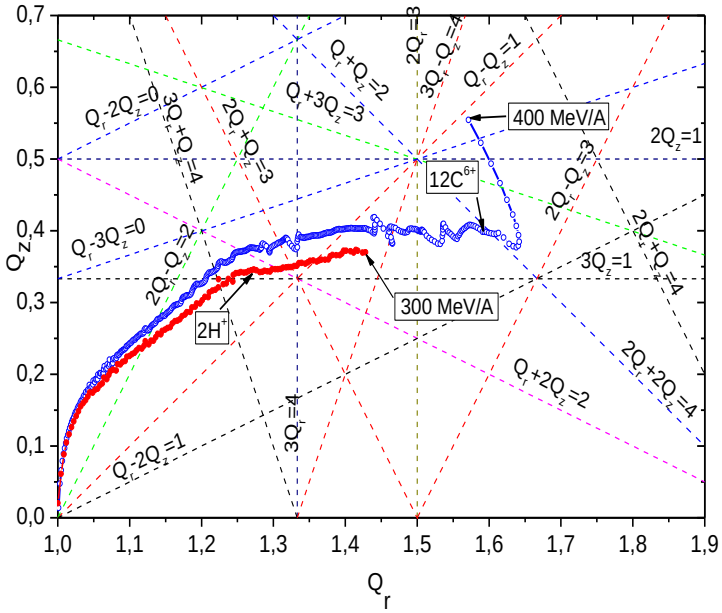

Figure 6: Working diagram of the cyclotron.

Acceleration of the beam will occur at the fourth harmonic of the orbital frequency, i.e. at 75 MHz. The acceleration will be obtained through two cavities placed in the opposite valleys. Two 45° dees working at the fourth harmonic will guarantee the maximum acceleration. The dee voltage increases from 80 kV at the center to 170 kV in the extraction region. A geometric model of the double gap delta cavity housed inside the valley of the magnetic system was developed in the Microwave Studio. The depth of the valley permits accommodation of the cavity with total height 116 cm. The vertical dee aperture was equal to 2 cm. The accelerating gap was 6 mm at the center and 80 mm in the extraction region. The distance between the dee and the back side of the cavity was 45 mm. The azimuth extension of the cavity (between the middles of the accelerating gaps) was 45º up to the radius 150 cm. The cavities have a spiral shape similar to the shape of the sectors. We inserted four stems with different transversal dimensions in the model and investigated different positions of the stems to ensure increasing voltage along the radius. The thickness of the dee was 20 mm. Edges of the dees are 10 mm wide. Basing on the 2D electric field simulations we have chosen the optimal form of the dee edges. RF heating simulation was performed to determine the cooling system layout.

During a whole range of acceleration the carbon beam crosses the lines of 15 resonances up to 4^{th} order. The working diagrams presented in Fig. 7 have been computed via an analysis of the small oscillations around the closed orbits. All resonances can be subdivided into two groups. The first group consists of 6 internal resonances ($nQ_r \pm kQ_z=4$, n, k=0, 1, 2, 3, 4, $n+k \leq 4$) having the main 4^{th} harmonic of the magnetic field as a driving term. The second group includes 11 external resonances ($nQ_r \pm kQ_z=m$, m=0, 1, 2, 3) that could be excited by the magnetic field perturbations.

Extraction of protons is supposed to be done by means of the stripping foil. It was found that 265 MeV is the minimal energy of protons for 2-turns extraction. The radius of foil in this case is 161.3 cm, azimuth is 51°.

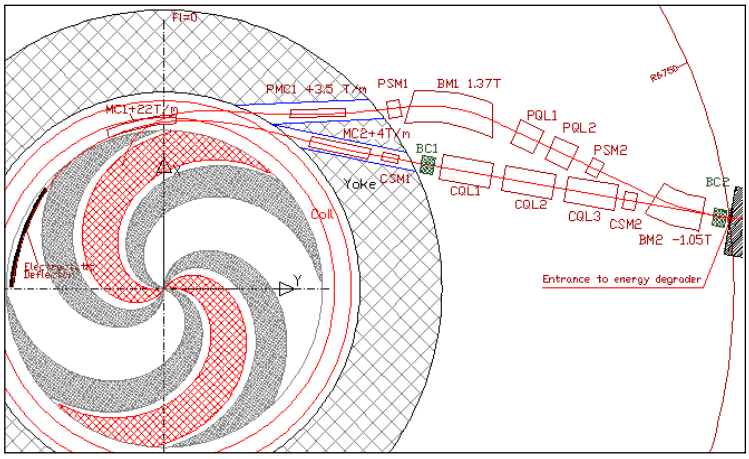

Figure 7: Layout of the cyclotron C400 with two extraction lines.

It is possible to extract the carbon beam by means of one electrostatic deflector (which is located in valley between sectors) with a 150 kV/cm field inside. Septum of the deflector was located at the radius 179.7 cm for tracking simulation. The extraction efficiency was estimated as 73% for the septum with increased (0.1 – 2) mm thickness along its length**.** The extraction of the carbon and proton beams by the separate channels and their further alignment by the bending magnets outside the cyclotron was chosen as the acceptable variant. The passive magnetic elements (correctors) are supposed to be used inside the cyclotron and the active current elements (quadrupole lenses and bending magnets) outside the yoke. A plan view of both lines is shown in Fig. 7. It is possible to align both beams into one direction just before the energy degrader (6750 mm from the cyclotron center). Both beams have a spot with $\sigma_{x,y}$<1 mm at this point. Transverse emittances are equal to 10 π mm·mrad and 4π mm·mrad for the extracted carbon beam.

4.20.5 **Detectors for Tomography**

The developed spectrometric CT tomographs of next generation should measure not only density of a substance but also its chemical composition. Colored X-ray imaging CT will ensure high-contrast imaging of a structure with different chemical compositions (tomography at different gamma ray energies selected near the K-edge of absorption lines of such elements as Ca, C, Fe, etc.) allowing, for example, clear-cut image of blood vessels including those behind bone structures with considerable shadowing of these structures. The gamma ray energy in the spectral CT tomography based on the JINR-TSU GaAs pixel detector [10] (Fig.8) is determined by a special chip involving a comparator of eight signal levels (eight colors) that allows spectrometry and determination of gamma ray energy from this information thus implementing colored X-ray imaging. The detecting systems of the spectrometric CT tomography are based on the semiconducting heterostructures. Together with spectrometric possibilities the pixel detectors on basis of GaAs(Cr) have a high space resolution(~100 μm), their sensitivity is one order of magnitude better comparing with Si detectors at photon energy of 30-35 kev (Fig.9).

A combined MRT/PET tomograph is under consideration in many research centers. The application of micro-pixel avalanche photodiodes (MAPDs) (Fig.10) allows

making a combined PET/MRT tomograph. This photodiode consists of many microcells, micropixels, each working in the yes/no Geiger mode with a high internal gain (up to 10^5) and being capable of detecting single photons. A special shop for assembly and testing of micropixel detectors is built at JINR. MAPDs are more and more widely used in nanoindustry (laser location, optical-fiber communication, optical information transmission lines, systems for optical readout of super high-density information from various carriers on the nanostructure basis, luminescence of quantum dots) and in development of medical diagnosis equipment (PET, combined PET/MRT, single-photon emission tomograph). The MAPD advantages comparing with photomultipliers [11] are high dynamic range (pixel densities of up to 4×10^4 mm^2); photon detection efficiency up to 30%; gain up 10^5; insensitivity to magnetic field; better radiation hardness; compact and rigid; low voltage supply (<100 V).

Figure 8: Spectrometric detector on basis of GaAs (Cr) pixel censor with 256×256 channels of 50 μm resolution and Medpix chip.

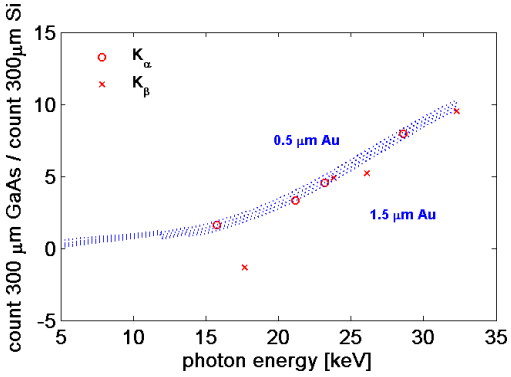

Figure 9: Dependence of count ratios of GaAs(Cr) and Si detectors on the photon energy.

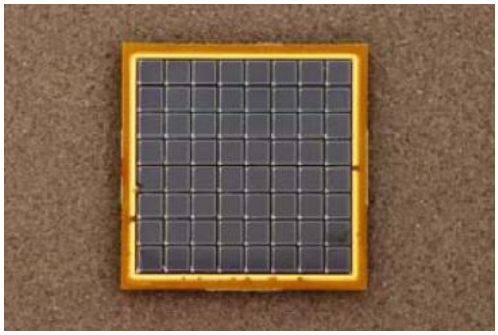

Figure 10: Micropixel avalanche photodiodes.

4.20.6 References

1. O.V. Savchenko, "40 years of proton therapy on synchrocyclotron and phasotron of LNP JINR", J. Medical physics (2007), № 3-4.
2. A.V. Agapov et al, "Methodic of 3D conformal proton therapy", Particle and Nuclei Letters, №6 (2005), 80-86.
3. S.V. Shvidky et al, "Proton Three-Dimensional Radiotherapy and Radiosurgery of

Intracranial targets in Dubna". Radioprotection, V.43, №5, (2008), p.7
4. G. Karamysheva et al, "Simulation of beam extraction from C235 cyclotron for proton therapy", Particle and Nuclei Letters, v.7, №4 (2010).
5. E.M. Syresin, Centers of hadron therapy on the basis of cyclotrons, RUPAC 08, Zelenograd, p.316 (2008).
6. Y. Jongen, "Design of a K=1600 SC cyclotron for Carbon therapy" ECPM, Nice (2006).
7. Y. Jongen et al., "Design Studies of the Compact Superconducting Cyclotron for Hadron Therapy", EPAC 06, p. 1678 (2006).
8. Y. Jongen et al., "IBA C400 Cyclotron Project for hadron therapy", Cyclotrons 2007, Italy, p. 151 (2007).
9. Y. Jongen et al.," Current status of the IBA C400 cyclotron project for hadron therapy" , EPAC 08, p.1806 (2008).
10. T. Lustos, G. Chelkov, O.Tolbanov "Characterization of GaAs(Cr) Medipix2 hybrid pixel detectors" in Proc. of iWoRid, Prague (2009).
11. Z. Sadygov et al. "Three advanced designs of micro-pixel avalanche photodiodes: Their present status, maximum possibilities and limitations", NIM A567(2006) 70-73.

5 Workshop and Conference Reports

5.1 HB2010 – the 46th ICFA Advanced Beam Dynamics Workshop on High Brightness, High Intensity Hadron Beams

Mike Seidel
Paul Scherrer Institut, CH-5232 Villigen, Switzerland
Mail to: mike.seidel@psi.ch

5.1.1 Workshop Theme and Organization

The 46th ICFA Advanced Beam Dynamics Workshop, HB2010, took place from September 27 to October 1 in Morschach, Switzerland. This fifth meeting in a series of workshops focusing on High Brightness, High Intensity Hadron Beams was hosted by the Paul Scherrer Institut, PSI. The Workshop continued with the tradition of previous editions, held in Batavia (2002), Bensheim (2004), Tsukuba (2006) and Nashville (2008), by providing an open forum for delegates to present and discuss their work, and to exchange experiences and ideas. The program covered experimental and theoretical advancements associated with high-intensity and/or high-brightness hadron beams, beam dynamics studies, reviews of planned projects, and practical experience gained with operating accelerators. The Workshop venue was set among the beautiful mountainous surroundings of Morschach, 200 m above Lake Lucerne. The final day of the Workshop was held at PSI and included a visit to the accelerator facilities.

The Workshop opened on the Monday with a plenary session comprising presentations from 8 invited speakers. The poster session followed in the afternoon with 54 presenters setting the stage for intense discussions among participating scientists. The following three days, from Tuesday to Thursday, were dedicated to the seven working groups, which hosted a total of 102 oral presentations and several discussion

sessions. Presentations were delivered in two parallel sessions, establishing a balance between a comprehensive program with numerous talks, and a forum for interaction across the various working groups. The majority of the oral presentations were invited by the working group conveners, while contributed papers were presented either as talks or posters.

On Friday, summary talks were presented at PSI by the conveners of the working groups. This was followed in the afternoon by a guided tour to the PSI accelerator facilities which included the cyclotron based 590 MeV proton accelerator with 1.3 MW average beam power and a new 250 MeV electron injector accelerator that serves as a test facility for the preparation of the planned free electron laser project SwissFEL at PSI.

The rising interest in high intensity hadron accelerators was reflected by an unprecedented 167 attendees, stemming from 15 countries, with the largest number from the US (46), Switzerland (43), Germany (26), UK (14), Japan (13) and China (6). As expected, many contributions were made from laboratories that operate large hadron facilities such as CERN, Fermilab, J-PARC, ORNL, GSI. However, it was also gratifying to receive first contributions from several new facilities, such as the Chinese Spallation Neutron Source (CSNS) and the European Spallation Neutron Source (ESS). Overall the workshop program covered a very wide range of topics ranging from practical operational aspects of beam dynamics to conceptual ideas.

5.1.2 **Scientific Program**

The plenary program focused on new results obtained from facilities that recently came into operation, on applications of hadron accelerators, and projects currently in the research and development phase. Following a motivating introduction by Kurt Clausen (board of directors, PSI), Richard Sheffield (LANL) talked about the application of high intensity accelerators for the transmutation of nuclear waste and energy production. John Galambos (ORNL) and Tadashi Koseki (J-PARC) respectively presented their experience with the SNS and the J-PARC accelerator complex, with emphasis on high intensity operation. Ralph Assmann (CERN) described the complex LHC collimation system, presented first experimental measurements, and gave a practical account of their operational experience. Two projects currently under development, FAIR and CSNS, were described by Peter Spiller (GSI) and Jingyu Tang (IHEP/Beijing). A special contribution from Wim Leemans (LBNL) addressed the application of high average power laser technology for charged particle beam acceleration. A joint task force between ICFA and ICUIL (International Committee on Ultra-High Intensity Lasers) has been formed to promote development in this promising accelerator technology. A related discussion session followed and different potential applications for high power lasers, such as very high gradient acceleration, medical applications and charge stripping were discussed in more detail. The opening day concluded with a stimulating poster session containing contributions from all working groups.

The subsequent three days were dedicated to the working group activities. Their subject matters, their conveners, and corresponding number of talks, are listed in Table 1.

Table 1: Working Groups at HB2010

Working Group	*Convener*	*No. Talks*
A) Beam Dynamics in High-Intensity Circular Machines	G. Franchetti (GSI) E. Metral (CERN)	23
B) Beam Dynamics in High-Intensity Linacs	J.-M. Lagniel (GANIL) A. Lombardi (CERN)	14
C) Accelerator System Design, Injection, Extraction	S. Cousineau (ORNL) D. Johnson (FNAL)	9
D) Commissioning, Operations and Performance	J. Galambos (ORNL) H. Hotchi (J-PARC) A. Mezger (PSI)	10
E) Computational Challenges in High-Intensity Linacs, Rings including FFAGs and Cyclotrons	P.N.Ostroumov (ANL) G. Pöplau (Univ. Rostock) R. Ryne (LBNL)	10
F) Beam Diagnostics and Instrumentation for High-Intensity Beams	R. Doelling (PSI) M. Wendt (FNAL) T. Toyama (J-PARC)	10
G) Beam Material Interaction	D. Kiselev (PSI) N. Mokhov (FNAL) R. Schmidt (CERN)	17

The majority of the papers at HB2010 were devoted to beam dynamics problems in circular and linear accelerators and simulation methods to treat such problems. The working group on circular machines received the largest number of contributions. Topics included high intensity related problems, such as space charge effects, impedance driven instabilities or strong beam-beam interaction in colliding beam facilities. New generic concepts such as a storage ring with non-linear optics in order to generate very strong Landau damping, were also discussed. In recent years considerable progress was made with applying high performance computing to beam dynamics problems. One working group focused specifically on computational methods. Beam-beam tracking simulations, space charge effects, beam induced wakefields or the prediction of low density beam tails are examples of problems that require high performance computing efforts.

High power accelerators typically have issues connected with beam losses, activation and heat load of collimators, targets, beam dumps or other accelerator components. A newly established working group on beam material interaction covered many of these aspects, discussing activation and disposal of components, predictions of nuclide inventories and cooling times, thermo-mechanical and cooling problems, and radiation damage. The example of the LHC collimation system demonstrated the close interaction of these issues with beam dynamics problems. Existing (e.g. BLIP at BNL) and planned (HiRadMat at CERN) facilities for experimental irradiation of material samples were highlighted.

The working groups on operation, instrumentation and accelerator system design mainly covered the technical and operational issues of existing accelerators. This included practical operational problems, reliability issues, commissioning strategies, critical subsystems for injection and extraction or diagnostic devices with a high dynamic range, as typically required in high intensity accelerators.

Apart from a few exceptions, papers at HB2010 made reference to existing or planned accelerator facilities. Hence, another way of summarizing the Workshop program is to classify the papers according to facilities. Table 2 lists the facilities sorted by their maturity. The three facilities, LHC, J-PARC, SNS, that are presently attempting to raise their intensities and to reach their design specifications, were the subject of the largest number of presentations at HB2010.

Table 2: Experimental Facilities in Contributions to HB2010

	Facilities	***Theory, Concepts***	***Components, Sub-systems***	***Operation, Procedures***
Well established	ISIS, TEVATRON, PSI-HIPA, COSY, CERN-PS, RHIC, UNILAC …	×	×	×
Operational, under development	LHC, J-PARC, SNS, (EMMA)	×	×	×
Planned	FAIR, Project-X, ESS; SPIRAL 2, LSPL, FRIB, CSNS, IFMIF …	×	×	×
Developing concepts	ADS, FFAG (EMMA), Laser Plasma Acceleration	×	×	

A report from the individual working groups can be found in the summary talks and papers prepared by the respective conveners [1].

5.1.3 **Conclusion**

HB2010 proved to be a successful and fruitful workshop that highlighted the rapid and comprehensive progress made in high intensity hadron accelerators from around the world. With new projects evolving, the growing interest in the field is further made evident by the continued rise of accelerator experts participating at the HB series.

Preliminary proceedings, which include copies of talks, are available on the PSI website of the workshop [1]. Once the editorial process is complete, the proceedings will be published electronically on the JACOW [2]. Selected papers are to be published in longer versions in a special edition of Physical Review Special Topics - Accelerators and Beams [3], to be edited by Andreas Adelmann (PSI).

The next workshop in this series, HB2012, will be hosted by the Institute of High Energy Physics in Beijing, China.

5.1.4 **References**

1. HB2010 website with preliminary proceedings: http://hb2010.web.psi.ch/
2. JACOW website (see “ABDW”): http://www.jacow.org/
3. PRST-AB special edition website: http://prst-ab.aps.org/speced/

5.2 ECLOUD2010 – the 49th ICFA Advanced Beam Dynamics Workshop on Electron Cloud Physics

The 49th ICFA ABDW was held October 8 through 12 at Cornell University, Ithaca, New York, USA. 59 researchers attended the meeting, with all major labs working in the field represented. The workshop began with a full day of tutorial lectures introducing the subject to those with a limited background. This overview covered the generation and build up of electron clouds in accelerators, the cloud induced beam instabilities, non-linear dynamics, and emittance growth. The tutorials concluded with a lecture on the control and mitigation of electron cloud in future high intensity accelerators.

The main body of the workshop included recent experimental results of diagnostic measurements at Fermilab, CERN, ANKA, DAFNE, Petra III, CESR-TA, INFN, and KEKB. A number of electron cloud mitigation techniques emphasizing surface coatings (TiN, amorphous carbon, NEG) or modifications (grooves) were presented with recent results. Many talks reviewed development of electron cloud simulation codes and it is clear that careful benchmarking of these codes and the further expansion of their capabilities to allow design of future machines is essential. Beam dynamics studies focused on the instabilities generated by electron clouds and the development of feedback techniques.

The workshop included tours of the facilities at Wilson Laboratory and a boat tour of nearby Cayuga Lake during the wonderful fall foliage season. A public lecture by Barry Barish, ILC Global Design Chair, on the science possible with the International Linear Collider made a strong case for the importance of continued work on electron cloud mitigation and advanced accelerators in general.

Contact:
Mark Palmer, ECloud 2010 Chair, Cornell University, USA
Email: ecloud10@lepp.cornell.edu

6 Recent Doctorial Theses

6.1 Determination of the Absolute Luminosity at the LHC

Simon Mathieu White
University of Paris-Sud and CERN
Mail to: simon.mathieu.white@cern.ch

Graduation date: 11 October 2010
Supervisors: H. Burkhardt (CERN) and P. Puzo (University of Paris-Sud)

Abstract:

For particle colliders, the most important performance parameters are the beam energy and the luminosity. High energies allow the particle physics experiments to study and observe new effects. The luminosity describes the ability of the collider to produce the required number of useful interactions or events. It is defined as the

proportionality factor between the event rate, measured by the experiments, and the cross section of the observed event, which describes its probability to occur. The absolute knowledge of the luminosity therefore allows for the experiments to measure the absolute cross sections.

The Large Hadron Collider (LHC) was designed to produce proton-proton collisions at center of mass energy of 14 TeV. This energy would be the highest ever reached in a particle accelerator. The knowledge and understanding of particle physics at such high energy is based on simulations and theoretical predictions. As opposed to electron-positron colliders, for which the Bhabba scattering cross section can be accurately calculated and used for luminosity calibration, there are no processes with well known cross sections and sufficiently high production rate to be directly used for the purpose of luminosity calibration in the early operation of the LHC.

The luminosity can also be expressed as a function of the numbers of charges per beam and the beam sizes at the interaction point. Using this relation the absolute luminosity can be determined from machine parameters. The determination of the absolute luminosity from machine parameters is an alternative to the cross section based calibration and provides complementary information to the fragmentation model.

In the LHC, it was proposed to use the method developed by S. van der Meer at the ISR to provide a luminosity calibration based on machine parameters to the physics experiments during the first year of operation.

After a review of some general accelerator physics concepts and the principle of the van der Meer method in the presence of various effects such as crossing angle and hourglass, this thesis presents the results obtained at the LHC and RHIC during luminosity calibration measurements. A detailed analysis of the systematic uncertainties associated to the measurement and proposals for future improvements are discussed. On the longer term, TOTEM and ATLAS plan to measure the proton-proton cross section using dedicated optics and beam conditions. An overview of the study and performance of this optics is also presented.

7 Forthcoming Beam Dynamics Events

7.1 DIPAC2011 – the 10th Biennial European Workshop on Beam Diagnostics and Instrumentation for Particle Accelerators

The 10th biennial European Workshop on Beam Diagnostics and Instrumentation for Particle Accelerators, DIPAC2011 (http://dipac2011.desy.de/), will take place from 16-18 May 2011 in Hamburg, Germany, hosted by the research centre DESY.

DIPAC provides a unique forum for experts and novices to share their experience and to exchange information and ideas in the field of particle accelerator beam diagnostics. The workshop aims to provide an atmosphere that fosters lively discussions regarding latest developments and new concepts in instrumentation at particle accelerator facilities worldwide, ranging from low energy gun and injector test facilities to high energy, high intensity hadron accelerators and colliders. Diagnostics and instrumentation issues at synchrotron radiation user facilities, accelerator-based cancer therapy centres and next generation LINAC-based FELs also form an integral part of the Workshop.

The DIPAC2011 Program Committee encourages those actively engaged in this rapidly advancing field of accelerator design to participate and contribute to the scientific program by submitting abstracts for poster or oral presentations. Further information concerning all aspects of the workshop can be found on the website http://dipac2011.desy.de/.

The venue of DIPAC2011 is the still fully functional freighter Cap San Diego (http://www.capsandiego.de/) which anchors (attached firmly (!)) at the Uberseebrücke in the centre of Hamburg. The talks and poster sessions will be held in the former cargo holds of the Cap San Diego, so you can expect a quite exciting atmosphere. All recommended hotels and quite a number of attractions you will find within walking distance to the ship. Registration, accommodation and abstract submission will be open from 1st Dec. 2010. For further details please visit the web-page where you may also download the conference poster. We are looking forward to welcome you on board of the Cap San Diego in Hamburg.

The meeting will include a tour of the facilities at the DESY laboratory.

Contact:

Kay Wittenburg (Chair), DESY: kay.wittenburg@desy.de
Conference Secretariat:
Helga Ahluwalia
Dept. MR Deutsches Elektronen-Synchrotron DESY
Notkestrasse 85, 22607 Hamburg, Germany
Phone: +49-40-8998-3311
Fax: +49-40-8998-4305
E-mail: helga.ahluwalia@desy.de

8 Announcements of the Beam Dynamics Panel

8.1 ICFA Beam Dynamics Newsletter

8.1.1 Aim of the Newsletter

The ICFA Beam Dynamics Newsletter is intended as a channel for describing unsolved problems and highlighting important ongoing works, and not as a substitute for journal articles and conference proceedings that usually describe completed work. It is published by the ICFA Beam Dynamics Panel, one of whose missions is to encourage international collaboration in beam dynamics.

Normally it is published every April, August and December. The deadlines are 15 March, 15 July and 15 November, respectively.

Categories of Articles

The categories of articles in the newsletter are the following:

1. Announcements from the panel.
2. Reports of beam dynamics activity of a group.

3. Reports on workshops, meetings and other events related to beam dynamics.
4. Announcements of future beam dynamics-related international workshops and meetings.
5. Those who want to use newsletter to announce their workshops are welcome to do so. Articles should typically fit within half a page and include descriptions of the subject, date, place, Web site and other contact information.
6. Review of beam dynamics problems: This is a place to bring attention to unsolved problems and should not be used to report completed work. Clear and short highlights on the problem are encouraged.
7. Letters to the editor: a forum open to everyone. Anybody can express his/her opinion on the beam dynamics and related activities, by sending it to one of the editors. The editors reserve the right to reject contributions they judge to be inappropriate, although they have rarely had cause to do so.

The editors may request an article following a recommendation by panel members. However anyone who wishes to submit an article is strongly encouraged to contact any Beam Dynamics Panel member before starting to write.

8.1.2 **How to Prepare a Manuscript**

Before starting to write, authors should download the template in Microsoft Word format from the Beam Dynamics Panel web site:

http://www-bd.fnal.gov/icfabd/news.html

It will be much easier to guarantee acceptance of the article if the template is used and the instructions included in it are respected. The template and instructions are expected to evolve with time so please make sure always to use the latest versions.

The final Microsoft Word file should be sent to one of the editors, preferably the issue editor, by email.

The editors regret that LaTeX files can no longer be accepted: a majority of contributors now prefer Word and we simply do not have the resources to make the conversions that would be needed. Contributions received in LaTeX will now be returned to the authors for re-formatting.

In cases where an article is composed entirely of straightforward prose (no equations, figures, tables, special symbols, etc.) contributions received in the form of plain text files may be accepted at the discretion of the issue editor.

Each article should include the title, authors' names, affiliations and e-mail addresses.

8.1.3 **Distribution**

A complete archive of issues of this newsletter from 1995 to the latest issue is available at

http://icfa-usa.jlab.org/archive/newsletter.shtml.

This is now intended as the primary method of distribution of the newsletter.

Readers are encouraged to sign-up for electronic mailing list to ensure that they will hear immediately when a new issue is published.

The Panel's Web site provides access to the Newsletters, information about future and past workshops, and other information useful to accelerator physicists. There are links to pages of information of local interest for each of the three ICFA areas.

Printed copies of the ICFA Beam Dynamics Newsletters are also distributed (generally some time after the Web edition appears) through the following distributors:

Weiren Chou	chou@fnal.gov	North and South Americas
Rainer Wanzenberg	rainer.wanzenberg@desy.de	Europe[++] and Africa
Susumu Kamada	susumu.kamada@kek.jp	Asia[**] and Pacific

++ Including former Soviet Union.
** For Mainland China, Jiu-Qing Wang (wangjq@mail.ihep.ac.cn) takes care of the distribution with Ms. Su Ping, Secretariat of PASC, P.O. Box 918, Beijing 100039, China.

To keep costs down (remember that the Panel has no budget of its own) readers are encouraged to use the Web as much as possible. In particular, if you receive a paper copy that you no longer require, please inform the appropriate distributor.

8.1.4 **Regular Correspondents**

The Beam Dynamics Newsletter particularly encourages contributions from smaller institutions and countries where the accelerator physics community is small. Since it is impossible for the editors and panel members to survey all beam dynamics activity worldwide, we have some Regular Correspondents. They are expected to find interesting activities and appropriate persons to report them and/or report them by themselves. We hope that we will have a "compact and complete" list covering all over the world eventually. The present Regular Correspondents are as follows:

Liu Lin	Liu@lnls.br	LNLS, Brazil
Sameen Ahmed Khan	Rohelakan@yahoo.com	SCOT, Oman
Jacob Rodnizki	Jacob.Rodnizki@gmail.com	Soreq NRC, Israel
Rohan Dowd	Rohan.Dowd@synchrotron.org.au	Australian Synchrotron

We are calling for more volunteers as Regular Correspondents.

8.2 ICFA Beam Dynamics Panel Members

Name	*eMail*	*Institution*
Rick Baartman	baartman@lin12.triumf.ca	TRIUMF, 4004 Wesbrook Mall, Vancouver, BC, V6T 2A3, Canada
Marica Biagini	marica.biagini@lnf.infn.it	LNF-INFN, Via E. Fermi 40, Frascati 00044, Italy
Yunhai Cai	yunhai@slac.stanford.edu	SLAC, 2575 Sand Hill Road, MS 26, Menlo Park, CA 94025, U.S.A.
Swapan Chattopadhyay	swapan@cockcroft.ac.uk	The Cockcroft Institute, Daresbury, Warrington WA4 4AD, U.K.
Weiren Chou (Chair)	chou@fnal.gov	Fermilab, P.O. Box 500, Batavia, IL 60510, U.S.A.
Wolfram Fischer	wfischer@bnl.gov	Brookhaven National Laboratory, Bldg. 911B, Upton, NY 11973, U.S.A.
Yoshihiro Funakoshi	yoshihiro.funakoshi@kek.jp	KEK, 1-1 Oho, Tsukuba-shi, Ibaraki-ken, 305-0801, Japan
Miguel Furman	mafurman@lbl.gov	Center for Beam Physics, LBL, 1 Cyclotron Road, Berkeley, CA 94720-8211, U.S.A.
Jie Gao	gaoj@ihep.ac.cn	Institute for High Energy Physics, P.O. Box 918, Beijing 100049, China
Ajay Ghodke	ghodke@cat.ernet.in	RRCAT, ADL Bldg. Indore, Madhya Pradesh, 452 013, India
Ingo Hofmann	i.hofmann@gsi.de	High Current Beam Physics, GSI Darmstadt, Planckstr. 1, 64291 Darmstadt, Germany
Sergey Ivanov	sergey.ivanov@ihep.ru	Institute for High Energy Physics, Protvino, Moscow Region, 142281 Russia
Kwang-Je Kim	kwangje@aps.anl.gov	Argonne Nat'l Lab, Advanced Photon Source, 9700 S. Cass Avenue, Argonne, IL 60439, U.S.A.
In Soo Ko	isko@postech.ac.kr	Pohang Accelerator Lab, San 31, Hyoja-Dong, Pohang 790-784, South Korea
Alessandra Lombardi	alessandra.lombardi@cern.ch	CERN, CH-1211, Geneva 23, Switzerland
Yoshiharu Mori	mori@kl.rri.kyoto-u.ac.jp	Research Reactor Inst., Kyoto Univ. Kumatori, Osaka, 590-0494, Japan
Toshiyuki Okugi	toshiyuki.okugi@kek.jp	KEK, 1-1 Oho, Tsukuba-shi, Ibaraki-ken, 305-0801, Japan
Mark Palmer	mark.palmer@cornell.edu	Wilson Laboratory, Cornell University, Ithaca, NY 14853-8001, USA
Chris Prior	c.r.prior@rl.ac.uk	ASTeC Intense Beams Group, STFC RAL, Chilton, Didcot, Oxon OX11 0QX, U.K.
Yuri Shatunov	yu.m.shatunov@inp.nsk.ru	Acad. Lavrentiev, prospect 11, 630090 Novosibirsk, Russia
Jiu-Qing Wang	wangjq@mail.ihep.av.cn	Institute for High Energy Physics, P.O. Box 918, 9-1, Beijing 100049, China
Rainer Wanzenberg	rainer.wanzenberg@desy.de	DESY, Notkestrasse 85, 22603 Hamburg, Germany